TARGETING THE WNT/β-CATENIN SIGNALING PATHWAY IN CANCER

EDITED BY: Simone Patergnani, Donald Buchsbaum and Gary Piazza
PUBLISHED IN: Frontiers in Oncology

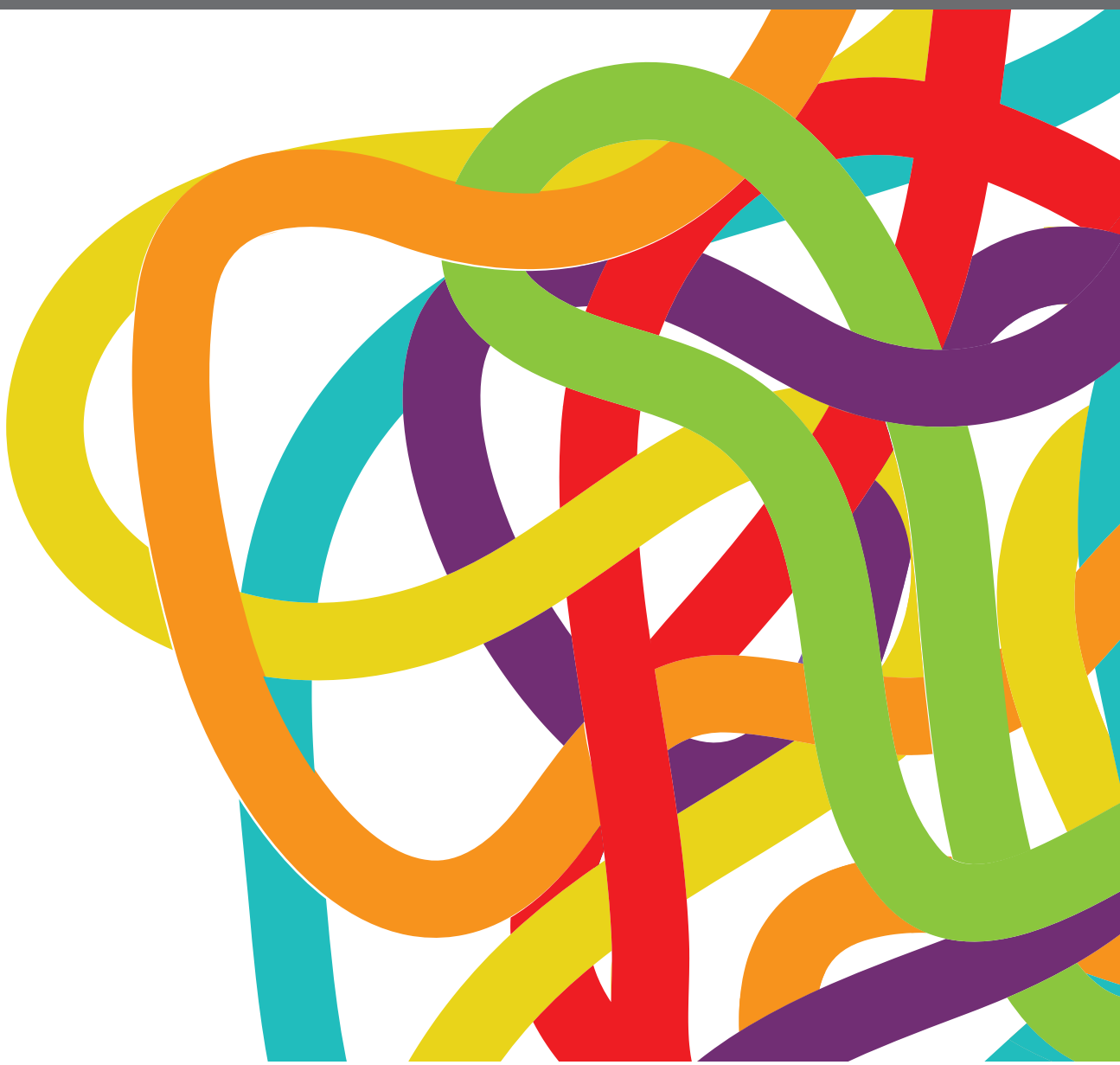

frontiers Research Topics

frontiers

ISSN 1664-8714
ISBN 978-2-83250-346-1
DOI 10.3389/978-2-83250-346-1

About Frontiers

Frontiers is more than just an open-access publisher of scholarly articles: it is a pioneering approach to the world of academia, radically improving the way scholarly research is managed. The grand vision of Frontiers is a world where all people have an equal opportunity to seek, share and generate knowledge. Frontiers provides immediate and permanent online open access to all its publications, but this alone is not enough to realize our grand goals.

Frontiers Journal Series

The Frontiers Journal Series is a multi-tier and interdisciplinary set of open-access, online journals, promising a paradigm shift from the current review, selection and dissemination processes in academic publishing. All Frontiers journals are driven by researchers for researchers; therefore, they constitute a service to the scholarly community. At the same time, the Frontiers Journal Series operates on a revolutionary invention, the tiered publishing system, initially addressing specific communities of scholars, and gradually climbing up to broader public understanding, thus serving the interests of the lay society, too.

Dedication to Quality

Each Frontiers article is a landmark of the highest quality, thanks to genuinely collaborative interactions between authors and review editors, who include some of the world's best academicians. Research must be certified by peers before entering a stream of knowledge that may eventually reach the public - and shape society; therefore, Frontiers only applies the most rigorous and unbiased reviews.
Frontiers revolutionizes research publishing by freely delivering the most outstanding research, evaluated with no bias from both the academic and social point of view. By applying the most advanced information technologies, Frontiers is catapulting scholarly publishing into a new generation.

What are Frontiers Research Topics?

Frontiers Research Topics are very popular trademarks of the Frontiers Journals Series: they are collections of at least ten articles, all centered on a particular subject. With their unique mix of varied contributions from Original Research to Review Articles, Frontiers Research Topics unify the most influential researchers, the latest key findings and historical advances in a hot research area! Find out more on how to host your own Frontiers Research Topic or contribute to one as an author by contacting the Frontiers Editorial Office: frontiersin.org/about/contact

TARGETING THE WNT/β-CATENIN SIGNALING PATHWAY IN CANCER

Topic Editors:
Simone Patergnani, University of Ferrara, Italy
Donald Buchsbaum, University of Alabama at Birmingham, United States
Gary Piazza, Auburn University, United States

Citation: Patergnani, S., Buchsbaum, D., Piazza, G., eds. (2022). Targeting the Wnt/β-Catenin Signaling Pathway in Cancer. Lausanne: Frontiers Media SA. doi: 10.3389/978-2-83250-346-1

Table of Contents

frontiers | Frontiers in Oncology

TYPE Editorial
PUBLISHED 13 September 2022
DOI 10.3389/fonc.2022.1022174

OPEN ACCESS

EDITED AND REVIEWED BY
Tao Liu,
University of New South Wales, Australia

*CORRESPONDENCE
Simone Patergnani
simone.patergnani@unife.it
Donald J. Buchsbaum
djb@uab.edu
Gary A. Piazza
gap0034@auburn.edu

†These authors have contributed equally to this work

SPECIALTY SECTION
This article was submitted to Molecular and Cellular Oncology, a section of the journal Frontiers in Oncology

RECEIVED 18 August 2022
ACCEPTED 19 August 2022
PUBLISHED 13 September 2022

CITATION
Patergnani S, Buchsbaum DJ and Piazza GA (2022) Editorial: Targeting the Wnt/β-catenin signaling pathway in cancer.
Front. Oncol. 12:1022174.
doi: 10.3389/fonc.2022.1022174

Editorial: Targeting the Wnt/β-catenin signaling pathway in cancer

Simone Patergnani[1*†], Donald J. Buchsbaum[2*†] and Gary A. Piazza[3*†]

[1]Department of Medical Sciences, Laboratory for Technologies of Advanced Therapies, University of Ferrara, Ferrara, Italy, [2]Department of Radiation Oncology, The University of Alabama at Birmingham, Birmingham, AL, United States, [3]Department of Drug Discovery and Development, Harrison College of Pharmacy, Auburn University, Auburn, AL, United States

KEYWORDS

Wnt/β-catenin, signaling, targeted therapy, molecular targets, cancer

Editorial on the Research Topic
Targeting the Wnt/β-catenin signaling pathway in cancer

Wnt/β-catenin signaling, also referred as canonical Wnt signaling, is a highly conserved cellular pathway that regulates multiple biological processes involved in normal physiological and disease processes, including cell proliferation and differentiation, tissue regeneration, migration, autophagy, and apoptosis. The main human disorder associated with dysfunctional Wnt/β-catenin signaling is cancer (1). Indeed, aberrant activation of Wnt/β-catenin signaling resulting from either Wnt overexpression or mutations in pathway components (e.g., APC) that stabilize β-catenin have been extensively reported in gastrointestinal, lung, liver, breast, and prostate cancers, as well as in leukemia and melanoma. Wnt/β-catenin signaling is known to drive Tcf/Lef transcription of proteins essential for cancer cell proliferation and survival, such as cyclin D, Myc, and survivin (2, 3). Wnt/β-catenin signaling also appears to be essential for cancer cell migration and invasion in the case of breast cancer and melanoma (4, 5) and the control of tumor dormancy in colorectal cancers (6). Another important aspect relating to cancer in which Wnt/β-catenin is involved is tumor immunology. Here, Wnt/β-catenin signaling appears to act as a major regulatory mechanism that causes primary resistance to T cell-based immune-oncology therapies (7). Finally, Wnt/β-catenin is involved in the maintenance and propagation of stem cells essential for normal cell turnover as well as tissue regeneration (8, 9). Consequently, Wnt/β-catenin signaling can cause resistance to certain cancer treatments (10), while inhibition can result in toxicity to normal tissues. Considering these aspects, it is not surprising that researchers have proposed multiple molecular strategies to target various nodes within this signaling pathway for cancer treatment. Indeed, the Wnt/β-catenin pathway is complex and embodies a wide number of components, which represent potential targets for cancer treatment or prevention. Furthermore, Wnt/β-catenin may have different roles among cancers of different histologic origins. Therefore, it is

necessary to consider all molecular relationships between Wnt/β-catenin signaling and other regulatory pathways in normal tissues and cancer in the development of novel anticancer drugs that target Wnt/β-catenin signaling.

This Research Topic entitled "Targeting the Wnt/β-catenin Signaling Pathway in Cancer" represents a review of the current knowledge of the intrinsic link between Wnt/β-catenin signaling and cancer. The published original research and review articles are briefly described below:

Zhou et al. investigated the molecular mechanisms by which uterine leiomyoma (UL) cells proliferate and unveiled that the specific long noncoding RNA Alu-mediated p21 transcriptional regulator (APTR) was overexpressed in UL human tissues and promoted cell proliferation by increasing the expression of the proteins of the Wnt/β-catenin signaling pathway and by directly interacting with the estrogen receptor alpha (ERα).

Raoul et al. reported the clinical outcome and molecular profile of two cases of metastatic pancreatoblastomas, a rare pancreatic tumor typically found in young children. In this report, they demonstrated that both patients benefited from systemic chemotherapy (FOLFIRINOX regimen). Furthermore, by performing high-throughput sequencing of the tumors analyzed, they found specific mutations of members of the Wnt/β-catenin pathway.

Behrooz and Syahir provides an overview of the state-of-the-art of the interplay between CD133, Wnt/β-catenin and TERT signaling pathways in glioblastoma multiforme (GBM) to demonstrate that this axis may represent a possible therapeutic target against this aggressive cancer type.

She et al. demonstrated that the Fas apoptotic inhibitory molecule 2 (FAIM2) is highly expressed in non-small cell lung cancer (NSCLC) tissues and NSCLC tissues with bone metastasis, and promotes cell proliferation, migration, and invasion, and inhibits cell apoptosis. Interestingly, the authors unveiled that FAIM2 exerts these effects by regulating the Wnt/β-catenin signaling pathway.

Ding et al. identified high expression levels of tumor endothelial marker 8 (TEM8) in samples and cells of lung adenocarcinoma. Such increased levels were associated with tumor size of primary tumor. Mechanistic investigations performed both *in vitro* and *in vivo* showed that TEM8 promoted lung cancer cell proliferation and invasion by activating Wnt/β-catenin signaling.

Ke et al. found that exposure to polycyclic aromatic hydrocarbons (which are widespread environmental pollutants associated with carcinogenicity) suppressed the microRNA (miR), 377-3p, and downregulated the expression of early growth response 1 (EGR1) to facilitate malignant transformation and tumor growth of lung cells by regulating the Wnt/β-catenin pathway.

Zheng et al. demonstrated that the protein A-kinase interacting protein 1 (AKIP1) was elevated in diverse thyroid carcinoma cells and regulated different aspects of tumorigenesis (including apoptosis, cell viability and invasion, and response to chemotherapy) by controlling the activity of PI3K/AKT and β-catenin pathways.

Shah et al. explored the current knowledge of the phosphorylation-dependent regulations of β-catenin and Wnt signaling in cancer providing a detailed overview of the main kinases which regulate the Wnt/β-catenin pathway.

Wang et al. performed a study aimed to investigate the significance of Wnt in the prognosis and tumor immunity in NSCLC and found that WNT2B and WNT7A might have prognostic value in lung adenocarcinoma and in squamous cell lung cancer. Authors performed this investigation by using a publicly available tumor database and validated their findings in NSCLC pathological tissues and cell lines.

Perspectives

The Wnt/β-catenin signaling pathway was discovered over 30 years ago and has been extensively studied as a key cellular pathway involved in both physiological and pathological processes. While it has been widely reported that Wnt/β-catenin signaling plays a critical role in multiple aspects of tumorigenesis from early stages of malignant transformation to invasion and metastasis, there are no approved anticancer drugs that target this pathway for either the treatment or prevention of cancer. Nonetheless, multiple lines of evidence suggests that targeting the Wnt/β-catenin pathway with small molecule inhibitors can selectively inhibit proliferation and induce apoptosis of cancer cells to inhibit tumor growth. Despite all these aspects, the exact function of Wnt/β-catenin signaling, all of its molecular components, and other intracellular signaling pathways (e.g., RAS/MAPK) that may intersect with Wnt/β-catenin signaling, within the context of normal physiology and cancer biology remain only partially understood. A more complete understanding of these questions holds promise for providing insight to novel molecular targets and the development of efficacious anticancer drugs for a wide range of malignancies that are driven by Wnt/β-catenin signaling.

Author contributions

All authors listed have made a substantial, direct, and intellectual contribution to the work and approved it for publication.

Funding

SP was supported by Fondazione Umberto Veronesi and by A-ROSE. DB was supported by the American Board of

Obstetsrics & Gynecology, the Norma Livingston Foundation, and the Foundation for Womens Cancer. GP was supported, in part, by the National Cancer Institute of the National Institutes of Health under awards R01CA197147, R01CA254197, and R01CA238514.

Acknowledgments

We thank all the authors who contributed to this Research Topic as well as various reviewers/editors of the respective manuscripts, for their efforts, timely responses and enthusiasm. We also thank the Frontiers Editorial Office for their assistance and support.

Conflict of interest

The authors declare that the research was conducted in the absence of any commercial or financial relationships that could be construed as a potential conflict of interest.

Publisher's note

References

1. Zhan T, Rindtorff N, Boutros M. Wnt signaling in cancer. *Oncogene* (2017) 36:1461–73. doi: 10.1038/onc.2016.304

2. Yu X, Wang Y, Degraff DJ, Wills ML, Matusik RJ. Wnt/beta-catenin activation promotes prostate tumor progression in a mouse model. *Oncogene* (2011) 30:1868–79. doi: 10.1038/onc.2010.560

3. Vilchez V, Turcios L, Marti F, Gedaly R. Targeting wnt/beta-catenin pathway in hepatocellular carcinoma treatment. *World J Gastroenterol* (2016) 22:823–32. doi: 10.3748/wjg.v22.i2.823

4. Yook JI, Li XY, Ota I, Hu C, Kim HS, Kim NH, et al. A wnt-Axin2-GSK3beta cascade regulates Snail1 activity in breast cancer cells. *Nat Cell Biol* (2006) 8:1398–406. doi: 10.1038/ncb1508

5. Damsky WE, Curley DP, Santhanakrishnan M, Rosenbaum LE, Platt JT, Gould Rothberg BE, et al. Beta-catenin signaling controls metastasis in braf-activated pten-deficient melanomas. *Cancer Cell* (2011) 20:741–54. doi: 10.1016/j.ccr.2011.10.030

6. Hiendlmeyer E, Regus S, Wassermann S, Hlubek F, Haynl A, Dimmler A, et al. Beta-catenin up-regulates the expression of the urokinase plasminogen activator in human colorectal tumors. *Cancer Res* (2004) 64:1209–14. doi: 10.1158/0008-5472.can-3627-2

7. Spranger S, Bao R, Gajewski TF. Melanoma-intrinsic beta-catenin signalling prevents anti-tumour immunity. *Nature* (2015) 523:231–5. doi: 10.1038/nature14404

8. Chakrabarti R, Wei Y, Hwang J, Hang X, Andres Blanco M, Choudhury A, et al. DeltaNp63 promotes stem cell activity in mammary gland development and basal-like breast cancer by enhancing Fzd7 expression and wnt signalling. *Nat Cell Biol* (2014) 16:1001–13. doi: 10.1038/ncb3040

9. Yue Z, Yuan Z, Zeng L, Wang Y, Lai L, Li J, et al. LGR4 modulates breast cancer initiation, metastasis, and cancer stem cells. *FASEB J* (2018) 32:2422–37. doi: 10.1096/fj.201700897R

10. Yamamoto TM, Mcmellen A, Watson ZL, Aguilera J, Ferguson R, Nurmemmedov E, et al. Activation of wnt signaling promotes olaparib resistant ovarian cancer. *Mol Carcinog* (2019) 58:1770–82. doi: 10.1002/mc.23064

frontiers in Oncology

ORIGINAL RESEARCH
published: 10 March 2021
doi: 10.3389/fonc.2021.536346

LncRNA APTR Promotes Uterine Leiomyoma Cell Proliferation by Targeting ERα to Activate the Wnt/β-Catenin Pathway

Weiqiang Zhou, Guocheng Wang, Bilan Li, Junjie Qu and Yongli Zhang *

Department of Obstetrics and Gynecology, Shanghai First Maternity and Infant Hospital, Tongji University School of Medicine, Shanghai, China

OPEN ACCESS

Edited by:
Zhe-Sheng Chen, St. John's University, United States

Reviewed by:
Xiaozhuo Liu, University at Buffalo, United States
Guangjian Fan, Shanghai General Hospital, China

***Correspondence:**
Yongli Zhang
doctorzhang2@163.com

Specialty section:
This article was submitted to Molecular and Cellular Oncology, a section of the journal Frontiers in Oncology

Received: *12 March 2020*
Accepted: *01 February 2021*
Published: *10 March 2021*

Citation:
Zhou W, Wang G, Li B, Qu J and Zhang Y (2021) LncRNA APTR Promotes Uterine Leiomyoma Cell Proliferation by Targeting ERα to Activate the Wnt/β-Catenin Pathway. Front. Oncol. 11:536346. doi: 10.3389/fonc.2021.536346

The molecular mechanisms by which uterine leiomyoma (UL) cells proliferate are unclear. Long noncoding RNA (lncRNA) is reported to participate in the occurrence and development of gynecological cancers. We investigated the molecular mechanisms that lncRNA uses in UL. We found that lncRNA Alu-mediated p21 transcriptional regulator (APTR) showed higher expression in UL tumor tissues compared with that in normal uterine tissues. APTR induced cell proliferation and colony formation both *in vitro* and *in vivo*. The JASPAR database showed that APTR was likely interacted with ERα, and these molecules were identified *via* laser scanning confocal microscopy and RNA immunoprecipitation analysis. To verify the correlation between APTR and ERα, we overexpressed and underexpressed APTR and simultaneously expressed ERα. The results showed that APTR function was suppressed. APTR increased the expressions of the proteins in the Wnt pathway, and inhibiting ERα eliminated these responses. In conclusion, our data suggest that APTR promoted leiomyoma cell proliferation through the Wnt pathway by targeting ERα, suggesting a new role of APTR in the Wnt signaling pathway in UL.

Keywords: long noncoding RNA (lncRNA) Alu-mediated p21 transcriptional regulator (APTR), uterine leiomyoma, proliferation, ERα, Wnt pathway

HIGHLIGHTS

►APTR induced uterine leiomyoma cell proliferation and colony formation
► APTR directly interacted with ERα and they were co-localized in the nucleus
►APTR promoted leiomyoma cell proliferation through the Wnt pathway by targeting ERα

INTRODUCTION

Uterine leiomyoma (UL) is the most common benign gynecological tumor, with an incidence rate of 30–40% in fertile women (1). UL may lead to asymptomatic complications such as uterine bleeding, severe dysmenorrhea, pelvic pain and infertility and is the leading indication for a hysterectomy (2). However, because the typical marriage age has increased, and many women have not completed childbearing, hysterectomies are often contraindicated (3). Therefore, nonsurgical treatments are urgently needed, and understanding the specific molecular mechanism of UL cell proliferation may improve patients' quality of life.

In vitro and *in vivo* experiments have shown that UL is an estrogen-dependent tumor, and estrogen affects UL promotion and progression (4). Estrogen binds to its receptors and initiates transcription, then promotes UL cell proliferation (5). Estrogen receptors include estrogen receptors (ERs) α and β, and estrogenic action can be influenced by selective estrogen receptors (6). However, whether ERα or ERβ mediate estrogen function and how estrogen affects UL cell proliferation remain unclear.

Aberrant activation of Wnt/β-catenin has been detected in ER-positive breast cancer cells (7). β-Catenin is involved in the canonical Wnt signaling pathway, regulating diverse sets of cellular activities including cell proliferation (8). Enhanced nuclear β-catenin can accelerate interphase by shortening the cell cycle phase and can activate cyclin-D1 and c-Myc (9).

Long noncoding RNA (lncRNA) is reported to participate in gynecological cancers and is associated with the epithelial-mesenchymal transition (EMT) (10). H19 generates miR-675, an EMT-associated gene in prostate cancer (11). LncRNA is also reported to participate in endometrial carcinoma occurrence and development (12).

LncRNA Alu-mediated p21 transcriptional regulator (APTR) is the inhibitor that represses the p21 promoter in human glioblastomas (13). APTR is reported to play a crucial role in osteosarcoma (14), be a potential biomarker for liver cirrhosis (15) and have potential diagnostic value for papillary thyroid cancer (16). In this study, we examined whether APTR plays a pivotal role in UL progression and elucidated the possible mechanism.

MATERIALS AND METHODS

Cells, Patients, and Samples

Three patients were included in the study, and UL tumor tissue and adjacent normal uterine tissue specimens were acquired at the follicular phase. Inclusion criteria for this study were patients who (a) were nonmenopausal, (b) had undergone a hysterectomy because of UL between 12/2016 and 08/2017, (c) were without medical complications, and (d) had no history of hormone therapy. Paraffin-embedded tissues of 34 UL patients were included in the study, and all histopathologic evaluations were performed by experienced pathologists from the Shanghai First Maternity and Infant Hospital.

Ht-UtLM primary cells were collected from 30 patients who had undergone total hysterectomies at the follicular phase and were selected according to the above criteria. All were diagnosed by a pathologist. The detailed steps were previously described (17). Ht-UtLM-1 and the Ht-UtLM-2 came from the same patient's primary cells. Because the primary cells cannot be subcultured, primary cells from different patients were used for different experiments and there were total 30 patients selected. It was investigated the cells culture was mycoplasma-free.

The Hospital's Protection of Human Subjects Committee approved the study protocols. Samples were acquired with written informed consent from the Shanghai First Maternity and Infant Hospital affiliated with Tongji University School of Medicine.

Immunohistochemistry

Immunohistochemical staining was performed using the two-step plus Poly-HRP Anti-IgG Detection System (ZSGB-Bio, Beijing, China) per the manufacturer's recommendations. Primary antibodies targeting ERα (C-311; cat. no. sc-787, Santa Cruz, CA, USA), ERβ (B-3; cat. no. 373853, Santa Cruz), Ki-67 (cat. no. 373853, Santa Cruz) and β-catenin (12F7; cat. no. sc-59737, Santa Cruz) were used.

RNA Extraction and Analysis

Total RNA extraction and reverse transcription were performed per the manufacturer's protocol. Semi-quantitative RT-PCR was performed using the standard protocol from the SYBR Green PCR kit (Toyobo, Osaka, Japan). GAPDH was used as the reference mRNA. DCt values were normalized to GAPDH levels. The $2^{-\triangle\triangle Ct}$ method was used to measure the gene expression levels. The primer pairs used were as follows: human lncRNA APTR forward: 5′-AGTAGCAGGAGACAG CAT-3′, reverse: 5′-TGACAGCCTTCCACAATC-3′; α-SMA forward: 5′-CTTTCAAGCTGTTCCTGTC-3′, reverse: 5′-TGT GTTTCTCCTCTGTCC-3′; vimentin forward: 5′-GATGGTGTT TGGTCGCATA-3′, reverse: 5′- CGAATGCGCAGCACCAG-3′; KRT-19 forward: 5′-GGCGCCACCATTGAGAA CT-3′, reverse: 5′-GCCAGGCGGGCATTG-3′; and GAPDH forward: 5′-GGC TCCCTTGGGTATATGGT-3′, reverse: 5′-TTGATTTTGGA GGGATCTCG-3′.

Western Blot Analysis

Western blot analysis was performed to assess protein expression as previously described (18). Primary antibodies included anti-GAPDH (cat. no. G9545) purchased from Sigma, all others were purchased from Santa Cruz, including anti-ERα (sc-8002), anti-KRT-19 (sc-376126), anti-α-SMA (sc-53142), anti-vimentin (sc-6260), anti-actin (sc-8432), anti-c-Myc (sc-373712), anti-β-catenin (sc-7963) and anti-cyclin-D1 (sc-8396).

Lentiviral Production and Infection

The full-length nucleotide sequence for APTR was obtained from the FLJ cDNA library. It was then inserted at the 3′ end of the

APTR in the lentivirus vector (Invitrogen, V49810). The shRNA was constructed as previously described (19).

Cell Cultures and Colony Formation

Cells were cultured in 10% Dulbecco's modified Eagle's medium containing 10% fetal bovine serum (Wisent, Canada) at 37°C with 5% CO2. For the colony-forming assay, cells (6×10^2) were transfected and incubated for 14 days. Colonies (>50 cells) were counted manually and plotted as previously described (18).

Cell Viability Assay

Cells were plated and grown for 96 h. The number of cells was determined using the 3-(4,5-dimethylthiazol-2yl)-2,5-diphenyltetrazolium bromide (MTT) assay as previously described (20).

RNA Immunoprecipitation

RIP analysis to assess RNA-binding protein expression was performed as previously described (21). Primary antibodies included mouse monoclonal antibody against ERα (cat. no. sc-787, Santa Cruz) and mouse monoclonal antibody against actin (C-2; cat. no. sc-8432, Santa Cruz).

Luciferase Assays

Cells were seeded at 1×10^5 cells/well in a 24-well cell plate one day prior to transfection with Superfect according to the manufacturer's protocol (Tiangen Biotech co LTD, Beijing, China). Luciferase activity was normalized for transfection efficiency using the mutant promoter reporter plasmid, FOPflash (vs. TOPflash, the un-mutated plasmid), as an internal control (22).

Illumina HiSeq

Total RNA was extracted from cells using TRIzol™ Reagent (#15596026, Invitrogen, Carlsbad, CA, USA) per the manufacturer's protocol, and ribosomal RNA was removed using the Ribo-Zero rRNA Removal Kit (Epicentre, Madison, WI, USA). Fragmented RNA (average length of ~200 bp) were subjected to first-strand and second-strand cDNA synthesis followed by adaptor ligation and enrichment with a low cycle per the instructions of the NEBNext® Ultra™ RNA Library Prep Kit for Illumina (NEB, USA). The purified library products were evaluated using the Agilent 2200 TapeStation and Qubit® 2.0 (Life Technologies, USA). The libraries were paired-end sequenced (PE150, sequencing reads were 150 bp) using the Illumina HiSeq Xten platform.

Fastp software (v0.17.0) was used to trim adaptor and remove low quality reads to get high quality clean reads. mRNA/LncRNA: hisat2 software (v2.04) was used to align the high quality clean reads to the human reference genome (UCSC hg19). Then, guided by the Ensembl GTF gene annotation file (v75), cuffdiff software (part of cufflinks, v2.2.1) was used to get the gene level FPKM as the expression profiles of mRNA, transcript level FPKM as the expression profiles of LncRNA, and fold change and p-value were calculated based on FPKM, differentially expressed mRNAs/LncRNAs were identified by cuffdiff software. Gene Ontology and KEGG pathway enrichment analysis were performed based on the differentially expressed mRNAs and LncRNA nearby genes. This part of the experiment was performed by Shanghai Yinxi Biomedical Technology Co., Ltd.

Nude Mouse Study

Ht-UtLM cells (5×10^6) with stably upregulated APTR were subcutaneously implanted into 4- to 6-week-old BALB/c nude mice purchased from Shanghai SLAC Laboratory Animal Company. Tumor growth was measured using a digital caliper every 5 days for 30 days. The mice were sacrificed on day 30 after cell implantation, and the tumor weights were measured.

Plasmids

The ERαcDNA and ERαRNAi plasmid were purchased from Origene (Maryland, USA) (23).

Fluorescence In Situ Hybridization

The cDNA encoding APTR was subcloned into the NheI and XhoI sites of pSL-MS2-12x vector (Addgene), named pSL-MS2-APTR, the sequence is as follow: ACTR-F-NheI 5'-TAGCTAGCAGTCCCGCTGACACCTT-3', ACTR-R-XhoI 5'-ACCTCGAGAACCGTGAGTCCATTAAACCTC -3'. A digoxin (Roche, Mannheim, Germany)-labeled lncRNA-APTR complementary DNA probe was synthesized *in vitro* used for RNA fluorescence *in situ* hybridization (FISH). The following procedures were performed as previously described (24) without slight modification.

Statistical Analysis

All experiments were repeated in triplicate. Data are expressed as the mean ± SD. Statistical significance between two groups was determined using Student's t-test. $P<0.05$ was considered statistically significant.

RESULTS

Alu-Mediated p21 Transcriptional Regulator Was Overexpressed in Uterine Leiomyoma

UL tissues and adjacent normal uterine tissues from three patients were used to confirm the APTR expression levels. Illumina HiSeq was used to further verify the higher expression of APTR. APTR expressions in the tissues from the three patients were significantly increased compared with those of the normal tissues (**Figures 1A, B**).

Increased levels of α-SMA and decreased levels of vimentin and KRT-19 identified the leiomyoma tumor cells (**Figure 1C**). Next, real-time PCR analysis confirmed the higher APTR levels in the UL tissues (**Figure 1D**). **Figures 1C, D** showed one representative sample.

Alu-Mediated p21 Transcriptional Regulator Overexpression Promoted Leiomyoma Cell Proliferation

APTR was overexpressed in UL tumor cells. Thus, we investigated the role of APTR in regulating cell proliferation.

We constructed APTR-overexpression and APTR-knockdown lentiviral vectors, infected Ht-UtLM cells, and selected stably infected cell clones for further study. The vectors were compared to a control (**Figure 2A**). MTT analysis showed that APTR-infected cells grew much faster than did the controls (**Figures 2B, C**). Colony-formation assays revealed that APTR-infected cells formed larger and more numerous colonies than did the controls (**Figures 2D, E**). Conversely, shRNA-infected cells had slower proliferation rates and formed smaller and fewer colonies than did the controls.

The stably infected cells were subcutaneously transplanted into BALB/c nude mice. We suspended the cells at 5×10^6 cells/ml, and 100 µl were injected into the flanks of nude mice (n=5). We measured tumor sizes starting 5 days postinjection using the formula, $W^2 \times L$, every 5 days for 30 days. Mice were then euthanized, and the tumors were excised (**Figure 2F**). Tumor sizes (**Figure 2G**) and weights (**Figure 2H**) from APTR-overexpressing cells were increased compared with the controls.

Alu-Mediated p21 Transcriptional Regulator Directly Interacted With ERα

According to the JASPAR database, lncRNA is likely interacted with ERα (**Figure 3A**). ENST00000447009 is lncRNA APTR, with an interaction strength of 10%. We next explored whether APTR interacts with ERα. The location of APTR was confirmed using FISH assay; APTR and ERα were co-localized in the nucleus (**Figure 3B**). We used RIP to verify the correlation between ERα and APTR, and the results showed that APTR is likely interacted with ERα (**Figure 3C**).

Alu-Mediated p21 Transcriptional + Regulator Induced Leiomyoma Tumor Cells Proliferation by Targeting ERα

In leiomyoma tumor cells, ERα promoted proliferation, as did APTR. Therefore, the correlation between ERα and APTR were measured. Western blot analysis was used to verify the overexpression and underexpression of ERα (**Figure 3D**). MTT

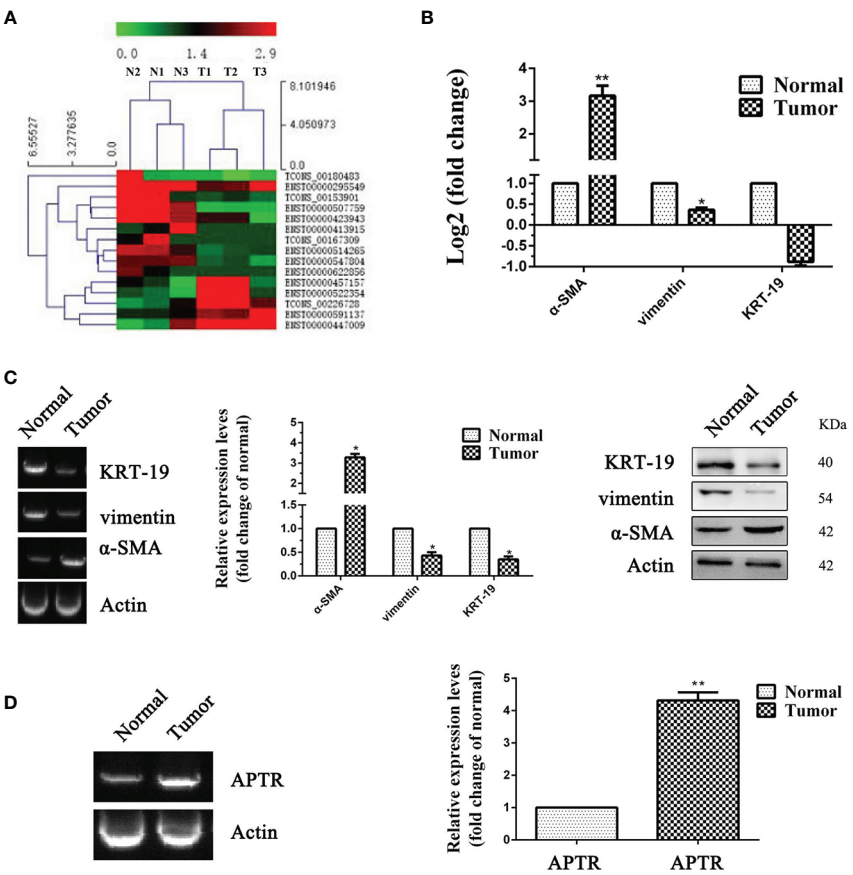

FIGURE 1 | LncRNA expression was high in leiomyoma tumors. **(A, B)** Differences in RNA transcription were detected between normal uterine tissues and leiomyoma tumors. High-level pathway sequencing showed that α-SMA expression was higher in leiomyoma tumors. **(C)** Gel electrophoresis, real-time PCR, and Western blot analyses confirmed higher α-SMA expression and lower vimentin and KRT-19 expression in leiomyoma tumors. **(D)** Gel electrophoresis and real-time PCR analyses confirmed higher APTR expression in leiomyoma tumors. (*$P < 0.05$, **$P < 0.01$).

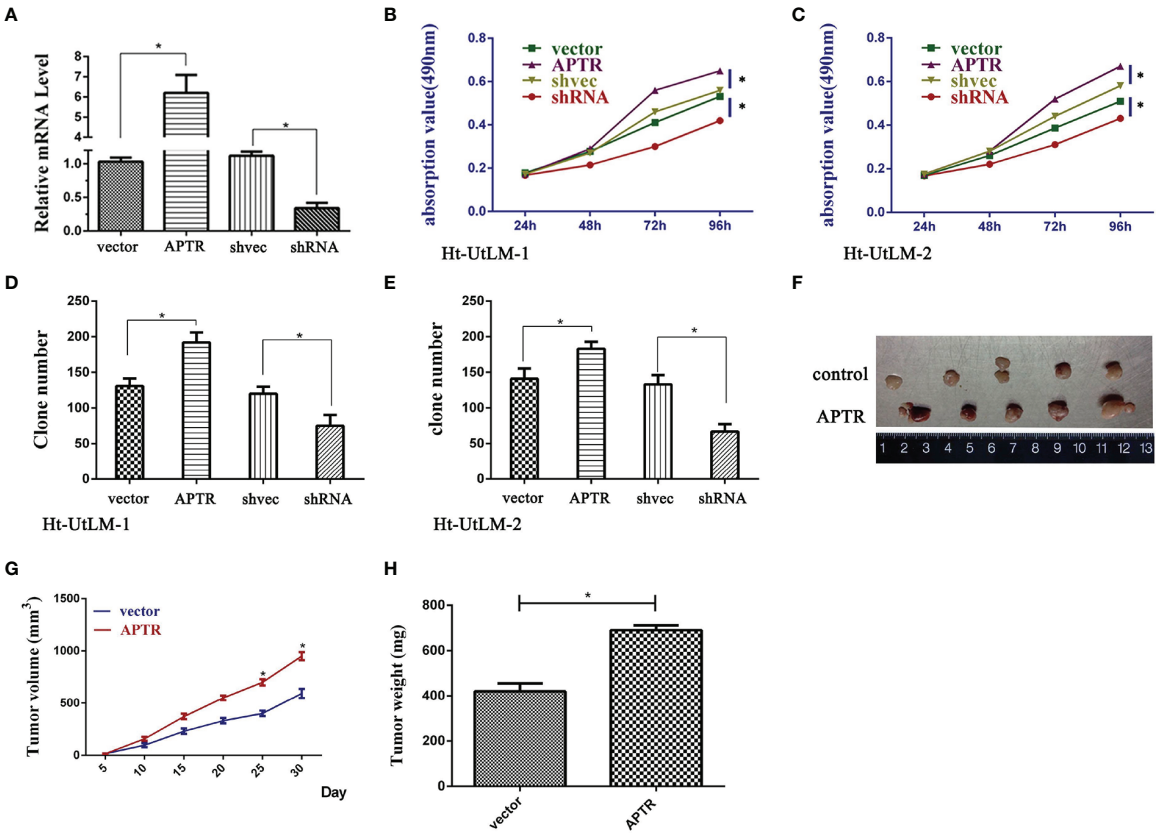

FIGURE 2 | LncRNA APTR induced leiomyoma tumor cell proliferation. Ht-UtLM primary cells derived from leiomyoma tumors were used. **(A)** Stably infected Ht-UtLM cells were generated and identified. Real-time PCR analyses confirmed the efficiency. **(B, C)** Cell proliferation testing was conducted using MTT assays. APTR overexpression increased cell proliferation. Conversely, knocking down APTR decreased cell proliferation. **(D, E)** Colony-formation assays were performed on stably overexpressed or underexpressed APTR for 2 weeks. **(F)** Tumors from xenograft-transplanted nude mice 30 days after subcutaneously injecting APTR-overexpressing or control Ht-UtLM cells. **(G)** Xenograft volumes 30 days after cell injection. **(H)** Xenograft weights 30 days after cell injection.

analysis showed that ERα overexpression cells grew much faster than controls (**Figure 3E**). Colony formation assays also revealed that ERα overexpression cells formed larger and more colonies than controls (**Figure 3F**). Conversely, ERα α cells had slower proliferation rates and formed smaller and fewer colonies than controls.

APTR levels were overexpressed and underexpressed (**Figure 3G**). The effect of APTR on growth was abolished when simultaneously infected with ERαRNAi (**Figures 3H, I**). Colony-formation assays revealed the same results. Colonies formed by the APTR- and ERαRNAi-infected cells did not significantly differ from those formed by the control cells (**Figures 3J, K**).

APTR Promoted Leiomyoma Cell Proliferation Through the Wnt Pathway by Targeting ERα

By bioinformatic analysis, β-catenin promoter has four ERα binding sites (**Figure 4A**). β-catenin promoter luciferase reporter (TOPflash) was used to investigate the regulation of β-catenin by APTR. The Ht-UtLM cells were coinfected with APTR or shRNA and TOPflash, and the activity was examined. The results showed that TOPflash activity was increased by cotransfection with APTR and decreased by shRNA (**Figures 4B, C**). When the cells were cotransfected with both APTR and ERαRNAi or shRNA and ERαRNAi, both cell groups lost their responses (**Figure 4D**).

Western blotting was used to further validate the effect of APTR. APTR upregulated β-catenin expression and simultaneously indirectly upregulated c-Myc and cyclin-D1, downstream proteins of the Wnt signaling pathway. Conversely, the β-catenin and downstream cyclin-D1 and c-Myc expression levels did not differ from those of the control groups. When the cells were coinfected with both APTR and ERαRNAi or shRNA and ERαRNAi, the changes in protein expressions between the two groups did not significantly differ (**Figures 4E, F**). These results indicated that APTR activated the Wnt pathway by targeting ERα.

DISCUSSION

In this study, we identified a new effect of lncRNA APTR, which targets the p21 promoter. We found high APTR expression levels in the leiomyoma tumor tissues using Illumina HiSeq and

A

Protein ID	RNA ID	Z-score	Discriminative Power (%)	Interaction Strength (%)
XP_016865869.1._183-252	ENST00000531508	0.91	96	99
XP_016865869.1._183-252	ENST00000447009	0.92	97	100
XP_016865869.1._183-252	ENST00000420160	0.92	97	100

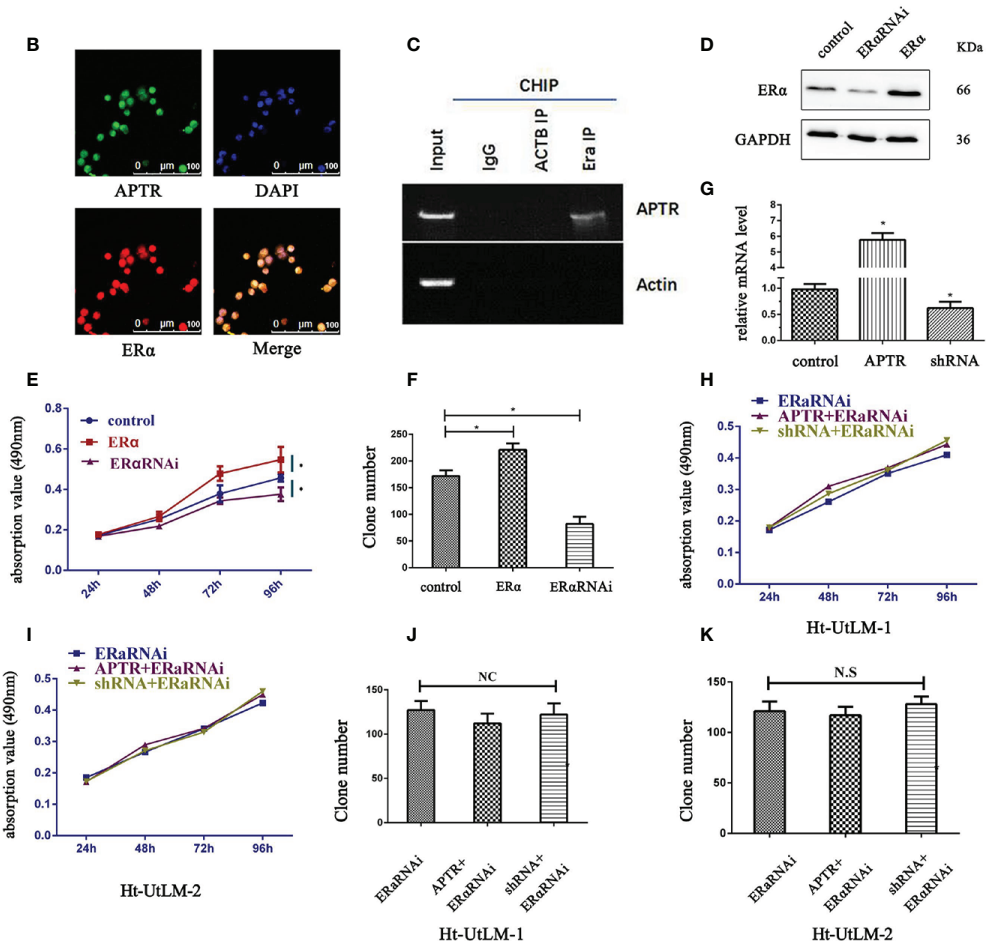

FIGURE 3 | LncRNA APTR induced tumor growth by targeting ERα. LncRNA APTR was likely interacted with ERα. **(A)** LncRNA ENST00000447009 was lncRNA APTR. According to the JASPAR database, APTR was likely interacted with ERα. **(B)** Ht-UtLM cells with elevated APTR expression were seeded in 96-well plates. FISH analysis showed that ERα (red) co-localized with APTR (green) in the nuclei of Ht-UtLM cells. **(C)** RIP showed that APTR was in contact with ERα. **(D)** Ht-UtLM cells were transfected with either ERα cDNA or shRNA plasmids. ERα expression was analyzed by western blot. **(E)** Cell viability was assessed by MTT assay daily for 4 days. **(F)** Colony formation assays were performed on Ht-UtLM cells for 2 weeks. **(G)** Ht-UtLM cells that stably overexpressed or underexpressed APTR were screened *via* real-time PCR. **(H, I)** After overexpressing or underexpressing APTR or ERαRNAi, the cell viability was assessed using MTT assays daily for 4 days. **(J, K)** Colony-formation assays were performed on cells stably overexpressed or underexpressed for 2 weeks. (*$P < 0.05$).

real-time PCR experiments to examine leiomyoma tumor tissues and adjacent normal cells. Bioinformatics analyses showed that APTR is likely interacted with ERα. Knocking down the ERα level abolished the effect of APTR on UL cell proliferation. This effect on APTR reveals a new role for ERα in the Wnt pathway and represents the first identification of the lncRNA and ERα pathway.

APTR represses the CDKN1A/P21 promoter, which has been correlated with cell proliferation in several cancers (13, 15). Downregulation of APTR has been correlated with tumorigenesis in papillary thyroid cancer and anaplastic thyroid cancer (16). In cirrhotic patients with portal hypertension, APTR was considered a prognostic marker, and higher APTR expression was associated with a poor prognosis (25).

Given the recently identified role of APTR, we first detected APTR expression in leiomyoma tissues and adjacent normal tissues. As expected, APTR had a higher expression in leiomyoma tissues. Further investigation of APTR's function would be of interest since APTR overexpression promoted

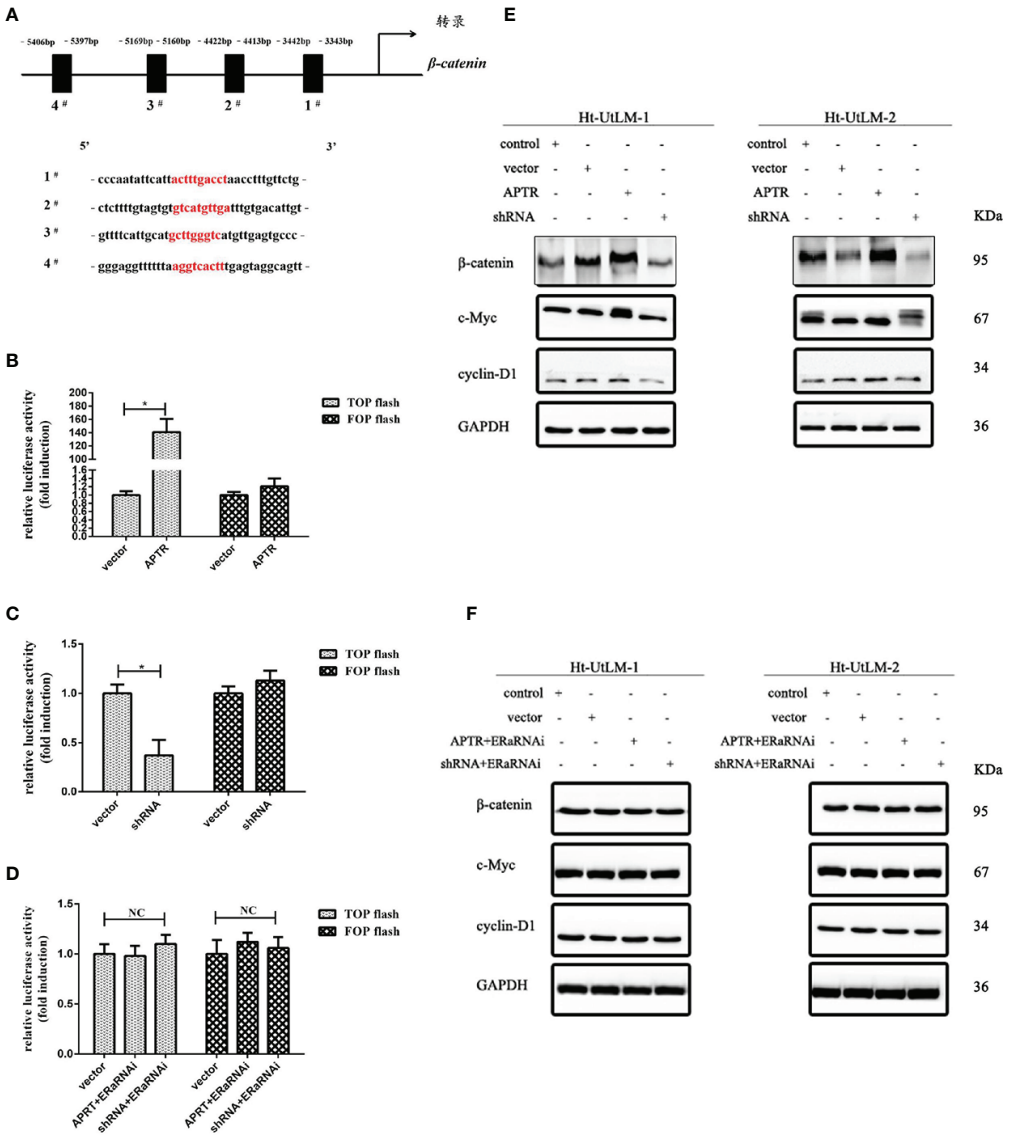

FIGURE 4 | APTR activated the canonical Wnt pathway in Ht-UtLM cells by targeting ERα. **(A)** β-Catenin promoter has four ERα binding sites. **(B)** Cells were infected with or without APTR together with the TCF-luciferase reporter (TOPflash) or mutant TCF-luciferase reporter (FOPflash) for 24 h. Upregulated APTR increased TOPflash activation in Ht-UtLM cells. **(C)** Downregulated APTR repressed TOPflash activation in Ht-UtLM cells. **(D)** Infection with APTR and ERαRNAi did not affect the basal TOPflash activity. **(E, F)** Ht-UtLM cells were infected with APTR or shRNA alone or together with the ERαRNAi. Western blot analysis was performed with GAPDH as the loading control. (*$P < 0.05$, **$P < 0.01$).

proliferation of the UL cell line, but underexpression of APTR had the opposite effect. Until now, the mechanism of APTR regulation as it relates to UL cell proliferation was unclear.

Long noncoding RNA (lncRNA) with more than 200 nucleotides is considered a transcript and is not translated into proteins (26). With little primary sequence conservation, many lncRNAs are localized to the nucleus (27), while some can encode small proteins (28). Bioinformatics analysis revealed that APTR was likely interacted with ERα, and we verified this using RIP. To further assess the function, we overexpressed APTR and underexpressed ERα simultaneously, which inhibited the effect of APTR. Underexpressing APTR and ERα simultaneously also inhibited the effect.

UL is reported to be estrogen-dependent (29), and estrogen that was uptaken or exposed bound to the estrogen receptor by acting with an estrogen-like effect (4). Estrogen can overexpress ERα and upregulate IGF-1 expression (30) and the VEGF pathways (31). The ERα signaling pathway can crosstalk with the TGF-β signaling pathway and mediate estrogen to promote UL cell proliferation (32).

Variant estrogen receptors have also been reported, such as ERα36, which is located in the mitochondria in Ht-UtLM cells.

These receptors are associated with mitochondrial proteins and considered to be nongenomic signals with pivotal functions. Bisphenol A induced UL cell proliferation through ERα36 as a nongenomic signaling pathway (33).

ERβ was also found in UL. ERα expression was shown to be higher than that of ERβ (34). In our study, specimens were taken at the follicular phase, and ERβ had low expression in leiomyoma tumor tissues (**Supplemental Figure 1**). Furthermore, the effect on the UL cell proliferation was related to ERα.

Interestingly, in this study, the effect of APTR on UL cell proliferation was offset by ERα. Studies have reported that different APTR levels affect the cellular biological activity; for example, knocking down APTR inhibited TGF-β1-induced upregulation of α-SMA in hepatic stellate cells (15).

Aberrant activated Wnt/β-catenin was detected in this study. We also detected β-catenin activity in ER-positive UL patients, which verified the effect of APTR in the Wnt/β-catenin pathway. Knocking down ERα depleted this effect. We also found a new checkpoint for ERα. LncRNA APTR promotes UL cell proliferation by activating the Wnt/β-catenin pathway, and ERα was the target of the effect of APTR.

Current studies are done in primary cells from only one patient for one and the same experiment, to avoid patient-specific issues, results will be confirmed in more patients in the near future.

DATA AVAILABILITY STATEMENT

The original contributions presented in the study are publicly available. This data can be found here: [https://www.ncbi.nlm.nih.gov/geo/query/acc.cgi?acc=GSE168497/GSE168497].

ETHICS STATEMENT

The studies involving human participants were reviewed and approved by The Hospital's Protection of Human Subjects Committee. The patients/participants provided their written informed consent to participate in this study. The animal study and study protocols were reviewed and approved by The Hospital's Protection of Human Subjects Committee. Written informed consent was obtained from the individual(s) for the publication of any potentially identifiable images or data included in this article.

AUTHOR CONTRIBUTIONS

All authors contributed equally to this paper. All authors contributed to the article and approved the submitted version.

ACKNOWLEDGMENTS

This study was supported by the National Natural Science Foundation of China (81871126), the Foundation Project of Shanghai Municipal Commission of Health and Family Planning (201640248), and the Shanghai Pudong new area health and family planning commission (PW2018D-13). We thank Traci Raley, MS, ELS, from Liwen Bianji, Edanz Editing China (www.liwenbianji.cn/ac) for editing a draft of this manuscript.

SUPPLEMENTARY MATERIAL

The Supplementary Material for this article can be found online at: https://www.frontiersin.org/articles/10.3389/fonc.2021.536346/full#supplementary-material

Supplementary Figure 1 | IHC staining shows ERα and ERβ expressions in uterine leiomyoma tumor compared to adjacent normal uterine tissues. The expressions of ERα and ERβ in uterine leiomyoma tumor and adjacent normal uterine tissues. The scale bar is 100 μm.

REFERENCES

1. Salimi S, Khodamian M, Narooie-Nejad M, Hajizadeh A, Fazeli K, Namazi L, et al. Association of polymorphisms and haplotypes in the cytochrome P450 1B1 gene with uterine leiomyoma: A case control study. *BioMed Rep* (2015) 3:201–6. doi: 10.3892/br.2014.413
2. Falcone T, Walters MD. Hysterectomy for benign disease. *Obstet Gynecol* (2008) 111:753–67. doi: 10.1097/AOG.0b013e318165f18c
3. Sato S, Maekawa R, Yamagata Y, Tamural I, Lee L, Okada M, et al. Identification of uterine leiomyoma-specific marker genes based on DNA methylation and their clinical application. *Sci Rep* (2016) 6:30652. doi: 10.1038/srep30652
4. Ishikawa H, Ishi K, Sema VA, Kakazu R, Bulun SE, Kurita T. Progesterone is essential for maintenance and growth of uterine leiomyoma. *Endocrinology* (2010) 15:2433–42. doi: 10.1210/en.2009-1225
5. Chuffa LG, Seiva FR, Fávaro WJ, Amorim JP, Teixeira GR, Mendes LO, et al. Melatonin and ethanol intake exert opposite effects on circulating estradiol and progesterone and differentially regulate sex steroid receptors in the ovaries, oviducts, and uteri of adult rats. *Reprod Toxicol* (2013) 39:40–9. doi: 10.1016/j.reprotox.2013.04.001
6. Ellmanns S, Sticht H, Thiel F, Bechmann MW, Strick R, Strissel PL. Estrogen and progesterone receptors: from molecular structures to clinical targets. *Cell Mol Life Sci* (2009) 66:2405–26. doi: 10.1007/s00018-009-0017-3
7. Sakunrangsit N, Ketchart W. Plumbagin inhibits cancer stem-like cells, angiogenesis and suppresses cell proliferation and invasion by targeting Wnt/β-catenin pathway in endocrine resistant breast cancer. *Pharmacol Res* (2019) 3:104517. doi: 10.1016/j.phrs.2019.104517
8. Mohammed MK, Shao C, Wang J, Wei Q, Wang X, Collier Z, et al. Wnt/β-catenin signaling plays an ever-expanding role in stem cell self-renewal, tumorigenesis and cancer chemoresistance. *Genes Dis* (2016) 3:11–40. doi: 10.1016/j.gendis.2015.12.004
9. Farahani R, Rezaei-Lotfi S, Simonian M, Hunter N. Bi-modal reprogramming of cell cycle by MiRNA-4673 amplifies human neurogenic capacity. *Cell Cycle* (2019) 18:848–68. doi: 10.1080/15384101.2019.1595873
10. Lin X, Qiu J, Hua K. Long non-coding RNAs as emerging regulators of epithelial to mesenchymal transition in gynecologic cancers. *Biosci Trends* (2018) 12:342–53. doi: 10.5582/bst.2018.01181
11. Zhu M, Chen Q, Liu X, Sun Q, Zhao X, Deng R, et al. lncRNA H19/miR-675 axis represses prostate cancer metastasis by targeting TGFBI. *FEBS J* (2014) 281:3766–75. doi: 10.1111/febs.12902

12. Li Q, Shen F, Zhao L. The relationship between lncRNA PCGEM1 and STAT3 during the occurrence and development of endometrial carcinoma. *BioMed Pharmacother* (2018) 107:918–28. doi: 10.1016/j.biopha.2018.08.091
13. Negishi M, Wongpalee SP, Sarkar S, Park J, Lee KY, Shibata Y, et al. A new lncRNA, APTR, associates with and represses the CDKN1A/p21 promoter by recruiting polycomb proteins. *PloS One* (2014) 9:e95216. doi: 10.1371/journal.pone.0095216
14. Guan H, Shang G, Cui Y, Liu J, Sun X, Cao W, et al. Long noncoding RNA APTR contributes to osteosarcoma progression through repression of miR-132-3p and upregulation of yes -associatied protein 1. *J Cell Physiol* (2019) 234:8998–9007. doi: 10.1002/jcp.27572
15. Yu F, Zheng J, Mao Y, Dong P, Li G, Lu Z, et al. Long non-coding RNA APTR promotes the activation of hepatic stellate cells and the progression of liver fibrosis. *Biochem Biophys Res Commun* (2015) 463:679–85. doi: 10.1016/j.bbrc.2015.05.124
16. Zhang K, Li C, Liu J, Li Z, Ma C. Down-Regulation of APTR and it's Diagnostic Value in Papillary and Anaplastic Thyroid Cancer. *Pathol Oncol Res* (2018) 26(1):559–65. doi: 10.1007/s12253-018-0561-y
17. Lee SM, Choi ES, Ha E, Ji KY, Shin SJ, Jung J. Gyejibongnyeong Hwan (Gui Zhi Fu Ling Wan) Ameliorates Human Uterine Myomas via Apoptosis. *Front Pharmacol* (2019) 10:1105. doi: 10.3389/fphar.2019.01105
18. Zhang Y, Bao W, Wang K, Lu W, Wang H, Tong H, et al. SOX17 is a tumor suppressor in endometrial cancer. *Oncotarget* (2016) 7:76036–46. doi: 10.18632/oncotarget.12582
19. Gui D, Peng W, Jiang W, Huang G, Liu G, Ye Z, et al. Ubiquitin-specific peptidase 46 (USP46) suppresses renal cell carcinoma tumorigenesis through AKT pathway inactivation. *Biochem Biophys Res Commun* (2019) 19:689–96. doi: 10.1016/j.bbrc.2019.09.036
20. Zhang Y, Jiang F, Bao W, Zhang H, He X, Wang H, et al. SOX17 increases the cisplatin sensitivity of an endometrial cancer cell line. *Cancer Cell Int* (2016) 16:29. doi: 10.1186/s12935-016-0304-7
21. Gagliardi M, Matarazzo MR. RIP: RNA Immunoprecipitation. *Methods Mol Biol* (2016) 1480:73–86. doi: 10.1007/978-1-4939-6380-5_7
22. Khan S, Kaur R, Shah BA, Malik F, Kumar A, Bhushan S, et al. A Novel cyano derivative of 11-Keto-beta-boswellic acid causes apoptotic death by disrupting PI3K/AKT/Hsp-90 cascade, mitochondrial integrity, and other cell survival signaling events in HL-60 cells. *Mol Carcinog* (2012) 51:679–95. doi: 10.1002/mc.20821
23. Xu N, Shen C, Luo Y, Xia L, Xue F, Xia Q, et al. Upregulated miR-130a increases drug resistance by regulating RUNX3 and Wnt signaling in cisplatin-treated HCC cell. *Biochem Biophys Res Commun* (2012) 425:468–72. doi: 10.1016/j.bbrc.2012.07.127
24. Xiangsong WU, Wang F, Li H, Hu Y, Jiang L, Zhang F, et al. LncRNA-PAGBC acts as a microRNA spong and promotes gallbladder tumorigenesis. *EMBO Rep* (2017) 10):1837–53. doi: 10.15252/embr.201744147
25. Yu S, Qi Y, Jiang J, Wang H, Zhou Q. APTR is a prognostic marker in cirrhotic patients with portal hypertension during TIPS procedure. *Gene* (2018) 645:30–3. doi: 10.1016/j.gene.2017.12.040
26. Kopp F, Mendell JT. Functional Classification and Experimental Dissection of Long Noncoding RNAs. *Cell* (2018) 172:393–407. doi: 10.1016/j.cell.2018.01.011
27. Li W, Notani D, Rosenfeld MG. Enhancers as non-coding RNA transcription units: recent insights and future perspectives. *Nat Rev Genet* (2016) 17:207–23. doi: 10.1038/nrg.2016.4
28. Matsumoto A, Pasut A, Matsumoto M, Yamashita R, Fung J, Monteleone E, et al. mTORC1 and muscle regeneration are regulated by the LINC00961-encodedSPAR polypeptide. *Nature* (2017) 541:228–32. doi: 10.1038/nature21034
29. Islam MS, Protic O, Giannubilo SR, Toti P, Tranguilli AL, Petraglia F, et al. Uterine leiomyoma: available medical treatments and new possible therapeutic options. *J Clin Endocrinol Metab* (2013) 98:921–34. doi: 10.1210/jc.2012-3237
30. Shen Y, Ren ML, Feng X, Gao YX, Xu Q, Cai YL. Does nonylphenol promote the growth of uterine fibroids? *Eur J Obstet Gynecol Reprod Biol* (2014) 178:134–7. doi: 10.1016/j.ejogrb.2014.04.038
31. Shen Y, Ren ML, Feng X, Cai YL, Gao YX, Xu Q. An evidence in vitro for the influence of bisphenol A on uterine leiomyoma. *Eur J Obstet Gynecol Reprod Biol* (2014) 178:80–3. doi: 10.1016/j.ejogrb.2014.03.052
32. Shen Y, Lu Q, Zhang P, Wu Y, Ren M. The effect of TGF-β signaling on regulating proliferation of uterine leiomyoma cell via ERα signaling activated by bisphenol A, octylphenol and nonylphenol in vitro. *J Cancer Res Ther* (2018) 14(Supplement):S276–81. doi: 10.4103/0973-1482.235342
33. Yu L, Das P, Vall AJ, Yan Y, Gao X, Sifre MI, et al. Bisphenol A induces human uterine leiomyoma cell proliferation through membrane-associated ERα36 via nongenomic signaling pathways. *Mol Cell Endocrinol* (2019) 484:59–68. doi: 10.1016/j.mce.2019.01.001
34. Shao R, Fang L, Xing R, Xiong Y, Fang L, Wang Z. Differential expression of estrogen receptor α and β isoforms in multiple and solitary leiomyomas. *Biochem Biophys Res Commun* (2015) 458:136–42. doi: 10.1016/j.bbrc.2015.10.145

Conflict of Interests: The authors declare that the research was conducted in the absence of any commercial or financial relationships that could be construed as a potential conflict of interest.

frontiers in Oncology

CASE REPORT
published: 16 March 2021
doi: 10.3389/fonc.2021.564506

Case Report: Two Cases of Metastatic Pancreatoblastoma in Adults: Efficacy of Folfirinox and Implication of the Wnt/β-Catenin Pathway in Genomic Analysis

Jean-Luc Raoul[1], Sandrine Oziel-Taieb[2], Thierry Lecomte[3], José Adelaide[4], Arnaud Guille[4], Max Chaffanet[4], Flora Poizat[5], Marie-Françoise Heymann[6], Louise Barbier[7] and François Bertucci[2,4]*

[1] Department of Medical Oncology, Institut de Cancérologie de l'Ouest, Saint-Herblain, France, [2] Department of Medical Oncology, Institut Paoli-Calmettes, Marseille, France, [3] Department of Hepatogastroenterology, CHU Tours, Tours, France, [4] Predictive Oncology Laboratory, Centre de Recherche en Cancérologie de Marseille, Marseille, France, [5] Department of Pathology, Institut Paoli-Calmettes, Marseille, France, [6] Department of Pathology, Institut de Cancérologie de l'Ouest, Saint-Herblain, France, [7] Department of Digestive Surgery, CHU Tours, Tours, France

OPEN ACCESS

Edited by:
Giuseppe Giaccone, Cornell University, United States

Reviewed by:
Lorenzo Antonuzzo, University of Florence, Italy
Anup Kumar Singh, La Jolla Institute for Immunology (LJI), United States

***Correspondence:**
Jean-Luc Raoul
jean-luc.raoul@ico.unicancer.fr

Specialty section:
This article was submitted to Molecular and Cellular Oncology, a section of the journal Frontiers in Oncology

Received: *29 May 2020*
Accepted: *16 February 2021*
Published: *16 March 2021*

Citation:
Raoul J-L, Oziel-Taieb S, Lecomte T, Adelaide J, Guille A, Chaffanet M, Poizat F, Heymann M-F, Barbier L and Bertucci F (2021) Case Report: Two Cases of Metastatic Pancreatoblastoma in Adults: Efficacy of Folfirinox and Implication of the Wnt/β-Catenin Pathway in Genomic Analysis. Front. Oncol. 11:564506. doi: 10.3389/fonc.2021.564506

Pancreatoblastomas are unfrequent tumors usually found in children. We report two cases of metastatic pancreatoblastomas observed in young women. A systemic chemotherapy (FOLFIRINOX regimen) was associated with a disease control in one case and a partial response in the second with an improvement of general status for both. A high-throughput sequencing of the tumor described in both cases alteration in the Wnt/β-catenin pathway: a mutation in *CTNNB1* (exon 3, c.110C>G, p.S37C, reported as a hotspot in COSMIC) in one case and a homozygous loss associated with breakage targeting *APC* (5q22.2) in the second.

Keywords: pancreatoblastoma, adult, genomics, chemotherapy—oncology, Wnt/β-catenin

INTRODUCTION

Pancreatoblastoma is a very rare malignant tumor of the pancreas, usually found in children <10 year-old (1). Less than 50 cases in adults have been reported in the literature (2–4), and their main clinical features are unspecific. Most adult patients are young or very young. They can have pain, weight loss, abdominal mass, or jaundice. Liver metastases are reported in <30% of the cases despite a primary size at diagnosis usually over 10 cm. The diagnosis is based on histopathology. Surgery, including removal of metastases, is the best therapeutic option allowing cures. Efficacy of systemic chemotherapy, particularly platinum salts and doxorubicin, can be impressive in children (5). These tumors seem to be more aggressive in adults than in children, but less aggressive than classical pancreatic ductal adenocarcinoma. Here, we report on two cases of young women diagnosed with a metastatic pancreatoblastoma, successfully treated by a FOLFIRINOX regimen and with alteration of the Wnt/β-catenin pathway identified by high-throughput sequencing of the tumor.

CASE REPORT n°1

This 33-year-old woman, with no prior familial or personal medical history, presented in 2009 epigastric pain and a palpable left upper abdomen quadrant mass. The diagnosis of large pancreatic tumor invading the gastric wall leads to perform a radical R0 distal pancreatectomy. On histopathological examination, the diagnosis of pancreatoblastoma was done in front of an encapsulated mass, with epithelial components with acini, some tubular structures and squamoid corpuscles. No adjuvant treatment was delivered. The follow-up was uneventful until 2012, when three liver metastases were found. Resection and external beam irradiation (Cyberknife®) of metastases were then performed. Liver metastases recurred a few months later (two in the left lobe and a large one in the remnant right lobe) but progressed at a very slow pace and were only submitted to radiological monitoring until October 2019. Then, a clear progression was observed on the large metastasis (**Figure 1A**) of the right lobe and associated with weight loss and pain, and an increase of serum Alkaline Phosphatases (1.6 ULN); CEA was normal and CA19-9 slightly increased (56 U/mL, normal <39 U/mL), as well as AFP (20.8 ng/mL; N < 7 ng/mL). A systemic chemotherapy based on the classical FOLFIRINOX regimen (6) was proposed. Six cycles were delivered from October to December 2019. Tolerance was mild (grade 2 asthenia, and grade 2 nausea despite symptomatic treatments) and no clinical benefit was immediately noticed. Biologically, Alkaline Phosphatase and CA19-9 went back to normal values. On contrast-enhanced CT-scan, we observed a minor response for the main metastasis (from 120 to 95 mm; **Figure 1B**), and stabilization for the two other ones, thus defining a RECIST 1.1 stable disease. A follow-up was initiated. After 6 months of therapeutic holidays, her general status improved and was by far better than before chemotherapy; the CT-scan remained stable until in mid-December 2020.

In 2014, in order to find out possibilities for targeted therapy, immunohistochemistry (IHC) of the primary tumor searching for ALK, CMET, and ROS-1 was negative as well as the search for gene mutations in *ALK* exons 23, 24, and 25, *MET* exons 14, 16, 17, and 18, and *BRAF* exon 15. On pathological exam, tumor cells displayed a strong cytoplasmic and nuclear staining for β-catenin by IHC. In 2019, after obtaining written informed consent from the patient, a NGS analysis (FOUNDATION ONE® CDx) from DNA extracted from one of the resected liver metastases was performed before initiating chemotherapy. The tumor was classified as MicroSatellite Stable (MSS), the Tumor Mutational Burden (TMB) was low (1 mutation/Mb), and only two somatic gene mutations were retained: *CTNNB1* (exon 3 c.110C>G, p.S37C; **Figure 1C**) and *NSD3* /*WHSC1L1* (NM 017778.2 exon 1c.121G>A, pA41T); these two mutations are hotspot mutations reported in COSMIC database (respectively COSM5679 and COSM750462). Some variants of unknown significance were also noted: *DIS3* (P666L), *DOT1L* (G724S and R544K), *FGF19* (S147T), *KDR* (R541G), *MYCL1* (S26R), *PTEN* (S294R), and *SPEN* (D1701E). No other base substitution, insertion/deletion, gene fusion, and copy number alteration was observed.

CASE REPORT n°2

A 33-year-old woman, with no familial medical history, presented on summer 2019, polyarthralgia and epigastric discomfort with no deterioration of clinical status. A cholecystectomy had been performed in April 2019 for gallbladder stones without any hepatic ultrasound abnormality. A CT-scan, performed as part of the assessment of a possible rheumatismal disease, showed a pancreatic tail tumor associated with multiple liver metastases confirmed by an abdominal MRI (**Figure 2A**). No thoracic lesion was found. Pathological examination of pancreatic and liver EUS-guided biopsies revealed a very heterogeneous tumor cell population with small cells associated with epithelioid cells; tumor cells displayed a strong cytoplasmic and nuclear staining for β-catenin by IHC. The retained diagnosis was pancreatoblastoma. Pancreatic lesion and liver metastases were hypermetabolic on ^{18}FDG-PET. The serum levels of CEA, CA19-9, Chromogranin A, AFP, and lipasemia were normal. Only NSE was slightly increased (36.2 μg/l, normal <16.3 μg/l) as well as γ-GT (6xN). Four cycles of FOLFIRINOX regimen were delivered from February to April 2020. As side effects the patient presented an asthenia (grade 2) and a thrombopenia (grade 3 then 2), requiring dose reduction and delays. CT-scan and hepatic MRI performed after the fourth cycle showed a RECIST 1.1 partial response with a decrease of the maximal diameter of the pancreatic lesion from 44 to 23 mm and a decrease in number and size of all hepatic lesions that became infracentimetric (**Figure 2B**). Four additionally cycles of FOLFIRINOX were proposed, followed by capecitabine only. After three cycles of capecitabine a progression was seen on the CT-scan and FOLFIRINOX was resumed, beginning mid December 2020. No genetic counceling was proposed.

The signed informed consent from the patient was obtained for genomic profiling. DNA extracted from the biopsied primary tumor (and normal blood) was submitted to NGS analysis (institutional Impact V1 panel including 754 genes) and array-CGH (Agilent 4x180k) as previously described (7). The lesion was classified as MSS, and the TMB was low (<1 mutation/Mb). No gene fusion was identified. A deletion associated with a breakage targeting *APC* (5q22.2: **Figure 3**) was observed. We also found a heterozygous loss of the 9p21 region including *CDKN2A* and the 13q14.2 region including *RB1*, and a focal amplification in the 6p22 region including many histones genes. No pathogenic somatic mutation was identified.

DISCUSSION

Pancreatoblastoma is a very rare tumor, typically found in young children and originating from fetal pancreatic stem cells. Some cases are associated with genetic syndromes (8), such as the Beckwith-Wiedermann syndrome (mainly caused by genetic or epigenetic defects within the chromosome 11p15.5 region, containing genes like *IGF2* and *CDKN1C*) (9), and Familial Adenomatous Polyposis (*APC* gene) (10). At diagnosis, the median patients' age is 5 years and <20% had metastases, most often hepatic. In adults, the clinical presentation is usually in

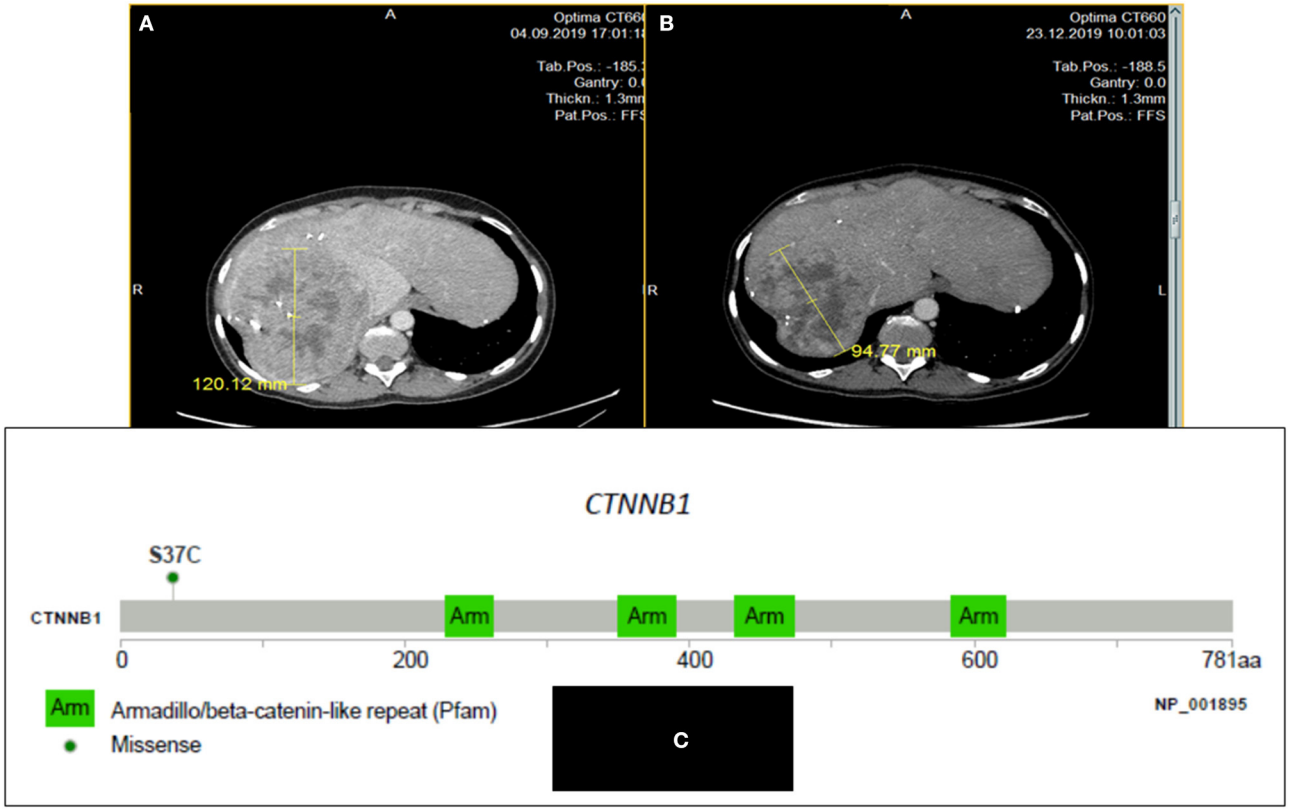

FIGURE 1 | CT scan images of the large liver metastasis of a pancreatoblastoma (patient # 1) in a 33 year-old woman: before **(A)** and after six cycles **(B)** of FOLFIRINOX regimen: minor response; **(C)**: Lolliplot of CTNNB1 gene showing the S37C mutation in exon 3.

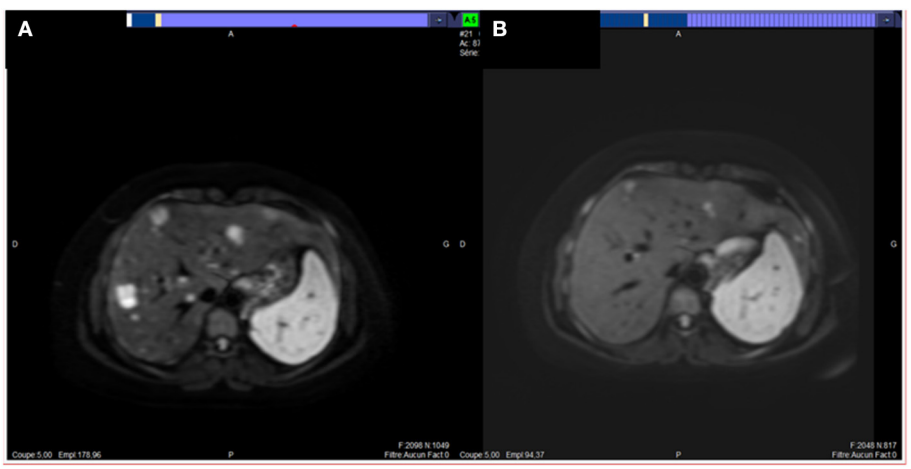

FIGURE 2 | MRI images of liver metastases of our second case of pancreatoblastoma (patient # 2) before **(A)** and after four cycles **(B)** of FOLFIRINOX regimen: partial response.

line with a large pancreatic malignant mass in a young adult with abdominal pain, jaundice, weight loss, and liver nodules. On imaging, these tumors are large, located in the pancreas head in 50% of cases, and have a mixed solid and cystic pattern; imaging can also show some aggressive patterns like invasion of adjacent structure or metastases at diagnosis. Pathologically, these tumors are considered as part of the "pancreatic carcinomas with acinar differentiation," with acinar cell carcinomas and carcinomas of mixed differentiation (11). Squamoid nests are the key morphologic feature of pancreatoblastoma; a neuroendocrine

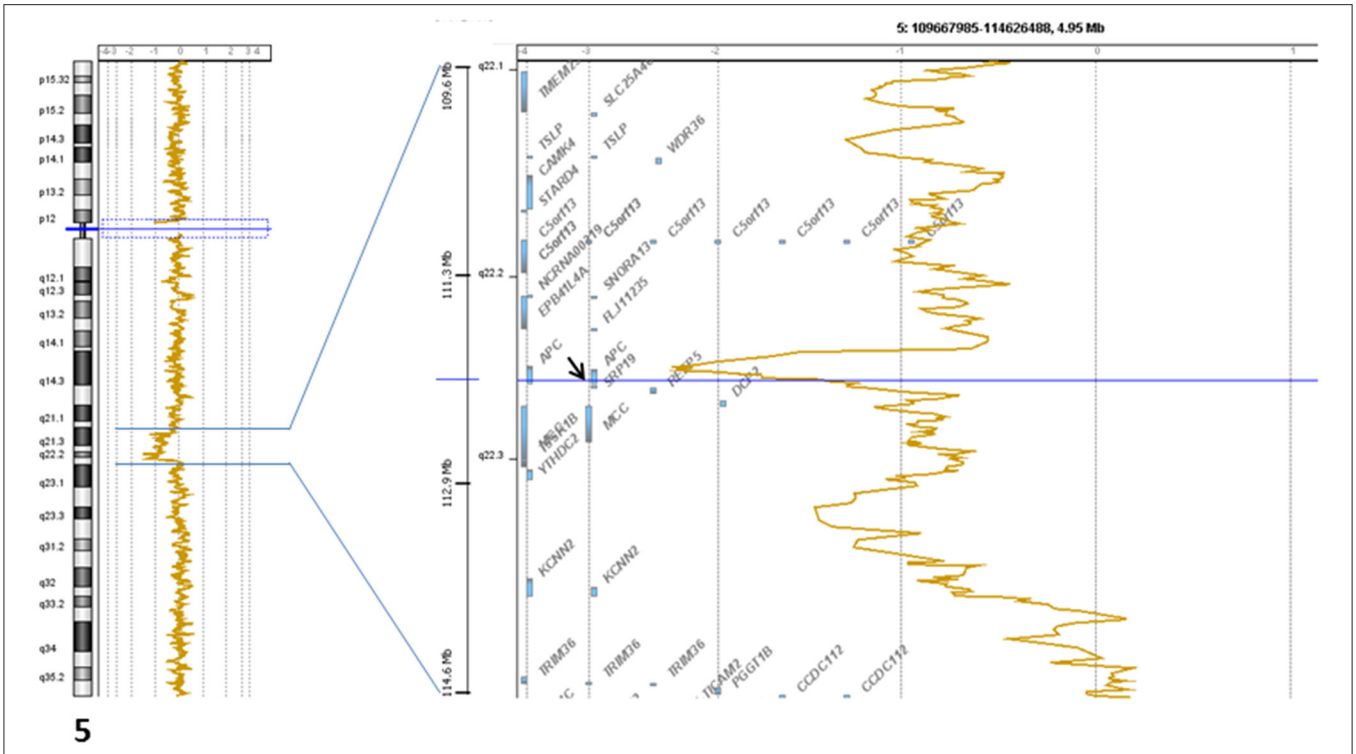

FIGURE 3 | Genomic profile of the 5q22.2 chromosomal region showing the breakage in *APC* gene.

component is frequently found (12). On IHC, a very distinctive feature is the abnormal nuclear and cytoplasmic localization of β-catenin, usually restricted to the squamoid nests (12).

Surgery of the primary tumor but also of the liver metastases is the first therapeutic option, but recurrences are frequent, and second surgery can be performed. When surgery is not possible, some chemotherapy regimens have been proposed. In our two patients, the FOLFIRINOX regimen, gold standard in pancreatic adenocarcinomas, allowed some improvement after respectively 6 and 4 cycles, with significant decrease in tumor size and improvement in the patients' performance status. As cases are scarce only a few reports with new systemic chemotherapy regimen has been published, but similar response has been reported in one case in the literature (4). The prognosis of pancreatoblastoma is better than that of other pancreatic malignancies with a median overall survival of 48 months. The main prognostic factors are metastases, surgical resectability and age (1). The development of effective systemic therapies is crucial, but the molecular pathogenesis of this rare disease remains poorly known.

During the last years, several studies aimed at defining the molecular landscape of pancreatoblastoma were performed, allowing to improve our knowledge. Clearly, pancreatoblastoma, like other pancreatic carcinomas with acinar differentiation and other rare malignant pancreatic tumors, has a molecular profile different of pancreatic ductal adenocarcinoma, and display frequent alterations of genes involved in the Wnt/β-catenin pathway, notably *CTNNB1* exon 3 mutations. Such mutations are rare in cancers other than liver, uterine, and adrenocortical carcinomas (13). Among a series of 328 pancreatic tumors, only 12 (3.7%) had *CTNNB1* exon 3 mutation, including eight solid pseudopapillary neoplasms, two pancreatic adenocarcinomas, and two pancreatoblastomas (cBioPortal database). In the pancreatic ductal adenocarcinoma, gene alterations are quite different: the most frequent ones concern *KRAS* (95% of the cases), *CDKN2A* (>90%), *TP53* (75%), and *SMAD4* (55%) (14), while *CTNNB1* mutations are very rare (1%) and only found in *KRAS* wild-type tumors (15).

The rare data reported in pancreatoblastoma, suggest similar and important role of the Wnt signaling pathway. On 2001, Abraham et al. (10) reported a series of nine cases, including seven pediatric cases and two adult cases: a nuclear accumulation of β-catenin was observed in 7/9 cases and a molecular alteration of *APC*/β-catenin pathway was observed in 6/9 cases (five activating *CTNNB1* exon 3 mutations and one biallelic *APC* inactivation). On 2003, Tanaka et al. reported a series of seven pediatric cases (16): a nuclear accumulation of β-catenin was observed in all cases and an activating *CTNNB1* mutation (exon 3) was found in 2/5 cases tested. On 2012, one case of congenital pancreatoblastoma in a 3-day-old child was reported with nuclear/cytoplasmic accumulation of β-catenin and an activating *CTNNB1* mutation in exon 3 (17). An integrated molecular analysis of 10 pediatric patients (median age of 3 years) revealed a very high frequency of

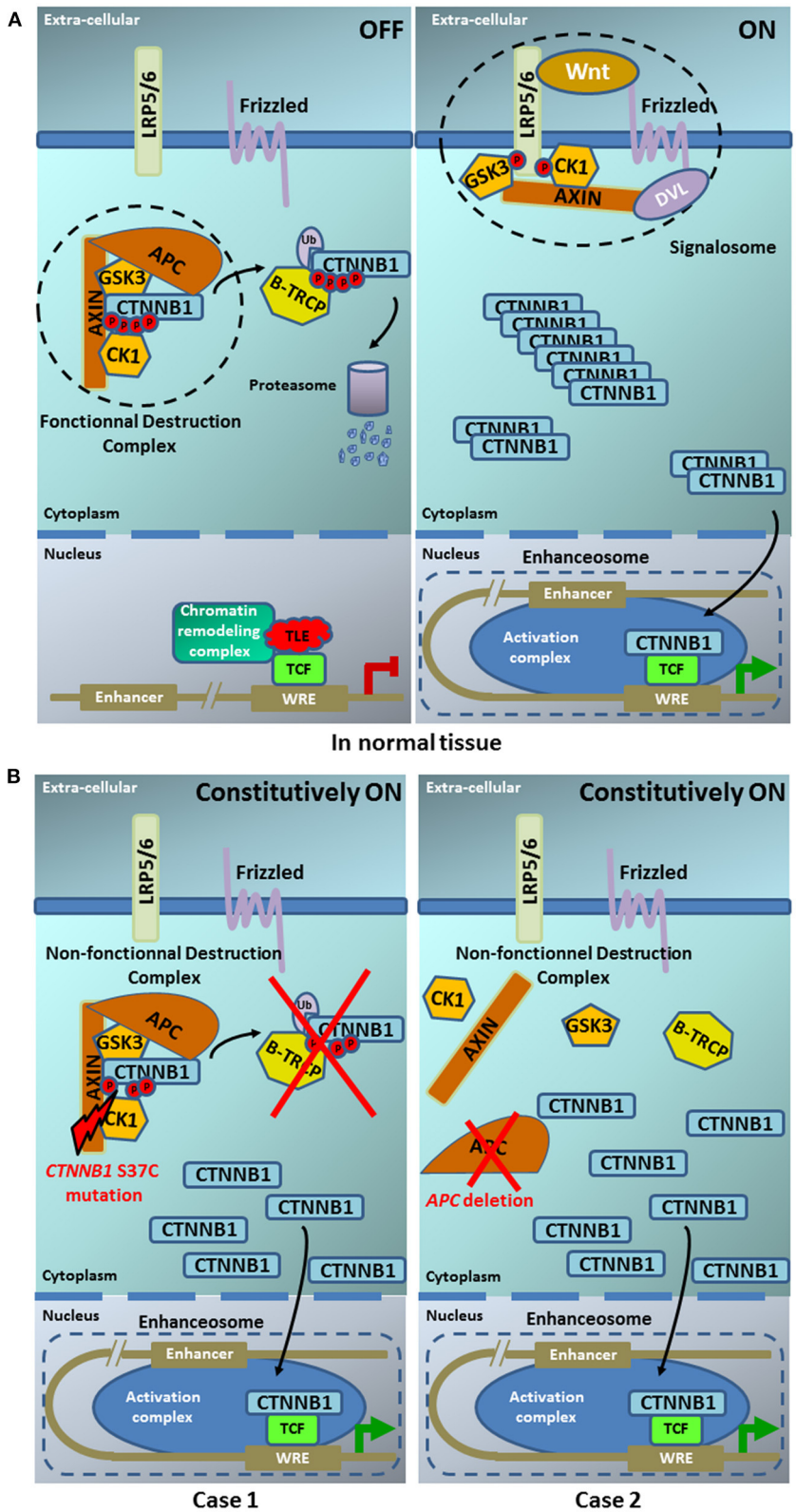

FIGURE 4 | Model of the Wnt pathway in normal tissue **(A)** and in our two pancreoblastoma cases **(B)**. **(A)** In normal tissue— (left part) In the absence of Wnt ligand, the β-catenin destruction complex maintains low cytoplasmic levels of β-catenin. In the destruction complex, β-catenin is phosphorylated at sites S33/S37 and T41/S45 by casein kinase 1 (CK1) and glycogen synthase kinase 3 (GSK3), respectively. Phosphorylated β-catenin is recognized by the β-Transducin Repeat

(Continued)

FIGURE 4 | Containing E3 Ubiquitin Protein Ligase (β-TRCP), which catalyzes its polyubiquitylation. Polyubiquitylated β-catenin, in turn, is degraded by the proteasome. (right part) In the presence of Wnt ligand, the signalosome is assembled and the β-catenin degradation is disrupted, leading to cytoplasmic accumulation. Entry of β-catenin into the nucleus promotes the formation of the enhanceosome to drive the transcription of Wnt target genes [Illustration adapted from Anthony et al. (19)]. **(B)** In our two pancreoblastoma cases. (left part) The CTNNB1 S37C mutation present in case 1 does not allow the β-catenin phosphorylation by CK1this site. (right part) The APC deletion in case 2 does not allow the building of β-catenin destruction complex. Both alterations, CTNNB1 S37C mutation and APC deletion, prevent the β-catenin interaction with E3 ubiquitine ligase and its degradation by the proteasome. The β-catenin accumulation in the cytoplasm leads to its constitutive translocation into the nucleus promoting the formation of the enhanceosome where its binding with TCF results in the constitutive activation of the Wnt signaling pathway.

activation of the Wnt signaling pathway, either *via* somatic mutations of *CTNNB1* (90%) or copy-neutral loss of heterozygoty of *APC* (10%), with concurrent imprinting dysregulation of IGF2 (8). Here too, all *CTNNB1* mutations were observed in exon 3.

On 2018, a somatic heterozygous missense mutation in *APC*, associated with the same heterozygous germline mutation, was reported in a 37-year-old woman with pancreatoblastoma (18). Functional analysis suggested this mutant *APC* attenuated repression of Wnt/β-catenin signaling activity, and was likely involved in the onset of disease. More recently, in a German series of four adult patients with metastatic disease (4), two (out of the three who had whole exome sequencing) had *CTNNB1* exon 3 mutations. Thus, out of the 23 pediatric samples sequenced through six studies, 16 displayed an activating *CTNNB1* mutation in exon 3 and one an inactivating *APC* alteration. Out of the eight adult samples sequenced through these six studies and our two present new cases, four displayed an activating *CTNNB1* mutation in exon 3 and three an inactivating *APC* alteration. Of note, in all cases, *APC* and *CTNNB1* alterations were mutually exclusive, and were associated, when analyzed, with nuclear accumulation of β-catenin.

Activation of the Wnt/β-catenin pathway participates to the tumorigenesis of many organs by regulating the expression of genes involved, for example, in proliferation, cell survival or adhesion. The proteins coded by *CTNNB1* and *APC* are crucial effectors of Wnt signaling. Several alterations in the pathway can cause ligand-independent β-catenin stabilization, which thus contributes to oncogenic β-catenin-regulated transcriptional activity. Many regulators have been identified which control the β-catenin subcellular location, nuclear abundance or transcriptional activity. **Figure 4** displays the Wnt/β-catenin pathway in normal tissues (**Figure 4A**) and in our two cases (**Figure 4B**). *CTNNB1* exon 3 mutations lead to alterations in the spatial characteristics of the β-catenin protein, decreasing its degradation, and resulting in accumulation in the nucleus (20). Such aberrant nuclear accumulation of β-catenin, hallmark of Wnt/β-catenin activation, is detectable by IHC (16), as observed in our case 1 and the literature. *APC* regulates the turnover of cytosolic β-catenin and is the key effector of the canonical Wnt pathway. Its loss-of-function, either by mutation or by deletion as in our case, reduces the ability to bind to β-catenin, decreasing its degradation, and resulting in accumulation in the nucleus, as observed in our case 2 and the literature. We did not analyse the transcriptional consequences of Wnt pathway activation in our two patients. But, Japanese authors [8] have shown in their pediatric cases that such *CTNNB1* or *APC* mutations resulted in Wnt/β-catenin activation and transcriptional consequences with an expression profile characteristic of early pancreas progenitor-like cells along with upregulation of the R-spondin/LGR5/RNF43 module, as well as overexpression of negative-feedback regulators of Wnt pathway (such as *NOTUM* and *NKD1*) and Wnt pathway effectors (such as *LEF1* and *TCF7*). Of note, the authors identified a concurrent imprinting dysregulation of IGF2, as already reported, although at lower frequency in other pediatric tumors like hepatoblasoma (21) and Wilm's tumor (22); such Wnt/IGF2 coactivation defines a consensus molecular subtype of colorectal cancer, characterized by intestinal stem cell–like phenotype and enriched LGR5 signature (23).

Today no targeted therapy has been clearly demonstrated as efficient for tumors with *CTNNB1* mutation, although everolimus plus letrozole (24) and cabozantinib (25) showed some efficacy in patients with endometrial carcinoma. The German series also reported molecular alterations in FGFR signaling in three out of four patients, leading to the delivery of nindetanib, a tyrosine kinase inhibitor targeting FGFRs 1-3. However, the treatment therapy was stopped after 4 weeks because of clinical deterioration (4). No FGFR alteration was observed in our cases. Clearly, the frequent alteration of the Wnt/β-catenin pathway in the reported cases suggests a role and thus a potential therapeutic interest of targeting this pathway. Clearly functional analyses on pre-clinical models are warranted to confirm such role and the interest for targeting the Wnt/β-catenin pathway. Over the past decades, a number of Wnt inhibitors have been identified, but none of them resulted in inhibition of Wnt signaling *via* direct β-catenin targeting. These disappointing observations, associated with the fact that β-catenin is a transcription factor, raised questions regarding its druggability (26). However, several strategies are ongoing to facilitate the development of new therapeutic agents against β -catenin (26, 27).

In conclusion, we report the clinical outcome and molecular profile of two additional cases of sporadic metastatic pancreatoblastoma in young adults. Both patients benefited from systemic FOLFIRINOX regimen that provided a long-lasting minor response in one case and an ongoing partial response in the second one. Exome sequencing showed a *CTNNB1* mutation (exon 3) in the first case and a deletion involving *APC* in the second case, likely responsible for activation of Wnt/β-catenin signaling pathway. These alterations are frequent in pediatric and adult cases, and can help to

differentiate acinar cell carcinomas, solid-pseudopapillary neoplasms and pancreatoblastoma from pancreatic ductal adenocarcinoma. Unfortunately, until now, no therapy targeting such alterations is available. Molecular analysis of larger series is warranted.

DATA AVAILABILITY STATEMENT

The original contributions presented in the study are included in the article/supplementary material, further inquiries can be directed to the corresponding author/s.

ETHICS STATEMENT

Written informed consent was obtained from the individual(s) for the publication of any potentially identifiable images or data included in this article.

AUTHOR CONTRIBUTIONS

J-LR, SO-T, and FB: writing of the manuscript. J-LR, SO-T, TL, and LB: cares of the patients. FP and M-FH: pathology. FB, JA, AG, and MC: genomics analysis. All authors: corrections, modifications, and final acceptation.

REFERENCES

1. Dhebri AR, Connor S, Campbell F, Ghaneh P, Sutton R, Neoptolemos JP. Diagnosis, treatment and outcome of pancreatoblastoma. *Pancreatology*. (2004) 4:441–51. doi: 10.1159/000079823
2. Cavallini A, Falconi M, Bortesi L, Crippa S, Barugola G, Butturini G. Pancreatoblastoma in adults: a review of the literature. *Pancreatology*. (2009) 9:73–80. doi: 10.1159/000178877
3. Omiyale AO. Clinicopathological review of pancreatoblastoma in adults. *Gland Surg*. (2015) 4:322–8. doi: 10.3978/j.issn.2227-684X.2015.04.05
4. Berger AK, Mughal SS, Allgauer M, Springfeld C, Hackert T, Weber TF, et al. Metastatic adult pancreatoblastoma: multimodal treatment and molecular characterization of a very rare disease. *Pancreatology*. (2020) 20:425–32. doi: 10.1016/j.pan.2020.02.017
5. Bien E, Godzinski J, Dall'igna P, Defachelles AS, Stachowicz-Stencel T, Orbach D, et al. Pancreatoblastoma: a report from the European cooperative study group for paediatric rare tumours (EXPeRT). *Eur J Cancer*. (2011) 47:2347–52. doi: 10.1016/j.ejca.2011.05.022
6. Conroy T, Desseigne F, Ychou M, Bouche O, Guimbaud R, Becouarn Y, et al. FOLFIRINOX versus gemcitabine for metastatic pancreatic cancer. *N Engl J Med*. (2011) 364:1817–25. doi: 10.1056/NEJMoa1011923
7. Bertucci F, Finetti P, Guille A, Adelaide J, Garnier S, Carbuccia N, et al. Comparative genomic analysis of primary tumors and metastases in breast cancer. *Oncotarget*. (2016) 7:27208–19. doi: 10.18632/oncotarget.8349
8. Isobe T, Seki M, Yoshida K, Sekiguchi M, Shiozawa Y, Shiraishi Y, et al. Integrated molecular characterization of the lethal pediatric cancer pancreatoblastoma. *Cancer Res*. (2018) 78:865–76. doi: 10.1158/0008-5472.CAN-17-2581
9. Brioude F, Kalish JM, Mussa A, Foster AC, Bliek J, Ferrero GB, et al. Expert consensus document: clinical and molecular diagnosis, screening and management of Beckwith-Wiedemann syndrome: an international consensus statement. *Nat Rev Endocrinol*. (2018) 14:229–49. doi: 10.1038/nrendo.2017.166
10. Abraham SC, Wu TT, Klimstra DS, Finn LS, Lee JH, Yeo CJ, et al. Distinctive molecular genetic alterations in sporadic and familial adenomatous polyposis-associated pancreatoblastomas : frequent alterations in the APC/beta-catenin pathway and chromosome 11p. *Am J Pathol*. (2001) 159:1619–27. doi: 10.1016/S0002-9440(10)63008-8
11. Al-Hader A, Al-Rohil RN, Han H, Von Hoff D. Pancreatic acinar cell carcinoma: a review on molecular profiling of patient tumors. *World J Gastroenterol*. (2017) 23:7945–51. doi: 10.3748/wjg.v23.i45.7945
12. Thompson ED, Wood LD. Pancreatic neoplasms with acinar differentiation: a review of pathologic and molecular features. *Arch Pathol Lab Med*. (2019). doi: 10.5858/arpa.2019-0472-RA. [Epub ahead of print].
13. Selenica P, Raj N, Kumar R, Brown DN, Arques O, Reidy D, et al. Solid pseudopapillary neoplasms of the pancreas are dependent on the Wnt pathway. *Mol Oncol*. (2019) 13:1684–92. doi: 10.1002/1878-0261.12490
14. Iacobuzio-Donahue CA, Velculescu VE, Wolfgang CL, Hruban RH. Genetic basis of pancreas cancer development and progression: insights from whole-exome and whole-genome sequencing. *Clin Cancer Res*. (2012) 18:4257–65. doi: 10.1158/1078-0432.CCR-12-0315
15. Cancer Genome Atlas Research Network. Electronic address aadhe, Cancer Genome Atlas Research N. Integrated genomic characterization of pancreatic ductal adenocarcinoma. *Cancer Cell*. (2017) 32:185–203 e13. doi: 10.1016/j.ccell.2017.07.007
16. Tanaka Y, Kato K, Notohara K, Nakatani Y, Miyake T, Ijiri R, et al. Significance of aberrant (cytoplasmic/nuclear) expression of beta-catenin in pancreatoblastoma. *J Pathol*. (2003) 199:185–90. doi: 10.1002/path.1262
17. Ismael O, Shimada A, Hama A, Takahashi Y, Sato Y, Hayakawa M, et al. Congenital pancreatoblastoma associated with beta-catenin mutation. *Pediatr Blood Cancer*. (2012) 58:827. doi: 10.1002/pbc.23337
18. Yamaguchi S, Fujii T, Izumi Y, Fukumura Y, Han M, Yamaguchi H, et al. Identification and characterization of a novel adenomatous polyposis coli mutation in adult pancreatoblastoma. *Oncotarget*. (2018) 9:10818–27. doi: 10.18632/oncotarget.24017
19. Anthony CC, Robbins DJ, Ahmed Y, Lee E. Nuclear regulation of Wnt/beta-catenin signaling: it's a complex situation. *Genes*. (2020) 11:80886. doi: 10.3390/genes11080886
20. Gao C, Wang Y, Broaddus R, Sun L, Xue F, Zhang W. Exon 3 mutations of CTNNB1 drive tumorigenesis: a review. *Oncotarget*. (2018) 9:5492–508. doi: 10.18632/oncotarget.23695
21. Honda S, Arai Y, Haruta M, Sasaki F, Ohira M, Yamaoka H, et al. Loss of imprinting of IGF2 correlates with hypermethylation of the H19 differentially methylated region in hepatoblastoma. *Br J Cancer*. (2008) 99:1891–9. doi: 10.1038/sj.bjc.6604754
22. Gadd S, Huff V, Huang CC, Ruteshouser EC, Dome JS, Grundy PE, et al. Clinically relevant subsets identified by gene expression patterns support a revised ontogenic model of Wilms tumor: a Children's Oncology Group Study. *Neoplasia*. (2012) 14:742–56. doi: 10.1593/neo.12714
23. Guinney J, Dienstmann R, Wang X, de Reynies A, Schlicker A, Soneson C, et al. The consensus molecular subtypes of colorectal cancer. *Nat Med*. (2015) 21:1350–6. doi: 10.1038/nm.3967
24. Slomovitz BM, Jiang Y, Yates MS, Soliman PT, Johnston T, Nowakowski M, et al. Phase II study of everolimus and letrozole in patients with recurrent endometrial carcinoma. *J Clin Oncol*. (2015) 33:930–6. doi: 10.1200/JCO.2014.58.3401
25. Dhani NC, Hirte HW, Wang L, Burnier JV, Jain A, Butler MO, et al. Phase II trial of cabozantinib in recurrent/metastatic endometrial cancer: a study of the Princess Margaret, Chicago and California Consortia (NCI9322/PHL86). *Clin Cancer Res*. (2020) 26:2477–86. doi: 10.1158/1078-0432.CCR-19-2576
26. Cui C, Zhou X, Zhang W, Qu Y, Ke X. Is beta-catenin a druggable target for cancer therapy? *Trends Biochem Sci*. (2018) 43:623–34. doi: 10.1016/j.tibs.2018.06.003

27. Grothey A, Sobrero AF, Shields AF, Yoshino T, Paul J, Taieb J, et al. Duration of adjuvant chemotherapy for stage III colon cancer. *N Engl J Med*. (2018) 378:1177–88. doi: 10.1056/NEJMoa1713709

Conflict of Interest: The authors declare that the research was conducted in the absence of any commercial or financial relationships that could be construed as a potential conflict of interest.

frontiers in Oncology

MINI REVIEW
published: 01 April 2021
doi: 10.3389/fonc.2021.642719

Could We Address the Interplay Between CD133, Wnt/β-Catenin, and TERT Signaling Pathways as a Potential Target for Glioblastoma Therapy?

Amir Barzegar Behrooz[1] *and Amir Syahir*[1,2]*

[1] Department of Biochemistry, Faculty of Biotechnology and Biomolecular Science, Universiti Putra Malaysia, Serdang, Malaysia, [2] MAKNA Cancer Research Laboratory, Institute of Bioscience, Universiti Putra Malaysia, Serdang, Malaysia

Glioblastoma multiforme (GBM) is one of the most lethal forms of primary brain tumors. Glioblastoma stem cells (GSCs) play an undeniable role in tumor development by activating multiple signaling pathways such as Wnt/β-catenin and PI3K/AKT/mTOR that facilitate brain tumor formation. CD133, a transmembrane glycoprotein, has been used to classify cancer stem cells (CSCs) in GBM. The therapeutic value of CD133 is a biomarker of the CSC in multiple cancers. It also leads to growth and recurrence of the tumor. More recent findings have confirmed the association of telomerase/TERT with Wnt/β-catenin and the PI3K/AKT/mTOR signaling pathways. Advance studies have shown that crosstalk between CD133, Wnt/β-catenin, and telomerase/TERT can facilitate GBM stemness and lead to therapeutic resistance. Mechanistic insight into signaling mechanisms downstream of surface biomarkers has been revolutionized by facilitating targeting of tumor-specific molecular deregulation. This review also addresses the importance of interplay between CD133, Wnt/β-catenin and TERT signaling pathways in GSCs and outlines the future therapeutic goals for glioblastoma treatment.

Keywords: glioblastoma stem cells, CD133, Wnt/β-catenin, PI3K/AKT/mTOR, telomerase

OPEN ACCESS

Edited by:
Maja Cemazar, Institute of Oncology Ljubljana, Slovenia

Reviewed by:
Barbara Breznik, National Institute of Biology (NIB), Slovenia
Anup Kumar Singh, La Jolla Institute for Immunology (LJI), United States

***Correspondence:**
Amir Syahir
amirsyahir@upm.edu.my

Specialty section:
This article was submitted to Molecular and Cellular Oncology, a section of the journal Frontiers in Oncology

Received: *16 December 2020*
Accepted: *15 March 2021*
Published: *01 April 2021*

Citation:
Behrooz AB and Syahir A (2021) Could We Address the Interplay Between CD133, Wnt/β-Catenin, and TERT Signaling Pathways as a Potential Target for Glioblastoma Therapy? Front. Oncol. 11:642719. doi: 10.3389/fonc.2021.642719

BACKGROUND

Glioblastoma multiform (GBM) is one of the calamitous kinds of aggressive primary glial brain tumor in adults, with a median overall survival between 10 to 20 months. Intriguingly, the recent study has demonstrated that outer radial glia-like cancer stem cells could impart to heterogenicity of GBM (1). The striking cellular-heterogeneity is one of the prominent hallmarks of GBM, and glioblastoma stem cells (GSCs) are placed at the apex of it (2). GSCs have been indicated to be involved in imperative processes of tumor growth, disseminated-metastases, chemo- and radio-therapy resistance and GBM relapse (3).

GSCs have been identified by many biomarkers of CSCs. CD133, also known as prominin-1, has been used as an essential marker for the detection of GSCs. Additionally, CD133 has been shown to be associated with GBM development, recurrence, and poor overall survival (4). Emerging

observations have suggested that CD133 could act as a novel receptor for PI3K/AKT/mTOR pathway (5). Further, CD133-Wnt/β-catenin axis was gained attention in GBM as a stemness regulatory pathway and lead to resistance to chemo- and radio-therapies (6). Accumulating data have indicated that AKT might activate Wnt/β-catenin pathway (7, 8). Furthermore, the results of studies have confirmed the interaction of telomerase/TERT with PI3K/AKT/mTOR and Wnt/β-catenin in various cancers which predominately participating in tumor invasion and metastasis and epithelial to mesenchymal transition (EMT) (9).

Each component of the CD133, Wnt/β-catenin, and TERT signaling pathways play a crucial role in the normal brain. CD133 is present in epithelial cells throughout the body, including the mammary gland, testis, digestive tract, trachea, and placenta, and is expressed in stem cells. CD133 is also present in non-epithelial cells, such as rod photoreceptor cells, and in many cancers (10). The Wnt/β-catenin signaling has a pivotal role in neural development. The underlying neural scaffolding that makes the diverse cognitive functions of the cerebral cortex is generated by a set of basic developmental processes. Production and differentiation of the immense diversity of nervous system cells entail a range of main activities, ranging from regional progenitor specification, separation and expansion of neural precursor populations, neuron generation, movement of young neurons to suitable locations, the evolution of neuronal processes, and the forming of complex synaptic connections (11). For both physiological processes and the transformation of human cells by stabilizing telomere length, TERT activation is necessary. TERT's telomere lengthening-independent roles contribute significantly to both physiological processes and cancer initiation or progression, including its effects on mitochondrial, ubiquitin-proteasomal (UPS) structures, gene transcription, expression of microRNA (miRNA), repair of DNA damage, and operation of RNA-dependent RNA polymerase (RdRP) (12).

The current review focuses on the significance of interplaying between CD133, Wnt/β-catenin and TERT signaling pathways in normal brain and GSCs. From a therapeutic perspective, targeting the interaction between CD133, Wnt/β-catenin and TERT will lead to the development of novel anti-cancer strategies and it would be important to examine if all these three signaling cascades can be inhibited concurrently by targeting CD133, thus killing many birds with one stone (**Figure 1**).

GENERAL OUTLINE OF CD133 ROLES IN GSCS AND NORMAL CELLS

A great deal of work has been made to classify CSCs in glioblastoma using the expression of unique surface biomarkers. Human CD133 (prominin-1), a 5-transmembrance glycoprotein, is one of these biomarkers and also commonly used in identification and isolation of GSCs (13, 14). Highly expressed CD133 indicates poor outcomes among cancer patients with colorectal cancer, rectal cancer, breast cancer, lung cancer, prostate cancer, and glioblastoma (15, 16). Whilst the primary role remains uncertain, it has been presumed that CD133 could be involved in signal transduction (10). CD133 is a CSCs surface marker and has been believed to have a prognostic (17, 18) and therapeutic qualities in GSCs (15). Evidence reveals that, CD133-targeted therapy of gastric, hepatocellular carcinoma (19), and glioblastoma (20) has greatly diminished cell proliferation and tumor growth within both *in vitro* and *in vivo* $CD133^{POS}$-marker cells. Furthermore, a study showed that CD133

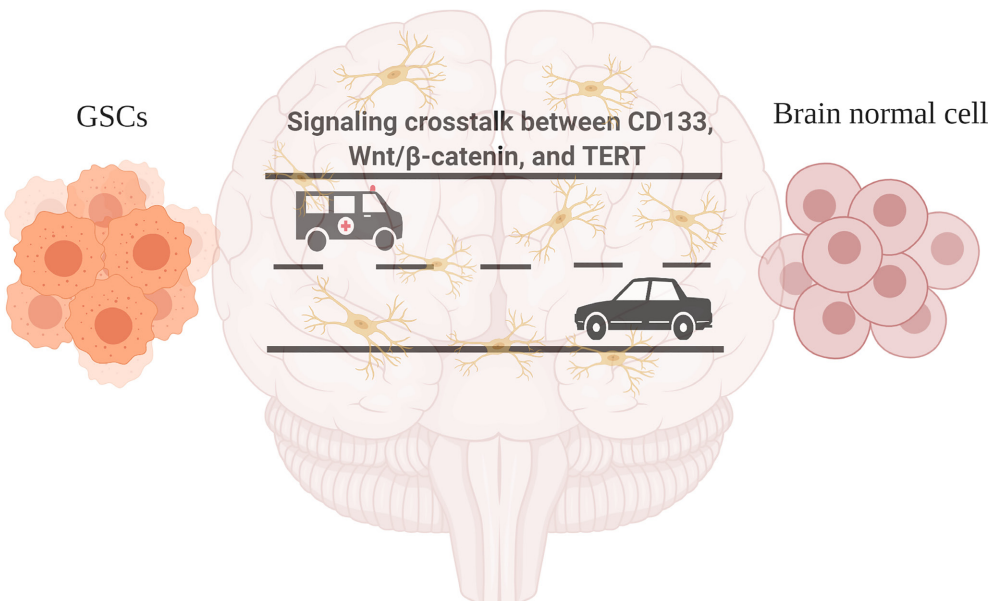

FIGURE 1 | Signaling crosstalk between CD133, Wnt/β-catenin, and TERT: Rescue and Rancor in brain that is a question. (Created with BioRender.com).

knockdown could inhibit cell proliferation of glioma (21). In light of the literature review, it is evident that CD133 is imperative for the harmful oncogenic potential of GSCs as its silencing prevents both the self-renewal and tumorigenic capacities of the GBM stem cells. Notwithstanding, a shred of slightly contradictory evidence shows that some $CD133^{Neg}$ cells can likewise develop aggressive malignancies (22). It was reported that $CD133^{Neg}$ glioma cells give rise to tumors *in vivo* as well as $CD133^{Pos}$ tumor cells and it was suggested that CD133 expression is needed for brain tumor initiation, however that it could be included during brain tumor progression (23). In support of this view, it was uncovered that there are CSCs in both $CD133^{Pos}$ and $CD133^{Neg}$ cell population originated from GBM patient, and both of $CD133^{Pos}$ and $CD133^{Neg}$ cells empowered the formation of tumor masses (24).

The formation of the central nervous system (CNS) of mammals, neurons, astrocytes and oligodendrocytes occurs from a reservoir of murine neuroepithelial (NE) cells, which are neural progenitor cells. Proliferative cell division changes to differentiating cell division as neurogenesis starts and it was shown that membrane particles containing CD133 have been shown to help cell differentiation. In addition to being restricted to NE progenitors, the presence of CD133 is also present in both epithelial and non-epithelial cell forms (10). Given the importance of its function it is unsurprising that it existed in most cells, however, the number of its expression is significantly different from one cell type to another. CD133 expression in normal cell is significantly lower compared to that of cancerous cells. Furthermore, this is also true when comparing normal cancer cells to their CSCs, with appear to have the highest number. CD133-mRNAs have been identified in several human tissues, like testis, digestive tract, and the pancreas, with the most notable expression in the kidney, placenta, salivary gland, and mammary gland. Non-epithelial cells, such as rod photoreceptor cells and bone marrow cells, also have CD133. CD133 appears to play a role in the formation of photoreceptor discs in this regard (10). The physiological role of CD133 in normal cell biology poorly understood. In spite of the lack of knowledge regarding the role of CD133 in normal cells, the vast majority of studies indicates that CD133 has a pivotal function in membrane organization. Moreover, the subcellular position of CD133 enables it to attach directly to the cholesterol-containing lipid rafts where it could be participated in different signaling cascade. It has been found that CD133 might be act as a scaffolding protein. Evidence indicates that, a lack of CD133 caused retinal degeneration and blindness. Additionally, it has suggested that CD133 might be has a function in maintaining of stemness properties (25). However, the exact molecular processes are still unknown. The adult mammalian brain harbors new neurons during life in two distinct locations: hippocampus and subventricular zone (SVZ). Immature neurons produced in the SVZ migrate along the rostral migratory stream (RMS) and become postmitotic interneurons in the olfactory bulb. The identity of the stem cells of the adult SVZ has been explored extensively. It was indicated that new neurons were generated by $CD133^{Pos}$ ependymal stem cells in the adult SVZ/RMS *in vivo* and it was reported that CD133 is specifically localized for ependyma, albeit not all ependymal cells are $CD133^{Pos}$ (26). In support of this view, the findings of another study have shown that CD133 is present neural stem cells in the embryonic brain, in the intermediate radial glial/ependymal cell type in the early postnatal stage, and in the adult brain. Based on these surveys, two competing scenarios for the origin of stem cell tumors in the brain were proposed: a derivation from CD133-expressing cells that are not usually found in the adult brain, or from $CD133^{Pos}$ ependymal cells in the adult brain. Additionally, stem cells of brain tumors may be produced from proliferative yet $CD133^{Neg}$ neurogenic astrocytes in adults brain (27).

ROLE OF WNT SIGNALING PATHWAY IN DEVELOPMENT OF GSCS AND NORMAL BRAIN

Wnt signaling pathway is mediated by Wnts proteins that are secreted by glycoproteins. This Wnts proteins are critical for cell proliferation, and differentiation of both normal and cancer stem cells (28, 29). Two kind of Wnt pathways could determine fate of the cell which are canonical Wnt pathway (Wnt/β-catenin) and non-canonical Wnt pathway. Embryonic development, cell movement, and tissue polarity are regulated by canonical and non-canonical Wnt pathways, respectively (30–32). The Wnt/β-catenin pathway is a strategically valuable molecular mechanism that provides proliferation of all types of stem cells. Increasing data show that hyperactivated-Wnt/β-catenin signaling exist in many cancers and it could adjust the self-renewal of CSCs and GSCS. It has also enhanced growth of tumor and tumor recurrence (33). As a part of the canonical Wnt pathway, β-catenin may control cell proliferation in different types of cells. Stabilized- β-catenin has been shown to translocate to the nucleus and to make T cell factor/lymphocyte enhancer factor 1 (Tcf/LEF1) complex. As a result of this complex, the target genes of Wnt, Cellular Myc (c-Myc) and Cyclin-D1, which are involved in the proliferation of glioma cells are activated (34). Intriguingly, it was speculated that the interaction of microglia-GBMs could be mediated by activated-Wnt/β-catenin pathway. Activated-Wnt/β-catenin in GBM cells might boost the recruitment of microglia by the release of Wnt3a, Wnt5a, Cyclooxygenase-2 (COX2), and metalloproteinases. As a consequence of this activation, microglia release factors such as Matrix metalloproteinases (MMPs), Nitric oxide (NOS), Stress inducible protein-1 (STI-1), Arginase-1 (ARG-1), Interleukins (ILS) and COX2 that can be influence the progression of GBM (35) (**Figure 2**).

It has been accepted that Wnt/β-catenin plays an inevitable role in neurogenesis and gliogenesis in the neocortex. Neurogenesis in neocortex occurs in the ventricular zone (VZ) of the dorsal telencephalon from radial glia (RG) and in the subventricular zone (SVZ) from neural intermediate progenitors (Ips) (37). During embryogenesis, the Wnt/β-catenin pathway is active in VZ zone (38–40). The β-catenin/TCF complex seems to specifically control the neurogenin 1 promoter, a gene involved

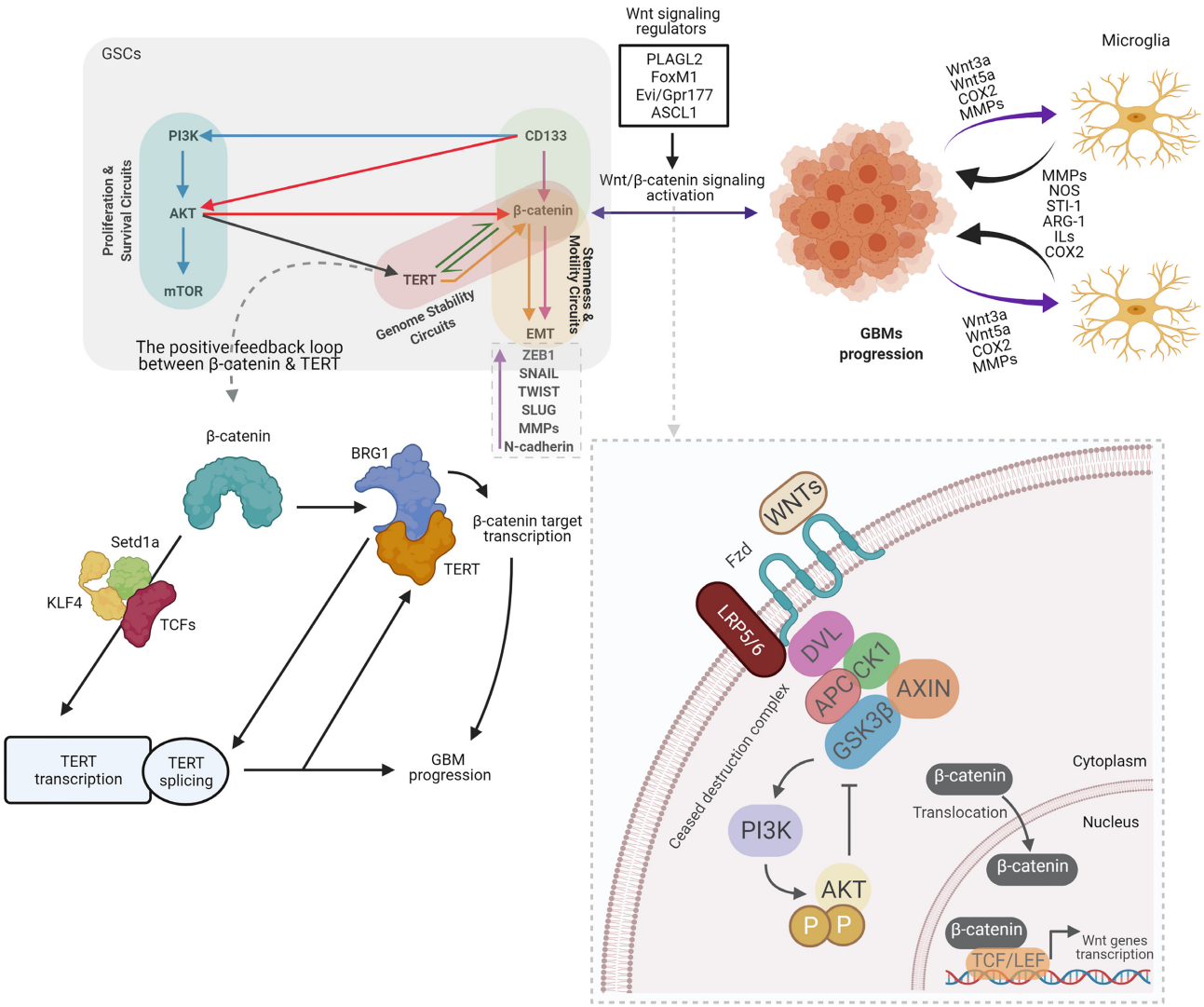

FIGURE 2 | Overview of crosstalk between CD133, Wnt/β-catenin, and telomerase/TERT in GSCs, old actors and new players. By contributing to tumor growth *via* secretion of anti-inflammatory and pro-tumor factors, particularly in GBMs, Microglia benefits glioma. Several microglia-released molecules, such as STI1, epidermal growth factor (EGF), type 1 membrane matrix metalloproteinase (MT1-MMP), NOS, ARG-1, ILs, and COX2 facilitate the proliferation and migration of GBM. Meanwhile, multiple factors that recruit microglial cells and modulate their polarization are secreted by gliomas, such as Wnt3a, Wnt5a, COX2, and MMPs. GBM cells release Wnt3a in response to Wnt/β-catenin activation, which could interfere with the low-density lipoprotein receptor-related protein 5/6 (LRP5/6) and the Frizzled receptor. β-catenin stabilized and translocated to the nucleus as a result of this association, and enhanced the transcription of target genes essential for stem and cell migration (35). The Wnt/β-catenin signaling functions in GBM are defined as follows: GSCs maintenance. Wnt/β-catenin signaling regulators such as PLAGL2, FoxM1, Evi/Gpr177, and ASCL1 activate Wnt/β-catenin signaling and increase the stemness of GBM. Invasiveness of GBM cells. Wnt/β-catenin signaling activation contributes to upregulation of EMT-related genes such as ZEB1, SNAIL, TWIST, SLUG, MMPs, and N-cadherin, leading to increased migration and invasion of GBM cells (36). Several lines of evidence suggest the positive feedback loop between β-catenin and TERT. β-catenin stimulates TERT transcription directly, while TERT serves as a co-factor to facilitate the transcription of the target genes of β-catenin *via* the recruitment of BRG1, resulting in the creation of a positive feedback loop. Furthermore, BRG1 and P54 (nrb) cooperate to control TERT splicing and facilitate full-length TERT mRNA generation. It has been shown that β-catenin binds directly to the TCF site in the TERT promoter and recruit's lysine methyltransferase Setd1a to the promoter region, while Setd1a catalyzes histone H3K4 trimethylation at the promoter site. TCF1, TCF4, and KLF4 can also be involved in β-catenin mediated TERT transcription. In the light of these findings, along with the influence of TERT on target genes for β-catenin, a positive feedback loop between TERT and β-catenin can be readily present in stem and cancer cells. However, it is not clear if BRG1 participates in the activation of TERT transcription by β-catenin, or whether TERT participates independently (12). PI3K, Phosphoinositide 3-kinases; AKT, Protein kinase B; mTOR, The mechanistic target of rapamycin; TERT, Telomerase Reverse Transcriptase; TWIST, Twist-related protein; COX2, Cyclooxygenase-2; MMPs, Matrix metalloproteinases; NOS, Nitric oxide; STI-1, Stress inducible protein-1; ILS, Interleukins; BRG1, brahma-related gene-1; setd1a, SET Domain Containing 1A; Histone Lysine Methyltransferase; KLF4, Kruppel-like factor 4; PLAGL2, Pleiomorphic adenoma gene-like 2; FoxM1, Forkhead box protein M1; Evi/GPr177, G protein-coupled receptor 177; ASCL1, Achaete-scute homolog 1; DVL, Dishevelled; APC, Adenomatous polyposis coli; CK1, The casein kinase 1; GSK3β, glycogen synthase kinase 3β. (Created with BioRender.com).

in cortical neuronal differentiation (41). The beta-catenin expression is highest in the brain during the developmental period and the cytoplasmic level increases in the neurons at day 5 in the mice (42). The amount of beta-catenin mRNA declines in the post-developmental period, which continues in adulthood. However, beta-catenin proteins show higher levels with progressive aging (43). Regulation of beta-catenin levels during brain development is significant, as overexpression of the gene may contribute to an increase in neural growth and a decrease in differentiation, whereas premature inhibition of beta-catenin expression before its natural decline can cause the progenitor neurons to exit the cell cycle early with increased neuronal differentiation (44). Beta-catenin will act as an adhesion protein where it acts as an anchor for cadherin, which is then bound to the actin cytoskeleton of the cell by means of alpha-catenin and thereby ties the cells together (45). As an adhesion protein, beta-catenin can influence synaptic stability during the estrous period between hippocampal neurons, hypothalamic neurons, and even within the amygdala neurons, where its activation correlates with the development and consolidation of brain memory (46–48). Beta-catenin-related dysfunctions have been involved in pathological disorders such as depression, neurodegenerative diseases, and cancer (49). In addition, experimental findings have shown that the activated-Wnt/β-catenin pathway increases the formation of tight junction proteins in the developing brain capillaries (50–52). However, the precise function of Wnt/β-catenin in GSCs and normal brain cells remains poorly elucidated.

FUNCTIONS OF TELOMERASE/TERT IN GSCS AND NORMAL BRAIN

It subsists ambiguous what self-defense mechanism are applied by GSCs against chemotherapeutic drugs. As of lately, it is believed that the DNA damage response (DDR) and DNA repair pathway have undeniable role in self-defense mechanism of cancer stem cells (CSCs) (53). Growing evidence demonstrated that direct correlation exists between elevated DDR and chemoresistance of the CSCs. In light of new observations indicating that maintaining genome stability CSCs might be on account of activation of DDR pathways. Activation of telomerase is one of the critical DDR pathways in GSCs (54). Guanine-rich repeated sequences are attached to the chromosomal terminals using the RNA template by telomerase which recompense the loss of DNA replication. Slight or no activity were reported for telomerase in normal human somatic cells (55). The enhanced activated-telomerase enzyme is one of the most significant molecular properties of cancer. Reactivated telomerase was shown in approximately 90% of tumors (56). It composed of catalytic protein telomerase reverse transcriptase (TERT) and RNA template (TERC). Irrespective of telomerase function, the TERC subunit is expressed in most cell types and the TERT subunit is heavily regulated through cell differentiation. The expression of TERT and TERC in normal cells is small, but the expression of TERT and TERC in tumor cells is indeed very substantial (54, 57). Telomerase is a reverse transcriptase enzyme that has a canonical and non-canonical function in cancer cells. The best-known canonical function of telomerase is maintaining telomere, and the non-canonical functions include DNA repair, anti-apoptotic activity, protection of mitochondrial DNA against oxidative stress, and pro-proliferative effects (58, 59).

In the majority of human primary cancers (~90%), TERT expression/telomerase activity is perceptible. Additionally, induced-TERT or activated-telomerase bestows immortality properties to cancer cells by stabilizing their telomere length (TL). However, current surveys have indicated that its oncogenic features independently of TL, which include DNA damage repair, gene transcription and microRNA expression (60). Moreover, mutated-TERT promoter have been observed in more than 50% of primary adult GBMs. Reports have pointed out that TERT was able to enhance stemness of glioma cells by modulation of epidermal growth factor receptor (EGFR) expression. Inversely, down-regulated TERT expression was coincided with declined expression of EGFR, basic fibroblast growth factor (bFGF) and glioma stem cell properties (61). How the molecular mechanistic details of TERT be able to modulate stemness of glioma remains unclear. Some suggested that GSCs have common properties with astrocyte-like neural stem cells (NSCs) of the SVZ and GBM might spring from the somatic mutations in NSCs of the SVZ. Thus, mutated-TERT promoter in NSCs could license them to expand a self-renewal capacity (62, 63).

Does activated-telomerase and expressed-TERT guard the neurons in our brain? Activated-telomerase is conjoined with cell proliferation during mammalian embryonic development, cell transformation, and in cancers. In adult animals the expression of telomerase is limited to the subventricular zone (SVZ) and olfactory bulb (62). It was shown that the proliferative capacity of somatic cells could be boosted by the up-regulation of TERT. Moreover, as somatic stem cells differentiate, the activity of telomerase and the expression of TERT decline (64, 65). The neurogenesis investigations have indicated that the activity of telomerase and expression of TERT are incremented in neuronal precursor cells in rats and mice brains during embryonic development. Furthermore, the declined-telomerase activity has coincided with a reduction of proliferation of neuroblasts, but the expression of TERT maintains boosted for an extended time period as neurons differentiate and migrate (66). Intriguingly, it was demonstrated that the activity of telomerase is increased in responses to brain injury and it seems that telomerase activity is enhanced in microglia and stem cells because brain tissue injury can induce proliferation of these cells (67).

THE SIGNALING CROSSTALK BETWEEN CD133, WNT/β-CATENIN, AND TERT IN NORMAL BRAIN

Meanwhile, CD133, also known as prominin-1, is one of the most used biomarkers for the isolation of cancer stem cells (CSCs). The rigorous function of CD133 maintains

unidentified, but it has been proposed that it would perform as a cell membrane topology organizer. Furthermore, by activating the Wnt/β-catenin pathway, CD133 could enhance growth, differentiation of nerve cells, and neurogenesis in the brain (10). The activated-Wnt/β-catenin pathway modulates brain development and adult function such as regulation of dendrite formation and synaptic function. By considering the findings stated above, the activated CD133-Wnt/β-catenin has a critical role in the function and integrity of adult brain (68). Importantly, it was reported that TERT has an ability to interact with brahma-related gene-1 (BRG1), chromatin-remodeling factor, and facilitates recruiting BRG1 to β-catenin genes for their transcriptional activation. Thus, the activated-TERT-Wnt/β-catenin axis might increase the proliferation of normal mouse stem cells (60, 69).

THE SIGNALING CROSSTALK BETWEEN CD133, WNT/β-CATENIN, AND TERT MIGHT DRIVE GSCS

Up-regulated CD133 in GBM, has been linked to the self-renewal ability of CSCs and chemotherapy resistance. As well as, it has demonstrated that overexpressed-CD133 is associated with GBM progression and tumorigenesis (70). The findings of study showed that the Wnt/β-catenin pathway could control the activity of GSCs. In this study, the expression levels of Wnt/β-catenin pathway proteins in $CD133^{Pos}$CSC and $CD133^{Neg}$ differentiated glioblastoma cells (DGCs) were compared ($P \leq 0.05$). The expression of eight Wnt proteins (APC, CSNK1E, CSNK1A, CSNK2A2, CSNK2B, CTNNB1, DVL1, RUVBL) was substantially increased. Interestingly, the expression of CTNNB1 (β-catenin) was enhanced 13.98-fold in $CD133^{Pos}$CSC relative to $CD133^{Neg}$ DGCs (71). Data suggest that CD133 is one of the main regulators for β-catenin signaling. Recently, CD133 has been shown to improve the proliferation of clones and the repair of kidneys by regulating the Wnt pathway *via* the modulation of β-catenin levels (72). Another research in liver cancers found that the risen clonogenic ability of CSCs is associated with modulation in Wnt/β-catenin signaling, which is positively linked to CD133 expression. It has been indicated that the CD133-Wnt/β-catenin axis has a critical role in regulating CSCs (73).

Interestingly, the Wnt/β-catenin pathway can do upregulate the stemness of brain cancer by modulating the CD44 CSC marker. It is important to note that Wnt/β-catenin highly activated sub-population of GSCs showed enhanced levels of expression of genes CD133, SRY-box 2 (SOX2), Nanog, Octamer-binding transcription factor-4 (Oct-4), and Nestin, which proposes the role of biomarkers-Wnt/β-catenin axis in remaining stemness traits of GBM (74). Additionally, the results of the study have indicated that CD133 may conceivably activate Wnt/β-catenin signaling pathway through AKT and leads to promote brain tumor-initiating cells in GBM. In other words, the outcome has shown that the CD133-AKT- Wnt/β-catenin axis drives glioblastoma-initiating cell tumor (4). The level of phosphorylate-Akt in $CD133^{Pos}$ cancer cells is greater than in $CD133^{Neg}$ cancer cells, notably in GSCs (5). Consequently, based on this, we may assume CD133 to be an activator of the PI3K-Akt pathway. The 5' regulatory area of TERT contains multiple binding sites for transcription factors, such as Wnt/β-catenin, c-Myc, estrogen receptor, Activator protein-1 (AP1), Signal transducer and activator of transcription proteins (STAT), Mas1 and Pax (Paired Box Proteins) (75–77). The PI3K/Akt/mTOR pathway enhances the expression of TERT thru many pathways (78). Activated-AKT through preventing interactions between mouse double minute 2 homolog (MDM2) and p14 (p19), induces a cell cycle that could impede ubiquitin-mediated p53 proteolysis and the mTOR-mediated degradation of the c-Myc competitor mitotic arrest deficiency-1 (MAD1) (79). Some investigations have shown that overexpressed-c-Myc oncogene plays a key role in the induction of telomerase enzyme activity by increasing TERT expression (80, 81).

Growing data has shown that TERT has mechanistically occupied Wnt/β-catenin promoters, including cyclin D1 and c-Myc. Of note, c-Myc (TERT stimulator) may be regulated by Wnt/β-catenin. On one hand, TERT may be regarded as one of the key targets of the Wnt/β-catenin signaling pathway. It has been shown that β-catenin can interact directly with the mouse and human cancer cells or cancer stem cells TERT promoter. In plain terms, these findings indicate that β-catenin controls the length of telomere by activating the transcription of TERT. Another research stated that TERT could stimulate EMT using Wnt/β-catenin. In addition, *in vitro* research findings showed that TERT expression levels were associated with Snail1 and vimentin expression levels (82–86). TERT activation is an essential step in GBM tumorigenesis and it was shown that TERT permits GBMs to attain CSC characteristics by inducing EGFR expression (61, 87). Of note, the investigations have revealed that TERT has direct interaction with β-catenin and presumably enhance transcriptional outputs of it. Besides, activated-TERT- β-catenin axis mayhap stimulate epithelial-mesenchymal transformation (EMT) in CSCs (54, 86, 88). CSCs and TERT could be linked together by Wnt/β-catenin pathway (85, 89). In summary, the crosstalk between each component of the CD133-Wnt/β-catenin-TERT axis may be considered a pivotal regulatory signaling pathway in the CSCs and GSCs.

CONCLUSION

In a nutshell, in the normal brain, each element of signaling pathways of CD133, Wnt/β-catenin, and TERT has a critical role in the integrity of the brain It is generally accepted that the expression of CD133 in normal cell is significantly lower compared to cancerous cells. This is also true and when comparing normal cancer cells to GSCs (i.e., expression in normal cancer cells is significantly less), especially in GSCs which has the highest expression. Upon minimizing toxicity effect towards normal cells targeting therapy is important. One can target CD133 surface receptor to specifically bring drugs to

CSCs leveraging on its significantly high expression in CSCs. The overexpressed-TERT would increase cell proliferation during embryonic development, whilst CD133 biomarker by activating Wnt/β-catenin pathway leads to neurogenesis. Thus, might be the cross-talk between each component of the mentioned axis has a neuroprotective effect on the normal brain. On the one hand, $CD133^{pos/high}$ sub-population of GSCs correlates to invasiveness and progression of tumor and besides, CD133-Wnt/β-catenin axis has an inevitable role in stemness of GBM. Recent evidence also demonstrated that interplay between Wnt/β-catenin pathway and TERT can be modulating the stemness of CSCs. Hence, activation of the above axis in the brain might be considered as a gate between "tranquility and turmoil" and targeting this pathway might shed a light on GBM therapy and prompt further investigations in this area. However, the bulk of these targeting techniques are of an experimental nature and their medical use is minimal. The biggest challenge is the heterogeneity of GSC's surface biomarkers, which render it challenging to detect and therefore aim therapy. In addition, answering the challenge of similarities between normal neural stem cells and GSCs makes treatment-associated toxicity possible.

AUTHOR CONTRIBUTIONS

AB: Conceptualization, Writing – Original draft. AS: Supervision, Writing – Reviewing, and Editing, Funding Acquisition. All authors contributed to the article and approved the submitted version.

ACKNOWLEDGMENTS

The authors thank Universiti Putra Malaysia for supporting this study under the 465 Putra Berimpak Grant FRGS/1/2020/STG02/UPM/02/13 (01-01-20-2223FR/5540355).

REFERENCES

1. Bhaduri A, Di Lullo E, Jung D, Müller S, Crouch EE, Espinosa CS, et al. Outer Radial Glia-like Cancer Stem Cells Contribute to Heterogeneity of Glioblastoma. *Cell Stem Cell* (2020) 26:48–63. doi: 10.1016/j.stem.2019.11.015
2. Gimple RC, Bhargava S, Dixit D, Rich JN. Glioblastoma stem cells: Lessons from the tumor hierarchy in a lethal cancer. *Genes Dev* (2019) 33:591–609. doi: 10.1101/gad.324301.119
3. Auffinger B, Spencer D, Pytel P, Ahmed AU, Lesniak MS. The role of glioma stem cells in chemotherapy resistance and glioblastoma multiforme recurrence. *Expert Rev Neurotherapeut* (2015) 15:741–52. doi: 10.1586/14737175.2015.1051968
4. Manoranjan B, Chokshi C, Venugopal C, Subapanditha M, Savage N, Tatari N, et al. A CD133-AKT-Wnt signaling axis drives glioblastoma brain tumor-initiating cells. *Oncogene* (2020) 39:1590–99. doi: 10.1038/s41388-019-1086-x
5. Wei Y, Jiang Y, Liu Y, Zou F, Liu YC, Wang S, et al. Activation of PI3K/Akt pathway by CD133-p85 interaction promotes tumorigenic capacity of glioma stem cells. *Proc Natl Acad Sci USA* (2013) 110:6829–34. doi: 10.1073/pnas.1217002110
6. Aghajani M, Mansoori B, Mohammadi A, Asadzadeh Z, Baradaran B. "New emerging roles of CD133 in cancer stem cell: Signaling pathway and miRNA regulation,". *J Cell Physiol* (2019) 234:21642–661. doi: 10.1002/jcp.28824
7. Mak AB, Nixon AML, Kittanakom S, Stewart JM, Chen GI, Curak J, et al. Regulation of CD133 by HDAC6 Promotes β-Catenin Signaling to Suppress Cancer Cell Differentiation. *Cell Rep* (2012) 2:951–63. doi: 10.1016/j.celrep.2012.09.016
8. Sastre-Perona A, Riesco-Eizaguirre G, Zaballos MA, Santisteban P. β-catenin signaling is required for RAS-driven thyroid cancer through PI3K activation. *Oncotarget* (2016) 7:49435–449. doi: 10.18632/oncotarget.10356
9. Ghareghomi S, Ahmadian S, Zarghami N. Biochimie Fundamental insights into the interaction between telomerase/TERT and intracellular signaling pathways. *Biochimie* (2021) 181:12–24. doi: 10.1016/j.biochi.2020.11.015
10. Barzegar Behrooz A, Syahir A, Ahmad S. CD133: beyond a cancer stem cell biomarker. *J Drug Targeting* (2018) 27:257–69. doi: 10.1080/1061186X.2018.1479756
11. Chenn A. Wnt/β-catenin signaling in cerebral cortical development. *Organogenesis* (2008) 4:76–80. doi: 10.4161/org.4.2.5852
12. Yuan X, Xu D. Telomerase reverse transcriptase (TERT) in action: Cross-talking with epigenetics. *Int J Mol Sci* (2019) 20:3338. doi: 10.3390/ijms20133338
13. Singh SK, Clarke ID, Terasaki M, Bonn VE, Hawkins C, Squire J, et al. Identification of a cancer stem cell in human brain tumors. *Cancer Res* (2003) 63:5821–28.
14. Singh SK, Hawkins C, Clarke ID, Squire JA, Bayani J, Hide T, et al. Identification of human brain tumour initiating cells. *Nature* (2004) 432:396–401. doi: 10.1038/nature03128
15. Liou GY. CD133 as a regulator of cancer metastasis through the cancer stem cells. *Int J Biochem Cell Biol* (2019) 106:1–7. doi: 10.1016/j.biocel.2018.10.013
16. Colman H, Zhang L, Sulman EP, McDonald M, Shooshtari NL, Rivera A, et al. A multigene predictor of outcome in glioblastoma. *Neuro Oncol* (2010) 12:49–57. doi: 10.1093/neuonc/nop007
17. Li B, McCrudden CM, Yuen HF, Xi X, Lyu P, Chan KW, et al. CD133 in brain tumor: The prognostic factor. *Oncotarget* (2017) 11144–59. doi: 10.18632/oncotarget.14406
18. Pallini R, Ricci-Vitiani L, Montano N, Mollinari C, Biffoni M, Cenci T, et al. Expression of the stem cell marker CD133 in recurrent glioblastoma and its value for prognosis. *Cancer* (2011) 117:162–174. doi: 10.1002/cncr.25581
19. Smith LM, Nesterova A, Ryan MC, Duniho S, Jonas M, Anderson M, et al. CD133/prominin-1 is a potential therapeutic target for antibody-drug conjugates in hepatocellular and gastric cancers. *Br J Cancer* (2008) 99:100–9. doi: 10.1038/sj.bjc.6604437
20. Vora P, Venugopal C, Salim SK, Tatari N, Bakhshinyan D, Singh M, et al. The Rational Development of CD133-Targeting Immunotherapies for Glioblastoma. *Cell Stem Cell* (2020) 26:832–44. doi: 10.1016/j.stem.2020.04.008
21. Yao J, Zhang T, Ren J, Yu M, Wu G. Effect of CD133/prominin-1 antisense oligodeoxynucleotide on *in vitro* growth characteristics of Huh-7 human hepatocarcinoma cells and U251 human glioma cells. *Oncol Rep* (2009) 22:781–87. doi: 10.3892/or_00000500
22. Ahmed SI, Javed G, Laghari AA, Bareeqa SB, Farrukh S, Zahid S, et al. CD133 Expression in Glioblastoma Multiforme: A Literature Review. *Cureus* (2018) 10:e3439. doi: 10.7759/cureus.3439
23. Wang J, Sakariassen P, Tsinkalovsky O, Immervoll H, Bøe SO, Svendsen A, et al. CD133 negative glioma cells form tumors in nude rats and give rise to CD133 positive cells. *Int J Cancer* (2008) 122:761–68. doi: 10.1002/ijc.23130
24. Joo KM, Kim SY, Jin X, Song SY, Kong DS, Lee JI, et al. Clinical and biological implications of CD133-positive and CD133-negative cells in glioblastomas. *Lab Investig* (2008) 88:808–15. doi: 10.1038/labinvest.2008.57
25. Glumac PM, LeBeau AM. The role of CD133 in cancer: a concise review. *Clin Transl Med* (2018) 7:18. doi: 10.1186/s40169-018-0198-1
26. Coskun V, Wu H, Blanchi B, Tsao S, Kim K, Zhao J, et al. CD133+ neural stem cells in the ependyma of mammalian postnatal forebrain. *Proc Natl Acad Sci U S A* (2008) 105:1026–1031. doi: 10.1073/pnas.0710000105
27. Pfenninger CV, Roschupkina T, Hertwig F, Kottwitz D, Englund E, Bengzon J, et al. CD133 is not present on neurogenic astrocytes in the adult subventricular zone, but on embryonic neural stem cells, ependymal cells

and glioblastoma cells. *Cancer Res* (2007) 67:5727–36. doi: 10.1158/0008-5472.CAN-07-0183
28. Anastas JN, Moon RT. WNT signalling pathways as therapeutic targets in cancer. *Nat Rev Cancer* (2013) 13:11–26. doi: 10.1038/nrc3419
29. Reya T, Clevers H. Wnt signalling in stem cells and cancer. *Nature* (2005) 434:843–50. doi: 10.1038/nature03319
30. Zhang L, Yang X, Yang S, Zhang J. The Wnt/β-catenin signaling pathway in the adult neurogenesis. *Eur J Neurosci* (2011) 33:1–8. doi: 10.1111/j.1460-9568.2010.7483.x
31. Nam JS, Turcotte TJ, Smith PF, Choi S, Jeong KY. Mouse cristin/R-spondin family proteins are novel ligands for the frizzled 8 and LRP6 receptors and activate β-catenin-dependent gene expression. *J Biol Chem* (2006) 281:13247–57. doi: 10.1074/jbc.M508324200
32. Guan R, Zhang X, Guo M. "Glioblastoma stem cells and Wnt signaling pathway: Molecular mechanisms and therapeutic targets. *Chin Neurosurg J* (2020) 6:25. doi: 10.1186/s41016-020-00207-z
33. Mao J, Fan S, Ma W, Fan P, Wang B, Zhang J, et al. Roles of Wnt/β-catenin signaling in the gastric cancer stem cells proliferation and salinomycin treatment. *Cell Death Dis* (2014) 5:e1039. doi: 10.1038/cddis.2013.515
34. Nager M, Bhardwaj D, Cantí C, Medina L, Nogués P, Herreros J. β -Catenin Signalling in Glioblastoma Multiforme and Glioma-Initiating Cells. *Chemother Res Pract* (2012) 2012:7. doi: 10.1155/2012/192362
35. Matias D, Predes D, Niemeyer Filho P, Lopes MC, Abreu JG, Lima FRS, et al. Microglia-glioblastoma interactions: New role for Wnt signaling. *Biochim Biophys Acta Rev Cancer* (2017) 1868:333–40. doi: 10.1016/j.bbcan.2017.05.007
36. Lee Y, Lee JK, Ahn SH, Lee J, Nam DH. WNT signaling in glioblastoma and therapeutic opportunities. *Lab Investig* (2016) 96:137–50. doi: 10.1038/labinvest.2015.140
37. Bem J, Brożko N, Chakraborty C, Lipiec MA, Koziński K, Nagalski A, et al. Wnt/β-catenin signaling in brain development and mental disorders: keeping TCF7L2 in mind. *FEBS Lett* (2019) 593:1654–74. doi: 10.1002/1873-3468.13502
38. Grove EA, Tole S, Limon J, Yip LW, Ragsdale CW. The hem of the embryonic cerebral cortex is defined by the expression of multiple Wnt genes and is compromised in Gli3-deficient mice. *Development* (1998) 125:2315–25.
39. Chodelkova O, Masek J, Korinek V, Kozmik Z, Machon O. Tcf7L2 is essential for neurogenesis in the developing mouse neocortex. *Neural Dev* (2018) 13:8. doi: 10.1186/s13064-018-0107-8
40. Machon O, Van Den Bout CJ, Backman M, Kemler R, Krauss S. Role of β-catenin in the developing cortical and hippocampal neuroepithelium. *Neuroscience* (2003) 122:129–43. doi: 10.1016/S0306-4522(03)00519-0
41. Hirabayashi Y, Itoh Y, Tabata H, Nakajima K, Akiyama T, Masuyama N, et al. The Wnt/β-catenin pathway directs neuronal differentation of cortical neural precursor cells. *Development* (2004) 131:2791–801. doi: 10.1242/dev.01165
42. Coyle-Rink J, Del Valle L, Sweet T, Khalili K, Amini S. Developmental expression of Wnt signaling factors in mouse brain. *Cancer Biol Ther* (2002) 1:640–45. doi: 10.4161/cbt.313
43. Lu T, Aron L, Zullo J, Pan Y, Kim H, Chen Y, et al. REST and stress resistance in ageing and Alzheimer's disease. *Nature* (2014) 507:448–54. doi: 10.1038/nature13163
44. Chenn A, Walsh CA. Regulation of cerebral cortical size by control of cell cycle exit in neural precursors. *Science* (2002) 297:365–69. doi: 10.1126/science.1074192
45. Drees F, Pokutta S, Yamada S, Nelson WJ, Weis WI. α-catenin is a molecular switch that binds E-cadherin-β-catenin and regulates actin-filament assembly. *Cell* (2005) 123:903–15. doi: 10.1016/j.cell.2005.09.021
46. Maguschak KA, Ressler KJ. β-catenin is required for memory consolidation. *Nat Neurosci* (2008) 11:1319–26. doi: 10.1038/nn.2198
47. Mills F, Bartlett TE, Dissing-Olesen L, Wisniewska MB, Kuznicki J, Macvicar BA, et al. Cognitive flexibility and long-term depression (LTD) are impaired following β-catenin stabilization *in vivo*. *Proc Natl Acad Sci USA* (2014) 111:8631–36. doi: 10.1073/pnas.1404670111
48. Barrera-Ocampo A, Gutierrez-Vargas J, Garcia-Segura LM, Cardona-Gómez GP. Glycogen synthase kinase-3β/β-catenin signaling in the rat hypothalamus during the estrous cycle. *J Neurosci Res* (2012) 90:1078–84. doi: 10.1002/jnr.22816
49. Teo CH, Soga T, Parhar IS. Brain Beta-Catenin Signalling during Stress and Depression. *NeuroSignals* (2019) 26:31–42. doi: 10.1159/000487764
50. Daneman R, Agalliu D, Zhou L, Kuhnert F, Kuo CJ, Barres BA. Wnt/β-catenin signaling is required for CNS, but not non-CNS, angiogenesis. *Proc Natl Acad Sci USA* (2009) 106:641. doi: 10.1073/pnas.0805165106
51. Harati R, Benech H, Villégier AS, Mabondzo A. P-glycoprotein, breast cancer resistance protein, organic anion transporter 3, and transporting peptide 1a4 during blood-brain barrier maturation: Involvement of Wnt/β-catenin and endothelin-1 signaling. *Mol Pharm* (2013) 10:1566–80. doi: 10.1021/mp300334r
52. Laksitorini MD, Yathindranath V, Xiong W, Hombach-Klonisch S, Miller DW. Modulation of Wnt/β-catenin signaling promotes blood-brain barrier phenotype in cultured brain endothelial cells. *Sci Rep* (2019) 9:19718. doi: 10.1038/s41598-019-56075-w
53. Abad E, Graifer D, Lyakhovich A. DNA damage response and resistance of cancer stem cells. *Cancer Lett* (2020) 1:106–17. doi: 10.1016/j.canlet.2020.01.008
54. Liu N, Guo XH, Liu JP, Cong YS. Role of telomerase in the tumour microenvironment. *Clin Exp Pharmacol Physiol* (2020) 47:357–64. doi: 10.1111/1440-1681.13223
55. Parkinson EK. Telomerase as a novel and potentially selective target for cancer chemotherapy. *Ann Med* (2003) 35:466–75. doi: 10.1080/07853890310006361
56. Podlevsky JD, Bley CJ, Omana RV, Qi X, Chen JL. The Telomerase Database. *Nucleic Acids Res* (2008) 36:D339–43. doi: 10.1093/nar/gkm700
57. Jiang J, Chan H, Cash DD, Miracco EJ, Ogorzalek Loo RR, Upton HE, et al. Structure of Tetrahymena telomerase reveals previously unknown subunits, functions, and interactions. *Science* (2015) 350:aab4070. doi: 10.1126/science.aab4070
58. Saretzki G. Does telomerase protein protect our neurons? *J Neurol Neuromed* (2016) 1:23–8. doi: 10.29245/2572.942X/2016/2.1025
59. Lu C, Fu W, Mattson MP. Telomerase protects developing neurons against DNA damage-induced cell death. *Dev Brain Res* (2001) 131:167–71. doi: 10.1016/S0165-3806(01)00237-1
60. Yuan X, Larsson C, Xu D. Mechanisms underlying the activation of TERT transcription and telomerase activity in human cancer: old actors and new players. *Oncogene* (2019) 38:6172–83. doi: 10.1038/s41388-019-0872-9
61. Beck S, Jin X, Sohn YW, Kim JK, Kim SH, Yin J, et al. Telomerase activity-independent function of TERT allows glioma cells to attain cancer stem cell characteristics by inducing EGFR expression. *Mol Cells* (2011) 31:9–15. doi: 10.1007/s10059-011-0008-8
62. Matarredona ER, Pastor AM. Neural stem cells of the subventricular zone as the origin of human glioblastoma stem cells. Therapeutic implications. *Front Oncol* (2019) 9:799. doi: 10.3389/fonc.2019.00779
63. Sanai N, Alvarez-Buylla A, Berger MS. Neural Stem Cells and the Origin of Gliomas. *N Engl J Med* (2005) 353:811–22. doi: 10.1056/NEJMra043666
64. Greenberg RA, Allsopp RC, Chin L, Morin GB, DePinho RA. Expression of mouse telomerase reverse transcriptase during development, differentiation and proliferation. *Oncogene* (1998) 16:1723–30. doi: 10.1038/sj.onc.1201933
65. Bodnar AG, Ouellette M, Frolkis M, Holt SE, Chiu CP, Morin GB, et al. Extension of life-span by introduction of telomerase into normal human cells. *Science* (1998) 279:349–52. doi: 10.1126/science.279.5349.349
66. Klapper W, Shin T, Mattson MP. Differential regulation of telomerase activity and TERT expression during brain development in mice. *J Neurosci Res* (2001) 64:252–60. doi: 10.1002/jnr.1073
67. Liu J, Solway K, Messing RO, Sharp FR. Increased neurogenesis in the dentate gyrus after transient global ischemia in gerbils. *J Neurosci* (1998) 18:7768–78. doi: 10.1523/JNEUROSCI.18-19-07768.1998
68. Zuccarini M, Giuliani P, Ziberi S, Carluccio M, Di Iorio P, Caciagli F, et al. The role of wnt signal in glioblastoma development and progression: A possible new pharmacological target for the therapy of this tumor. *Genes* (2018) 9:105. doi: 10.3390/genes9020105
69. Il Park J, Venteicher AS, Hong JY, Choi J, Jun S, Shkreli M, et al. Telomerase modulates Wnt signalling by association with target gene chromatin. *Nature* (2009) 460:66–72. doi: 10.1038/nature08137
70. Hassn Mesrati M, Behrooz AB, Abuhamad AY, Syahir A. Understanding Glioblastoma Biomarkers: Knocking a Mountain with a Hammer. *Cells* (2020) 9:1236. doi: 10.3390/cells9051236
71. Shevchenko V, Arnotskaya N, Zaitsev S, Sharma A, Sharma HS, Bryukhovetskiy A, et al. Proteins of Wnt signaling pathway in cancer stem cells of human glioblastoma. In: *International Review of Neurobiology*, vol. 151. (2020). p. 185–200. doi: 10.1016/bs.irn.2020.03.006

72. Brossa A, Papadimitriou E, Collino F, Incarnato D, Oliviero S, Camussi G, et al. Role of CD133 Molecule in Wnt Response and Renal Repair. *Stem Cells Transl Med* (2018) 7:283–94. doi: 10.1002/sctm.17-0158
73. Aghajani M, Mansoori B, Mohammadi A, Asadzadeh Z, Baradaran B. New emerging roles of CD133 in cancer stem cell: Signaling pathway and miRNA regulation. *J Cell Physiol* (2019) 234:21642–661. doi: 10.1002/jcp.28824
74. Prasad S, Ramachandran S, Gupta N, Kaushik I, Srivastava SK. Cancer cells stemness: A doorstep to targeted therapy. *Biochim Biophys Acta Mol Basis Dis* (2020) 18866:165424. doi: 10.1016/j.bbadis.2019.02.019
75. Artandi SE, Alson S, Tietze MK, Sharpless NE, Ye S, Greenberg RA, et al. Constitutive telomerase expression promotes mammary carcinomas in aging mice. *Proc Natl Acad Sci U S A* (2002) 99:8191–96. doi: 10.1073/pnas.112515399
76. González-Suárez E, Samper E, Ramírez A, Flores JM, Martín-Caballero J, Jorcano JL, et al. Increased epidermal tumors and increased skin wound healing in transgenic mice overexpressing the catalytic subunit of telomerase, mTERT, in basal keratinocytes. *EMBO J* (2001) 20:2619–2630. doi: 10.1093/emboj/20.11.2619
77. Ramlee MK, Wang J, Toh WX, Li S. Transcription regulation of the human telomerase reverse transcriptase (hTERT) gene. *Genes* (2016) 7:50. doi: 10.3390/genes7080050
78. Daniel M, Peek GW, Tollefsbol TO. Regulation of the human catalytic subunit of telomerase (hTERT). *Gene* (2012) 498:135–46. doi: 10.1016/j.gene.2012.01.095
79. Peek GW, Tollefsbol TO. Down-regulation of hTERT and Cyclin D1 transcription *via* PI3K/Akt and TGF-β pathways in MCF-7 Cancer cells with PX-866 and Raloxifene. *Exp Cell Res* (2016) 344:95–102. doi: 10.1016/j.yexcr.2016.03.022
80. Wu KJ, Grandori C, Amacker M, Simon-Vermot N, Polack A, Lingner J, et al. Direct activation of TERT transcription by c-MYC. *Nat Genet* (1999) 21:220–4. doi: 10.1038/6010
81. Khattar E, Tergaonkar V. Transcriptional regulation of telomerase reverse transcriptase (TERT) by MYC. *Front Cell Dev Biol* (2017) 5:1. doi: 10.3389/fcell.2017.00001
82. Li J, Huang X, Xie X, Wang J, Duan M. Human telomerase reverse transcriptase regulates cyclin D1 and G1/S phase transition in laryngeal squamous carcinoma. *Acta Otolaryngol* (2011) 131:546–51. doi: 10.3109/00016489.2011.557393
83. Yang C, Przyborski S, Cooke MJ, Zhang X, Stewart R, Anyfantis G, et al. A Key Role for Telomerase Reverse Transcriptase Unit in Modulating Human Embryonic Stem Cell Proliferation, Cell Cycle Dynamics, and In Vitro Differentiation. *Stem Cells* (2008) 26:850–63. doi: 10.1634/stemcells.2007-0677
84. Zhang Y, Toh LL, Lau P, Wang X. Human telomerase reverse transcriptase (hTERT) is a novel target of the Wnt/β-catenin pathway in human cancer. *J Biol Chem* (2012) 287:32494–511. doi: 10.1074/jbc.M112.368282
85. Hoffmeyer K, Raggioli A, Rudloff S, Anton R, Hierholzer A, Del Valle I, et al. Wnt/β-catenin signaling regulates telomerase in stem cells and cancer cells. *Science* (2012) 336:1549–54. doi: 10.1126/science.1218370
86. Liu Z, Li Q, Li K, Chen L, Li W, Hou M, et al. Telomerase reverse transcriptase promotes epithelial-mesenchymal transition and stem cell-like traits in cancer cells. *Oncogene* (2013) 32:4203–13. doi: 10.1038/onc.2012.441
87. Pestana A, Vinagre J, Sobrinho-Simões M, Soares P. TERT biology and function in cancer: Beyond immortalisation. *J Mol Endocrinol* (2017) 58:R129–46. doi: 10.1530/JME-16-0195
88. Zhang K, Guo Y, Wang X, Zhao H, Ji J, Cheng C, et al. WNT/β-catenin directs self-renewal symmetric cell division of hTERThigh prostate cancer stem cells. *Cancer Res* (2017) 77:2534–47. doi: 10.1158/0008-5472.CAN-16-1887
89. Greider CW. Wnt regulates TERT - Putting the horse before the cart. *Science* (2012) 336:1519–20. doi: 10.1126/science.1223785

Conflict of Interest: The authors declare that the research was conducted in the absence of any commercial or financial relationships that could be construed as a potential conflict of interest.

frontiers in Oncology

ORIGINAL RESEARCH
published: 23 August 2021
doi: 10.3389/fonc.2021.699004

miR-377-3p-Mediated EGR1 Downregulation Promotes B[a]P-Induced Lung Tumorigenesis by Wnt/Beta-Catenin Transduction

Xinxin Ke[1], Lulu He[1], Runan Wang[1], Jing Shen[2], Zhengyang Wang[3], Yifei Shen[4], Longjiang Fan[4], Jimin Shao[1,5] and Hongyan Qi[1]**

[1] Department of Pathology and Pathophysiology, and Department of Radiation Oncology of the Second Affiliated Hospital, School of Medicine, Zhejiang University, Hangzhou, China, [2] Department of Pathology and Pathophysiology, and Department of Medical Oncology of the Second Affiliated Hospital, School of Medicine, Zhejiang University, Hangzhou, China, [3] Department of Pulmonary and Critical Care Medicine, Sir Run Run Shaw Hospital, School of Medicine, Zhejiang University, Hangzhou, China, [4] Institute of Crop Science and Institute of Bioinformatics, Zhejiang University, Hangzhou, China, [5] Key Laboratory of Disease Proteomics of Zhejiang Province, Key Laboratory of Cancer Prevention and Intervention of China National Ministry of Education, and Research Center for Air Pollution and Health, School of Medicine, Zhejiang University, Hangzhou, China

OPEN ACCESS

Edited by:
Zhong Liu,
Jinan University, China

Reviewed by:
Junjian Wang,
Sun Yat-Sen University, China
Srinivas Patnaik,
KIIT University, India
Yao Wang,
Wuyi University, China

***Correspondence:**
Hongyan Qi
qihongyan@zju.edu.cn
Jimin Shao
shaojimin@zju.edu.cn

Specialty section:
This article was submitted to Molecular and Cellular Oncology, a section of the journal Frontiers in Oncology

Received: *27 May 2021*
Accepted: *26 July 2021*
Published: *23 August 2021*

Citation:
Ke X, He L, Wang R, Shen J, Wang Z, Shen Y, Fan L, Shao J and Qi H (2021) miR-377-3p-Mediated EGR1 Downregulation Promotes B[a]P-Induced Lung Tumorigenesis by Wnt/Beta-Catenin Transduction. Front. Oncol. 11:699004. doi: 10.3389/fonc.2021.699004

Polycyclic aromatic hydrocarbons (PAHs), particularly benzo[a]pyrene (B[a]P), found in cigarette smoke and air pollution, is an important carcinogen. Nevertheless, early molecular events and related regulatory effects of B[a]P-mediated cell transformation and tumor initiation remain unclear. This study found that EGR1 was significantly downregulated during human bronchial epithelial cell transformation and mice lung carcinogenesis upon exposure to B[a]P and its active form BPDE, respectively. In contrast, overexpression of EGR1 inhibited the BPDE-induced cell malignant transformation. Moreover, miR-377-3p was strongly enhanced by BPDE/B[a]P exposure and crucial for the inhibition of EGR1 expression by targeting the 3'UTR of EGR1. MiR-377-3p antagomir reversed the effect of EGR1 downregulation in cell malignant transformation and tumor initiation models. Furthermore, the B[a]P-induced molecular changes were evaluated by IHC in clinical lung cancer tissues and examined with a clinic database. Mechanistically, EGR1 inhibition was also involved in the regulation of Wnt/β-catenin transduction, promoting lung tumorigenesis following B[a]P/BPDE exposure. Taken together, the results demonstrated that bBenzo[a]pyrene exposure might induce lung tumorigenesis through miR-377-3p-mediated reduction of EGR1 expression, suggesting an important role of EGR1 in PAHs-induced lung carcinogenesis.

Keywords: early growth response protein 1, miR-377-3p, malignant transformation, lung tumorigenesis, Wnt/β-catenin pathway

INTRODUCTION

Lung cancer has the highest morbidity and mortality worldwide. Late diagnosis and poor prognosis are the main causes of cancer-related death (1, 2), and smoking is a common risk factor. Yet, over the years, the increased non-smoking-related risk associated with ambient air pollution has been frequently reported (3). Polycyclic aromatic hydrocarbons (PAHs) are widespread environmental pollutants that have been associated with carcinogenicity (in gas or particle phase) (4). The most widely studied PAH is Benzo[a]pyrene (B[a]P), which is frequently chosen as a substitute for evaluating the carcinogenic PAHs (5).

B[a]P is a human group 1 carcinogen capable of initiating and promoting lung tumorigenesis (6). BPDE is the main biologically active metabolite of B[a]P that can form DNA adducts of guanine N2, thus exerting its carcinogenic effect (7). In cell-based models, B [a]P or its metabolite BPDE induce cell malignant transformation, while in mice models, it can reduce lung tumors. Recent studies have shown that B[a]P-induced tumorigenesis involves DNA methylation, oxidative stress, cell cycle, inflammation, apoptosis, and other biological processes (7–9). Yet, the exact molecular mechanism behind this remains unclear.

Transient activation and regulation of immediate-early genes are considered primary cellular responses to an external signal in cancer development (10). Early growth response 1 (EGR1) is an immediate-early gene that can be directly activated by growth factors, hypoxia, ischemia, tissue injury, and apoptotic signals in different cells (11). Different roles of EGR1 have been observed in different tumors. EGFR1 can have double-edged effects in tumor development. For example, EGR1 has an oncogenic function in prostate cancer by promoting cell proliferation and survival, but it can also act as a tumor suppressor in various cancers such as glioma, lung, and bladder cancer by directly upregulating PTEN, P53, and fibronectin (12–16).

MicroRNAs (miRNAs), an endogenous short non-coding RNA, have important functions in many developmental systems (17). miRNAs regulate gene expression in multicellular organisms by affecting both the stability and translation of mRNAs. They can target the 3'-UTR of mRNA transcripts *via* complementary sequences and repress the gene expression by post-transcriptional level (18). Their deregulation has been closely related to cancer initiation and progression (19).

miR-377-3p is a novel tumor regulatory miRNA whose biological functions are wildly unknown. MiR-377-3p has been shown to possess tumor-inhibiting effects in clear cell renal cell carcinoma and hepatocellular carcinoma (20, 21). Contrary, previous studies have shown that miR-377 promotes the proliferation and EMT process in colon cancer, while the low level of miR-377 was associated with a good prognosis of periampullary adenocarcinoma (22, 23). Moreover, recent studies demonstrated that miRNAs are also involved in B[a]P-induced carcinogenicity (24, 25). However, the potential contribution of miRNAs in environmental carcinogens-induced lung tumorigenesis is still not clear.

In the present study, we found that EGR1 expression was strongly reduced in the malignant transformation of human lung bronchial epithelial cells and lung tumorigenicity following B[a]P and its active metabolite BPDE exposure. Moreover, miR-377-3p mediated EGR1 downregulation facilitates cell malignant transformation and tumor formation by regulating the Wnt/β-catenin pathway, suggesting an important role of the miR-377-3p/EGR1 axis in the malignant transformation of lung tumorigenesis induced by environmental carcinogen.

MATERIALS AND METHODS

Patient Samples

A total of 114 non-small-cell lung cancer (NSCLC) clinical samples of the Second Affiliated Hospital of Zhejiang University were used in this study. The study was approved by the ethics committee of the hospital. The clinical characteristics of these samples are shown in **Table 1**. The cancer tissues were formalin-fixed and paraffin-embedded for immunohistochemistry (IHC).

Cells and Reagents

Human bronchial normal epithelium cell BEAS-2B (Cell Bank of the Chinese Academy of Science, Xiangya, China) and 293T cells (ATCC, Manassas, VA, USA) were cultured in DMEM (Gibco, Grand Island, NY, USA.) supplemented with 10% FBS (Gibco), streptomycin (100 g/mL), and penicillin (100 U/mL) in a humidified atmosphere containing 5%CO_2/95% air at 37°C. The authenticity of the cell lines used in this study has been verified by STR profiling.

BPDE was purchased from the National Cancer Institute Chemical Carcinogen Reference Standard Repository (Kansas City, MO, USA), dissolved in DMSO, and stocked in -80°C.

Cell Transformation Assays

Cells were exposed to 0.2 μM or 0.5 μM BPDE for 2 hours in a serum-free medium. Then, the treated medium was removed, and cells were recovered in a fresh medium at 37°C. BPDE exposure was repeated once a week for 12 weeks. After 12 weeks of treatment, the malignant phenotype was analyzed and DMSO was used as solvent control.

QRT-PCR

Total RNA was extracted from cell lines or tumor and normal tissue samples with TRIzol reagent (Invitrogen, Carlsbad, CA, USA). For gene expression, RNA was reverse transcribed using a Prime-Script RT reagent Kit (TaKaRa). QRT-PCR was carried out with an SYBR Premix Ex Taq (TaKaRa). For miRNA expression, RNA was reverse transcribed using an SYBR® Premix Ex Taq II (TliRnaseH Plus) (TaKaRa, Dalian, China). QRT-PCR was performed using a Mir-X miRNAFirst-Strand Synthesis kit (Clontech, Madison, WI, USA). Experiments were performed in triplicate, and the values were normalized to GAPDH or RNU6B using the $2(-\Delta\Delta Ct)$ method for gene and miRNA expression analysis, respectively.

Immunoblot Analysis

Cell lysates (50 mg) were separated on a 10% SDS-PAGE gel and then transferred onto a nitrocellulose membrane (Whatman, Maidstone, UK). The membrane was blocked with 5% skim milk solution for 2 hours and incubated overnight at 4°C with the

following diluted primary antibody: rabbit monoclonal anti-human EGR1 (ab194357, Abcam, Hanghzou, China), and the mouse monoclonal anti-human GADPH (sc-47724) and anti-human β-catenin (sc-7963) both purchased from Santa Cruz Biotechnology (Santa Cruz, CA, USA). Then, the membrane was incubated in IRDye® 800CW- or IRDye 680-conjugated secondary antibody (LI-COR Biosciences, Lincoln, NE, USA) and detected by an Odyssey® infrared imaging system.

Animal Models

A/J mice (4 weeks) and Balb/c nude mice (4 weeks) were obtained from Model Animal Research Center, Nanjing, China and SLAC Laboratory Animal, Shanghai, China. All the animals were housed in an environment with a temperature of 22 ± 1°C, relative humidity of 50 ± 1%, and a light/dark cycle of 12/12 h. All animal studies (including the mice euthanasia procedure) were done in compliance with Zhejiang University institutional animal care regulations and guidelines, and conducted according to the AAALAC and the IACUC guidelines.

A/J mice (4 weeks) were randomly divided into two groups (12 mice/group). B[a]P group was intraperitoneally injected with B[a]P (25 mg/kg, in tricaprylin solvent) (Sigma), and the control group was intraperitoneally injected with the tricaprylin solvent. B[a]P treatment was given on a weekly basis for 8 weeks. The control group was treated as the same. After 4 months of restoration following the treatment period, mice were sacrificed, and the lung tissues were obtained and histologically examined. The tricaprylin solvent-treated group was used as a control group.

Balb/c nude mice (4 weeks) were subcutaneously injected with 5×10^6 transformed cells in 100 μl volume mixed with Matrigel (1:1). Three days after injection, miR-377-3p antagomir (5 nmol/mouse) or scramble control was performed by intratumor injection twice a week. The long diameter (a) and short diameter (b) of the tumors were measured; after which, the volume (V) was calculated using the formula $V = 1/2 \times a \times b2$. Mice were sacrificed, and the tumor tissues were obtained and weighed.

Soft Agar Assay

The cells (1,000 cells/well) were suspended in a culture medium containing 0.4% agarose (Sigma, St Louis, MO, USA) and seeded onto a base layer of 0.7% agar bed in 12-well plates. After 2 weeks, colonies were stained with crystal violet and photographed. Colonies ≥ 0.05 mm in diameter were counted.

Scratch Test

Cells (1×10^5 cells/ml) were plated in 6-well plates. The monolayer was scratched by a 10 ml sterile pipette tip. The cells were gently rinsed twice with PBS to remove floating cells and incubated in 2 ml of serum free medium in 37°C, 5% CO2 air environment. Images of the scratches were taken by using an inverted microscope at 0, 24, and 48 hours of incubation. ImageJ software was used to analyze the percentage of wound closure.

Transwell Assay

We performed a cell migration assay with an 8 μm-pore in 24-well transwell plates (Costar, Cambridge, MA, USA). Briefly, 400 ml of complete DMEM medium was added under the chambers, whereas cells (2×10^4) were added above the chambers in a serum-free medium. After 48 hours of incubation at 37°C, the migrated cells were fixed with 4% paraformaldehyde and stained with 0.5% crystal violet. Then, the filter membrane was examined and photographed under a microscope.

Immunohistochemistry

The IHC was performed using an Envision Detection System (DAKO, Carpinteria, CA) according to the instructions of the manufacturer. Rabbit monoclonal anti-mouse Ki67 (ab194357) was purchased from Abcam; rabbit polyclonal anti-mouse EGR1 (sc-110) was purchased from Santa Cruz Biotechnology. The IHC staining results were assessed and confirmed by two independent investigators blinded to the clinical data.

Cell Transfection

For lentiviral-mediated transfection, 293T cells were co-transfected with the lentiviral and packaging vectors. After 72 h, the supernatant was collected. Supernatants were then collected and centrifuged at 1,000 × g for 15 min at 4°C to pellet debris. Before performing the infection, the lentiviruses were recovered and re-suspended in a fresh medium with 6 g/ml of polybrene. Stable cells with EGR1 knockdown or EGR1 overexpression were selected following transduction with 0.5 mg/ml of puromycin for 2 weeks. Transfection efficiency of EGR1 knockdown or EGR1 overexpression was examined by Western blot.

For miR-377-3p mimic, inhibitor, antagomir, miRNA control (GenePharma, Shanghai, China) transfection, cells were transfected using Lipofectamine® RNAiMAX (Invitrogen) following the instructions of the manufacturer. After 72 h of transfection, the cells were collected for further experiments.

Dual-Luciferase Reporter Assay

The full-length and mutated miR-377-3p recognition elements of 3'UTR-EGR1 were synthesized and constructed into a pGL3-Basic vector (Promega, Madison, WI, USA). After seeding the cells for 24 h, the mimic or inhibitor of miR-377-3p (GenePharma) was co-transfected with either pGL3-EGR1-3'UTR wild-type or mutant into BEAS-2B and 293T cells. Dual-Luciferase Reporter Assay System was used for testing the relative luciferase activity (Promega).

Immunofluorescence

The BPDE-transformed cells were plated in culture. After overexpression of EGR1, the cells were fixed for 15 min in 4% formaldehyde solution. Then, the cells were washed with PBS and treated with 0.1% Triton X-100 in PBS for 10 min. After permeabilizing the cells, we blocked the cells for 1 h in an antibody blocking buffer (10% normal goat serum, 1% BSA in PBS). Then, the cells were washed with PBS and incubated with anti-human β-catenin primary antibody. The presented IF staining pictures are the overlaid images of β-catenin staining in green fluorescence with nuclear 4'6-diamidino-2-phenylindole (DAPI) staining in blue fluorescence. The IF staining images were taken and overlaid using the Nikon NIS-Elements software.

Statistical Analysis

The two-tailed Student's t-test and one-way analysis of variance were used for statistical data analysis. The data was expressed of three separate experiments, as mean ± standard deviation (SD). $P \leq 0.05$ was considered to be statistically significant.

RESULTS

BPDE/B[a]P Downregulates the Expression of EGR1 *In Vitro* and *In Vivo*

B[a]P and its ultimate carcinogenic metabolite, BPDE, are the strong lung carcinogens found in tobacco smoke and air pollution (26). However, the molecular mechanisms underlying PAH-induced lung tumorigenesis, particularly in the early stage, remain unclear. To indicate the critical genes involved in this process, human lung epithelial cells and A/J mice were exposed to BPDE/B[a]P, respectively. Malignant transformation of BEAS-2B cells was identified upon 12 weeks of BPDE exposure (**Figures 1** and **S1**). **Figure 1A** shows a schematic map of the strategy used to generate the BPDE-induced malignant transformation of BEAS-2B cells. Cell proliferation assay and soft agar assay revealed that BPDE treatment enhanced the reproductive capacity of cells and the anchorage-independent growth capability, respectively (**Figures 1B, C**). We also observed that the cell migration was enhanced upon BPDE treatment (**Figures S1A, B**). Xenograft assay further confirmed the malignant phenotype of BPDE-induced BEAS-2B cells (**Figure 1D**). In addition, we also confirmed the above tumorigenic effects with the BPDE-induced HBE malignant transformation cell model by malignant phenotype analysis (data not shown).

To investigate the genes implicated in the BPDE-induced malignant transformation process, we performed RNA-sequencing analysis. Our results showed that EGR1 was the most obviously downregulated gene in the transformed cells (**Figure S1C**). The downregulation of EGR1 expression was confirmed in both BEAS-2B and HBE BPDE-induced cell transformed models (**Figures 1E, F**). Moreover, the EGR1 protein content was also reduced in different lung cancer cells contrasted with normal cells (**Figure 1G**).

To further evaluate the effect of B[a]P on EGR1 expression *in vivo*, we established a B[a]P-treated A/J mice model (**Figure S2A**). Most mice treated with B[a]P developed primary lung tumors within 6 months; this was observed by PET-CT detection and histopathological analysis (**Figures 2A** and **S2B, C**). Our results also showed that EGR1 mRNA expression and protein level were decreased in the lung tumor tissues compared to the adjacent normal tissues (**Figures 2B, C**). Ki67 was extensively assessed and reported as a predictive proliferative marker of cancer cells. Moreover, the downregulation of EGR1 was not only observed in adenocarcinoma but also B[a]P-treated mice adenoma (**Figure 2D**), indicating that EGR1 reduction could be the early event in B[a]P-induced tumorigenesis.

To further determine whether EGR1 downregulation was involved in human lung carcinoma development, we expanded our study by investigating the expression of EGR1 in clinical cancer tissues. In eight pairs of fresh cancer and adjacent normal tissues from clinical NSCLC patients, we found the reduction of EGR1 expression in cancer tissues (**Figure S3A**). TCGA (The Cancer Genome Atlas) database and the other two datasets supported in Lung Cancer Explorer confirmed that EGR1 was downregulated in NSCLC patient tissues compared to normal tissues (**Figures 2E** and **S3B, C**). Collectively, the results indicated that the inhibition of EGR1 was involved in cell malignant transformation and mice lung tumorigenesis induced by BPDE/B[a]P exposure. The EGR1 reduction was also observed in clinical cancer tissues. The above data suggested that EGR1 could have a tumor-suppressive role in the lung cancer process.

TABLE 1 | Association of immunohistochemical staining for EGR1 with the tumor clinic pathological characteristic.

Clinicopathological features	Case N. (%)	Egr1 expression		*p*-value
		High	Low	
Gender				
Male	63 (55)	27	36	
Female	51 (45)	20	31	0.296
Age				
Mean (Range)	62 (37-85)			
<60	65 (57)	26	39	
>60	49 (43)	21	28	0.476
Tumor size[a]				
<2.5cm	46 (51)	21	25	
>2.5cm	45 (49)	19	26	0.565
Depth of invasion				
T1	46 (40)	38	16	
T2	53 (46)	28	25	
T3	11 (10)	1	10	
T4	4 (4)	2	2	0.013*
Lymph node metastasis				
N0	50 (44)	31	19	
N1	29 (25)	7	22	
N2	35 (31)	9	26	0.000**
Distant metastasis				
M0	107 (94)	44	63	
M1	7 (6)	3	4	0.750
TNM stage				
I	44 (39)	29	15	
II	29 (25)	8	21	
2III	36 (32)	8	28	
IV	5 (4)	2	3	0.000**
Histological grade[b]				
High	31 (28)	19	12	
Moderate	63 (58)	25	38	
Poor	15 (14)	3	12	0.003*

[a]*23 cases without tumor size.*
[b]*5 cases without tumor histological grade.*
**P < 0.05 and **P < 0.01.*

EGR1 Reduction Mediates BPDE-Induced Malignant Transformation

To investigate the potential role of EGR1 downregulation in lung tumorigenic effects upon BPDE exposure, we established stable EGR1 overexpression models in BPDE-induced transformed cells with lenti-EGR1 lentivirus (**Figure S4A**). The ectopic expression of EGR1 led to a reduced malignancy in BPDE-induced transformed cells (**Figure 3**). Moreover, EGR1 overexpression reduced the cell migration ability (**Figures 3A–C**) and xenograft tumor growth (**Figures 3D, E**). The suppressive effect of EGR1 on

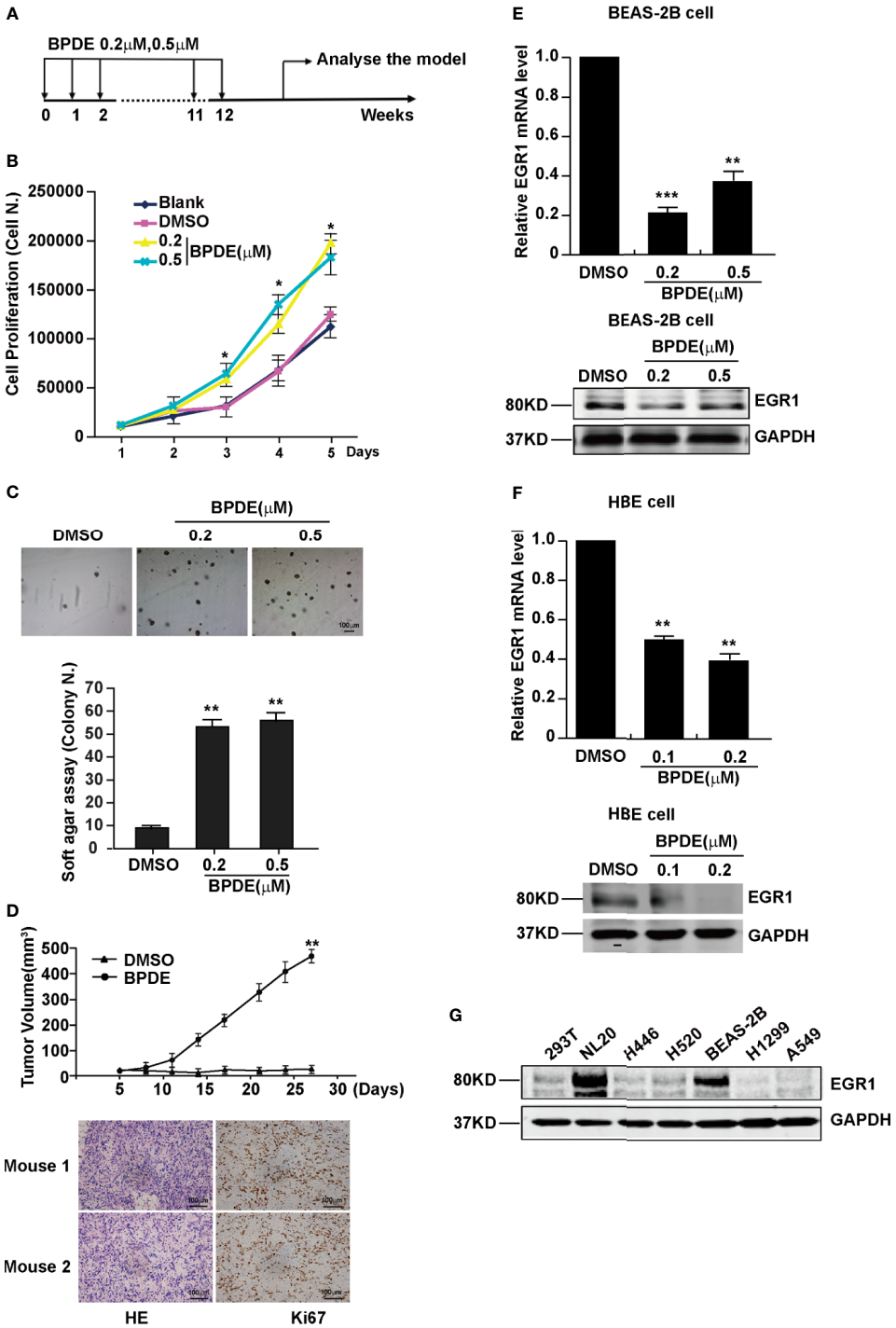

FIGURE 1 | EGR1 was downregulated in BPDE-induced malignant transformation of normal human lung epithelial cells. **(A)** Schematic map of BPDE-induced malignant transformation model. **(B)** Cell proliferation ability of BPDE-treated and control cells. **(C)** Cell anchorage-independent growth in soft agar. Top, representative images; bottom, quantitative results of cell colony per field. **(D)** Top, Tumor growth curve of the transformed cells induced by BPDE and control cells injected subcutaneously in nude mice (n = 12 tumors per group); bottom, representative photos of the HE staining and Ki67 immunohistochemical staining of the tumor mass. **(E, F)** EGR1 expression analyzed by qRT-PCR and Western Blot in transformed BEAS-2B and HBE cells. **(G)** Egr-1 expression in different lung epithelial and lung cancer cells. Normal bronchial epithelial cell: NL-20, BEAS-2B; lung cancer cell: H446, H520, H1299, A549. The analyses were repeated three times, and the results were expressed as mean ± SD. $^{*}P < 0.05$, $^{**}P < 0.01$ and $^{***}P < 0.001$.

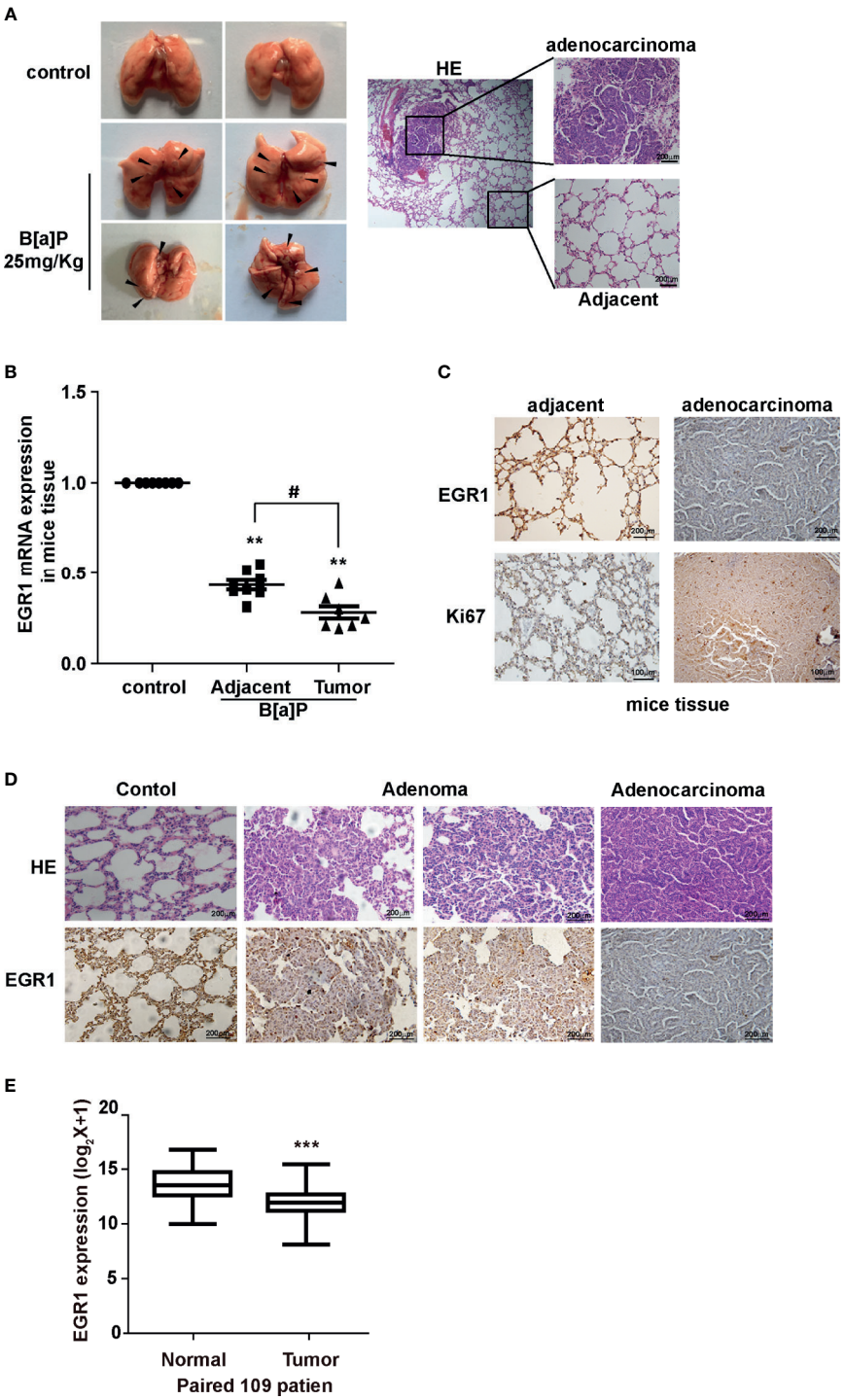

FIGURE 2 | B[a]P downregulated EGR1 expression *in vivo*. **(A)** B[a]P-induced A/J mice lung tumorigenesis. Left, representative images of primary lung tumor in mice with or without B[a]P treatment (25mg/kg); right, representative images of HE staining. **(B)** EGR1 mRNA expression in B[a]P-induced murine lung tumor and adjacent normal tissues, vehicle lung tissues. **(C, D)** Representative images of EGR1, Ki67 immuno-histochemical staining of B[a]P-treated murine lung tumor tissues and adjacent tissues, vehicle lung tissues. **(E)** Analysis of the TCGA database of EGR1 mRNA expression in paired lung cancer and normal tissues. The analyses were repeated three times, and the results were expressed as mean ± SD. $^{\#}P < 0.05$, $^{**}P < 0.01$, and $^{***}P < 0.001$.

cell malignant phenotypes was further confirmed by EGR1 knockdown. EGR1 shRNAs introduction through lentiviral vectors resulted in an increased malignancy of BEAS-2B cells (**Figures S4C–E**). Moreover, the rescue of EGR1 also reversed the effect of EGR1-knockdown in promoting cell transformation (**Figures S4F, G**). The knockdown efficiency of EGR1 was supported in **Figure S4B**. Our results suggested that EGR1 downregulation was critical for promoting BPDE-induced cell malignant transformation.

mir-377-3p Targets EGR1 and Induces its Inhibition Following BPDE Exposure

Notably, we found that the expression of EGR1 was inhibited during the BPDE-induced cell malignant transformation (data

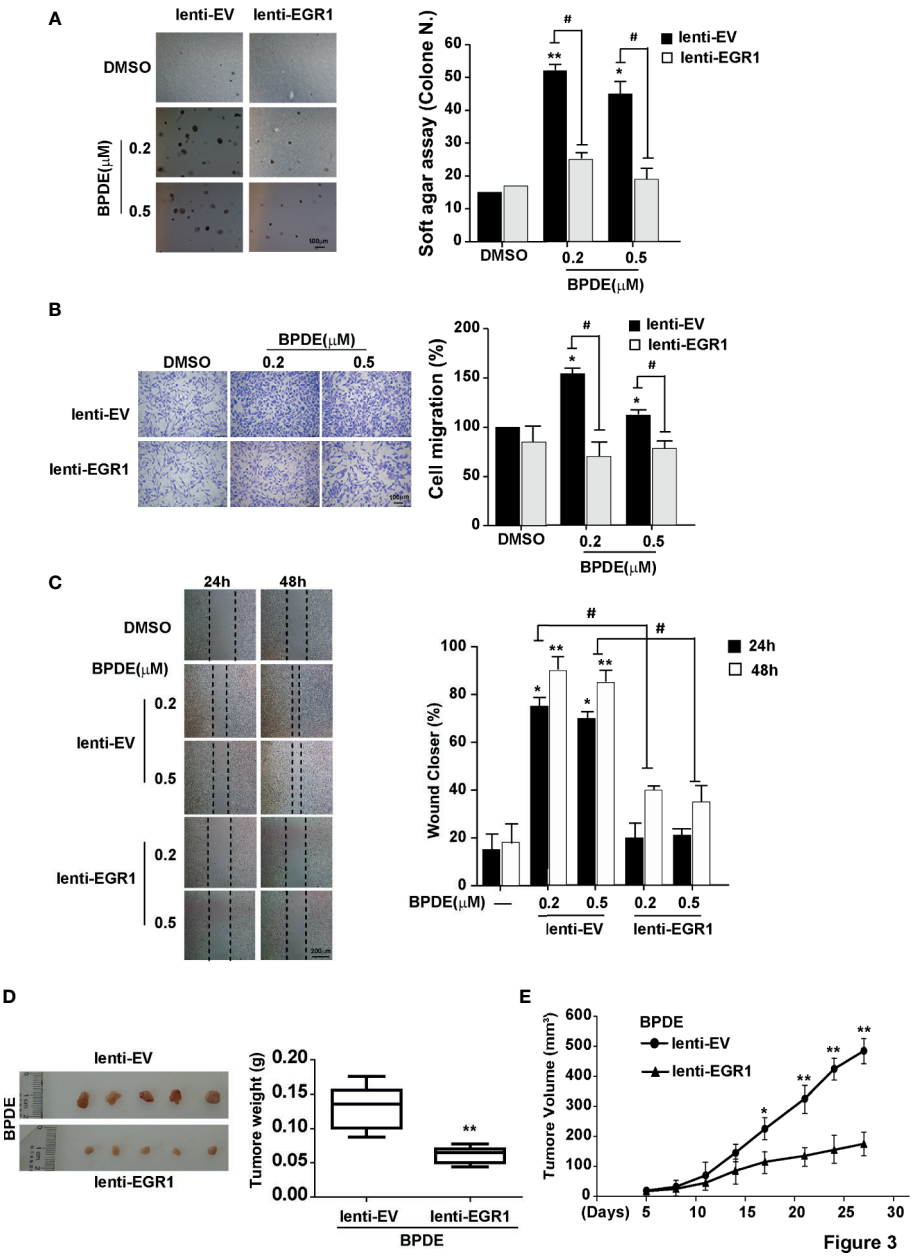

FIGURE 3 | EGR1 downregulation is crucial for BPDE-induced cell malignant transformation. **(A)** Soft-agar colony formation assays of BPDE-induced transformed cells infected with EGR1 overexpression lentivirus. Left, representative images; right, quantitative results of cell colony per field. **(B, C)** Left, representative images of transwell migration and wound healing assays; right, relative numbers of migration cell and percentage wound closure after treatment. **(D)** Representative images of xenograft tumors in nude mice at 4 weeks after inoculation (Left) and the tumor weight of BPDE-induced transformed cells infected with EGR1 overexpression. **(E)** Tumor growth curve of xenograft assays (n = 10 tumors per group). The analyses were repeated three times, and the results were expressed as mean ± SD. $^{\#}$,$^{*}P < 0.05$ and $^{**}P < 0.01$.

not shown). To investigate the molecular mechanism underlying EGR1 reduction upon BPDE treatment, we first evaluated EGR1 promoter DNA methylation level by bisulfite sequencing PCR. The DNA methylation level of the EGR1 promoter sequence did not change after BPDE exposure (**Figure S3D**). Over the past decade, it has been widely reported that miRNAs regulate gene expression by recognizing the 3'UTR sequence. Using the microRNA database and target prediction tools (miRanda, PicTar, and TargetScan), we predicted the potential microRNAs that could target EGR1 and regulate its mRNA transcription. qRT-PCR revealed that miR-377-3p levels were markedly increased in BPDE-treated cells (**Figure 4A**). Transient transfection with mimics and inhibitor of miR-377-3p showed that miR-377-3p regulates EGR1 expression (**Figures 4B, C**).

To further identify the effect of miR-377-3p on EGR1 expression regulation, we constructed the luciferase reporter containing wild-type regulatory sequence with or without EGR1 binding site mutation (**Figure 4D**). The result showed that miR-377-3p mimic reduced the reporter activity of the full-length EGR1 3'UTR-containing luciferase construct, and the inhibitor of miR-377-3p augmented the reporter activity in BEAS-2B and 293T cells. The effect of miR-377-3p on the reporter activity was abrogated with the mutant-type EGR1 3'UTR-containing luciferase construct (**Figures 4E, F**). These results indicated that miR-377-3p mediated the downregulation of EGR1 in BPDE-induced malignant transformed cells by directly targeting its 3'UTR sequence.

mir-377-3p Antagomir Rescued the Effect of EGR1 Downregulation in Cell Malignant Transformation and Lung Carcinogenesis

To detect whether the inhibition of miR-377-3p allows for the re-expression of EGR1 and reduces the malignancy of BPDE-induced transformed cells, we transfected the cells with miR-377-3p antagomir. Our results revealed that the antagomir of miR377-3p reduced the malignancy phenotypes of the transformed cells induced by BPDE exposure (**Figures 5A–D**). Moreover, miR-377-3p upregulation was identified in mice lung tumor tissues induced by B[a]P, concomitantly with EGR1 downregulation (**Figure 5E**). Furthermore, we observed a negative relevance between EGR1 and miR-377-3p in mice lung tumor tissues by the correlation analysis (**Figure 5F**). Consistent with our findings, the TCGA database analysis revealed the increase of miR-377-3p and the decrease of EGR1 in human lung adenocarcinoma tissues (**Figures 5G, H**). Besides, the expression of EGR1 and miR-377-3p in fresh lung cancer tissues also showed a negative relevance (**Figure S5A**).

To confirm the tumor repressive effect of EGR1 in NSCLC, we performed IHC staining to evaluate the clinical relevance of EGR1 expression. Our results showed a high EGR1 immunoreactivity in the nuclei of adjacent normal cells compared with cancer cells. In 114 paired cases, EGR1 was significantly inhibited in tumor tissues (**Figures 5I, J** and **S5B**). EGR1 expression was negatively associated with tumor invasion, lymph node status, histological grade, and TNM stage (**Table 1**). Our results suggested that EGR1 functions as an onco-suppressor, and the inhibition of EGR1 was associated with tumor aggressiveness in lung cancer. Taken together, our results suggest that the upregulation of miR-377-3p inhibits EGR1 transcription, which is implicated in BPDE/B[a]P-induced cell malignant transformation and lung tumorigenesis.

EGR1 Inhibition is Involved in the Regulation of Wnt/β-Catenin Transduction in PAHs-Induced Tumorigenesis

EGR1 is an important transcription factor for regulating the cell cycle, differentiation, apoptosis, and stress. To identify the potential EGR1-downstream genes involved in the BPDE/B[a]P-induced tumorigenesis, we performed the RNA-sequencing by knocking down EGR1 expression. As expected, Kyoto Encyclopedia of Genes and Genomes (KEGG) analysis indicated that the Wnt/β-catenin pathway is one of the most significantly altered gene set concepts in EGR1 knockdown cells, and gene set enrichment analysis (GSEA) revealed a large fraction of Wnt/β-catenin downstream genes that displayed significant alterations (**Figures 6A, B**). Moreover, we also observed the upregulation of β-catenin in BPDE-induced malignant transformed cells and mice primary lung cancer tissue (**Figures 6C–E**). By transient transfection, EGR1 overexpressing led to a reduction of CTNNB1 gene expression. Moreover, EGR1 knockdown upregulated the CTNNB1 gene expression (**Figure 6F**). Also, the rescue of EGR1 expression abrogated the upregulation and nuclear localization of β-catenin induced by BPDE exposure (**Figures 6G, H**). These data suggested that the Wnt/β-catenin pathway is the potential downstream signal in EGR1-mediated cell malignant transformation.

Furthermore, we detected the most altered genes of RNA-sequencing by knocking down EGR1 in the transformed cells. Our result revealed that ATF3 and ANKRD1 were downregulated in malignant cells and mice primary lung cancer tissues induced by PAHs (**Figures S5C, D**). Ectopic expression of EGR1 resulted in the upregulation of ATF3 and ANKRD1. Moreover, siRNA of EGR1 reduced the expression of ATF3 and ANKRD1 (**Figure S5E**). Besides, the rescue of EGR1 expression in BPDE-induced transformed cells abrogated the inhibition of ATF3 and ANKRD1 expression induced by BPDE (**Figure S5F**). To sum up, our data indicated that the downregulation of EGR1 could alter the downstream cell signals and the expression of its target genes to contribute to the cell malignant transformation and lung carcinogenesis.

DISCUSSION

B[a]P can directly induce lung carcinogenesis by inducing DNA damage and activating the signaling pathways (26–28). This study further investigated early events and the molecular mechanisms of gene dysregulation that lead to cell malignant transformation and lung tumorigenesis following B[a]P/BPDE exposure. We discovered that B[a]P/BPDE treatment led to miR-377-3p induction, which targeted EGR1-3'UTR and inhibited its expression, subsequently resulting in the activation of Wnt/β-catenin signal and promotion of cell malignant transformation, thus further contributing to lung tumorigenesis. Consequently,

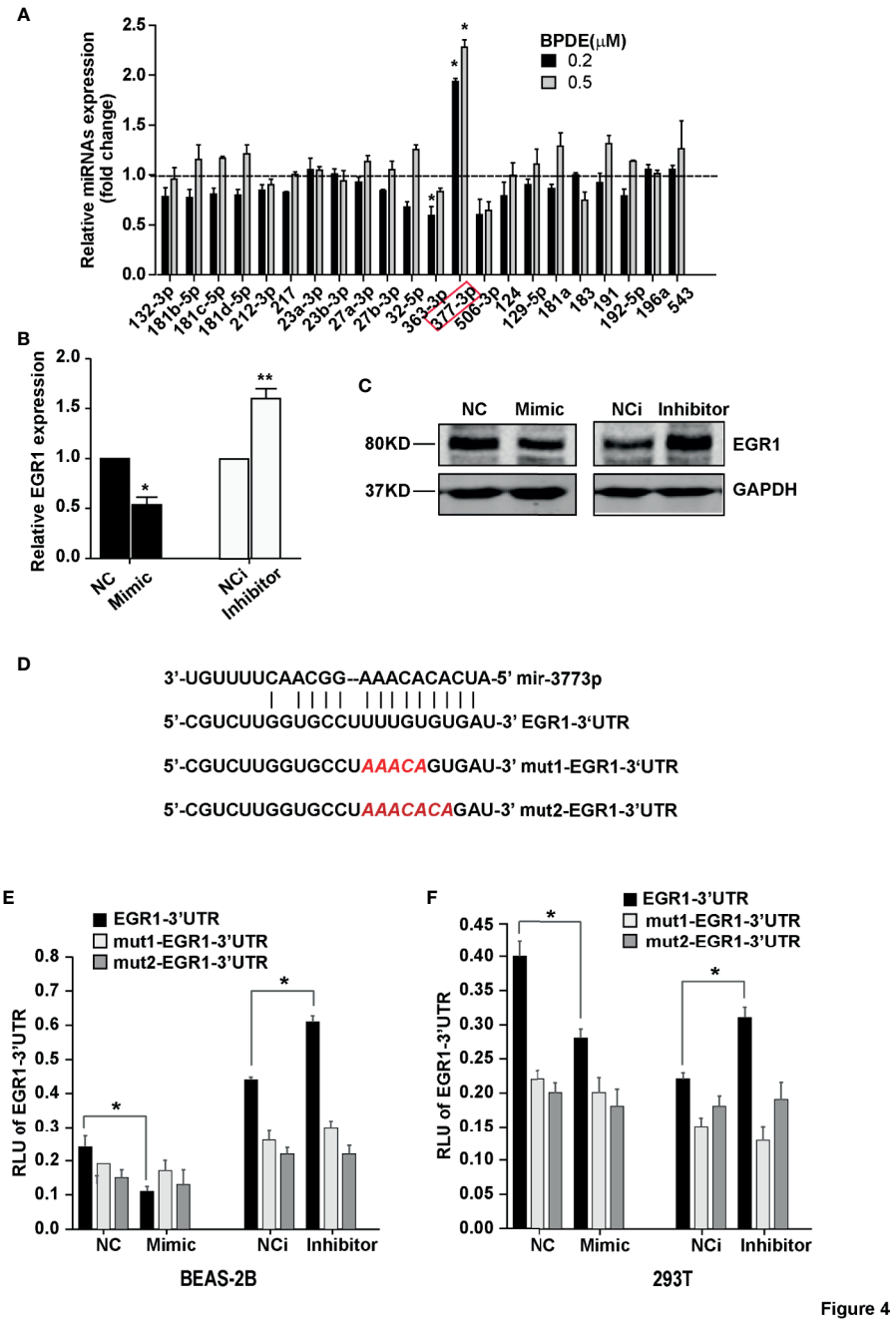

Figure 4

FIGURE 4 | MiR-377-3p activation mediated EGR1 inhibition following BPDE exposure. **(A)** Expression profile of predicted miRNAs in BPDE-treated BEAS-2B cells by qRT-PCR. **(B, C)** EGR1 expression after transfection of miR-377-3p mimic and inhibitor in BEAS-2B cells was analyzed by QRT-PCR and Western blot. **(D)** The putative target site of miR-377-3p in the 3'UTR of EGR1 (upper panel); red letters indicate the mutant luciferase reporter gene sequence (lower panel). **(E, F)** EGR1 3'UTR luciferase reporter assays in BEAS-2B cells and 293T cells. The analyses were repeated three times, and the results were expressed as mean ± SD. *$P < 0.05$ and **$P < 0.01$.

EGR1 could be considered a potential target for B[a]P initiation of lung carcinogenic actions.

As a transcription factor, EGR1 has a crucial role in human cancers. EGR1 has been increasingly attracting research attention due to its tumor-suppressing role in the occurrence and development of tumors. The expression of EGR1 decreases or even disappears in a variety of human malignancies, and its expression level is associated with tumor sensitivity to

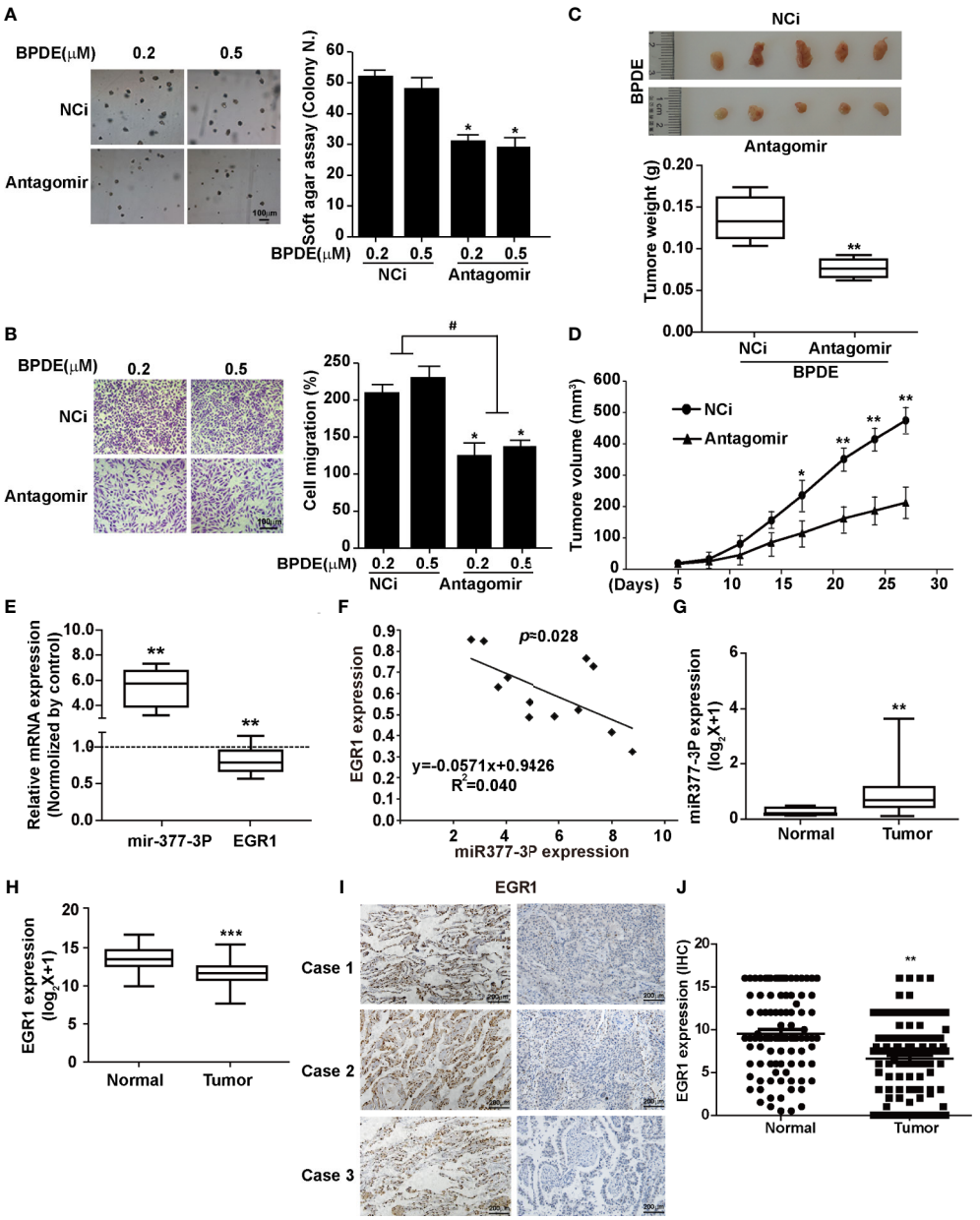

FIGURE 5 | MiR-377-3p antagomir rescued the effect of EGR1 downregulation in cell malignant transformation and lung carcinogenesis. **(A)** Soft-agar colony formation assays. Left, representative images; right, quantitative results of cell colony per field. **(B)** Transwell migration assays. Left, representative images; right, quantitative results of migratory cells per field. **(C)** Representative xenograft tumor images at 4 weeks after inoculation (top) and tumor weight (bottom) of BPDE-induced transformed cells treated with miRNA-377-3p antagomir or control. **(D)** The tumor growth curve of xenograft. **(E)** MiR-377-3p expression and EGR1 mRNA expression in B[a]P-induced murine lung cancer tissues by qRT-PCR. The analyses were repeated three times, and the results were expressed as mean ± SD. **(F)** The correlation analysis of EGR1 and miR-377-3p mRNA expression in mice carcinogenesis model. Y-axis showed EGR1 mRNA expression; X-axis showed miR-377-3p mRNA expression. **(G, H)** TCGA database analysis of miR-377-3p expression and EGR1 mRNA expression in human lung adenocarcinoma tissues. **(I)** Representative image of IHC staining of EGR1 in human lung cancer tissues. **(J)** Quantification of EGR1 staining in the adjacent normal lung epithelial cells and lung cancer cells in 114 paired patient tissues. $^{\#}$,$^{*}P < 0.05$, $^{**}P < 0.01$, and $^{***}P < 0.001$.

chemotherapy (29). EGR1 depletion has been associated with tumor anti-apoptotic and invasion events, whereas its overexpression may depress the tumorigenicity and metastasis in different cancer cells, including lung cancer (30). Mechanistically, EGR1 can directly transactivate P53 and PTEN, implicated in the proliferation inhibition of lung tumor cells (31, 32). It can also suppress the EMT transition and cell migration in lung cancer by regulating TGFβ activity (33). Recent studies have

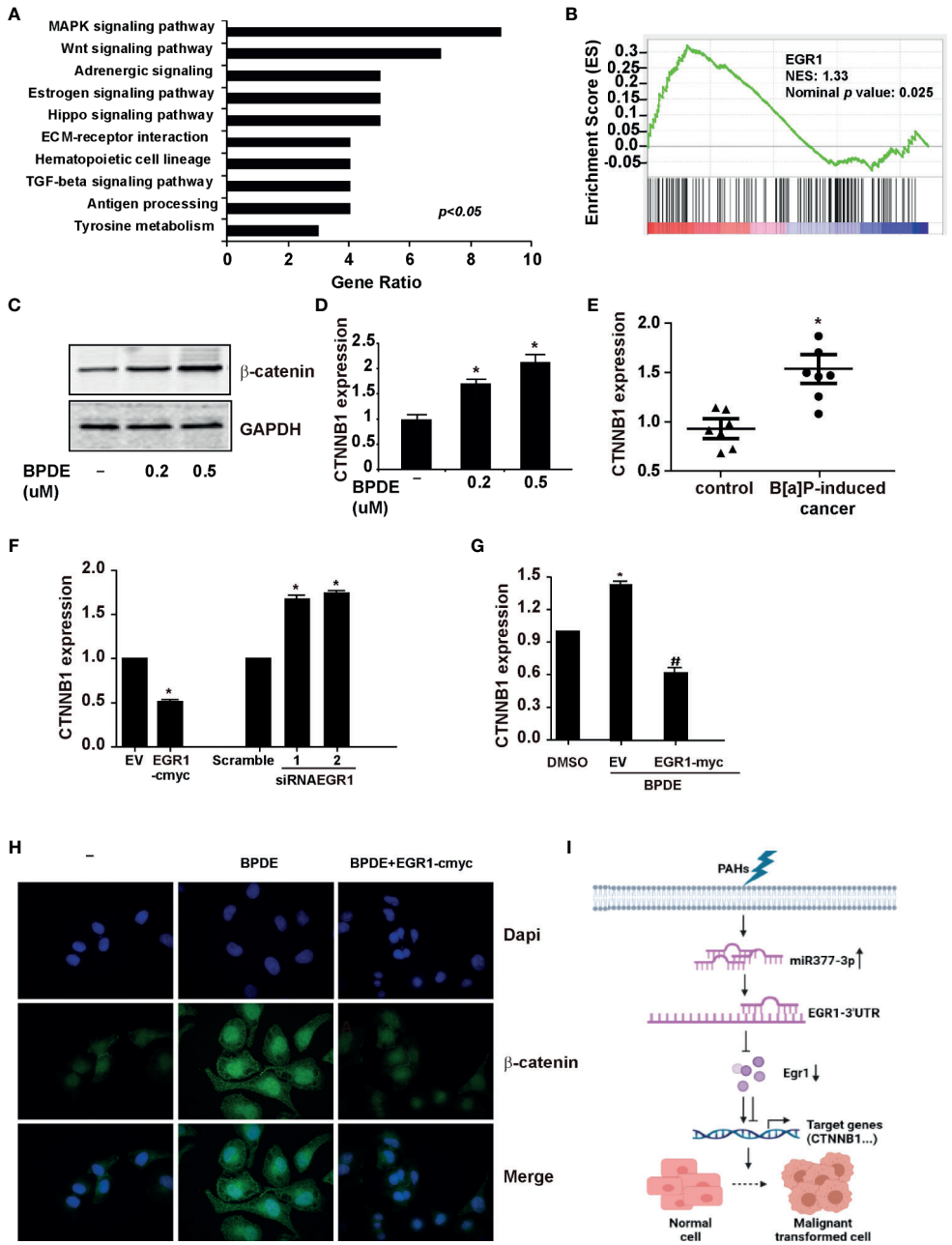

FIGURE 6 | EGR1 inhibition was involved in the regulation of Wnt/β-catenin transduction in PAH-induced tumorigenesis. **(A, B)** KEGG analysis of differentially expressed genes and Gene set enrichment plots of differentially expressed genes belonging to the Wnt pathway in EGR1 knockdown cells. **(C, D)** β-catenin protein content and mRNA gene expression of CTNNB1 in BPDE-induced transformed cells. **(E)** mRNA level of CTNNB1 gene in mice primary lung cancer tissues. **(F, G)** CTNNB1 gene expression in BEAS-2B cells upon EGR1 overexpression and knockdown and in BPDE-induced transformed cells upon EGR1 overexpression. **(H)** Immunostaining of β-catenin in malignant transformed cells with or without EGR1 overexpression. **(I)** Schematic diagram of the regulatory mechanism of miRNA-377-3p/EGR1 axis in tumorigenesis. The analyses were repeated three times, and the results were expressed as mean ± SD. $^{\#}$,$^{*}P < 0.05$.

shown that EGR1 can directly and negatively regulate cell growth in different epithelial tumor cell lines (34). It can also regulate KRT18 expression to inhibit the malignancy of human NSCLC cells (35). Our data showed that EGR1 was strongly decreased in the early stage of malignant cell transformation upon BPDE exposure. The inhibition of EGR1 promoted the progression of BPDE-induced tumorigenicity. Moreover, the downregulation of EGR1 was also confirmed in B[a]P-induced lung tumors *in vivo*.

The results indicated that EGR1 has a tumor repressive effect in cell malignant transformation and lung tumorigenesis upon B[a]P/BPDE treatment.

DNA methylation and miRNA dysregulation are important molecular mechanisms of gene expression, which are critical for epigenetic regulation in tumor formation and development by negatively regulating targeting downstream genes (36, 37). Recent studies reported that miR-301b, miR-191, and miR-146a could target EGR1 mRNA and inhibit its expression, thus contributing to oncogenesis (16, 38, 39). In this study, EGR1 was persistently decreased after BPDE exposure but without variation of its promoter DNA methylation level. miRNA screening analysis demonstrated that miR-377-3p is a new regulator of EGR1 by directly binding to its 3'UTR. miR-377-3p was significantly increased in BPDE-induced malignant transformed cells, as well as in the lung tumor tissues of B[a]P-treated A/J mice. Antagonized miR-377-3p reversed the effect of EGR1 in cell malignant transformation, thus supporting the critical role of miR-377-3p in regulating EGR1 expression to promote cell transformation and tumor formation. Recent studies reported that miR-377 displays an ambiguous role in different cancers. miR-377-3p can drive malignancy characteristics by upregulating GSK-3β expression and activating the NF-κB pathway in CRC cells (22). It can also target the pro-oncogenic genes, like E2F3, VEGF, and CDK6, or negatively regulate the Wnt/β-catenin signaling to suppress the proliferation of cancer cells (40–43). However, the dual effect of miR-377 in tumor inhibition and promotion needs to be further explored.

Clinical studies reported that the depletion of EGR1 sensitizes the chemotherapy of cisplatin in ovarian tumors (44). The low levels of EGR1, associated with the expression of PTEN, can predict poor outcomes after surgical resection of NSCLC (45). In this study, clinic tissue analysis showed a downregulation of EGR1 expression in cancer tissues compared with the normal tissue. The repression of EGR1 was associated with the local invasion depth, lymph nodes, and TNM stages. It was also negatively associated with histological grade (**Table 1**). Our result confirmed that the deactivation of EGR1 was associated with cancer aggressiveness.

Furthermore, it is reported that EGR1 can be increased by chemotherapy, and negatively regulate the Wnt/β–catenin signaling pathway in CML cells (46). In this study, we observed an enrichment of Wnt/β–catenin downstream genes after EGR1 knockdown. Besides, β–catenin, the key effector of canonical Wnt signaling, was activated in malignant transformed cells and lung cancer tissues following EGR1 inhibition. The rescue of EGR1 expression reversed the upregulation and nuclear staining of β–catenin after BPDE exposure. The Wnt/β–catenin pathway is a cell signaling that promotes cancer initiation and development. It has an important role in crucial cellular processes, including cell fate determination, embryonic development, homeostasis, motility, polarity, and stem cell renewal (47). It has also been reported that the activation of canonical Wnt/β-catenin signaling is critical for the initiation and progression of NSCLC (48). In patient-derived xenograft models of lung cancer, the activation of WNT/β-catenin signaling and nuclear β-catenin staining was associated with a poor prognosis in patients with lung cancer (49). Previous studies also reported that the Wnt/β-catenin pathway contributes to the induction of EMT by transactivating several EMT-related transcriptional factors, such as Snail, Slug, Twist, ZEB1, and ZEB2 in lung adenocarcinoma (50). Moreover, we also observed that ANKRD1 and ATF3, as the target genes of EGR1, were significantly downregulated in malignant transformed cells and mice lung cancer tissues. ATF3, a highly conserved transcription factor, was described as a principal target of EGR1 and discussed as a tumor suppressor and promoter (51–53). A recent study also reported that ATF3 and EGR1 are involved at the beginning of the inflammatory processes related to cancer (54). ANKRD1 is a tumor-suppressive downstream gene of the Hippo pathway, downregulated in different human cancers (55, 56). A previous study demonstrated that ANKRD1 could be inhibited by lncRNA, resulting in the promotion of pancreatic cancer proliferation and metastasis (57). Therefore, EGR1 could regulate its downstream signals and target genes, thus having a tumor-suppressive role in human lung cancer.

In summary, our current study demonstrated the regulation mechanism of EGR1 inhibition induced by miR-377-3p activation following exposure to environmental carcinogen B[a]P/BPDE. We also discovered that EGR1 has a repressive effect on lung tumorigenesis by regulating the Wnt/β-catenin signaling pathway (**Figure 6I**). Our findings provided a novel molecular regulatory mechanism through which the miR-377-3p/EGR1 axis was implicated in cell malignant transformation and tumorigenesis induced by PAH.

DATA AVAILABILITY STATEMENT

The datasets presented in this study can be found in online repositories. The names of the repository/repositories and accession number(s) can be found in the article/**Supplementary Material**.

ETHICS STATEMENT

The studies involving human participants were reviewed and approved by the ethics committee of the Second Affiliated Hospital of Zhejiang University. The patients/participants provided their written informed consent to participate in this study. The animal study was reviewed and approved by The Committee on the Use of Animals of Zhejiang University.

AUTHOR CONTRIBUTIONS

XK: Conceptualization, Investigation, Resources, and Writing - original draft. LH and RW: Investigation, Methodology, and Validation. YS and LF: Software, Validation. ZW: Methodology, Validation. JShe: Review and Editing, Supervision, and Project administration. JSha: Review and Editing, Resources, and Supervision. HQ: Writing - Review and Editing, Investigation, Methodology, Formal analysis, Project administration, and Funding

acquisition. All authors contributed to the article and approved the submitted version.

FUNDING

This work was supported by the Zhejiang Provincial Natural Science Foundation of China (No. LY18H160024, LY20H160040), the National Natural Science Foundation of China (No. 81472543, No. 81772919), the National Key R&D Program of China (2016YFC1303401), and the Zhejiang Medical and Health Science and Technology Foundation (2018KY119).

SUPPLEMENTARY MATERIAL

The Supplementary Material for this article can be found online at: https://www.frontiersin.org/articles/10.3389/fonc.2021.699004/full#supplementary-material

REFERENCES

1. McGuire S. World Cancer Report 2014. Geneva, Switzerland World Health Organization, International Agency for Research on Cancer, WHO Press, 2015. *Adv Nutr* (2016) 7(2):418–9.
2. Bray F, Ferlay J, Soerjomataram I, Siegel RL, Torre LA, Jemal A. Global Cancer Statistics 2018: GLOBOCAN Estimates of Incidence and Mortality Worldwide for 36 Cancers in 185 Countries. *CA: A Cancer J Clin* (2018) 0:1–31. doi: 10.3322/caac.21492
3. IARC Working Group on the Evaluation of Carcinogenic Risks to Humans. Outdoor Air Pollution. *IARC Monogr Eval Carcinog Risks Hum* (2016) 109:9–444.
4. Chen H, Ma S, Yu Y, Liu R, Li G, Huang H, et al. Seasonal Profiles of Atmospheric PAHs in an E-Waste Dismantling Area and Their Associated Health Risk Considering Bioaccessible PAHs in the Human Lung. *Sci Total Environ* (2019) 683:371–9. doi: 10.1016/j.scitotenv.2019.04.385
5. Hong WJ, Jia H, Ma W, Sinha RK, Moon H, Nakata H, et al. Distribution, Fate, Inhalation Exposure and Lung Cancer Risk of Atmospheric Polycyclic Aromatic Hydrocarbons in Some Asian Countries. *Environ Sci Technol* (2016) 50(13):7163–74. doi: 10.1021/acs.est.6b01090
6. Kasala ER, Bodduluru LN, Barua CC, Sriram CS, Gogoi R. Benzo(a)pyrene Induced Lung Cancer: Role of Dietary Phytochemicals in Chemoprevention. *Pharmacol Rep* (2015) 67(5):996–1009. doi: 10.1016/j.pharep.2015.03.004
7. He Z, Li D, Ma J, Chen L, Duan H, Zhang B, et al. TRIM36 Hypermethylation Is Involved in Polycyclic Aromatic Hydrocarbons-Induced Cell Transformation. *Environ Pollut* (2017) 225:93–103. doi: 10.1016/j.envpol.2017.03.001
8. Shahid A, Ali R, Ali N, Hasan SK, Bernwal P, Afzal SM, et al. Modulatory Effects of Catechin Hydrate Against Genotoxicity, Oxidative Stress, Inflammation and Apoptosis Induced by Benzo(a)Pyrene in Mice. *Food Chem Toxicol* (2016) 92:64–74. doi: 10.1016/j.fct.2016.03.021
9. Li E, Xu Z, Zhao H, Sun Z, Wang L, Guo Z, et al. Macrophages Promote Benzopyrene-Induced Tumor Transformation of Human Bronchial Epithelial Cells by Activation of NF-κb and STAT3 Signaling in a Bionic Airway Chip Culture and in Animal Models. *Oncotarget* (2015) 6(11):8900–13. doi: 10.18632/oncotarget.3561
10. Bahrami S, Drabløs F. Gene Regulation in the Immediate-Early Response Process. *Adv Biol Regul* (2016) 62:37–49. doi: 10.1016/j.jbior.2016.05.001
11. Gitenay D, Baron VT. Is EGR1 a Potential Target for Prostate Cancer Therapy? *Future Oncol* (2009) 5:993–1003. doi: 10.2217/fon.09.67
12. Calogero A, Arcella A, De Gregorio G, Porcellini A, Mercola D, Liu C, et al. The Early Growth Response Gene EGR-1 Behaves as a Suppressor Gene That is Down-Regulated Independent of ARF/Mdm2 But Not P53 Alterations in Fresh Human Gliomas. *Clin Cancer Res* (2001) 7(9):2788–96.
13. Baron V, De Gregorio G, Krones-Herzig A, Virolle T, Calogero A, Urcis R, et al. Inhibition of Egr-1 Expression Reverses Transformation of Prostate Cancer Cells *In Vitro* and *In Vivo*. *Oncogene* (2003) 22(27):4194–204. doi: 10.1038/sj.onc.1206560
14. Sun M, Nie FQ, Zang C, Wang Y, Hou J, Wei C, et al. The Pseudogene DUXAP8 Promotes Non-Small-Cell Lung Cancer Cell Proliferation and Invasion by Epigenetically Silencing EGR1 and RHOB. *Mol Ther* (2017) 25 (3):739–51. doi: 10.1016/j.ymthe.2016.12.018
15. Huang RP, Fan Y, Belleet I, Niemeyer C, Gottardis MM, Mercola D, et al. Decreased Egr-1 Expression in Human, Mouse and Rat Mammary Cells and Tissues Correlates With Tumor Formation. *Int J Cancer* (1997) 72:102–9. doi: 10.1002/(SICI)1097-0215(19970703)72:1<102::AID-IJC15>3.0.CO;2-L
16. Yan L, Wang Y, Liang J, Liu Z, Sun X, Cai K. MiR-301b Promotes the Proliferation, Mobility, and Epithelial-to-Mesenchymal Transition of Bladder Cancer Cells by Targeting EGR1. *Biochem Cell Biol* (2017) 95(5):571–7. doi: 10.1139/bcb-2016-0232
17. O'Connell RM, Rao DS, Chaudhuri AA, Baltimore D. Physiological and Pathological Roles for microRNAs in the Immune System. *Nat Rev Immunol* (2010) 10(2):111–22. doi: 10.1038/nri2708
18. Ventura A, Jacks T. MicroRNAs and Cancer: Short RNAs Go a Long Way. *Cell* (2009) 136(4):586–91. doi: 10.1016/j.cell.2009.02.005
19. Hanahan D, Weinberg RA. Hallmarks of Cancer: The Next Generation. *Cell* (2011) 144(5):646–74. doi: 10.1016/j.cell.2011.02.013
20. Chen G, Lu L, Liu C, Shan L, Yuan D. MicroRNA-377 Suppresses Cell Proliferation and Invasion by Inhibiting TIAM1 Expression in Hepatocellular Carcinoma. *PloS One* (2015) 10(3):e0117714. doi: 10.1371/journal.pone.0117714
21. Wang R, Ma Y, Yu D, Zhao J, Ma P. MiR-377 Functions as a Tumor Suppressor in Human Clear Cell Renal Cell Carcinoma by Targeting ETS1. *BioMed Pharmacother* (2015) 70:64–71. doi: 10.1016/j.biopha.2015.01.012
22. Liu WY, Yang Z, Sun Q, Yang X, Hu Y, Xie H, et al. miR-377-3p Drives Malignancy Characteristics *via* Upregulating GSK-3β Expression and Activating NF-κb Pathway in hCRC Cells. *J Cell Biochem* (2018) 119:2124–34. doi: 10.1002/jcb.26374
23. Sandhu V, Bowitz Lothe IM, Labori KJ, Lingjaerde OC, Buanes T, Dalsgaard AM, et al. Molecular Signatures of mRNAs and miRNAs as Prognostic Biomarkers in Pancreatobiliary and Intestinal Types of Periampullary Adenocarcinomas. *Mol Oncol* (2015) 9(4):758–71. doi: 10.1016/j.molonc.2014.12.002
24. Caiment F, Gaj S, Claessen S, Kleinjans J. High-Throughput Data Integration of RNA-miRNA-circRNA Reveals Novel Insights Into Mechanisms of Benzo [a]Pyrene-Induced Carcinogenicity. *Nucleic Acids Res* (2015) 43(5):2525–34. doi: 10.1093/nar/gkv115
25. Marrone AK, Tryndyak V, Beland FA, Pogribny IP. MicroRNA Responses to the Genotoxic Carcinogens Aflatoxin B1 and Benzo[a]pyrene in Human HepaRG Cells. *Toxicol Sci* (2016) 149(2):496–502. doi: 10.1093/toxsci/kfv253
26. Wang GZ, Cheng X, Zhou B, Wen Z, Huang Y, Chen H, et al. CXCL13 in Lung Cancers Associated With Environmental Polycyclic Aromatic Hydrocarbons Pollution. *Elife* (2015) pii:e09419. doi: 10.7554/eLife.09419
27. Li J, Tang MS, Liu B, Shi X, Huang C. A Critical Role of PI-3k/Akt/JNKs Pathway in Benzo[a]Pyrene Diol-Epoxide (B[a]PDE)-Induced AP-1 Transactivation in Mouse Epidermal Cl41 Cells. *Oncogene* (2004) 23 (22):3932–44. doi: 10.1038/sj.onc.1207501
28. Li W, Hu J, Adebali O, Adar S, Yang Y, Chiou Y, et al. Human Genome-Wide Repair Map of DNA Damage Caused by the Cigarette Smoke Carcinogen Benzo[a]Pyrene. *Proc Natl Acad Sci U S A* (2017) 114(26):6752–7. doi: 10.1073/pnas.1706021114
29. Calogero A, Porcellini A, Lombari V, Fabbiano C, Arcella A, Miscusi M, et al. Sensitivity to Cisplatin in Primary Cell Lines Derived From Human Glioma Correlates With Levels of EGR−1 Expression. *Cancer Cell Int* (2011) 11:5. doi: 10.1186/1475-2867-11-5
30. Hann SS, Tang Q, Zheng F, Zhao S, Chen J, Wang Z. Repression of Phosphoinositide-Dependent Protein Kinase 1 Expression by Ciglitazone *via* Egr-1 Represents a New Approach for Inhibition of Lung Cancer Cell Growth. *Mol Cancer* (2014) 13:149. doi: 10.1186/1476-4598-13-149
31. Fang L, Min L, Lin Y, Ping G, Rui W, Ying Z, et al. Downregulation of Stathmin Expression Is Mediated Directly by Egr1 and Associated With P53 Activity in Lung Cancer Cell Line A549. *Cell Signal* (2010) 22(1):166–73. doi: 10.1016/j.cellsig.2009.09.030

32. Yamamoto C, Basaki Y, Kawahara A, Nakashima K, Kage M, Izumi H, et al. Loss of PTEN Expression by Blocking Nuclear Translocation of EGR1 in Gefitinib-Resistant Lung Cancer Cells Harboring Epidermal Growth Factor Receptor-Activating Mutations. *Cancer Res* (2010) 70(21):8715–25. doi: 10.1158/0008-5472.CAN-10-0043
33. Shan LN, Song YG, Su D, Liu YL, Shi XB, Lu SJ. Early Growth Response Protein-1 Involves in Transforming Growth Factor-β1 Induced Epithelial-Mesenchymal Transition and Inhibits Migration of Non-Small-Cell Lung Cancer Cells. *Asian Pac J Cancer Prev* (2015) 16(9):4137–42. doi: 10.7314/APJCP.2015.16.9.4137
34. Kobayashi K, Sakurai K, Hiramatsu H, Inada K, Shiogama K, Nakamura S, et al. The miR-199a/Brm/EGR1 Axis Is a Determinant of Anchorage-Independent Growth in Epithelial Tumor Cell Lines. *Sci Rep* (2015) 5:8428. doi: 10.1038/srep08428
35. Zhang H, Chen X, Wang J, Guang W, Han W, Zhang H, et al. EGR1 Decreases the Malignancy of Human Non-Small Cell Lung Carcinoma by Regulating KRT18 Expression. *Sci Rep* (2014) 4:5416. doi: 10.1038/srep05416
36. Fabbri M, Calore F, Paone A. Epigenetic Regulation of miRNAs in Cancer. *Adv Exp Med Biol* (2013) 754:137–48. doi: 10.1007/978-1-4419-9967-2_6
37. Jones PA, Baylin SB. The Epigenomics of Cancer. *Cell* (2007) 128(4):683–92. doi: 10.1016/j.cell.2007.01.029
38. Gao X, Xie Z, Wang Z, Chen K, Liang K, Song Z, et al. Overexpression of miR-191 Predicts Poor Prognosis and Promotes Proliferation and Invasion in Esophageal Squamous Cell Carcinoma. *Yonsei Med J* (2017) 58(6):1101–10. doi: 10.3349/ymj.2017.58.6.1101
39. Contreras JR, Palanichamy JK, Tran TM, Fernando TR, Rodriguez-Malave NI, Goswami N, et al. MicroRNA-146a Modulates B-Cell Oncogenesis by Regulating Egr1. *Oncotarget* (2015) 6(1):11023–37. doi: 10.18632/oncotarget.3433
40. Yang B, Du K, Yang C, Xiang L, Xu Y, Cao C, et al. CircPRMT5 Circular RNA Promotes Proliferation of Colorectal Cancer Through Sponging miR-377 to Induce E2F3 Expression. *J Cell Mol Med* (2020) 24:3431–7. doi: 10.1111/jcmm.15019
41. Li B, Xu WW, Han L, Chan KT, Tsao SW, Lee NPY, et al. MicroRNA-377 Suppresses Initiation and Progression of Esophageal Cancer by Inhibiting CD133 and VEGF. *Oncogene* (2017) 36(28):3986–4000. doi: 10.1038/onc.2017.29
42. Zhang J, Zhao M, Xue ZQ, Xue Y, Wang YX. miR-377 Inhibited Tumorous Behaviors of Non-Small Cell Lung Cancer Through Directly Targeting CDK6. *Eur Rev Med Pharmacol Sci* (2016) 20(21):4494–9.
43. Huang L, Liu Z, Hu J, Luo Z, Zhang C, Wang L, et al. MiR-377-3p Suppresses Colorectal Cancer Through Negative Regulation on Wnt/β-Catenin Signaling by Targeting XIAP and ZEB2. *Pharmacol Res* (2020) 156:104774. doi: 10.1016/j.phrs.2020.104774
44. He J, Yu JJ, Xu Q, Wang L, Zheng JZ, Liu LZ, et al. Downregulation of ATG14 by EGR1-MIR152 Sensitizes Ovarian Cancer Cells to Cisplatin-Induced Apoptosis by Inhibiting Cyto-Protective Autophagy. *Autophagy* (2015) 11 (2):373–84. doi: 10.1080/15548627.2015.1009781
45. Ferraro B, Bepler G, Sharma S, Cantor A, Haura EB. EGR1 Predicts PTEN and Survival in Patients With Non-Small-Cell Lung Cancer. *J Clin Oncol* (2005) 23 (9):1921–6. doi: 10.1200/JCO.2005.08.127
46. Ma W, Liu F, Yuan L, Zhao C, Chen C. Emodin and AZT Synergistically Inhibit the Proliferation and Induce the Apoptosis of Leukemia K562 Cells Through the EGR1 and the Wnt/β−Catenin Pathway. *Oncol Rep* (2020) 43 (1):260–9. doi: 10.3892/or.2019.7408
47. Koni M, Pinnarò V, Felice Brizzi M. The Wnt Signalling Pathway: A Tailored Target in Cancer. *Int J Mol Sci* (2020) 21(20):7697. doi: 10.3390/ijms21207697
48. Yang J, Chen J, He J, Li J, Shi J, Cho WC, et al. Wnt Signaling as Potential Therapeutic Target in Lung Cancer. *Expert Opin Ther Targets* (2016) 20:999–1015. doi: 10.1517/14728222.2016.1154945
49. Ka M. Multi−layered Prevention and Treatment of Chronic Inflammation, Organ Fibrosis and Cancer Associated With Canonical WNT/β-Catenin Signaling Activation. *Int J Mol Med* (2018) 42:713–25. doi: 10.3892/ijmm.2018.3689
50. Puisieux A, Brabletz T, Caramel J. Oncogenic Roles of EMT-Inducing Transcription Factors. *Nat Cell Biol* (2014) 16:488–94. doi: 10.1038/ncb2976
51. Fan F, Jin S, Amundson SA, Tong T, Fan W, Zhao H, et al. ATF3 Induction Following DNA Damage is Regulated by Distinct Signaling Pathways and Over-Expression of ATF3 Protein Suppresses Cells Growth. *Oncogene* (2015) 21(49):7488–96. doi: 10.1038/sj.onc.1205896
52. Xie JJ, Xie YM, Chen B, Pan F, Guo JC, Zhao Q, et al. ATF3 Functions as a Novel Tumor Suppressor With Prognostic Significance in Esophageal Squamous Cell Carcinoma. *Oncotarget* (2014) 5(18):8569–82. doi: 10.18632/oncotarget.2322
53. Tanaka Y, Nakamura A, Morioka MS, Inoue S, Adachi MT, Yamada K, et al. Systems Analysis of ATF3 in Stress Response and Cancer Reveals Opposing Effects on Pro-Apoptotic Genes in P53 Pathway. *PloS One* (2011) 6(10): e26848. doi: 10.1371/journal.pone.0026848
54. Schoen I, Koitzsch S. ATF3-Dependent Regulation of EGR1 *In Vitro* and *In Vivo*. *ORL J Otorhinolaryngol Relat Spec* (2017) 79(5):239–25. doi: 10.1159/000478937
55. Dethlefsen C, Hansen LS, Lillelund C, Andersen C, Gehl J, Christensen JF, et al. Exercise-Induced Catecholamines Activate the Hippo Tumor Suppressor Pathway to Reduce Risks of Breast Cancer Development. *Cancer Res* (2017) 77 (18):4894–904. doi: 10.1158/0008-5472.CAN-16-3125
56. Jiménez AP, Traum A, Boettger T, Hackstein H, Richter AM, Dammann RH. The Tumor Suppressor RASSF1A Induces the YAP1 Target Gene ANKRD1 That is Epigenetically Inactivated in Human Cancers and Inhibits Tumor Growth. *Oncotarget* (2017) 8(51):88437–52. doi: 10.18632/oncotarget.18177
57. Hui B, Ji H, Xu Y, Wang J, Ma Z, Zhang C, et al. RREB1-Induced Upregulation of the lncRNA AGAP2-AS1 Regulates the Proliferation and Migration of Pancreatic Cancer Partly Through Suppressing ANKRD1 and ANGPTL4. *Cell Death Dis* (2019) 10(3):207. doi: 10.1038/s41419-019-1384-9

Conflict of Interest: The authors declare that the research was conducted in the absence of any commercial or financial relationships that could be construed as a potential conflict of interest.

frontiers in Oncology

ORIGINAL RESEARCH
published: 09 September 2021
doi: 10.3389/fonc.2021.690142

FAIM2 Promotes Non-Small Cell Lung Cancer Cell Growth and Bone Metastasis by Activating the Wnt/β-Catenin Pathway

Kelin She[1,2,3,4*†], *Wensheng Yang*[3†], *Mengna Li*[1,2,4], *Wei Xiong*[1,2,4] *and Ming Zhou*[1,2,4*]

[1] National Health Commission (NHC) Key Laboratory of Carcinogenesis, Hunan Cancer Hospital and the Affiliated Cancer Hospital of Xiangya School of Medicine, Central South University, Changsha, China, [2] Cancer Research Institute, Central South University, Changsha, China, [3] Department of Thoracic Surgery, The Affiliated Shaoyang Hospital, Hengyang Medical School, University of South China, Shaoyang, China, [4] The Key Laboratory of Carcinogenesis and Cancer Invasion of the Chinese Ministry of Education, Central South University, Changsha, China

OPEN ACCESS

Edited by:
Daniele Vergara,
University of Salento, Italy

Reviewed by:
Miguel F. Segura,
Vall d'Hebron Research Institute (VHIR), Spain
Xiaolong Yan,
Tangdu Hospital, China
Xinyuan Ding,
Suzhou Municipal Hospital, China

***Correspondence:**
Kelin She
shekelin@163.com
Ming Zhou
zhouming2001@163.com

[†]These authors have contributed equally to this work and share first authorship

Specialty section:
This article was submitted to Molecular and Cellular Oncology, a section of the journal Frontiers in Oncology

Received: 06 April 2021
Accepted: 09 August 2021
Published: 09 September 2021

Citation:
She K, Yang W, Li M, Xiong W and Zhou M (2021) FAIM2 Promotes Non-Small Cell Lung Cancer Cell Growth and Bone Metastasis by Activating the Wnt/β-Catenin Pathway. Front. Oncol. 11:690142. doi: 10.3389/fonc.2021.690142

Aim: Bone metastasis is the major reason for the poor prognosis and high mortality rate of non-small cell lung cancer (NSCLC) patients. This study explored the function and underlying mechanism of Fas apoptotic inhibitory molecule 2 (FAIM2) in the bone metastasis of NSCLC.

Methods: Samples of normal lung tissue and NSCLC tissue (with or without bone metastasis) were collected and analyzed for FAIM2 expression. HARA cells with FAIM2 overexpression and HARA-B4 cells with FAIM2 knockdown were tested for proliferation, migration, invasion, anoikis, and their ability to adhere to osteoblasts. Next, whether FAIM2 facilitates bone metastasis by regulating the epithelial mesenchymal transformation (EMT) process and Wnt/β-catenin signaling pathway were investigated. Finally, an *in vivo* model of NSCLC bone metastasis was established and used to further examine the influence of FAIM2 on bone metastasis.

Results: FAIM2 was highly expressed in NSCLC tissues and NSCLC tissues with bone metastasis. FAIM2 expression was positively associated with the tumor stage, lymph node metastasis, bone metastasis, and poor prognosis of NSCLC. FAIM2 upregulation promoted HARA cell proliferation, migration, and invasion, but inhibited cell apoptosis. FAIM2 knockdown in HARA-B4 cells produced the opposite effects. HARA-B4 cells showed a stronger adhesive ability to osteocytes than did HARA cells. FAIM2 was found to be related to the adhesive ability of HARA and HARA-B4 cells to osteocytes. FAIM2 facilitated bone metastasis by regulating the EMT process and Wnt/β-catenin signaling pathway. Finally, FAIM2 was found to participate in regulating NSCLC bone metastasis *in vivo*.

Conclusions: FAIM2 promoted NSCLC cell growth and bone metastasis by regulating the EMT process and Wnt/β-catenin signaling pathway. FAIM2 might be useful for diagnosing and treating NSCLC bone metastases.

Keywords: NSCLC, FAIM2, bone metastasis, Wnt pathway, EMT

INTRODUCTION

Lung cancer is one of the most malignant cancers and accounts for nearly 12% of all human cancers worldwide, making it the leading cause of cancer-related death in both men and women (1). In general, lung cancer can be divided into categories of non-small cell lung cancer (NSCLC) and small cell lung cancer (SCLC), which account for 85% and 15% of all cases, respectively (2). Although targeted therapy and immune therapy have progressed in recent years due to the discovery of the epidermal growth factor receptor gene (*EGFR*), K-RAS, MET, and PD-l, the overall prognosis for lung cancer patients remains unsatisfactory (3, 4). Further studies of the underlying mechanism of lung cancer carcinogenesis and progression should provide novel options for treating lung cancer.

Distant metastasis is a major reason for the death of lung cancer patients. In NSCLC patients, bone tissue is a frequent site of metastasis and accounts for 13.2% of all metastasis sites (5). Although bone metastasis is a negative prognostic factor for NSCLC, the molecular mechanism of bone metastasis remains largely unknown (6, 7). Several studies have identified the molecules involved in modulating the bone metastasis of NSCLC. For instance, an upregulation of LIGHT/tumor necrosis factor superfamily member 14 (TNFSF14) signaling was found to result in the destruction of bone homeostasis in NSCLC patients and subsequent bone metastasis (8). Moreover, Wu et al. (9) reported that an ERBB2 mutation existed in 2% of NSCLC patients, and was responsible for bone metastasis. More investigations are needed to further explore the molecular mechanism of bone metastasis in NSCLC patients.

Tumor metastasis is a complicated process involving multiple steps, including epithelial mesenchymal transformation (10), effusion from blood vessels (11), formation of a pre-metastasis niche (12), and the colonization and proliferation of seeded cells (13). During the process of tumor metastasis, tumor cells fail to undergo apoptosis. Fas apoptotic inhibitory molecule 2 (FAIM2) is a member of the Fas apoptosis inhibitory molecule family, which can protect against the effects of Fas by direct interaction with the Fas receptor or regulate calcium release *via* interaction with Bcl-xL (14). Recent studies reported that FAIM2 participates in regulating tumor initiation and progression. For example, Wang et al. (15) discovered that microRNA-612 can modulate the tumorigenesis of neurofibromatosis type 1 by targeting FAIM2. Ziaee et al. (16) reported that FAIM2 expression was upregulated in colorectal adenocarcinoma tissues. With regard to lung cancer, Kang et al. (17) found that FAIM2 was highly expressed in SCLC tissue, and could serve as a novel diagnostic marker and potential therapeutic target for SCLC. Our previous studies revealed that FAIM2 was highly expressed in NSCLC tissues and played a role in modulating NSCLC cell proliferation, migration, invasion, and apoptosis (18, 19). However, until now, it has remained unclear whether FAIM2 participates in regulating NSCLC bone metastasis.

In this study, we investigated the expression profile of FAIM2 in NSCLC and examined its prognostic value, role in bone metastasis, and molecular mechanism. Our results suggest that FAIM2 could possibly serve as a biomarker and molecular target for treating NSCLC.

MATERIALS AND METHODS

Clinical Specimens

Samples of NSCLC tissue and corresponding adjacent normal tissue (distance > 3 cm from the tumor tissue) were collected during the time period of September 2017 to October 2018. For patients without bone metastasis, the tissues were acquired during surgical resection. For patients with bone metastasis, the tissues were acquired during the pathological examination process (puncture biopsy). All diagnoses were independently confirmed by two pathologists. All tissue samples were obtained from patients who had not received any prior chemotherapy, radiotherapy, or other therapy, and had no other type of tumor. All patients provided their written informed consent for their participation in the study. Clinical information regarding the patients is shown in **Supplementary Material**. The protocols for all studies involving human participants were reviewed and approved by the Ethics Committee of the Affiliated Cancer Hospital of Xiangya School of Medicine.

Cell Lines and Culture Procedure

Human NSCLC cell lines, including the lung squamous cell carcinoma HARA cell line and its bone seeking subclone HARA-B4, lung adenocarcinoma NCI-H1395 and A549 cells, embryonic fibroblast NIH3T3 cells, and primary osteoblasts (Primary OB) and osteoblasts (MC3T3E1) were all purchased from the National Infrastructure of Cell Line Resource (Beijing, China). All cells were subjected to the STR assay before being sent to the purchaser and were cultured in Dulbecco's Modified Eagle Media (DMEM) medium containing penicillin (100 units/mL), streptomycin (100 μg/mL), and fetal bovine serum [FBS, 10% (v/v)] at 37°C in a humidified incubator containing 5% CO_2. To inactivate the Wnt signaling pathway, 30 μmol/L of IWP-2 (Sigma-Aldrich, St. Louis, MO, USA) was added to the culture medium for 72 h.

Quantitative Real-Time PCR

The tissues and cell were washed with PBS (pH 7.4), and the total RNA in tissues and cells was extracted using the Trizol reagent (Takara, Japan). cDNA was synthesized using a PrimeScript RT-PCR kit (Takara, Japan). Gene expression was detected by real-time PCR performed on a 7500 real-time PCR system (Applied Biosystems, Waltham, MA, USA). The $2^{-\triangle\triangle CT}$ method was used to calculate relative levels of gene expression, and GAPDH served as a housekeeping gene. The primers used for qRT-PCR are shown in **Table 1**.

Western Blotting

The total proteins in tissues and cells were extracted using the IP lysis buffer (Thermo Fisher) containing a proteinase and phosphatase inhibitor cocktail (Roche, Basel, Switzerland). The protein concentration in each extract was measured using a BCA

TABLE 1 | The information of the primers for real-time PCR.

Name	Sequence (5'-3')	Length (bp)
FAIM2 F	CCAGGGAAAGCTCTCCGTG	203
FAIM2 R	GGTCCACATAGGCCCAGCTA	
ALP F	ACTGGGGCCTGAGATACCC	185
ALP R	TCGTGTTGCACTGGTTAAAGC	
RUNX2 F	TGGTTACTGTCATGGCGGGTA	101
RUNX2 R	TCTCAGATCGTTGAACCTTGCTA	
GAPDH F	TGTTCGTCATGGGTGTGAAC	154
GAPDH R	ATGGCATGGACTGTGGTCAT	

protein assay kit (Thermo Fisher). Next, an aliquot of protein from each sample was diluted with a loading buffer and separated by sodium dodecyl sulfate polyacrylamide gel electrophoresis (SDS-PAGE). The protein bands were transferred onto a NC membrane (Merck, Kenilworth, NJ, USA), which was subsequently blocked with 5% fat-free milk at room temperature for 1 h. Next, the membrane was incubated with the primary antibody overnight at 4°C. The following antibodies against the proteins were used: FAIM2 (1:1,000, Abcam, Cat#: ab194435), ALP (1:1,000, Abcam, Cat#: ab154100), RUNX2 (1:1,000, Abcam, Cat#: ab23981), E-cadherin (1:1,000, Cell Signaling Technology, Cat#: #24E10), N-cadherin (1:1,000, Abcam, Cat#: ab18203), Vimentin (1:1,000, Abcam, Cat#: ab137321), and GAPDH (1:10,000, Abcam, Cat#: ab181602). The next day, the membrane was washed three times with TBST (pH 7.4) and then incubated with a secondary antibody (Thermo Fisher) at room temperature for 1 h. Finally, the protein bands were visualized and measured for staining intensity with an Odyssey imaging system (LI-COR Biosciences, Lincoln, NE, USA).

Hematoxylin-Eosin Staining

Samples of normal lung tissue and lung cancer tissue were fixed in 10% paraformaldehyde solution. Following gradient dehydration and paraffin embedding, the tissues were cut into 6-μm thick sections, de-paraffinized in xylene solution, and then re-hydrated using a decreasing concentration gradient of ethanol solution. Next, the sections were stained with hematoxylin solution and eosin solution, respectively. After dehydration with ethanol solution and xylene solution, the staining results were observed under a microscope (Nikon, Japan).

Immunohistochemistry Assay

IHC assays were carried out to test FAIM2 expression. Briefly, following the deparaffinization and hydration steps that were similar to those used in H&E staining, the sections were incubated with citrate antigen retrieval solution for 15 min and then with 0.2% Triton X-100 solution for 20 min. Internal peroxidase activity was quenched with 3% H_2O_2 solution. After being incubated with 5% normal goat serum to block non-specific binding, the sections were incubated overnight with the primary antibody against FAIM2 (1:2,000, Thermo Fisher Scientific, Cat#: PA520311). On the next day, the sections were incubated with the secondary antibody (1:4,000, Abcam, Cat#: ab205718) for 1 h. Finally, the sections were stained with hematoxylin solution and observed under a microscope.

FAIM2 Overexpression, Knockdown, and Plasmid Transfection

To construct the FAIM2 overexpression plasmid, the full-length sequence of FAIM2 was inserted into the pcDNA3.0 plasmid, which was subsequently designated as pcD-FAIM2. Three shRNAs targeting FAIM2 (shFAIM2) were specifically designed to knock down FAIM2 expression in cells. Because HARA cells exhibited lower levels of FAIM2 expression, pcD-FAIM2 was transfected into HARA cells. shFAIM2 was transfected into HARA-B4 cells due to their higher levels of FAIM2 expression. Briefly, cells were cultured in 6-well plates until reaching 60% to 70% confluence; after which, they were transfected with pcD-FAIM2 or shFAIM2 by using Lipofectamine 2000 (Thermo Fisher, 11668027). pcDNA3.0 and shCTRL served as the negative controls. The transfection efficacies were evaluated *via* qRT-PCR and Western blotting.

Cell Counting Kit-8 Assay

The viability of HARA and HARA-B4 cells was determined using the cell counting kit-8 (CCK-8) assay (Dojindo, Japan). Following stimulation, the cells were cultured in a 96-well plate (1×10^4 cells per well) at 37°C in a 5% CO_2 atmosphere for 0, 24, 48, or 72 h. Next, 10 μL of CCK-8 solution was added to each well and the cells were incubated for an additional 4 h at 37°C. Finally, the absorbance of each well at 450 nm was measured with a Microplate Reader (Bio-Tek Inc., Winooski, VT, USA).

Colony Formation Assay

Following stimulation, cells were cultivated in a 6-well plate (1,000 cells per well) with the culture medium being replaced by fresh medium every 3 days for a period of 2 weeks. Next, the plate was washed with PBS and the cells were fixed with 1% paraformaldehyde solution for 20 min. A 0.1% crystal violet/40% methanol solution was used to stain the clones overnight. After removing the crystal violet and washing the culture plate with PBS, results of the colony formation assay were obtained using a scanner and subsequently analyzed using the Image J software.

Edu Labeling and Immunofluorescence

Following stimulation, the cells were cultured on coverslips (Fisher, Pittsburgh, PA, USA) overnight at a density of 500 cells/mL; after which, they were incubated with Edu buffer for 1 h and then stained with anti-Edu antibody (Upstate, Temecula, CA, USA) according to the instructions provided by the manufacturer. DAPI (Merck, Germany) was used to stain the cell nucleus. Finally, images of the stained cells were obtained under a microscope (Nikon, Japan), and the percentages of EdU^+ cells were calculated using the Image J software.

In Vitro Osteogenic Differentiation

NIH3T3, primary OB, and MC3T3E1 cells were cultured in 6-well plates to 40%–50% confluence. Next, the culture medium was changed to α-MEM containing 10 nmol/L dexamethasone, 5 mmol/L glycerol phosphate, 100 units of penicillin, 100 μg/mL

streptomycin, 0.25 μg/mL amphotericin B, 100 μmol/L L-ascorbic acid, and 10% FBS. To induce osteogenic differentiation, lipopolysaccharides (LPSs, 100 ng/mL) and a tumor growth factor beta 2 (TGF-β2) inhibitor were added to the culture medium. ALP activity was examined by using reagents in a QuantiChrom assay kit (BioAssay Systems, Hayward, CA, USA) after 7 days. Alizarin red solution was used for staining cells to visualize calcium accumulation. Finally, photographs were obtained under a microscope. A mixture of 20% methanol and 10% acetic acid was used to quantify Alizarin red S staining.

Cell Adhesion Assay

HARA and HARA-B4 cells were transfected with GFP plasmid NIH3T3. Primary OB and MC3T3E1 cells were seeded into a 6-well plate and cultured overnight. Next, the HARA and HARA-B4 cells were added to the 6-well plate and co-cultured with the OB and MC3T3E1 cells for 24 h. Then, the cells were washed with PBS and fixed with 4% paraformaldehyde. Photographs were taken under a microscope and analyzed using the Image J software.

Cell Anoikis Assay

To analyze HARA and HARA-B4 cell death due to a loss of adherence, the two cell types were stimulated and then seeded into low-adhesive plates at a density of 10×10^5 cells per well. After 1, 4, or 7 days, the cells in each group were harvested and centrifuged at 1,000 rpm for 5 min; after which, they were washed with PBS, and then stained with Annexin V (Invitrogen, Carlsbad, CA, USA) solution and propidium iodide (PI) solution according to the instructions of the manufacturer. The percentage of cells with anoikis was analyzed by flow cytometry.

Cell Apoptosis Assay

After receiving the appropriate stimulation, the cells in each group were harvested and centrifuged at 1,000 rpm for 5 min. The cells were then washed with PBS and stained with Annexin V (Invitrogen, USA) solution and propidium iodide (PI) solution according to the instructions of the manufacturer. The percentage of apoptotic cells was analyzed by flow cytometry.

Two-Chamber Transwell Assay

The two-chamber Transwell assay was used to detect cell migration and invasion. After receiving the designated stimulation, HARA and HARA-B4 cells (2×10^4 cells in 100 μL of FBS-free medium) were added to the upper chamber, and 700 μL of culture medium containing 10% FBS was added to the lower chamber. After being cultured at 37°C in a 5% CO_2 atmosphere for 48 h, the non-migrated cells in the upper chamber were carefully removed, and the migrated cells on the Transwell membrane were washed with PBS, fixed with 4% paraformaldehyde, and stained using violet solution. Cell migration results were observed and photographed under a microscope (Nikon, Japan). The number of migrated cells in each field was counted.

Cell invasion was detected in a similar manner, except that the Transwell membrane was pre-coated with Matrigel (Corning, Corning, NY, USA).

Cell Scratch Assay

After receiving the designated stimulation, 5×10^5 HARA or HARA-B4 cells were cultured in a 6-well plate overnight. Next, a 200 μL pipette tip was used to remove cells and generate scratches on the cell monolayer. After rinsing with PBS to clear the redundant cells, the cells were cultured in FBS-free medium for 24 or 48 h. The scratches were then observed and photographed under a microscope (MOTIC, Xiamen, China). The data were analyzed using the IPP software.

Immunofluorescence Staining

E-cadherin, N-cadherin, and Vimentin expression in cells was detected by immunofluorescence. Briefly, cells were seeded into immunofluorescence-specialized 12-well plates at a concentration of 1×10^5 cells/well and cultured overnight. After being washed with PBS, the cells were fixed with 4% polyformaldehyde for 15 min, permeabilized with 0.1% TritonX-100 for 30 s, and then blocked with 10% BSA for 1 h. Next, the cells were washed three times with PBS and then incubated overnight with primary antibodies against E-cadherin (1:500, ab40772), N-cadherin (1:500, ab18203), and Vimentin (1:1,000, ab92547) at 4°C. On the next day, the cells were washed with PBS and then incubated with an Alexa Fluor 488 (1: 300, ab150077) secondary antibody for 60 min at room temperature. Finally, the cells were incubated with DAPI, covered with sealing liquid, and photographed under a microscope (Nikon, Japan).

In Vivo Animal Experiments

Female BALB/c nude mice (4–5 weeks old) were housed in the SPF level barrier system at 26°C– 28°C with a free access to food and water. After the mice had been fed at our facility for 1 week, 1×10^6 HARA cells transfected with pcDNA3.0 or pcD-FAIM2, as well as HARA-B4 cells transfected with shCTRL or shFAIM2, were injected into the outer tibia stick to observe the growth of tibia tumors in the hind limbs of the nude mice (20). A total of five mice were included in each group. After 5 weeks, the mice were sacrificed by the induction of an acute hemorrhage. The lung and tibia tissues of the mice were collected and stained with H&E to observe changes in the microstructure and test for FAIM2 expression. All experiments using mice were performed in accordance with guidelines in the *National Institute of Health's Guide for the Care and Use of Laboratory Animals*, and the protocols were approved by the Ethics Committee of the Affiliated Cancer Hospital of Xiangya School of Medicine.

Statistical Analysis

SPSS 13.0 software and GraphPad 7.0 software were used to perform all statistical analyses. *P*-values for differences between two groups were calculated using the two-tailed student's t-test, and *P*-values for differences among three or more groups were determined by ANOVA. The Kaplan-Meier method was used to calculate cumulative survival curves, and the significance of a difference was assessed by the log-rank test. Chi-square values were calculated for correlation analyses. Data are presented as a mean value ± S.D. Statistical significance is indicated as follows: $P > 0.05$ = ns; $P < 0.05$ = *, #; $P < 0.01$ = **, ##.

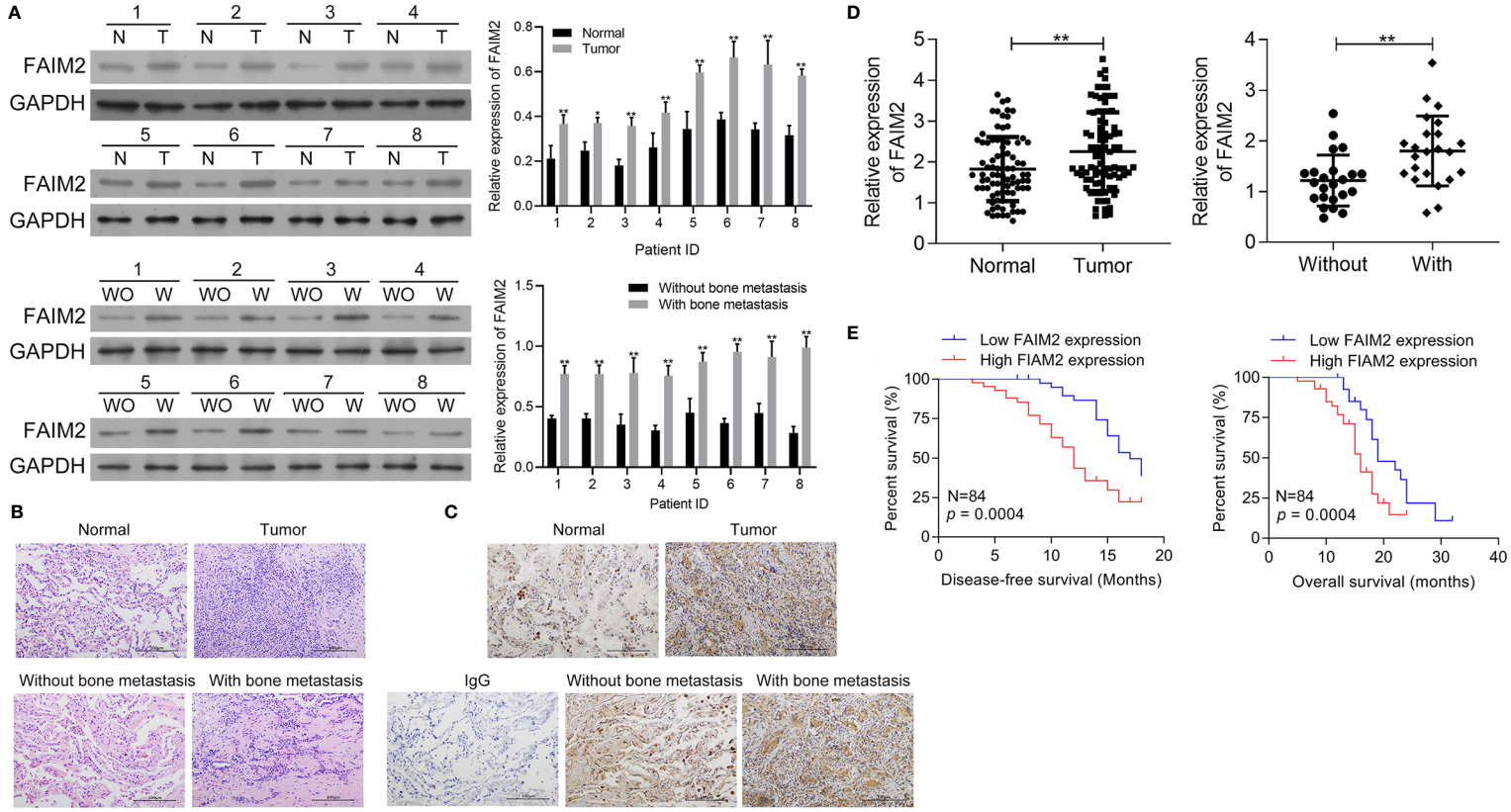

FIGURE 1 | FAIM2 was highly expressed in NSCLC and correlated with bone metastasis and a poor prognosis. **(A)** The levels of FAIM2 protein expression in normal lung tissues and NSCLC tissues, as well as in NSCLC tissues with (W) or without (WO) bone metastasis, were examined by Western blotting. **(B)** The microstructure of normal lung tissues and NSCLC tissues, as well as NSCLC tissues with (W) or without (WO) bone metastasis. **(C, D)** FAIM2 protein and mRNA expression in normal lung tissues and NSCLC tissues, as well as in NSCLC tissues with (W) or without (WO) bone metastasis, were examined by IHC and qRT-PCR. **(E)** Kaplan-Meier curves for the disease-free survival (DFS) and overall survival (OS) of patients with high and low levels of FAIM2. $P < 0.05$, *; $P < 0.01$, ** *vs.* Normal lung tissues or NSCLC tissues without bone metastasis.

RESULTS

FAIM2 Was Highly Expressed in NSCLC Tissues and Correlated With Bone Metastasis and a Poor Prognosis

First, the levels of FAIM2 expression in NSCLC tumor tissues and adjacent normal tissues, as well as in NSCLC tissues with or without bone metastasis were examined by Western blotting. Those results showed that when compared to normal lung tissues, FAIM2 was more highly expressed in NSCLC tissues ($P < 0.05$ or $P < 0.01$, **Figure 1A**). Moreover, when compared to NSCLC tissues without bone metastasis, FAIM2 expression was upregulated in NSCLC tissues with bone metastasis ($P < 0.01$). H&E staining was performed to reveal the microstructure of normal lung tissues and NSCLC tissues, as well as NSCLC tissues with or without bone metastasis (**Figure 1B**). The normal lung tissues showed a normal microstructure with blue-purple nuclei and pink cytoplasm, while NSCLC tissues had an increased number of cells. Furthermore, relative to the NSCLS tissues without bone metastasis, the NSCLC tissues with bone metastasis displayed increased cell numbers and unclear cell boundaries. IHC assay results (**Figure 1C**) also showed that FAIM2 expression was increased in the NSCLC tissues relative to the normal lung tissues. When compared to the NSCLC tissues without bone metastasis, FAIM2 expression was increased in the NSCLC tissues with bone metastasis. Similar results were found for FAIM2 mRNA expression in the normal lung tissues and NSCLC tissues, as well as in the NSCLC tissues with or without bone metastasis ($P < 0.01$, **Figure 1D**). Moreover, we also analyzed the clinical significance of FAIM2 in NSCLC. Our results indicated that a high level of FAIM2 predicted a poor prognosis for NSCLC patients, including shorter disease-free survival (DFS) and overall survival (OS) times (**Figure 1E**). By exploring the association between FAIM2 expression and multiple clinicopathological characteristics of NSCLC patients, we discovered that FAIM2 was an independent factor correlated with the tumor stage (P = 0.0024), lymph node metastasis ($P = 0.0161$), and bone metastasis ($P = 0.0010$) (**Table 2**). The results above demonstrated that FAIM2 was highly expressed in NSCLC tissues and correlated with bone metastasis and a poor prognosis.

TABLE 2 | Correlation between FAIM2 expression and multiple clinicopathological characteristics in NSCLC patients.

Clinicopathological characteristics		FIAM2 expression		Total	χ^2	*p*-value
		Low	High			
Age	≤60	23	22	45	0.0478	0.8268
	>60	19	20	39		
Gender	Female	21	22	44	0.1112	0.7833
	Male	21	19	40		
Tumor stage	I	21	8	29	12.09	**0.0024**
	II	14	14	28		
	III	7	20	27		
Lymph node metastasis	Negative	25	14	39	5.791	**0.0161**
	Positive	17	28	45		
Bone metastasis	Negative	27	12	39	10.77	**0.0010**
	Positive	15	30	45		
T stage	T1	19	16	35	0.4431	0.8031
	T2	9	10	19		
	T3	14	16	30		
	Total			84		

Bold values means p < 0.05.

FAIM2 Was Highly Expressed in NSCLC Cells and Associated With Cell Metastasis

To further evaluate the function of FAIM2 in the bone metastasis of NSCLC, we compared the levels of FAIM2 expression in Beas-2B cells, NCI-H1395 cells, HARA cells, A549 cells, and HARA-B4 cells. Our results showed that when compared to Beas-2B cells, the levels of FAIM2 protein and mRNA expression in NSCLC cells were increased (**Figures 2A, B**, $P < 0.01$ for the mRNA level). Moreover, relative to HARA cells, the levels of FAIM2 were increased in HARA-B4 cells ($P < 0.01$ for the mRNA level), indicating a correlation between FAIM2 and bone metastasis. To analyze the relationship between anchorage-dependent cell growth and FAIM2 expression, the HARA and HARA-B4 cells were cultured in low-adhesive dishes and FAIM2 mRNA expression was measured. **Figure 2C** shows that FAIM2 expression in the HARA and HARA-B4 cells gradually decreased from day 1 to day 7, suggesting that FAIM2 is related to an anchorage-dependent cell growth. Next, HARA cells were transfected with pcD-FAIM2 to upregulate FAIM2 expression, while HARA-B4 cells were transfected with shFAIM2 to knockdown FAIM2 expression. Results in **Figure 2D** show that following pcD-FAIM2 transfection, the levels of FAIM2 protein and mRNA expression in HARA cells were increased ($P < 0.01$ for the mRNA level). Three shRNAs targeting FAIM2 were designed. ShRNA3 showed the best FAIM2 knockdown efficiency (**Figure 2E**), and was selected for use in subsequent experiments. Following shFAIM2 transfection, the levels FAIM2 protein and mRNA expression in HARA-B4 cells were both reduced (**Figure 2F**, $P < 0.01$ for the mRNA level). Moreover, anoikis was detected in HARA cells transfected with pcD-FAIM2 and in HARA-B4 cells transfected with shFAIM2. Transfection with pcD-FAIM2 reduced the anoikis of HARA cells on Day 4 ($P < 0.05$) and Day 7 ($P < 0.01$) (**Figure 2G**), while transfection with shFAIM2 increased the anoikis of HARA-B4 cells on Day 4 ($P < 0.01$) and Day 7 ($P < 0.01$) (**Figure 2H**). The results above demonstrated that FAIM2 was highly expressed in NSCLC cells and related to cell metastasis.

Upregulation of FAIM2 Promoted HARA Cell Proliferation, Migration, and Invasion, but Reduced Cell Apoptosis

After being transfected with pcD-FAIM2, the viability, proliferation, migration, and invasion of HARA cells were detected. As shown in **Figure 3A**, pcD-FAIM2 transfection increased the OD_{450} values of HARA cells after 24, 48, and 72 h of culture, suggesting that pcD-FAIM2 promoted HARA cell viability. Furthermore, pcD-FAIM2 also promoted HARA cell proliferation, as evidenced by an increase in the colony numbers ($P < 0.01$) and percentage of EdU^+ cells ($P < 0.01$, **Figures 3B, C**). Moreover, pcD-FAIM2 also inhibited the apoptosis of HARA cells ($P < 0.01$, **Figure 3D**). Both the numbers of migrated and invaded HARA cells in the pcD-FAIM2 group were notably increased

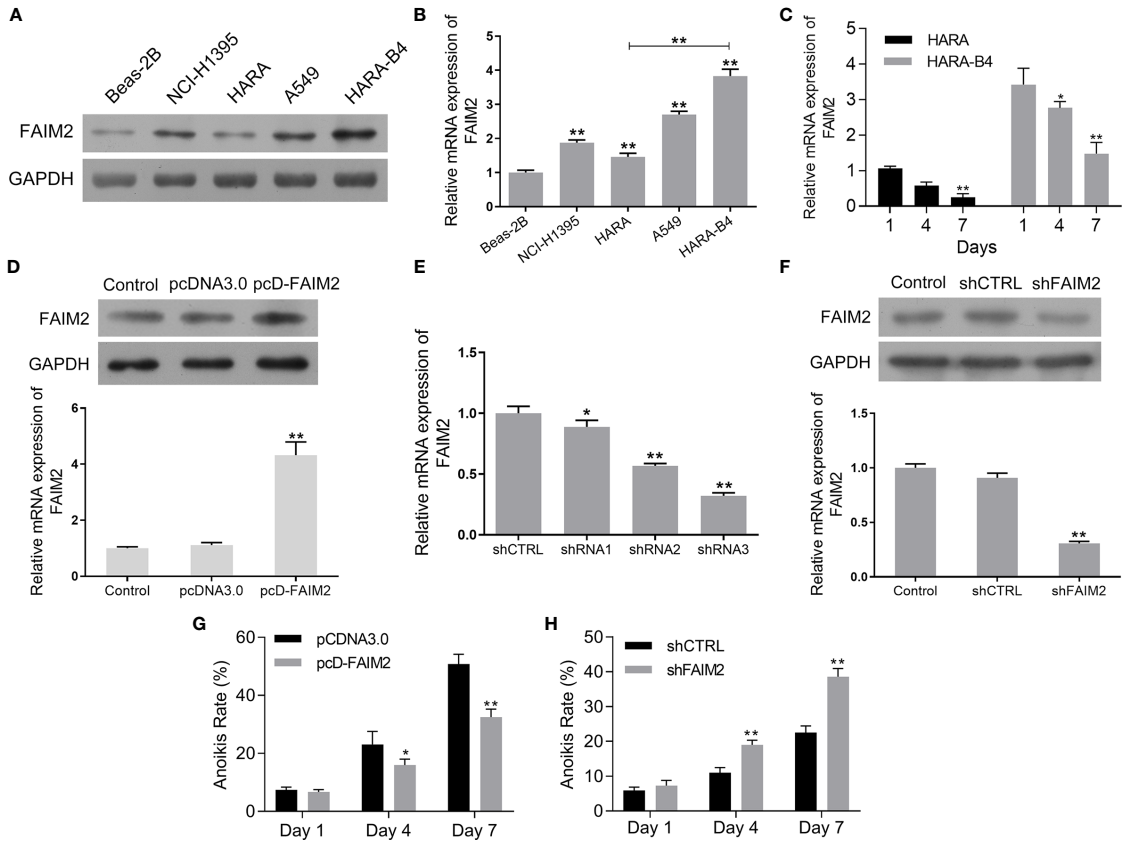

FIGURE 2 | FAIM2 was highly expressed in NSCLC cells and related to cell metastasis. **(A, B)** FAIM2 protein and mRNA expression in Beas-2B, NCI-H1395, HARA, A549, and HARA-B4 cells was examined by Western blotting and qRT-PCR. **(C)** qRT-PCR was used to detect FAIM2 mRNA expression in HARA and HARA-B4 cells cultured under anchorage-dependent conditions during day 1 to day 7. **(D)** Following pcDNA3.0 or pcD-FAIM2 transfection, FAIM2 protein and mRNA expression in HARA cells was examined by Western blotting and qRT-PCR. **(E)** FAIM2 mRNA expression in HARA-B4 cells transfected with shRNA1, shRNA2, or shRNA3 was examined by qRT-PCR. **(F)** FAIM2 protein and mRNA expression in HARA cells transfected with shCTRL or sh-FAIM2 was examined by Western blotting and qRT-PCR. **(G)** Following transfection with pcDNA3.0 or pcD-FAIM2, HARA cell anoikis due to a loss of adherence for 1, 4, and 7 days was detected. **(H)** Following transfection with shCTRL or sh-FAIM2, HARA-B4 cell anoikis due to a loss of adherence for 1, 4, and 7 days was detected. $P < 0.05$, *; $P < 0.01$, ** *vs.* Beas-2B, Day1, the pcDNA3.0 or shCTRL group.

($P < 0.01$, **Figure 3E**), indicating that pcD-FAIM2 promoted HARA cell migration and invasion. The increased migration ability of the transfected cells was also demonstrated by the decreased relative wound areas in the pcD-FAIM2-transfected group at 24 and 48 h ($P < 0.01$, **Figure 3F**). The results above suggested that the overexpression of FAIM2 increased HARA cell proliferation, migration, and invasion, and inhibited cell apoptosis.

Downregulation of FAIM2 Reduced HARA-B4 Cell Proliferation, Migration, and Invasion, but Promoted Cell Apoptosis

After shFAIM2 transfection, the viability, proliferation, migration, and invasion of HARA-B4 cells were detected. As shown in **Figure 4A**, shFAIM2 transfection lowered the OD_{450} nm values at 24, 48, and 72 h, suggesting that shFAIM2 reduced HARA-B4 cell viability. **Figures 4B, C** show that shFAIM2 inhibited HARA-B4 cell proliferation, as evidenced by the decreased colony numbers ($P < 0.01$) and percentages of EdU^+ cells ($P < 0.01$). Moreover, shFAIM2 increased the apoptosis of HARA-B4 cells ($P < 0.01$, **Figure 4D**), but decreased the numbers of migrated and invaded HARA-B4 cells ($P < 0.01$, **Figure 4E**), indicating that shFAIM2 inhibited HARA-B4 cell migration and invasion. Finally, shFAIM2 reduced HARA-B4 cell migration, as evidenced by the increased relative wound areas in the shFAIM2 group at 24 and 48 h ($P < 0.01$, **Figure 4F**). These results showed that downregulation of FAIM2 reduced HARA-B4 cell proliferation, migration, and invasion, and promoted cell apoptosis.

Primary OB and MC3T3E1 Cells Were Effective for Inducing Osteoblast Differentiation

Embryonic fibroblast NIH3T3, primary OB, and osteoblast MC3T3E1 cells were used to induce osteoblast differentiation. Following the induction of osteoblast differentiation, the levels of ALP and RUNX2 protein and mRNA in the cells were measured. Results showed that after the induction of osteoblast

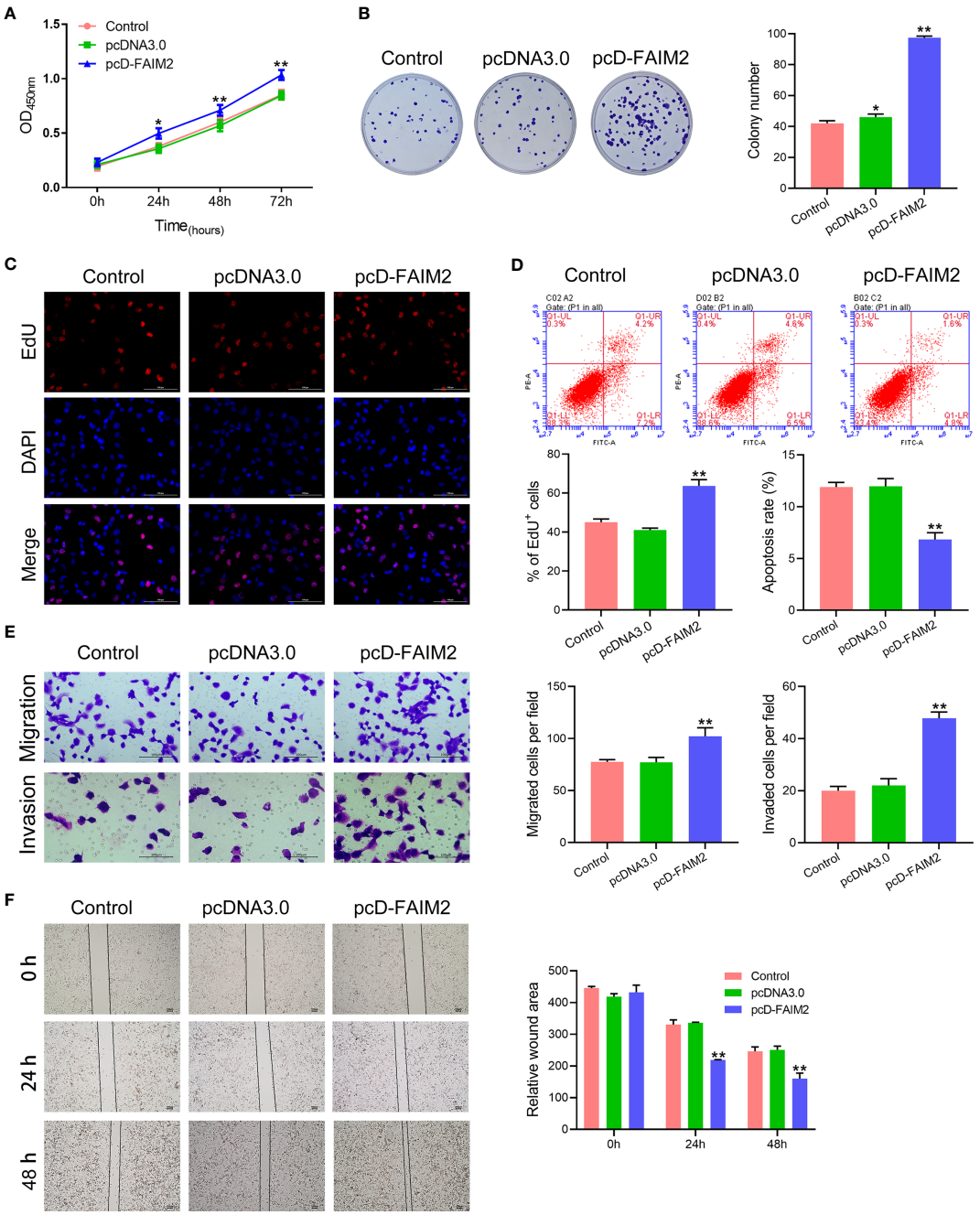

FIGURE 3 | Upregulation of FAIM2 promoted HARA cell proliferation, migration, and invasion, but reduced cell apoptosis. Following pcDNA3.0 or pcD-FAIM2 transfection, **(A)** the viability of HARA cells was detected *via* the CCK-8 assay. **(B, C)** HARA cell proliferation was evaluated *via* the colony formation assay and EdU staining. **(D)** HARA cell apoptosis was assessed by flow cytometry. **(E)** HARA cell migration and invasion were measured *via* the two-chamber Transwell assay. **(F)** The cell scratch assay was conducted to further test for HARA cell migration. $P < 0.05$, *; $P < 0.01$, ** *vs.* the pcDNA3.0 group.

differentiation, the levels of both ALP and RUNX2 expressions in NIH3T3, Primary OB and MC3T3E1 cells were upregulated ($P < 0.05$ or $P < 0.01$ for the mRNA level) (**Supplementary Figures 1A, B**). ALP staining and Alizarin Red staining were performed to further verify the successful establishment of an osteoblast differentiation model. Those staining results showed that primary OB and MC3T3E1 cells induced a more intense staining than did NIH3t3 cells ($P < 0.01$, **Supplementary Figure 1C**). These results suggested that the primary OB and MC3T3E1 were effective for inducing osteoblast differentiation.

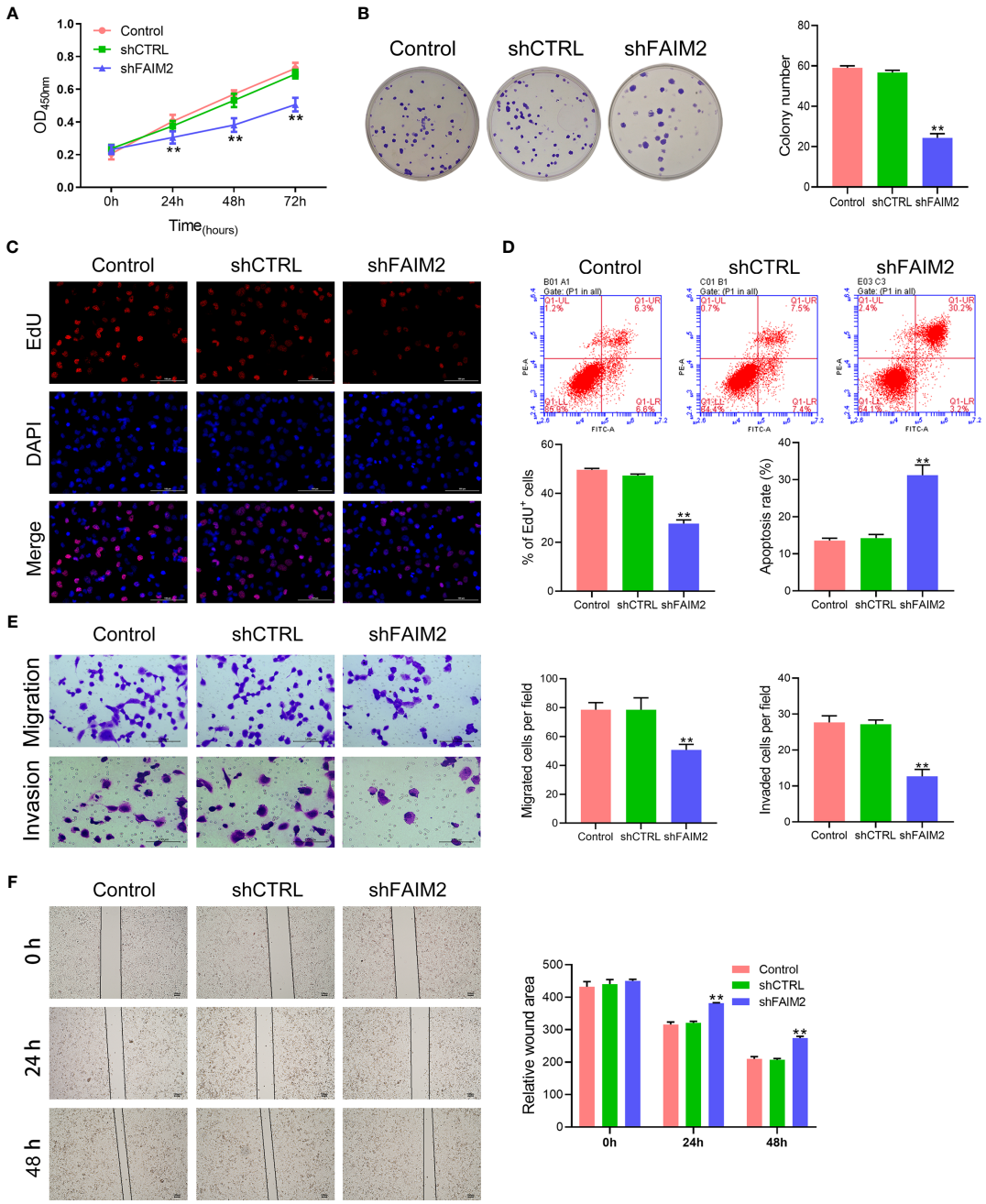

FIGURE 4 | Downregulation of FAIM2 reduced HARA-B4 cell proliferation, migration, and invasion, but promoted cell apoptosis. Following shCTRL or shFAIM2 transfection, **(A)** the viability of HARA-B4 cells was detected *via* the CCK-8 assay. **(B, C)** HARA-B4 cell proliferation was evaluated *via* the colony formation assay and EdU staining. **(D)** HARA-B4 cell apoptosis was assessed by flow cytometry. **(E)** HARA-B4 cell migration and invasion were measured *via* the two-chamber Transwell assay. **(F)** The cell scratch assay was conducted to further test for HARA-B4 cell migration. $P < 0.01$, ** *vs.* the shCTRL group.

HARA-B4 Cells Showed a Stronger Adhesive Ability to Osteocytes Than Did HARA Cells

Because HARA-B4 is a bone-seeking cell line, it was assumed that those cells would show a stronger adhesive ability to osteocytes. To verify this assumption, HARA and HARA-B4 cells were transfected with a plasmid containing GFP to detect the luciferase signaling. Next, following the co-culture of HARA (or HARA-B4) cells and NIH3T3 cells (or primary OB and MC3T3E1, cells that were subjected to the induction of osteoblast differentiation), the adhesive abilities of HARA-B4 and HARA cells were detected. Those results showed that

HARA-B4 cells had a stronger ability to bind to osteocytes than did HARA cells (**Supplementary Figures 2A–C**, $P < 0.01$ in the MC3T3E1 and Primary OB cell groups).

FAIM2 Was Related to the Ability of HARA and HARA-B4 Cells to Adhere to Osteocytes

Next, we assessed how FAIM2 modulated the adhesive ability of HARA and HARA-B4 cells to osteocytes. Following the co-culture with MC3T3E1 (cells were subjected to an induction of osteoblast differentiation), the relative numbers of adherent HARA and HARA-B4 cells were measured. Those measurements showed that an upregulation of FAIM2 expression in HARA cells significantly increased the adhesion of HARA cells to osteocytes ($P < 0.01$, **Figure 5A**), and a downregulation of FAIM2 expression in HARA-B4 cells reduced the adhesion of HARA-B4 cells to osteocytes ($P < 0.01$, **Figure 5B**). Those results suggested that FAIM2 could modulate the adhesive ability of NSCLC cells, and plays a role in promoting bone metastasis.

FAIM2 Facilitated Bone Metastasis by Regulating the Epithelial Mesenchymal Transformation

To explore whether FAIM2 plays a role in regulating the EMT process in HARA and HARA-B4 cells, we detected the levels of E-cadherin, N-cadherin, and Vimentin expression in pcD-FAIM2-transfected HARA cells and shFAIM2-transfected HARA-B4 cells. IF assay results (**Figure 6A**) showed that pcD-FAIM2 transfection reduced E-cadherin expression, but increased N-cadherin and Vimentin expression in HARA cells, indicating that pcD-FAIM2 promoted the EMT process in HARA cells. When compared to HARA cells in the pcDNA3.0 group, HARA cells in the pcD-FAIM2 group displayed a spindle-shaped morphology. Moreover, shFAIM2 transfection enhanced E-cadherin expression, but decreased the levels of N-cadherin and Vimentin expression in HARA-B4 cells (**Figure 6B**), indicating that shFAIM2 attenuated the EMT process in HARAB4 cells. Similar results were shown by Western blotting ($P < 0.01$, **Figure 6C**). These results suggested that FAIM2 participates in modulating the EMT process in NSCLC cells, and can thereby promote bone metastasis.

FAIM2 Promoted HARA Cell Migration and Invasion by Activating the Wnt Signaling Pathway

Previous reports suggested that the Wnt signaling pathway is associated with the bone metastasis of NSCLC (21). Therefore, we examined whether FAIM2 might regulate HARA cell migration and invasion by modulating the Wnt signal pathway. We found that pcD-FAIM2 activated the Wnt pathway in HARA cells, as evidenced by the increased levels of Wnt3a and β-catenin protein and mRNA expression ($P < 0.01$, **Figure 7**). Next, IWP-2 was used to inactivate the Wnt pathway. Results showed that IWP-2 treatment significantly attenuated the Wnt pathway activation induced by pcD-FAIM2 ($P < 0.01$). When compared to the pcD-FAIM2 group, the levels of FAIM2 mRNA in HARA cells were significantly lower in the pcD-FAIM2+IWP-2 group ($P < 0.01$, **Figure 7B**). Furthermore, IWP-2 significantly reversed the pcD-FAIM2-induced increase

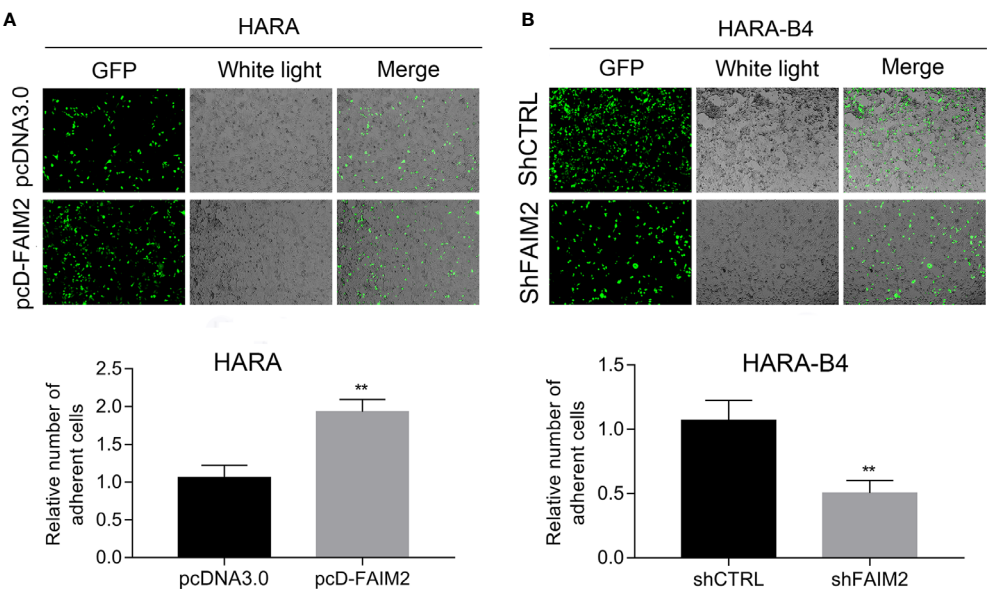

FIGURE 5 | FAIM2 was related to the ability of HARA and HARA-B4 cells to adhere to osteocytes. **(A)** Following pcDNA3.0 or pcD-FAIM2 transfection, the ability of HARA cells to adhere to MC3T3E1 cells (cells were subjected to induction of osteoblast differentiation) was evaluated. **(B)** Following shCTRL or shFAIM2 transfection, the ability of HARA-B4 cells to adhere to MC3T3E1 cells (cells were subjected to induction of osteoblast differentiation) was evaluated. $P < 0.01$, ** *vs.* the pcDNA3.0 or shCTRL group.

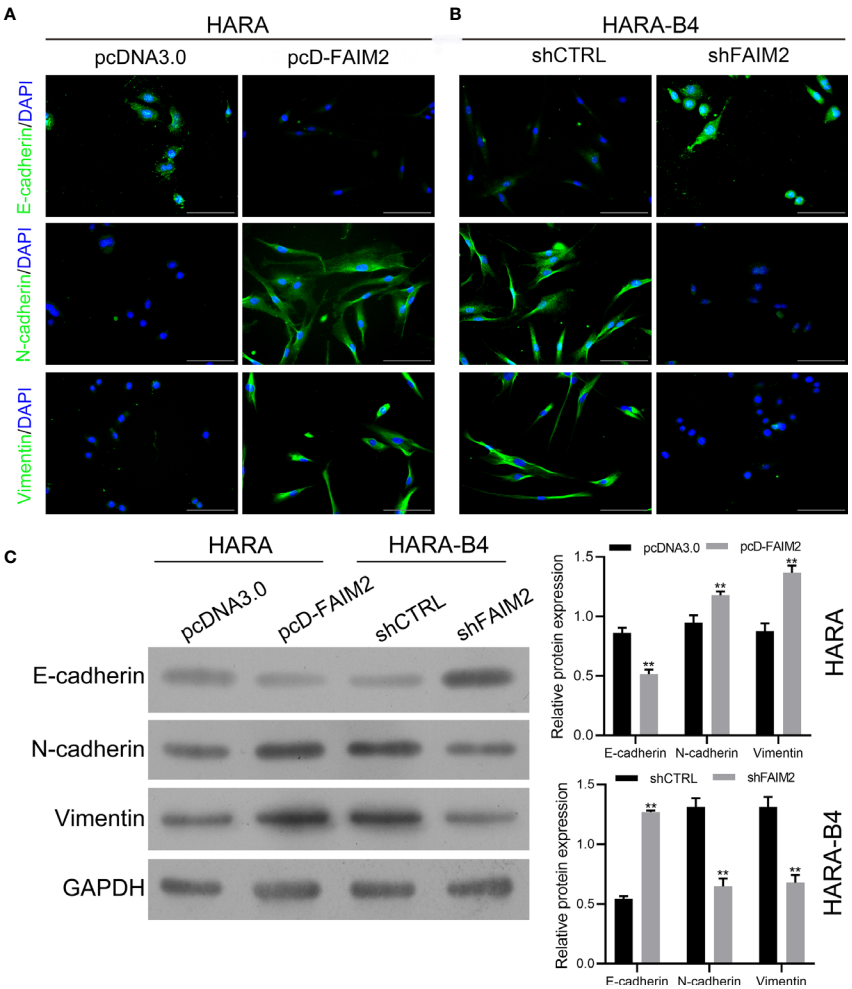

FIGURE 6 | FAIM2 facilitated bone metastasis by regulating the EMT processes. Following pcDNA3.0 or pcD-FAIM2 transfection of HARA cells, as well as shCTRL or shFAIM2 transfection of HARA-B4 cells, **(A, B)** the expression of EMT markers, including E-cadherin, N-cadherin, and Vimentin was examined by immunofluorescence staining. **(C)** The levels of E-cadherin, N-cadherin, and Vimentin protein expression were determined by Western blotting. $P < 0.01$, ** *vs.* the pcDNA3.0 group.

in HARA cell viability ($P < 0.01$, **Figure 7C**). Moreover, when compared to the pcD-FAIM2 group, the numbers of migrated and invaded HARA cells in the pcD-FAIM2+IWP-2 group were notably decreased ($P < 0.01$, **Figure 7D**), indicating that IWP-2 also attenuated the migration and invasion of HARA cells induced by pcD-FAIM2. In addition, IWP-2 attenuated HARA cell migration, as evidenced by the increased relative wound areas in the pcD-FAIM2+IWP-2 group at 24 and 48 h ($P < 0.05$ or $P < 0.01$, **Figure 7E**). These results suggested that FAIM2 promoted HARA cell migration and invasion by activating the Wnt signaling pathway.

FAIM2 Participated in Regulating NSCLC Bone Metastasis *In Vivo*

Finally, we investigated whether FAIM2 participates in modulating NSCLC bone metastasis *in vivo*. As shown in **Figure 8A**, the rate of HARA cell metastasis to bone tissue was higher in the pcD-FAIM2 group than in the pcDNA3.0 group, while the rate of HARA-B4 cell metastasis in the shFAIM2 group was lower than that in the shCTRL group. Furthermore, a comparison of bone tumor tissue microstructure showed that the blood supply available to tumors in the pcD-FAIM2 group was greater than that in the shFAIM2 group. IHC assays were performed to test for FAIM2 expression. Those results showed that the levels of FAIM2 expression in lung tissue and bone metastasis NSCLC tissues were higher in the pcD-FAIM2 group than in the shFAIM2 group (**Figure 8B**). Those results further suggest that FAIM2 participates in regulating NSCLC bone metastasis.

DISCUSSION

Tumor metastasis is the main reason for the poor prognosis of NSCLC patients (22). Because bone is the major metastasis site of

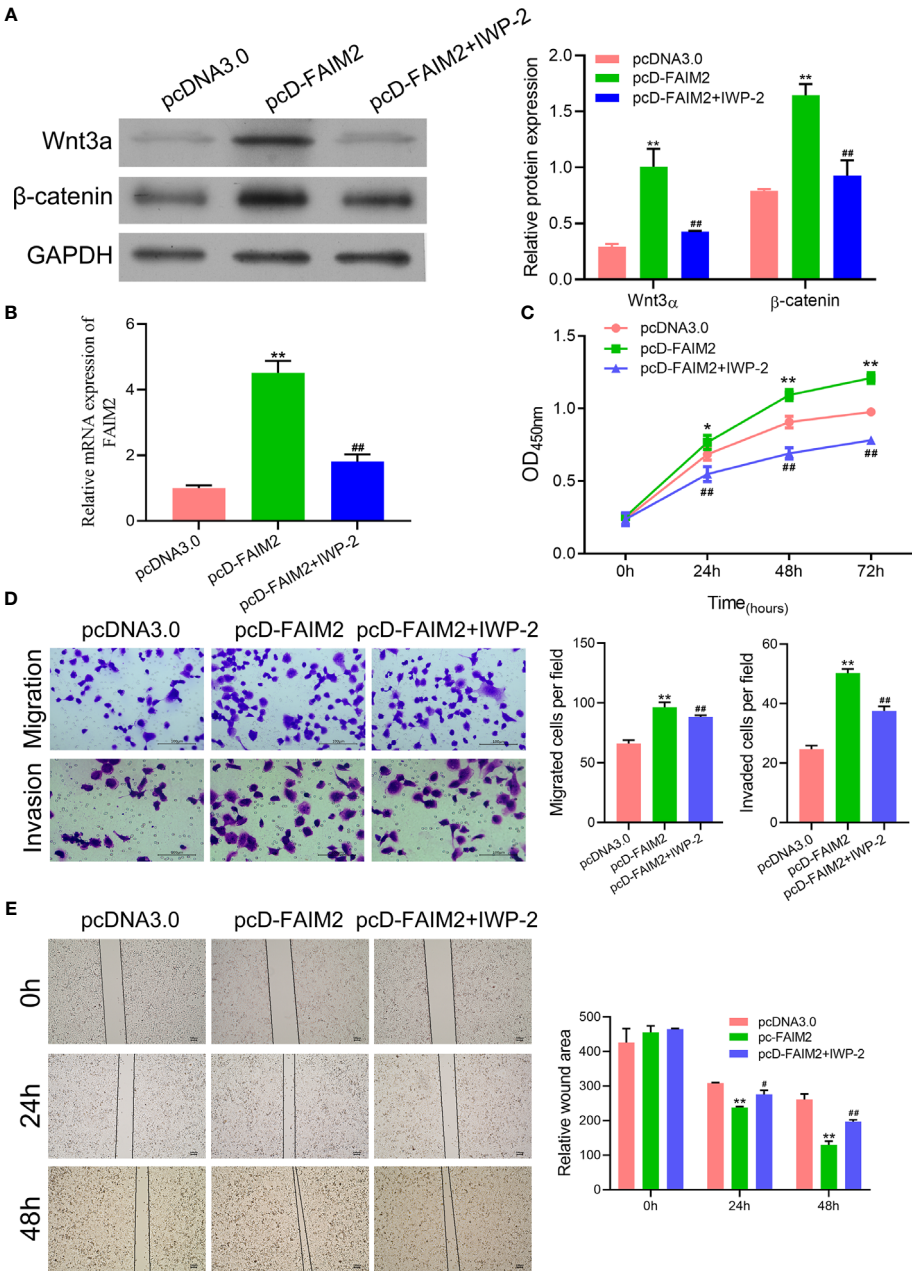

FIGURE 7 | FAIM2 promoted HARA cell migration and invasion by activating the Wnt signaling pathway. Following pcD-FAIM2 transfection and IWP-2 treatment, **(A)** the levels of Wnt3a and β-catenin protein expression were examined by Western blotting. **(B)** FAIM2 mRNA expression was measured by qRT-PCR. **(C)** Cell viability was detected by the CCK-8 assay. **(D)** Cell migration and invasion were evaluated *via* the two-chamber Transwell assay. **(E)** The cell scratch assay was conducted to further test for HARA cell migration. $P < 0.05$, *; $P < 0.01$, ** *vs.* the pcDNA3.0 group; $P < 0.05$, $^{\#}$; $P < 0.01$, $^{\#\#}$ *vs.* the pcD-FAIM2 group.

NSCLC, inhibition of NSCLC bone metastasis is considered to be helpful for increasing the survival rate of NSCLC patients (7). FAIM2 belongs to the Fas apoptosis inhibitory molecule family (14). In the current study, we comprehensively investigated the expression pattern of FAIM2 in NSCLC. Moreover, we explored the influence of FAIM2 on the bone metastasis of NSCLC. In summary, our main findings were as follows: 1) FAIM2 was overexpressed in NSCLC tissues and NSCLC tissues with bone metastasis, and a high level of FAIM2 expression was correlated with a poor clinical prognosis; 2) FAIM2 was highly expressed in NSCLC cells and related to cell metastasis; 3) an upregulation of FAIM2 promoted HARA cell proliferation, migration, and invasion, but reduced cell apoptosis; 4) a downregulation of FAIM2 impaired HARA-B4 cell proliferation, migration, and invasion, but promoted cell apoptosis; 5) HARA-B4 cells showed a stronger adhesive ability than HARA cells, and FAIM2

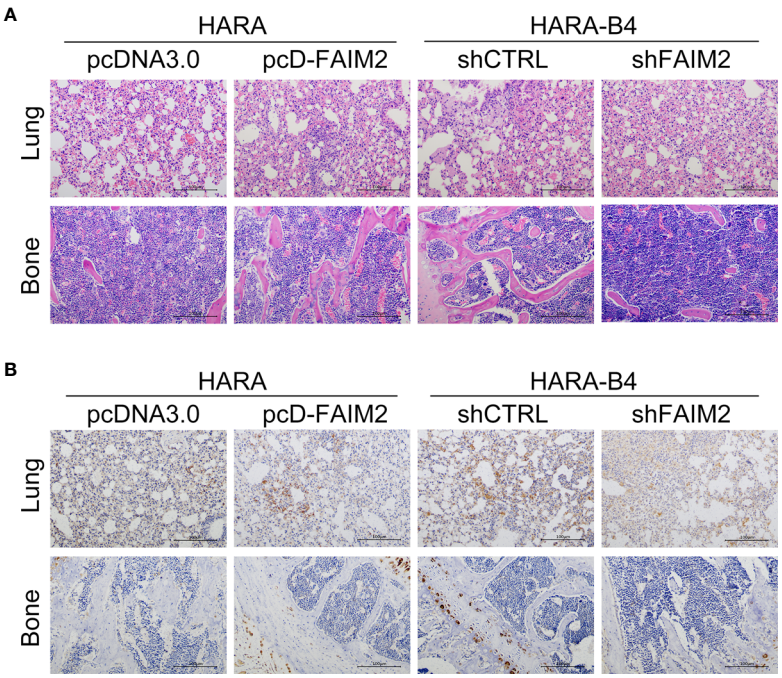

FIGURE 8 | FAIM2 participated in regulating NSCLC bone metastasis *in vivo*. An *in vivo* NSCLC bone metastasis model was established. **(A)** The lung and bone tissues were collected and stained with H&E to observe changes in the microstructure. **(B)** The lung and bone tissues were collected to test for FAIM2 expression *via* IHC.

promoted the adhesive ability of HARA-B4 cells to osteocytes; 6) FAIM2 promoted NSCLC bone metastasis by regulating the EMT process and activating the Wnt signaling pathway. Based on the results above, we deduced that FAIM2 might be a promising biomarker and target for inhibiting or treating bone metastasis in NSCLC patients.

FAIM2 is an anti-apoptotic protein that is upregulated in B cells, leading to apoptotic resistance and Fas-mediated cell death. In addition to their anti-apoptosis effect, FAIM family members have been discovered to participate in several physiological processes and pathological conditions, including cell proliferation, metabolic regulation, tumorigenesis, and Alzheimer's disease (23). With regard to carcinogenesis, FAIM family members have been reported to be upregulated in multiple myeloma, which could promote cancer cell proliferation by activating the IGF-1 and AKT signaling pathways (24).

In recent years, numerous reports have provided evidence supporting the oncogenic role of FAIM2. Pan et al. (25) reported that de-differentiated OS cells with upregulated FAIM2 levels could acquire a survival ability that enhances their metastatic potential. Moreover, Chen et al. (26) reported that the LncRNA DCST1-AS1/miR-1254/FAIM2 axis facilitated tumor progression in hepatocellular carcinoma. In lung cancer, the upregulation of lncRNA-SNHG7 was reported to accelerate the proliferation, migration, and invasion of lung cancer cells by upregulating FAIM2 expression (18, 19). However, those previous studies focused on the upstream regulation of FAIM2, and ignored the downstream effectors of FAIM2 in tumor cells. In this study, we found that FAIM2 regulated the EMT process and Wnt pathway to promote tumor proliferation and metastasis. These results provide a useful supplement to former studies.

Bone metastasis is a comprehensive process which includes the development of osteogenic/osteolytic bone lesions (27). The Wnt signaling pathway plays an important role in bone development under physiological conditions, but is also deeply involved in tumor initiation and progression (28). EMT is an important process that tumor cells must complete to obtain their metastatic potential; as it enables them to detach from the original tumor, enter the circulation, and disseminate to the bone (28). Multiple studies have proven that the Wnt signaling pathway promotes the EMT process (29). For example, the activation of Wnt receptors FZD8 and LRP5 was reported to facilitate cell migration and invasion by accelerating EMT in prostate cancer (30, 31). Moreover, an upregulation of APC and β-catenin was shown to significantly increase the levels of matrix MMP-9 and MMP-2 (members of the metalloproteinase family) expression and downregulate E-cadherin, Snail1, and Zeb1 expression, which ultimately resulted in EMT and bone metastasis in lung cancer (32, 33).

Several unanswered questions remain to be explored in future studies. For example, the direct effector that was regulated by FAIM2 in the Wnt pathway remains unknown. Also, a quantitative evaluation of possible diagnostic tools and therapeutic agents based on FAIM2 must still be conducted.

In conclusion, our research showed that FAIM2 was significantly upregulated in NSCLC tissues and performed an oncogenic function in tumor progression, including tumor cell proliferation and bone metastasis. With regard to the molecular

mechanism, we found that an upregulation of FAIM2 expression activated the EMT process and Wnt signaling pathway. FAIM2 also exhibited a diagnostic value in tumor progression. We found that FAIM2 expression was independently correlated with a poor survival and disease outcomes of NSCLC patients. Taken together, these results suggest FAIM2 as a potential diagnostic biomarker and therapeutic target for NSCLC patients.

DATA AVAILABILITY STATEMENT

The raw data supporting the conclusions of this article will be made available by the authors, without undue reservation.

ETHICS STATEMENT

The studies involving human participants were reviewed and approved by the Ethics Committee of the Affiliated Cancer Hospital of Xiangya School of Medicine. The patients/participants provided their written informed consent to participate in this study.

AUTHOR CONTRIBUTIONS

MZ and KS conceived and designed the study, and provided administrative support. KS, WY, and ML performed the experiments. WX and MZ analyzed and interpreted the data. KS and WY wrote the manuscript. All authors contributed to the article and approved the submitted version.

FUNDING

The study was supported by the Key Scientific and Technological project of Shaoyang City (2020NS36).

SUPPLEMENTARY MATERIAL

The Supplementary Material for this article can be found online at: https://www.frontiersin.org/articles/10.3389/fonc.2021.690142/full#supplementary-material

Supplementary Figure 1 | Primary OB and MC3T3E1 cells were effective for inducing osteoblast differentiation. Following the induction of osteoblast differentiation, **(A)** the levels of ALP and RUNX2 protein and mRNA expression in cells were measured by qRT-PCR and western blotting. **(B)** ALP staining and Alizarin Red staining were performed to evaluate osteoblast formation. P * 0.05, *; $P < 0.01$, ** *vs.* Control group.

Supplementary Figure 2 | HARA-B4 cells showed a stronger adhesive ability to osteocytes than did HARA cells HARA and HARA-B4 cells that had been transfected with the GFP plasmid were co-cultured with NIH3T3, Primary OB or MC3T3E1 cells. **(A–C)** The adhesive ability of HARA and HARA-B4 cells was measured. NS: not significant. $P < 0.01$, ** *vs.* HARA cells.

REFERENCES

1. Siegel RL, Miller KD, Jemal A. Cancer Statistics, 2020. *CA Cancer J Clin* (2020) 70(1):7–30. doi: 10.3322/caac.21590
2. Ferrer L, Giaj Levra M, Brevet M, Antoine M, Mazieres J, Rossi G, et al. A Brief Report of Transformation From NSCLC to SCLC: Molecular and Therapeutic Characteristics. *J Thorac Oncol* (2019) 14(1):130–4. doi: 10.1016/j.jtho.2018.08.2028
3. Osmani L, Askin F, Gabrielson E, Li QK. Current WHO Guidelines and the Critical Role of Immunohistochemical Markers in the Subclassification of Non-Small Cell Lung Carcinoma (NSCLC): Moving From Targeted Therapy to Immunotherapy. *Semin Cancer Biol* (2018) 52(Pt 1):103–9. doi: 10.1016/j.semcancer.2017.11.019
4. Nagasaka M, Gadgeel SM. Role of Chemotherapy and Targeted Therapy in Early-Stage Non-Small Cell Lung Cancer. *Expert Rev Anticancer Ther* (2018) 18(1):63–70. doi: 10.1080/14737140
5. da Silva GT, Bergmann A, Thuler LCS. Incidence and Risk Factors for Bone Metastasis in Non-Small Cell Lung Cancer. *Asian Pac J Cancer Prev* (2019) 20 (1):45–51. doi: 10.31557/APJCP.2019.20.1.45
6. Rinaldi S, Santoni M, Leoni G, Fiordoliva I, Marcantognini G, Meletani T, et al. Prognostic and Predictive Role of Hyponatremia in Patients With Advanced Non-Small Cell Lung Cancer (NSCLC) With Bone Metastases. *Support Care Cancer* (2019) 27(4):1255–61. doi: 10.1007/s00520-018-4489-2
7. Niu FY, Zhou Q, Yang JJ, Zhong WZ, Chen ZH, Deng W, et al. Distribution and Prognosis of Uncommon Metastases From Non-Small Cell Lung Cancer. *BMC Cancer* (2016) 16:149. doi: 10.1186/s12885-016-2169-5
8. Brunetti G, Belisario DC, Bortolotti S, Storlino G, Colaianni G, Faienza MF, et al. LIGHT/TNFSF14 Promotes Osteolytic Bone Metastases in Non-Small Cell Lung Cancer Patients. *J Bone Miner. Res* (2020) 35(4):671–80. doi: 10.1002/jbmr.3942
9. Wu Y, Ni J, Chang X, Zhang X, Zhang L. Successful Treatment of Pyrotinib for Bone Marrow Metastasis Induced Pancytopenia in a Patient With Non-Small-Cell Lung Cancer and ERBB2 Mutation. *Thorac Cancer* (2020) 11 (7):2051–5. doi: 10.1111/1759-7714.13480
10. Lourenco AR, Ban Y, Crowley MJ, Lee SB, Ramchandani D, Du W, et al. Differential Contributions of Pre- and Post-EMT Tumor Cells in Breast Cancer Metastasis. *Cancer Res* (2020) 80(2):163–9. doi: 10.1158/0008-5472.CAN-19-1427
11. Xie SL, Yang MH, Chen K, Huang H, Zhao XW, Zang YS, et al. Efficacy of Arsenic Trioxide in the Treatment of Malignant Pleural Effusion Caused by Pleural Metastasis of Lung Cancer. *Cell Biochem Biophys* (2015) 71(3):1325–33. doi: 10.1007/s12013-014-0352-3
12. Han P, Cao P, Hu S, Kong K, Deng Y, Zhao B, et al. Esophageal Microenvironment: From Precursor Microenvironment to Premetastatic Niche. *Cancer Manag Res* (2020) 12:5857–79. doi: 10.2147/CMAR.S258215
13. Hamidi H, Ivaska J. Every Step of the Way: Integrins in Cancer Progression and Metastasis. *Nat Rev Cancer* (2018) 18(9):533–48. doi: 10.1038/s41568-018-0038-z
14. Planells-Ferrer L, Urresti J, Coccia E, Galenkamp KM, Calleja-Yagüe I, López-Soriano J, et al. Fas Apoptosis Inhibitory Molecules: More Than Death-Receptor Antagonists in the Nervous System. *J Neurochem* (2016) 139(1):11–21. doi: 10.1111/jnc.13729
15. Wang M, Wang Z, Zhu X, Guan S, Liu Z. NFKB1-miR-612-FAIM2 Pathway Regulates Tumorigenesis in Neurofibromatosis Type 1. *In Vitro Cell Dev Biol Anim* (2019) 55(7):491–500. doi: 10.1007/s11626-019-00370-3
16. Ziaee F, Hajjari M, Kazeminezhad RS, Behmanesh M. SNHG7 and FAIM2 Are Up-Regulated and Co-Expressed in Colorectal Adenocarcinoma Tissues. *Klin Onkol* (2020) 33(6):445–9. doi: 10.48095/ccko2020445
17. Kang HC, Kim JI, Chang HK, Woodard G, Choi YS, Ku JL, et al. FAIM2, as a Novel Diagnostic Maker and a Potential Therapeutic Target for Small-Cell Lung Cancer and Atypical Carcinoid. *Sci Rep* (2016) 6:34022. doi: 10.1038/srep34022
18. She K, Huang J, Zhou H, Huang T, Chen G, He J. lncRNA-SNHG7 Promotes the Proliferation, Migration and Invasion and Inhibits Apoptosis of Lung

Cancer Cells by Enhancing the FAIM2 Expression. *Oncol Rep* (2016) 36 (5):2673–80. doi: 10.3892/or.2016.5105
19. She K, Yan H, Huang J, Zhou H, He J. miR-193b Availability Is Antagonized by LncRNA-SNHG7 for FAIM2-Induced Tumour Progression in Non-Small Cell Lung Cancer. *Cell Prolif* (2018) 51(1):e12406. doi: 10.1111/cpr.12406
20. Wang M, Chao CC, Chen PC, Liu PI, Yang YC, Su CM, et al. Thrombospondin Enhances RANKL-Dependent Osteoclastogenesis and Facilitates Lung Cancer Bone Metastasis. *Biochem Pharmacol* (2019) 166:23–32. doi: 10.1016/j.bcp.2019.05.005
21. Xu Y, Li H, Weng L, Qiu Y, Zheng J, He H, et al. Single Nucleotide Polymorphisms Within the Wnt Pathway Predict the Risk of Bone Metastasis in Patients With Non-Small Cell Lung Cancer. *Aging (Albany N Y)* (2020) 12(10):9311–27. doi: 10.18632/aging.103207
22. Ou SI, Zhu VW. CNS Metastasis in ROS1+ NSCLC: An Urgent Call to Action, to Understand, and to Overcome. *Lung Cancer* (2019) 130:201–7. doi: 10.1016/j.lungcan.2019.02.025
23. Huo J, Xu S, Lam KP. FAIM: An Antagonist of Fas-Killing and Beyond. *Cells* (2019) 8(6):541. doi: 10.3390/cells8060541
24. Huo J, Xu S, Lin B, Chng WJ, Lam KP. Fas Apoptosis Inhibitory Molecule Is Upregulated by IGF-1 Signaling and Modulates Akt Activation and IRF4 Expression in Multiple Myeloma. *Leukemia* (2013) 27(5):1165–71. doi: 10.1038/leu.2012.326
25. Pan Y, Zhang Y, Tang W, Zhang Y. Interstitial Serum Albumin Empowers Osteosarcoma Cells With FAIM2 Transcription to Obtain Viability *via* Dedifferentiation. *In Vitro Cell Dev Biol Anim* (2020) 56(2):129–44. doi: 10.1007/s11626-019-00421-9
26. Chen J, Wu D, Zhang Y, Yang Y, Duan Y. An Y. LncRNA DCST1-AS1 Functions as a Competing Endogenous RNA to Regulate FAIM2 Expression by Sponging miR-1254 in Hepatocellular Carcinoma. *Clin Sci (Lond)* (2019) 133(2):367–79. doi: 10.1042/CS20180814
27. Fornetti J, Welm AL, Stewart SA. Understanding the Bone in Cancer Metastasis. *J Bone Miner Res* (2018) 33(12):2099–113. doi: 10.1002/jbmr.3618
28. Taciak B, Pruszynska I, Kiraga L, Bialasek M, Krol M. Wnt Signaling Pathway in Development and Cancer. *J Physiol Pharmacol* (2018) 69(2):185–96. doi: 10.26402/jpp.2018.2.07
29. Patel S, Alam A, Pant R, Chattopadhyay S. Wnt Signaling and Its Significance Within the Tumor Microenvironment: Novel Therapeutic Insights. *Front Immunol* (2019) 10:2872. doi: 10.3389/fimmu.2019.02872
30. Murillo-Garzón V, Gorroño-Etxebarria I, Åkerfelt M, Puustinen MC, Sistonen L, Nees M, et al. Frizzled-8 Integrates Wnt-11 and Transforming Growth Factor-β Signaling in Prostate Cancer. *Nat Commun* (2018) 9 (1):1747. doi: 10.1038/s41467-018-04042-w
31. Guo Y, Zi X, Koontz Z, Kim A, Xie J, Gorlick R, et al. Blocking Wnt/LRP5 Signaling by a Soluble Receptor Modulates the Epithelial to Mesenchymal Transition and Suppresses Met and Metalloproteinases in Osteosarcoma Saos-2 Cells. *J Orthop Res* (2007) 25(7):964–71. doi: 10.1002/jor.20356
32. Yang X, Li L, Huang Q, Xu W, Cai X, Zhang J, et al. Wnt Signaling Through Snail1 and Zeb1 Regulates Bone Metastasis in Lung Cancer. *Am J Cancer Res* (2015) 5(2):748–55. doi: 10.26402/jpp.2018.2.07
33. Liu X, Zhang Z, Pan S, Shang S, Li C. Interaction Between the Wnt/β-Catenin Signaling Pathway and the EMMPRIN/MMP-2, 9 Route in Periodontitis. *J Periodontal Res* (2018) 53(5):842–52. doi: 10.1111/jre.12574

Conflict of Interest: The authors declare that the research was conducted in the absence of any commercial or financial relationships that could be construed as a potential conflict of interest.

Publisher's Note: All claims expressed in this article are solely those of the authors and do not necessarily represent those of their affiliated organizations, or those of the publisher, the editors and the reviewers. Any product that may be evaluated in this article, or claim that may be made by its manufacturer, is not guaranteed or endorsed by the publisher.

frontiers in Oncology

ORIGINAL RESEARCH
published: 14 October 2021
doi: 10.3389/fonc.2021.712371

Tumor Endothelial Marker 8 Promotes Proliferation and Metastasis *via* the Wnt/β-Catenin Signaling Pathway in Lung Adenocarcinoma

Chen Ding[1†], Jun Liu[1†], Jiali Zhang[1], Yang Wan[1], Linhui Hu[1], Alice Charwudzi[1], Heqin Zhan[2], Ye Meng[1], Huimin Zheng[1], HuiPing Wang[1], Youliang Wang[3], Lihua Gao[3], Xianwen Hu[3], Jingrong Li[4*] and Shudao Xiong[1,5*]*

[1] Department of Hematology/Oncology Lab, The Second Hospital of Anhui Medical University, Hefei, China, [2] Department of Pathology, School of Basic Medical Sciences, Anhui Medical University, Hefei, China, [3] Laboratory of Cell Engineering, Beijing Institute of Biotechnology, Beijing, China, [4] Department of Emergency, The Second Hospital of Anhui Medical University, Hefei, China, [5] Center of Hematology Research, Anhui Medical University, Hefei, China

Tumor endothelial marker 8 (TEM8), also known as ANTXR1, was highly expressed in cancers, and was identified as a biomarker for early diagnosis and prognosis in some cancers. However, the clinical role and molecular mechanisms of TEM8 in lung adenocarcinoma (LUAD) are still unclear. The present study aimed to explore its clinical value and the molecular mechanisms of TEM8 underlying the progression of LUAD. Our study found the elevation of TEM8 in LUAD cell lines and tissues. What's more, we observed that the TEM8 expression level was associated with tumor size, primary tumor, and AJCC stage, and LUAD patients with high TEM8 expression usually have a poor prognosis. Then, we conducted a series of experiments by the strategy of loss-of-function and gain-of-function, and our results suggested that the knockdown of TEM8 suppressed proliferation, migration, and invasion and induced apoptosis in LUAD whereas overexpression of TEM8 had the opposite effect. Molecular mechanistic investigation showed that TEM8 exerted its promoting effects mainly through activating the Wnt/β-catenin signaling pathway. In short, our findings suggested that TEM8 played a crucial role in the progression of LUAD by activating the Wnt/β-catenin signaling pathway and could serve as a potential therapeutic target for LUAD.

Keywords: TEM8, ANTXR1, LUAD, proliferation, prognosis

OPEN ACCESS

Edited by:
Simone Patergnani, University of Ferrara, Italy

Reviewed by:
Fei Han, Army Medical University, China
Daniel Peña-Oyarzun, Pontifical Catholic University of Chile, Chile

****Correspondence:***
Shudao Xiong
xshdao@ahmu.edu.cn
Jingrong Li
412201761@qq.com
Xianwen Hu
huxw1969@163.com

[†]These authors have contributed equally to this work

Specialty section:
This article was submitted to Molecular and Cellular Oncology, a section of the journal Frontiers in Oncology

Received: *20 May 2021*
Accepted: *28 September 2021*
Published: *14 October 2021*

Citation:
Ding C, Liu J, Zhang J, Wan Y, Hu L, Charwudzi A, Zhan H, Meng Y, Zheng H, Wang H, Wang Y, Gao L, Hu X, Li J and Xiong S (2021) Tumor Endothelial Marker 8 Promotes Proliferation and Metastasis via the Wnt/β-Catenin Signaling Pathway in Lung Adenocarcinoma. Front. Oncol. 11:712371. doi: 10.3389/fonc.2021.712371

Abbreviations: LUAD, Lung adenocarcinoma; NSCLC, Non-small cell lung cancer; TEM8, Tumor endothelial marker 8; ANTXR1, Anthrax toxin receptor; AJCC, American Joint Committee on Cancer; OS, Overall survival; CI, Confidence Intervals; HR, Hazard Ratio; NC, Negative control; siRNA, Small interfering RNA; qRT-PCR, Quantitative real-time PCR; pGSK-3β, Phosphorylated GSK-3β; Phosphorylated ERK1/2; CCK-8, Cell counting kit-8; PBS, Phosphate buffered solution; FBS, Fetal bovine serum; IHC, Immunohistochemistry; KM, Kaplan–Meier; ROC, Receiver operating characteristic; ECOG, Eastern Cooperative Oncology Group.

INTRODUCTION

Lung cancer is the major cause of tumor-related death worldwide (1). Non-small cell lung cancer (NSCLC), which includes adenocarcinoma, squamous cell carcinoma, and large cell carcinoma, represents approximately 85% of all lung cancer cases (2, 3). Among them, the incidence of lung adenocarcinoma (LUAD) is rising and is gradually occupying a center stage (4). In addition, although molecular targeted therapy and immunotherapy for LUAD have made great progress in recent years, the 5-year overall survival (OS) rate historically remains very poor (5–8). Hence, a deeper understanding of the molecular mechanisms underlying the development of LUAD might establish effective therapeutic targets that are urgently needed.

Tumor endothelial marker 8 (TEM8), an integrin-like cell surface protein, was demonstrated as a tumor-associated marker in colorectal cancer by St. Croix in 2000 (9). Initially, TEM8 was found as an anthrax toxin receptor, so it was alternatively named ANTXR1 (10). A previous study also reported TEM8 as a specific protein molecule upregulated in tumor endothelial cells, required for tumor angiogenesis (11). With the deepening of research, an increasing number of mechanisms of TEM8 in cancer were revealed, such as in gastric cancer (12), breast cancer (13), and ovarian cancer (14). Among these, Tiara et al. (15) investigated the role of TEM8 in cancer progression and metastasis in invasive breast cancer; they proved that TEM8 regulates cancer progression by affecting the expression levels of cell cycle-related genes. Furthermore, in early 2020, researchers had reported that TEM8 might be used as an early diagnostic indicator of lung cancer, providing a reference for the early diagnosis of lung cancer in future clinical practice (16). However, the mechanism and clinical value in LUAD are not clear and need to be elucidated.

In this study, we explored the role and mechanism of TEM8 in LUAD. Our experiments *in vitro* and *in vivo* elucidated that the TEM8 in LUAD cell lines remarkably induced cell proliferation, invasion and migration, and suppressed apoptosis. In addition, our mechanistic investigations showed that TEM8 promoted lung cancer cell proliferation and invasion by activating Wnt/β-catenin. Moreover, we also found that TEM8 was associated with reduced overall survival (OS). Collectively, our results revealed that TEM8 played a crucial role in the progression of LUAD by activating the Wnt/β-catenin signaling pathway and might be a novel biomarker and therapeutic target for LUAD.

METHODS

Cell Culture and Regents

Human LUAD cell lines (A549, and H1299) and human normal bronchial epithelial cell line (BEAS-2B) were acquired from American Type Culture Collection (Manassas, VA, USA) and maintained in RPMI-1640 medium (Hyclone Logan, Utah, USA) supplemented with 10% fetal bovine serum. All cell lines were maintained at 37°C and 5% CO2 in a humid environment.

ICG001 (SF6827) was purchased from Beyotime Institute of Biotechnology and dissolved in DMSO. And the TEM8-overexpressed cells were treated with ICG001 for 24 hours at the recommended concentration of 25 μM.

Cell Transfection

SiRNA for TEM8 was designed and synthesized by Gene Pharma (Shanghai, China),and the sequence was: si-TEM8 (1) F: 5'-GCC AGUGAGCAGAUUUAUUTT-3' (forward), R: 5'-AAU AAAUCUGCUCACUGGCTT-3' (reverse). si-TEM8 (2) F: 5'-GCGGAUUUGACCUGUACUUTT-3' (forward), R: 5'-AAG UACAGGUCAAAUCCGCTT-3' (reverse). The corresponding negative control (NC) sequence was also purchased from the same company: F 5'-UUCUCCGAACGUGUCACGUTT-3' (forward), R: 5'-ACGUGACACGUUCGGAGAATT-3' (reverse). The cells were transfected with the siRNA using Lipofectamine 2000 (Life Technologies, Grand Island, NY, USA) according to the manufacturer's protocol.

Meanwhile, the stably TEM8 overexpressing cell lines and control cell lines were established by lentiviral transfection. Overexpression plasmids lentiviral vector carrying GFP was synthesized by GeneChem (shanghai, China). And the cells were transfected with overexpression plasmids and empty vectors according to the manufacturer's instructions. Then puromycin (1ug/ml) (Bioss, Beijing, China) was used to select the stably transfected cell lines.

The knockdown and overexpression efficiencies were evaluated by quantitative real-time PCR (qRT-PCR) and western blotting.

Real-Time Quantitative PCR Analysis

Total RNA was extracted using Trizol reagent (Invitrogen, Carlsbad, CA, USA) an extracted following the manufacturer's protocol. The cDNA was obtained *via* reverse transcription using the reverse transcription kit (Thermofisher Scientific, USA) according to the manufacturer's manual. Quantitative real-time PCR (qRT-PCR) was performed using TB Green PCR Mix (TaKaRa, Dalian, China) according to the manufacturer's manual. The primer sequences are: (1) TEM8: F: 5'-TGCA ACACAGAAATGCTCTGCCTG-3' (forward), R: 5'-TTTAT CCCTGGGTGATGAAGCCCA-3' (reverse), (2) GAPDH: F: 5'-AGCAAGAGCACAAGAGGAAG-3' (forward), R: 5'-GGT TGAGCACAGGGTACTTT-3' (reverse). The relative expression ratio of TEM8 in each group was calculated by the $2^{-\Delta\Delta Ct}$ method.

Western Blot

The cells were collected, and total proteins were extracted. The total proteins were resolved by SDS-polyacrylamide gel electrophoresis on 12% gels and transferred onto polyvinylidene difluoride transfer membrane (Merck Millipore, Billerica, USA). Primary antibody incubation was performed overnight at 4°C. The primary antibodies used were TEM8 (1:500 dilution) (Affinity, America), Wnt1 (1:1000 dilution) (Abcam, Cambridge, UK), β-catenin, pGSK-3β, GSK-3β, cyclin D1, P21, β-actin (1:1000 dilution) (Cell Signaling Technology, Danvers, MA, USA). Then, the blots were developed with a

peroxidase-conjugated secondary antibody (1:5000 dilution) (Cell Signaling Technology, Danvers, MA, USA), and the proteins were visualized using the ECL Plus detection Reagent (Tanon, Shanghai, China). The gray-scale value was assessed by *ImageJ* (ImageJ v1.47).

Flow Cytometry Analysis

Flow cytometry analysis was conducted to detect apoptotic cells. After transfecting the lung cancer cell lines with TEM8-siRNA and NC-siRNA, the cells were harvested into centrifuge tubes. The cells were then washed with PBS and stained using 5ul Annexin V reagents and 5ul PI reagents (BestBio, Shanghai, China) for 15min in the light-proof condition. The mixture was added to 400ul of Binding Buffer after the reaction. Cell apoptosis was analyzed using the *CytoFlex* (Beckman CytoFlex, USA).

Cell Proliferation Assay

The cell counting kit-8 (CCK-8) assay was used to evaluate the level of cell proliferation. After 24h of transfection with TEM8 siRNA and NC siRNA, the cells were cultured in 96-well plates (5×10^4/well). The cells were then incubated for 24, 48, and 72h at 37°C. Thereafter, 10μl of CCK−8 solution (Beyotime Institute of Biotechnology, China) was added to each well and cultured at 37°C for 2h according to the manufacturer's instruction. The absorbance at 450nm was measured using a microplate autoreader (Bio Tek Instruments Inc., Winooski, VT, USA).

Colony Formation Assay

For the colony formation assays, the transfected cells (1×10^3/well) were placed into six-well plates and cultured for two weeks. The colonies were then washed with PBS, fixed in methanol, stained with crystal violet, photographed, and counted.

Wound-Healing Assay

Cells (1×10^5/well) were pretreated or not with mitomycin C (5ug/ml) (Selleck, USA), seeded in six-well plates, and serum-starved for 24h. Then we used a 200ul pipette tip to make a scratch after cells were grown to 80% confluence. The wound healing process was observed and photographed at a magnification of 100× at the indicated time points (0 and 24h).

Transwell Invasion Assay

Cells (10×10^4/well) were pretreated with mitomycin C(5ug/ml) (Selleck, USA), and seeded in the top chambers in 100μL serum-free medium; the lower chambers were filled with a 600ul complete medium with 20% FBS. After 48h incubation, 0.1% crystal violet dye was used to stain cells. The images were analyzed by *ImageJ* (ImageJ v1.47).

Dual-Luciferase Report Assay

Cells (5×10^3/well) were seeded into a 96-well plate. And the cells of the knockdown group were transfected with 200ng Top/Fop-flash reporter plasmids (Beyotime Institute of Biotechnology, China) and 0.25ul siRNA using Lipofectamine 2000. The stably selected overexpression cells were just transfected with 200ng Top/Fop-flash reporter plasmids using Lipofectamine 2000. After 24h of incubation, the luciferase activity was detected by the Dual-Luciferase Reporter Assay System (Beyotime Institute of Biotechnology, China).

Immunohistochemistry

IHC staining was performed as described previously (17). The Human LUAD tissue array was purchased from Outdo Biotech (Shanghai, China). TEM8 expression was assessed by multiplying scores representing the reaction degree of positive cells and staining intensity. Staining intensity was graded as 0 (no staining), 1 (weak staining=light yellow), 2 (moderate staining=yellow brown), and 3 (strong staining=brown). The extent (0–100%) of reactivity was scored as follows: 0 (≤25% positive cells), 1 (26%-50% positive cells), 2 (51%-74% positive cells), 3 (≥75% positive cells). Scores of 0–4 were classified as low expression, whereas all other scores were classified as high expression. Two pathologists without knowledge of the clinic-pathological variables independently scored staining on each slide. Staining assessment and the allocation of tumors by the two pathologists were similar. All immunohistochemical images were obtained using an Olympus BX51 microscope equipped with a 200× objective lens (Olympus) and a DP 50 camera (Olympus).

In Vivo Tumorigenic Assay

Female BALB/c nude mice (4 weeks old) were purchased from GemPharmatech Co.Ltd (Nanjing, China) and maintained under specific pathogen-free conditions. The mice were randomly assigned into NC and TEM8-knockdown groups (n=5 mice/group). H1299 cells were transfected with siRNA-TEM8 or siRNA-NC for 24h. And cells were collected with PBS and mixed with an equal volume of Matrigel at a final concentration of 1×10^8/ml. Then each mouse was injected with 100ul of the cell suspensions. When the volumes of tumors grew to about 1 cm^3, the nude mice were killed, and the tumor was extracted. Meanwhile, the tumor volumes and body weights were measured every 3 days. All animal studies were carried out with the approval of the Ethics Committee of AnHui Medical University (Approval No. LLSC20190462).

Statistical Analysis

Statistical analyses were performed using SPSS (version 16.0 for Windows, SPSS Inc., Chicago, IL, USA) and GraphPad Prism 8.0 (GraphPad 8.0, San Diego, CA, USA). The quantitative data were expressed as means ± SD. Significant differences were determined by the independent t-test or ANOVA. Survival curves were estimated by the Kaplan–Meier (KM) method. Chi-square analysis was used to explore relations between TEM8 expression in tumor tissues and clinicopathologic characteristics of LUAD patients. The independent prognostic factors in LUAD were determined by Cox regression. And factors with $P<0.05$ in the univariate analysis were entered into the multivariate analysis. Regarding Kaplan-Meier plotter (http://kmplot.com/) analysis, patients with adenocarcinoma were chosen; the patients were divided into 2 groups based on the median value of TEM8, higher than median TEM8 value was defined as a high group, otherwise was assigned a low group. What's more, the gene expression data set was derived from

220092_s_at probe. A p-value less than 0.05 was used as the criterion for statistical significance.

RESULTS

TEM8 Was Upregulated in LUAD Tissues and Cell Lines

To determine whether TEM8 is aberrantly expressed, we performed Western Blot by using A549, H1299 and BEAS-2B cells. Our data showed that TEM8 was highly expressed in LUAD cell lines (A549 and H1299) compared with normal bronchial epithelial cell lines (BEAS-2B) (**Figure 1A**). To investigate the level of TEM8 expression in patients with LUAD, we applied IHC to examine its expression in a human LUAD tissue array (HLugA180Su07). We found TEM8 remarkably upregulated in the tumor tissues compared with the matched adjacent normal tissues (**Figure 1B**). Taken together, these findings suggested that TEM8 was significantly elevated in LUAD tissues and cell lines.

High TEM8 Expression Was Associated With Poor Prognosis of LUAD Patients

Based on the above analysis, we further investigated whether TEM8 expression is associated with the clinical outcome of LUAD. As presented in **Figures 2A, B**, the expression levels of TEM8 correlated with the tumor stage. Given this, we deeply analyzed the human LUAD tissue array (HLugA180Su07), which contained gene expression profiles of 95 human LUAD with clinical follow-up information. The samples were divided into two groups (low and high) according to the IHC staining score. As shown in the KM survival analysis, LUAD patients with high-TEM8 expression usually had shorter OS (**Figure 2C**). The result of the Kaplan-Meier plotter (http://kmplot.com/) confirmed our finding, demonstrating that high TEM8 expression remarkably correlated with a poorer OS in patients with LUAD (HR= 1.54; 95% CI, 1.22-1.96; P = 0.00031; **Figure 2D**).

Notably, TEM8 expression was correlated with tumor size ($p<0.05$), primary tumor ($p<0.05$), and AJCC stage ($p<0.05$) based on the Chi-square test (**Table 1**). As presented in the univariate Cox regression analysis, TEM8 expression, primary tumor, and AJCC stage were risk factors for LUAD ($P < 0.05$). But the multivariate Cox regression analysis indicated that TEM8 expression was not an independent predictor of OS (**Table 2**). Anyway, all these results proved that TEM8 expression was upregulated in human LUAD tissues, which may be associated with poor prognosis in LUAD.

TEM8 Promoted Malignancy Phenotypes of Lung Cancer Cells *In Vitro*

Next, to explore the impact of TEM8 on the malignancy development of LUAD, we constructed the loss-of-function in both H1299 and A549 cells and gain-of-function in A549 cells. After TEM8 silencing with siRNA (**Figures 3A, C**), TEM8 was expressed at a lower level in Si-TEM8 groups than in the NC group. The results of CCK-8 assays showed that the proliferation rates of repressed TEM8 cells presented a remarkable decrease relative to the NC cells (**Figure 3D**). The data revealed that suppressing TEM8 levels reduced the number of proliferative LUAD cells. Moreover, clone formation assay proved that the colony formation abilities also decreased after knocking down

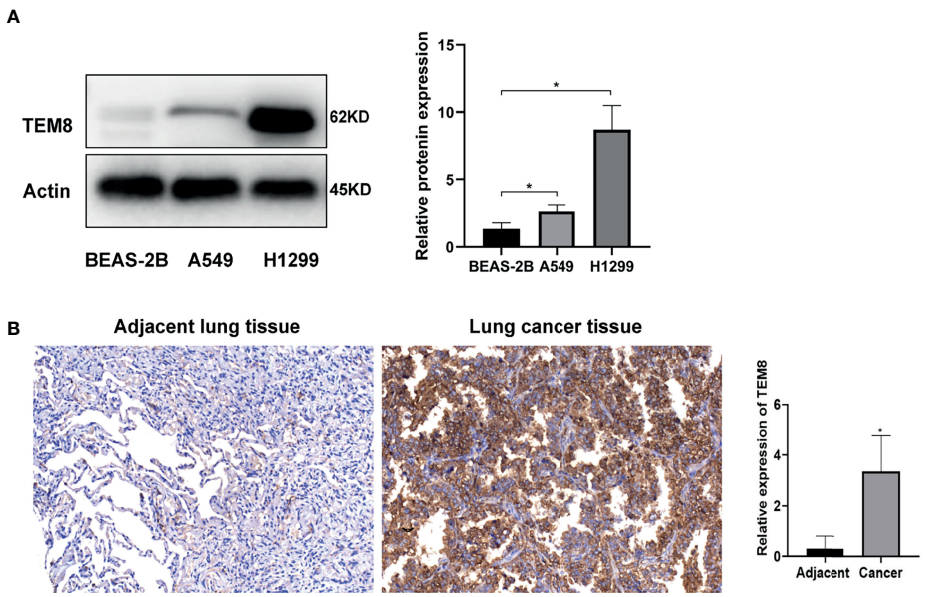

FIGURE 1 | TEM8 expression is increased in LUAD tissue and LUAD cell lines. **(A)** Relative expression of TEM8 protein in human LUAD cell lines (A549 and H1299) and normal bronchial epithelial cell lines (BEAS-2B) by western blotting. **(B)** Representative images and quantitative results of TEM8 expression in LUAD tissue and adjacent normal tissue by immunohistochemistry. All experiments were repeated at least three times and representative as shown. Data are means ± SD, *p < 0.05.

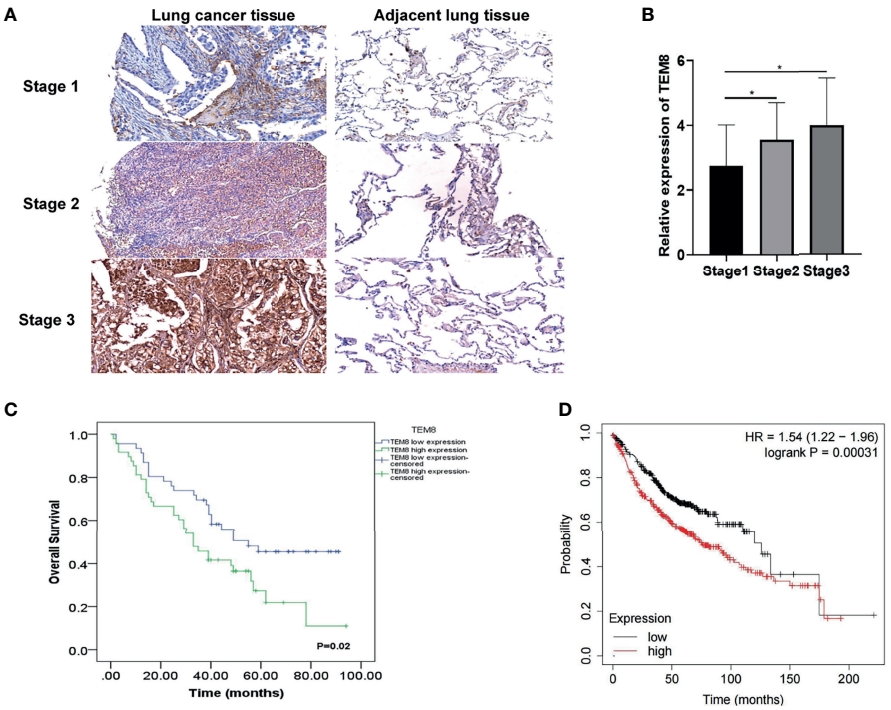

FIGURE 2 | TEM8 expression correlated with poor prognosis in LUAD patients. **(A)** Representative images of TEM8 IHC staining in samples from human LUAD tissue array (magnification, 200×). **(B)** Quantitative results of TEM8 expression levels in LUAD tissue arrays. **(C, D)** Kaplan-Meier curves of overall survival in LUAD patients stratified by TEM8 expression. Each subgroup was divided into low and high TEM8 expression groups. Patients with higher TEM8 expression had a poorer prognosis. All experiments were repeated at least three times and representative as shown. Data are means ± SD, *p < 0.05.

TABLE 1 | Correlation between TEM8 expression in tumor tissues and clinicopathologic characteristics of LUAD patients.

Characteristic	Patients	TEM8 expression		P-value
		Low (n = 46)	High (n = 49)	
Gender				0.784
Male	53	25	28	
Female	42	21	21	
Age (years)				0.363
<60	45	24	21	
≥60	50	22	28	
Tumor size (cm)				0.000*
<4	43	36	8	
≥4	51	10	41	
Primary tumor (T)				0.000*
$T_1 - T_2$	67	44	23	
$T_3 - T_4$	26	0	26	
Tumor stage				0.199
I+II	62	33	29	
III+IV	33	13	20	
AJCC stage				0.001*
1-2 stage	50	32	18	
3-4 stage	44	13	31	

represent P value less than 0.05.

TEM8 (**Figure 3E**). In addition, apoptosis assay was performed by the flow cytometry analyses, and our data showed that the apoptotic rate of LUAD cells in the si-TEM8 group was higher than that in the NC group (**Figure 3F**).

Meanwhile, we performed overexpression experiments proved by western blotting and qRT-PCR (**Figures 3B, C**). As expected, the CCK8 and colony formation assays suggested that the ability of LUAD cell proliferation was enhanced as the

TABLE 2 | Univariate and multivariate analyses of prognostic factors in LUAD patients.

Characteristic	Univariate analysis			Multivariate analysis		
	HR	95% CI	P-value	HR	95% CI	P-value
Gender						
Male *vs.* Female	1.110	0.668-1.844	0.688			
Age (years)						
<60 *vs.* ≥60	1.451	0.868-2.426	0.156			
Tumor size (cm)						
<4 *vs.* ≥4	1.229	0.839-1.800	0.289			
Primary tumor (T)						
T1–T2 *vs.* T3–T4	1.875	1.089-3.229	0.023*	1.196	0.659-2.170	0.555
Tumor stage						
I+II *vs.* III+IV	1.016	0.598-1.725	0.953			
AJCC stage						
1-2 *vs.* 3-4	3.493	2.029-6.013	0.000*	3.736	1.773-7.871	0.001*
TEM8 expression						
Low *vs.* High	1.239	1.011-1.518	0.039*	1.132	0.837-1.532	0.422

**represent P value less than 0.05.*

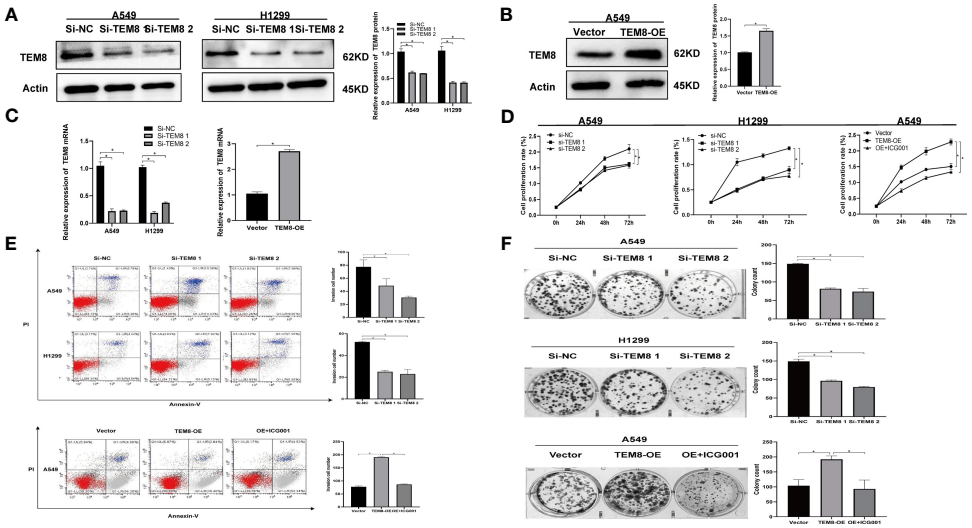

FIGURE 3 | Effects of expression of TEM8 on LUAD cell proliferation and apoptosis *in vitro*. **(A–C)** Knockdown of TEM8 in H1299 and A549 cells and overexpression of TEM8 in A549 cells were identified by quantitative PCR and western blot. **(D, F)** CCK8 and colony formation assays were carried out in A549 and H1299 cells expressing the negative control or siRNA of TEM8 and in A549 cells expressing the vector control, TEM8-OE or OE+inhibitor ICG0001. **(E)** Flow cytometry assays were used to examine the effect of TEM8 on cell apoptosis. All experiments were repeated at least three times and representative as shown. Data are means ± SD, *p < 0.05.

overexpression level of TEM8 (**Figures 3D, F**). What's more, the results of the apoptosis assay were opposite to the results obtained when the TEM8 was knocked down (**Figure 3E**).

Together, these results collectively proved that TEM8 accelerates the LUAD cells' proliferation and decreases apoptosis.

TEM8 Accelerated the Metastatic Potentials of LUAD Cells

As mentioned above, the elevated expression level of TEM8 might contribute to the development of LUAD. We next investigated the effect of TEM8 on LUAD metastasis. Firstly, we treated cells with mitomycin C to exclude the effects of proliferation on metastasis, and the wound-healing assays showed that TEM8 deficiency reduced the wound closures of LUAD cells when compared with NC cells, whereas the TEM8-overexpressed A549 cells exhibited stronger migration capabilities than control vector cells (**Figure 4A**). Moreover, we conducted transwell analyses, and the results also certified that the suppression of TEM8 resulted in markedly decreased invasive cell numbers. In contrast, cells stably overexpressing TEM8 showed stronger invasion ability (**Figure 4B**). Above all, these findings proved that TEM8 had a facilitation effect on LUAD cell migration and invasion.

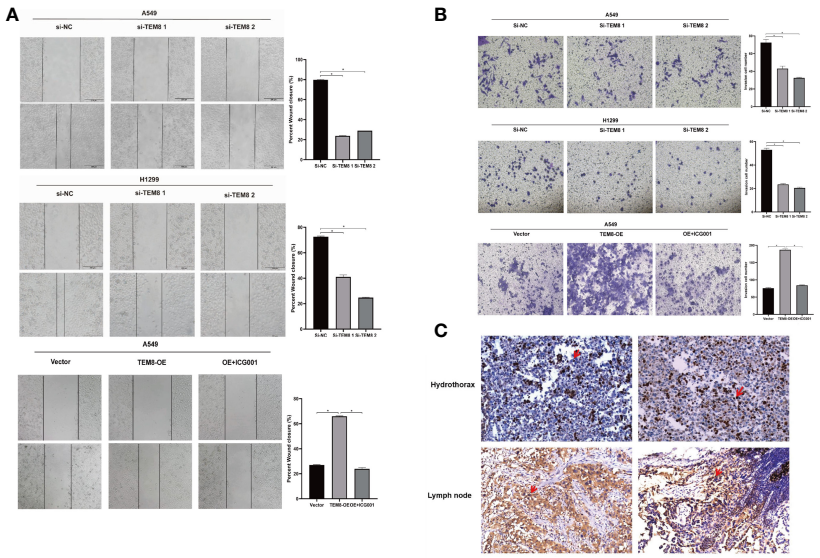

FIGURE 4 | The inhibition of TEM8 suppresses the metastatic potentials of LUAD. **(A, B)** Representative images of cell migration based on wound-healing assays and transwell assays in knockdown groups and overexpression groups, and quantitative analysis of cell migration based on transwell assays. **(C)** Representative images of TEM8 IHC staining in samples from patients with hydrothorax and lymph node metastasis (magnification, 200×). All experiments were repeated at least three times and representative as shown. Data are means ± SD, *p < 0.05.

Besides, we performed IHC for TEM8 on 20 pleural fluid samples and 20 lymph node metastasis samples obtained from patients with LUAD. We found that TEM8 was highly expressed in cancer cells in the hydrothorax and lymph node metastasis specimens from late-stage LUAD patients (**Figure 4C**). This result further suggested that TEM8 induced the metastatic potentials of LUAD.

TEM8 May Promote LUAD Progression Through The Wnt/β-Catenin Signaling Pathway

After elucidating the effect of TEM8 on LUAD progression, we investigated the mechanisms involved in this process. Some reports show the constant upregulation of the Wnt/β-catenin signaling pathway in various cancers (18). Evidence suggests that the Wnt/β-catenin signaling pathway is involved in the proliferation and apoptosis of lung cancer (19). Therefore, we further explored if the tumorigenic effects of TEM8 were dependent on the Wnt/β-catenin signaling pathway. As shown in **Figure 5A**, the expression levels of Wnt1, GSK3β, pGSK3β, and β-catenin were decreased in the TEM8-knockdown (KD) groups but increased in TEM8-overexpressed groups. To further confirm these results, rescue experiments were performed. We used the Wnt/β-catenin signaling pathway inhibitor ICG001 to treat TEM8-overexpressed A549 cells. Then we found that ICG001 significantly reduced proliferation capacity in the CCK8, colony formation, and apoptosis assays (**Figures 3D–F**). Also, ICG001 treatment inhibited the promotional effects on migration and invasion caused by TEM8 overexpression (**Figures 4A, B**). Importantly, we also used the dual-luciferase reporter assay to investigate the regulation of Wnt/β-catenin signaling activity. As shown in **Figure 5C**, the results showed that TEM8 knockdown significantly reduced Wnt reporter activity. In contrast, the overexpression of TEM8 enhanced Wnt reporter activity. Collectively, these results consistently proved that TEM8 played a key role in the activation of the Wnt/β-catenin signaling pathway.

In addition, previous studies have proved that p21 and cyclin-D1 are the Wnt targets associated with the proliferation of tumor cells (20–22). Therefore, we investigated whether TEM8 activated the Wnt/β-catenin signaling pathway to regulate the p21 and cyclin D1. Expectedly, the results proved that the expression level of p21 in the Si-TEM8 groups was higher compared with the Si-NC groups. In contrast, the expression of p21 was remarkably downregulated in the TEM8-overexpressed group. Additionally, the cyclin D1 expression level was lower with TEM8 knockdown but higher with TEM8 overexpression (**Figure 5B**). Above all, our findings indicated that the Wnt/β-catenin pathway might be the major downstream signaling pathway activated by TEM8 (**Figure 5D**).

TEM8 Promotes LUAD Cell Tumorigenesis *In Vivo*

To investigate the effect of TEM8 on LUAD cell tumorigenesis *in vivo*, we injected mice with H1299 cells expressing si-NC and si-TEM8 *via* subcutaneous injections. As shown in **Figures 6A, B**, the H1299/TEM8-KD-injected animals had fewer and smaller tumors than the H1299/NC-injected animals. Additionally, as indicated by the xenograft tumor size, tumor growth curves, and mice body weight curves (**Figures 6C–E**), TEM8-KD cells had a significantly weaker capacity to form tumor nodules in nude mice. The findings suggest TEM8 expression is critical for the development of LUAD cells. The tissues were further examined

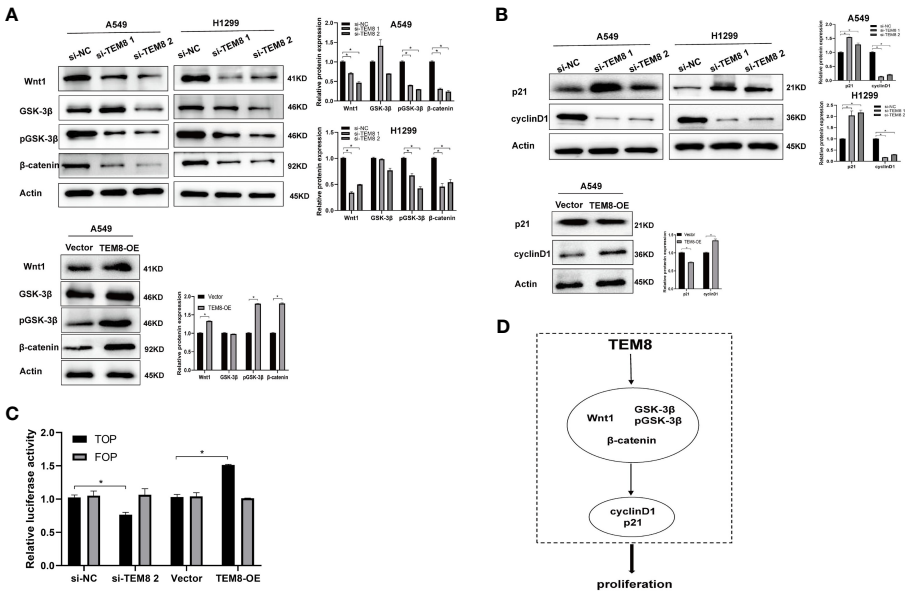

FIGURE 5 | TEM8 may promote LUAD progression *via* activating the Wnt/β-catenin signaling pathway. **(A)** Western blotting was used to investigate the effect of TEM8 downregulation or overexpression on the expression levels of Wnt1, GSK-3β, pGSK-3β and β-catenin in A549 and H1299 cells. **(B)** Western blot analysis for p21 and cyclinD1 in TEM8-silenced cells, TEM8-overexpressed cells, and TEM8-overexpressed cells treated with ICG001. **(C)** The luciferase activity of Wnt/β-catenin signaling was detected using a TOP-flash assay with FOP-flash as a negative control. **(D)** Schematic diagram of the regulatory mechanism of TEM8 in promoting lung cancer cells proliferation. TEM8 could activate the Wnt/β-catenin signaling pathway, then activate the p21 and cyclin D1, thereby mediating the proliferation of LUAD cells. All experiments were repeated at least three times and representative as shown. Data are means ± SD, *p < 0.05.

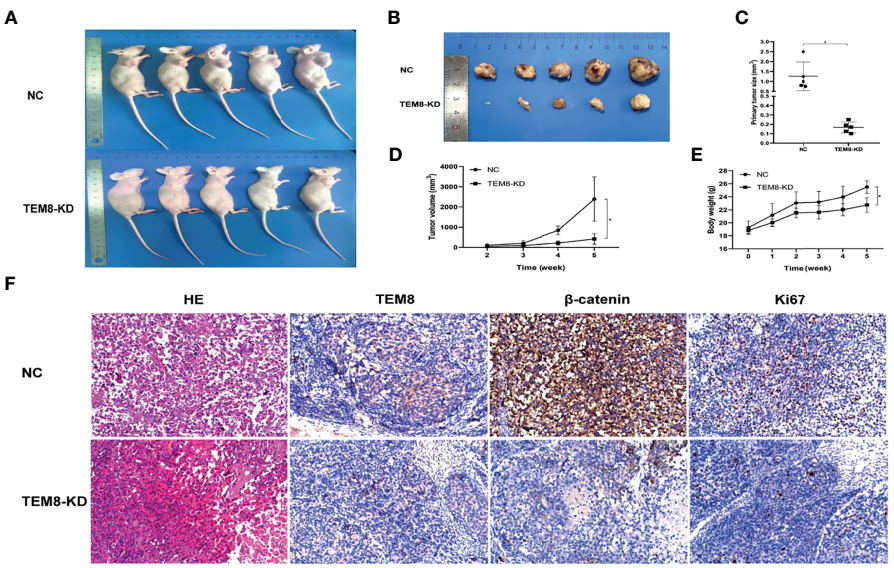

FIGURE 6 | TEM8 promotes tumorigenesis of LUAD cells in nude mice. **(A, B)** Knockdown (KD) of TEM8 attenuated tumor growth in the nude mice model by xenograft growth assay. Xenograft tumors **(B)** from **(A)** were dissected and photographed. **(C)** Tumor size from the negative control or TEM8-knockdown groups. Each group contained five mice. **(D, E)** The tumor growth curve and mice growth curve of TEM8-knockdown cells were compared with negative control cells. Each group contained five mice. **(F)** HE staining and immunohistochemistry for TEM8, β-catenin, and Ki67 in the negative control group and the TEM8-knockdown group. Data are means ± SD, *p < 0.05.

by HE staining to confirm the presence of tumors. IHC demonstrated that TEM8-KD groups had fewer expression levels of TEM8 than NC groups. Moreover, to verify if TEM8 exerts its effect by activating Wnt/β-catenin signaling pathway *in vivo*, the expression of β-catenin was examined in the xenograft tumor samples, and the results showed that β-catenin was expressed in the cell nucleus at a lower level in the TEM8-KD group. Additionally, the IHC also found that the TEM8-KD group had fewer Ki67-positive cells than the NC group (**Figure 6F**). All these data suggested that TEM8 is capable of promoting the development in LUAD.

DISCUSSION

TEM8, an anthrax toxin receptor, is reported as a tumor-associated biomarker in cancers (10, 23), however, the role and mechanism in LUAD are not clear. In our study, our results demonstrated the elevation of TEM8 in LUAD cell lines and cancer tissues. Our data also found that the TEM8 expression level was associated with cancer behaviors, including tumor size, primary tumor, and AJCC stage, and TEM8 is a poor prognosis factor in LUAD patients. Importantly, we firstly reported that the TEM8 promoted LUAD proliferation and metastasis *via* the Wnt/β-catenin signaling pathway.

Previous studies have proved that TEM8 is broadly expressed in tumor endothelial cells (9, 11). Meanwhile, some researchers found that TEM8 positively regulates the proliferation of endothelial cells in cancer while negatively regulating the proliferation in normal endothelial cells (24, 25). But few reports indicated that TEM8 is highly expressed in lung cancer (16, 26). In the study of Sun (16), they measured the serum TEM8 expression in 204 patients with lung cancer by PCR, and the results showed that the expression level of TEM8 in patients with lung cancer was significantly higher than that in healthy subjects. Their report was based on serum TEM8 levels, and LUAD was not mentioned, so the results and conclusions need to be elucidated in LUAD tissues. In addition, Gong et al. (26) also revealed that TEM8 was highly expressed in lung cancer tissues and cells and potentially involved in tumor angiogenesis. Thus, our results about the expression level of TEM8 were roughly consistent with the two previous studies and suggested that a high level of TEM8 may induce progression in LUAD.

Our data also found that the TEM8 expression level was associated with cancer behaviors, including tumor size, primary tumor, and AJCC stage in LUAD patients. The univariate Cox regression analysis demonstrated that TEM8 expression, primary tumor, and AJCC stage were risk factors for LUAD. However, TEM8 was not the independent risk factor of OS for LUAD by multivariate Cox regression analysis, this maybe caused by the partly missing clinical data including Eastern Cooperative Oncology Group (ECOG) Scale of performance status in the patients' tissue array samples, so a larger sample size and longer follow-up time are needed to demonstrate the clinical value in the future. Simultaneously, a recent study has shown that TEM8 could be an excellent indicator for early clinical diagnosis and prognosis of lung cancer (16). In the study, they plotted the receiver operating characteristic (ROC) curve and found that TEM8 has a diagnostic value in patients with lung cancer (pathological type was not mentioned). In the light of their study, TEM8 expression correlated with smoking, lymphatic metastasis, TNM stage, and pleural invasion. Anyway, our findings extended previous observations and supported the notion that TEM8 expression level was associated with cancer behavior and was a poor factor in LUAD.

Recent studies have reported that TEM8 positively regulates the proliferation in varieties of cancers, including breast cancer, gastric cancer, and so on (12, 14, 27–29). Subsequently, our loss-of-function and gain-of-function experiments and a series of functional experiments *in vitro* and *in vivo* indicated that TEM8 accelerates the proliferation but suppresses the apoptosis of LUAD cells. Also, the elevation of TEM8 has a facilitating effect on the migration and invasion of LUAD cells. What's more, higher TEM8 expression was validated in the pleural effusion and lymph nodes from the late stage of LUAD patients. These results were similar to Gong's previous study (26). Thus, all these data suggested that TEM8 plays a vital role in the development of LUAD.

Moreover, we further set up experiments to explore the underlying mechanism through which TEM8 promotes LUAD progression. Studies have reported that Wnt/β-catenin signaling is important in LUAD cell lines, and the inhibition of Wnt reduces proliferation (30–33). Thus, we speculated that TEM8 might activate the Wnt/β-catenin signaling pathway to promote the development of LUAD. In this study, we verified the above signaling pathway proteins in the TEM8-knockdown and TEM8-overexpression groups. The results suggested that the levels of Wnt1, pGSK-3β, and β-catenin were decreased in the TEM8-knockdown group but increased in the TEM8-overexpression group. Additionally, Wnt/β-catenin inhibitor ICG001 rescued the function of overexpressed TEM8 in LUAD cells. Importantly, as expected, the data validated that the TEM8 knockdown inhibited the activity of the Wnt/β-catenin signaling pathway *via* the TOP/FOP flash luciferase reporter system. Hence, these findings collectively indicated that TEM8 promoted the malignant biological behavior of LUAD cells by activating the Wnt/β-catenin signaling pathway.

Moreover, previous pieces of evidence have demonstrated that TEM8 promoted the proliferation of osteosarcoma and ovarian cancer by regulating the expression of p21 and cyclin D1 (14, 27). Meanwhile, multiple previous studies have demonstrated that cyclinD1 and p21 are the downstream target genes of the Wnt/β-catenin signaling pathway (34–38). Besides, we found that the expression level of cyclin D1 was reduced while the expression level of p21 was increased in TEM8-siRNA cells. Furthermore, these results in the TEM8-OE group contradicted those in the TEM8-KD group. Above all, these findings firstly demonstrated that TEM8-induced progression of LUAD may be due to modulation of Wnt/β-catenin activity. Our novel findings may provide new insights into the mechanisms of TEM8 and suggest TEM8 could be a potential therapeutic target of LUAD.

This study aimed to systematically explore the clinical role and the molecular mechanisms of TEM8 underlying the progression of LUAD and establish effective therapeutic targets. However, due to the limited conditions of this study, there are still some shortcomings in the relevant clinical prognostic analysis. Therefore, additional studies are needed to refine and expand our findings.

In conclusion, our study showed that the expression of TEM8 in LUAD was significantly upregulated and closely associated with the poor prognosis of LUAD patients. Simultaneously, our results firstly demonstrated that TEM8 played a crucial role in promoting LUAD cell progression by activating the Wnt/β-catenin signaling pathway *in vitro* and *in vivo*. Our findings suggested that TEM8 could serve as a biomarker and potential therapeutic target for LUAD.

DATA AVAILABILITY STATEMENT

The original contributions presented in the study are included in the article/**Supplementary Material**. Further inquiries can be directed to the corresponding authors.

ETHICS STATEMENT

The animal study was reviewed and approved by Anhui Medical University.

AUTHOR CONTRIBUTIONS

SX and JuL designed the study. CD and JuL performed the experiments. CD and JuL interpreted the results. JZ and YaW supervised the study. SX provided the funding. CD and LH wrote the draft. AC and YM revised the draft. All authors contributed to the article and approved the submitted version.

FUNDING

This work was partly supported by the Key Research and Development Plan of Anhui Province, China (201904a07020058), Higher School of Anhui Provincial Natural Science Research Project (KJ2018A0198), Foundation of Anhui Medical University (2019xkj134), National Science Foundation of China (81272259, 82172858), Basic and Clinical Cooperative Research Promotion Plan of Anhui Medical University[2020xkjT021], Scientific Research Foundation of the Institute for Translational Medicine (SRFITMAP, 2017zhyx13).

ACKNOWLEDGMENTS

We thank our laboratory colleagues for their continuous support and fellowship.

SUPPLEMENTARY MATERIAL

The Supplementary Material for this article can be found online at: https://www.frontiersin.org/articles/10.3389/fonc.2021.712371/full#supplementary-material

Supplementary Figure 1 | The rate of pGSK-3β/GSK-3β was decreased with the knockdown of TEM8 **(A, B)**, whereas elevated with the overexpression of TEM8 **(C)**.

Supplementary Figure 2 | Nuclear localization of β-catenin is observed in IHCs of patient samples.

Supplementary Figure 3 | The expression of TEM8 in lung cancer cell lines (A549, H1299, H1395, and 95D) and normal bronchial epithelial cell lines.

REFERENCES

1. Siegel RL, Miller KD, Fuchs HE, Jemal A. Cancer Statistics, 2021. *CA: Cancer J Clin* (2021) 71(1):7–33. doi: 10.3322/caac.21654
2. Hahn EJ, Rayens MK, Wiggins AT, Gan W, Brown HM, Mullett TW. Lung Cancer Incidence and the Strength of Municipal Smoke-Free Ordinances. *Cancer* (2018) 124(2):374–80. doi: 10.1002/cncr.31142
3. Wang R, Yamada T, Kita K, Taniguchi H, Arai S, Fukuda K, et al. Transient IGF-1R Inhibition Combined With Osimertinib Eradicates AXL-Low Expressing EGFR Mutated Lung Cancer. *Nat Commun* (2020) 11(1):4607. doi: 10.1038/s41467-020-18442-4
4. Chen Z, Fillmore CM, Hammerman PS, Kim CF, Wong KK. Non-Small-Cell Lung Cancers: A Heterogeneous Set of Diseases. *Nat Rev Cancer* (2014) 14 (8):535–46. doi: 10.1038/nrc3775
5. William WN, Kim JS, Liu DD, Solis L, Behrens C, Lee JJ, et al. The Impact of Phosphorylated AMP-Activated Protein Kinase Expression on Lung Cancer Survival. *Ann Oncol Off J Eur Soc Med Oncol* (2012) 23(1):78–85. doi: 10.1093/annonc/mdr036
6. Yang F, Xu J, Li H, Tan M, Xiong X, Sun Y. FBXW2 Suppresses Migration and Invasion of Lung Cancer Cells *via* Promoting Beta-Catenin Ubiquitylation and Degradation. *Nat Commun* (2019) 10(1):1382. doi: 10.1038/s41467-019-09289-5
7. Garon EB, Hellmann MD, Rizvi NA, Carcereny E, Leighl NB, Ahn MJ, et al. Five-Year Overall Survival for Patients With Advanced NonSmall-Cell Lung Cancer Treated With Pembrolizumab: Results From the Phase I KEYNOTE-001 Study. *J Clin Oncol Off J Am Soc Clin Oncol* (2019) 37 (28):2518–27. doi: 10.1200/JCO.19.00934
8. Dolly SO, Collins DC, Sundar R, Popat S, Yap TA. Advances in the Development of Molecularly Targeted Agents in Non-Small-Cell Lung Cancer. *Drugs* (2017) 77(8):813–27. doi: 10.1007/s40265-017-0732-2
9. St Croix B, Rago C, Velculescu V, Traverso G, Romans KE, Montgomery E, et al. Genes Expressed in Human Tumor Endothelium. *Science* (2000) 289 (5482):1197–202. doi: 10.1126/science.289.5482.1197
10. Bradley KA, Mogridge J, Mourez M, Collier RJ, Young JA. Identification of the Cellular Receptor for Anthrax Toxin. *Nature* (2001) 414(6860):225–9. doi: 10.1038/n35101999
11. Carson-Walter EB, Watkins DN, Nanda A, Vogelstein B, Kinzler KW, St Croix B. Cell Surface Tumor Endothelial Markers Are Conserved in Mice and Humans. *Cancer Res* (2001) 61(18):6649–55.
12. Cai C, Dang W, Liu S, Huang L, Li Y, Li G, et al. Anthrax Toxin Receptor 1/Tumor Endothelial Marker 8 Promotes Gastric Cancer Progression Through Activation of the PI3K/AKT/mTOR Signaling Pathway. *Cancer Sci* (2020) 111 (4):1132–45. doi: 10.1111/cas.14326

13. Byrd TT, Fousek K, Pignata A, Szot C, Samaha H, Seaman S .Correction: TEM8/ANTXR1-Specific CAR T Cells as a Targeted Therapy for Triple-Negative Breast Cancer. *Cancer Res* (2018) 78(12):3403. doi: 10.1158/0008-5472.CAN-16-1911
14. Wang CX, Xiong HF, Wang S, Wang J, Nie X, Guo Q, et al. Overexpression of TEM8 Promotes Ovarian Cancer Progression *via* Rac1/Cdc42/JNK and MEK/ERK/STAT3 Signaling Pathways. *Am J Trans Res* (2020) 12(7):3557–76.
15. Byrd TT, Fousek K, Pignata A, Szot C, Samaha H, Seaman S, et al. TEM8/ANTXR1-Specific CAR T Cells as a Targeted Therapy for Triple-Negative Breast Cancer. *Cancer Res* (2018) 78(2):489–500. doi: 10.1158/0008-5472.CAN-16-1911
16. Sun M, Li H, Liu J, Ning L, Zhao D, Liu S. The Relationship Between TEM8 and Early Diagnosis and Prognosis of Lung Cancer. *Minerva Med* (2020) 112 (3):359–64. doi: 10.23736/S0026-4806.20.06444-7
17. Zhou L, Li M, Yu X, Gao F, Li W. Repression of Hexokinases II-Mediated Glycolysis Contributes to Piperlongumine-Induced Tumor Suppression in Non-Small Cell Lung Cancer Cells. *Int J Biol Sci* (2019) 15(4):826–37. doi: 10.7150/ijbs.31749
18. Zhang Y, Wang X. Targeting the Wnt/beta-Catenin Signaling Pathway in Cancer. *J Hematol Oncol* (2020) 13(1):165. doi: 10.1186/s13045-020-00990-3
19. Cai J, Fang L, Huang Y, Li R, Xu X, Hu Z, et al. Simultaneous Overactivation of Wnt/beta-Catenin and TGFbeta Signalling by miR-128-3p Confers Chemoresistance-Associated Metastasis in NSCLC. *Nat Commun* (2017) 8:15870. doi: 10.1038/ncomms15870
20. Cho YH, Ro EJ, Yoon JS, Mizutani T, Kang DW, Park JC, et al. 5-FU Promotes Stemness of Colorectal Cancer *via* P53-Mediated WNT/beta-Catenin Pathway Activation. *Nat Commun* (2020) 11(1):5321. doi: 10.1038/s41467-020-19173-2
21. Kanwar SS, Yu Y, Nautiyal J, Patel BB, Majumdar AP. The Wnt/beta-Catenin Pathway Regulates Growth and Maintenance of Colonospheres. *Mol Cancer* (2010) 9:212. doi: 10.1186/1476-4598-9-212
22. Kolligs FT, Bommer G, Goke B. Wnt/beta-Catenin/Tcf Signaling: A Critical Pathway in Gastrointestinal Tumorigenesis. *Digestion* (2002) 66(3):131–44. doi: 10.1159/000066755
23. Miles LA, Burga LN, Gardner EE, Bostina M, Poirier JT, Rudin CM. Anthrax Toxin Receptor 1 Is the Cellular Receptor for Seneca Valley Virus. *J Clin Invest* (2017) 127(8):2957–67. doi: 10.1172/JCI93472
24. Jiang Q, Qin X, Yoshida CA, Komori H, Yamana K, Ohba S, et al. Antxr1, Which Is a Target of Runx2, Regulates Chondrocyte Proliferation and Apoptosis. *Int J Mol Sci* (2020) 21(7):24–5. doi: 10.3390/ijms21072425
25. Hotchkiss KA, Basile CM, Spring SC, Bonuccelli G, Lisanti MP, Terman BI. TEM8 Expression Stimulates Endothelial Cell Adhesion and Migration by Regulating Cell-Matrix Interactions on Collagen. *Exp Cell Res* (2005) 305 (1):133–44. doi: 10.1016/j.yexcr.2004.12.025
26. Gong Q, Liu C, Wang C, Zhuang L, Zhang L, Wang X. Effect of Silencing TEM8 Gene on Proliferation, Apoptosis, Migration and Invasion of XWLC05 Lung Cancer Cells. *Mol Med Rep* (2018) 17(1):911–7. doi: 10.3892/mmr.2017.7959
27. Cao C, Wang Z, Huang L, Bai L, Wang Y, Liang Y, et al. Down-Regulation of Tumor Endothelial Marker 8 Suppresses Cell Proliferation Mediated by ERK1/2 Activity. *Sci Rep* (2016) 6:23419. doi: 10.1038/srep23419
28. Davies G, Cunnick GH, Mansel RE, Mason MD, Jiang WG. Levels of Expression of Endothelial Markers Specific to Tumour-Associated Endothelial Cells and Their Correlation With Prognosis in Patients With Breast Cancer. *Clin Exp Metastasis* (2004) 21(1):31–7. doi: 10.1023/B:CLIN.0000017168.83616.d0
29. Davies G, Rmali KA, Watkins G, Mansel RE, Mason MD, Jiang WG. Elevated Levels of Tumour Endothelial Marker-8 in Human Breast Cancer and its Clinical Significance. *Int J Oncol* (2006) 29(5):1311–7. doi: 10.3892/ijo.29.5.1311
30. Stewart DJ. Wnt Signaling Pathway in Non-Small Cell Lung Cancer. *J Natl Cancer Institute* (2014) 106(1):djt356. doi: 10.1093/jnci
31. Xiong SD, Yu K, Liu XH, Yin LH, Kirschenbaum A, Yao S, et al. Ribosome-Inactivating Proteins Isolated From Dietary Bitter Melon Induce Apoptosis and Inhibit Histone Deacetylase-1 Selectively in Premalignant and Malignant Prostate Cancer Cells. *Int J Cancer* (2009) 125(4):774–82. doi: 10.1002/ijc.24325
32. Tammela T, Sanchez-Rivera FJ, Cetinbas NM, Wu K, Joshi NS, Helenius K, et al. A Wnt-Producing Niche Drives Proliferative Potential and Progression in Lung Adenocarcinoma. *Nature* (2017) 545(7654):355–9. doi: 10.1038/nature22334
33. Tennis M, Van Scoyk M, Winn RA. Role of the Wnt Signaling Pathway and Lung Cancer. *J Thorac Oncol Off Publ Int Assoc Study Lung Cancer* (2007) 2 (10):889–92. doi: 10.1097/JTO.0b013e318153fdb1
34. Chikazawa N, Tanaka H, Tasaka T, Nakamura M, Tanaka M, Onishi H, et al. Inhibition of Wnt Signaling Pathway Decreases Chemotherapy-Resistant Side-Population Colon Cancer Cells. *Anticancer Res* (2010) 30(6):2041–8.
35. Flahaut M, Meier R, Coulon A, Nardou KA, Niggli FK, Martinet D, et al. The Wnt Receptor FZD1 Mediates Chemoresistance in Neuroblastoma Through Activation of the Wnt/beta-Catenin Pathway. *Oncogene* (2009) 28(23):2245–56. doi: 10.1038/onc.2009.80
36. Shtutman M, Zhurinsky J, Simcha I, Albanese C, D'Amico M, Pestell R, et al. The Cyclin D1 Gene Is a Target of the Beta-Catenin/LEF-1 Pathway. *Proc Natl Acad Sci USA* (1999) 96(10):5522–7. doi: 10.1073/pnas.96.10.5522
37. Zhang DY, Wang HJ, Tan YZ. Wnt/beta-Catenin Signaling Induces the Aging of Mesenchymal Stem Cells Through the DNA Damage Response and the P53/P21 Pathway. *PloS One* (2011) 6(6):e21397. doi: 10.1371/journal.pone.0021397
38. Dannheisig DP, Bachle J, Tasic J, Keil M, Pfister AS. The Wnt/beta-Catenin Pathway is Activated as a Novel Nucleolar Stress Response. *J Mol Biol* (2021) 433(2):166719. doi: 10.1016/j.jmb.2020.11.018

Conflict of Interest: The authors declare that the research was conducted in the absence of any commercial or financial relationships that could be construed as a potential conflict of interest.

Publisher's Note: All claims expressed in this article are solely those of the authors and do not necessarily represent those of their affiliated organizations, or those of the publisher, the editors and the reviewers. Any product that may be evaluated in this article, or claim that may be made by its manufacturer, is not guaranteed or endorsed by the publisher.

frontiers in Oncology

REVIEW
published: 14 March 2022
doi: 10.3389/fonc.2022.858782

Phosphorylation-Dependent Regulation of WNT/Beta-Catenin Signaling

Kinjal Shah[1,2] *and Julhash U. Kazi*[1,2]*

[1] Division of Translational Cancer Research, Department of Laboratory Medicine, Lund University, Lund, Sweden, [2] Lund Stem Cell Center, Department of Laboratory Medicine, Lund University, Lund, Sweden

WNT/β-catenin signaling is a highly complex pathway that plays diverse roles in various cellular processes. While WNT ligands usually signal through their dedicated Frizzled receptors, the decision to signal in a β-catenin-dependent or -independent manner rests upon the type of co-receptors used. Canonical WNT signaling is β-catenin-dependent, whereas non-canonical WNT signaling is β-catenin-independent according to the classical definition. This still holds true, albeit with some added complexity, as both the pathways seem to cross-talk with intertwined networks that involve the use of different ligands, receptors, and co-receptors. β-catenin can be directly phosphorylated by various kinases governing its participation in either canonical or non-canonical pathways. Moreover, the co-activators that associate with β-catenin determine the output of the pathway in terms of induction of genes promoting proliferation or differentiation. In this review, we provide an overview of how protein phosphorylation controls WNT/β-catenin signaling, particularly in human cancer.

Keywords: β-catenin, *CTNNB1*, GSK3β, adherens junctions, AXIN, CK1, frizzled

OPEN ACCESS

Edited by:
Simone Patergnani,
University of Ferrara, Italy

Reviewed by:
Wioletta Skronska-Wasek,
Boehringer Ingelheim, Germany
Claudio Cantù,
Linköping University Hospital, Sweden
Simon Söderholm,
in collaboration with reviewer CC

***Correspondence:**
Julhash U. Kazi
kazi.uddin@med.lu.se

Specialty section:
This article was submitted to Molecular and Cellular Oncology, a section of the journal Frontiers in Oncology

Received: *20 January 2022*
Accepted: *16 February 2022*
Published: *14 March 2022*

Citation:
Shah K and Kazi JU (2022) Phosphorylation-Dependent Regulation of WNT/Beta-Catenin Signaling. Front. Oncol. 12:858782. doi: 10.3389/fonc.2022.858782

INTRODUCTION

WNT/β-catenin signaling is a tightly controlled and highly conserved pathway that regulates cell fate during embryogenesis, hepatobiliary development, liver homeostasis, repair in adulthood, cell proliferation, differentiation, and cell polarity (1, 2). The intracellular responses that WNT ligands trigger can be classified into canonical (β-catenin-dependent) and non-canonical (β-catenin-independent) signaling (2, 3). WNT is a family of nineteen hydrophobic cysteine-rich secreted glycoproteins which serve as ligands for ten members of the Frizzled (Fz) family of 7-transmembrane receptors, the co-receptors low-density lipoprotein receptor-related proteins 5/6 (LRP 5/6), and non-classical WNT receptors like RYK and ROR (4–8). Abnormal WNT/β-catenin signaling is involved in many diseases including Alzheimer's disease, heart disease, osteoarthritis, and cancer (9, 10). β-catenin is one of the core molecules in the canonical WNT signaling pathway. It is also involved in E-cadherin and cytoskeleton-associated cell-cell adhesion when localized to the plasma membrane (11, 12). However, cytosolic β-catenin acts as the molecular effector of the WNT ligands (1, 13). This review discusses the phosphorylation-dependent regulations of β-catenin and WNT signaling in cancer.

STRUCTURE, LOCATION, AND FUNCTION OF β-CATENIN

β-catenin is a multifunctional protein encoded by the *CTNNB1* gene in humans and is the vertebrate homolog of the Drosophila Armadillo (14). It is a 781-amino-acid-long protein consisting of the N-terminal domain (NTD), twelve armadillo (ARM) domains in the middle of the protein, and the C-terminal domain (CTD) (**Figure 1**). Each ARM domain contains three α-helices and, together, all twelve ARM domains create a compact superhelix with a positively charged groove spanning all the ARM domains (15, 16). This core ARM domain structure serves as a scaffold and interacts with various β-catenin binding partners that are critical for both WNT signaling and the formation of adherens junctions (16, 17). β-catenin can exist in three distinct pools inside the cell: membranous, cytoplasmic, and nuclear (18). β-catenin normally interacts with E-cadherin at the cell membrane and plays an important structural role in the adherens junctions. β-catenin that is free in the cytoplasm is captured by the destruction complex for degradation. However, when some of the components of the destruction complex are compromised, β-catenin evades degradation; instead, it translocates to the nucleus and contributes to the transcriptional regulation of genes (18). β-catenin thus acts as both an adaptor protein and a transcriptional coregulator (19). This spatial separation of β-catenin at the plasma membrane, cytoplasm, and the nucleus is regulated by specific phosphorylation mechanisms.

STABILIZATION OF β-CATENIN AT THE PLASMA MEMBRANE AS AN INTRACELLULAR ADHESION REGULATOR

β-catenin acts as an adaptor protein and binds to the intracellular part of E-cadherin present at the plasma membrane *via* its C-terminal region. Apart from β-catenin, the cytoplasmic tail of E-cadherin can interact with various molecules such as γ-catenin and other regulatory proteins, while its extracellular part interacts with other cadherins present on adjacent cells (20, 21). The N-terminus of β-catenin interacts with α-catenin, which links β-catenin to the actin cytoskeleton. This entire structure of actin filaments-α-catenin-β-catenin-E-cadherin interactions promote clustering of the adhesion junction proteins, thereby stabilizing cell adhesion (22). In the absence of WNT, the majority of β-catenin localizes to the plasma membrane, building an epithelial barrier and restricting cell invasion and metastasis (23). However, the β-catenin-E-cadherin complex gets weakened by the phosphorylation of β-catenin at the plasma membrane (24). Tyrosine phosphorylation in the different armadillo repeats probably specifies interactions with α-catenin and E-cadherin. Phosphorylation of Tyr142/Tyr654 results in the dissociation of the adherens junctions, which leads to the cytoplasmic accumulation of β-catenin followed by its nuclear translocation to promote gene transcription (25).

TRANSCRIPTIONAL REGULATIONS THROUGH STABILIZATION OF β-CATENIN IN THE CYTOPLASM AND NUCLEUS

In the absence of WNT signaling, β-catenin is sequestered in the cytoplasm by the 'destruction complex' composed of the scaffolding protein AXIN, tumor suppressor adenomatous polyposis coli (APC), and two serine/threonine kinases: casein kinase 1 (CK1) and glycogen synthase kinase 3β (GSK3β) (**Figure 2A**). AXIN directly binds with APC, GSK3β, CK1, and β-catenin and holds the destruction complex (26–29). Besides interaction with kinases, AXIN has an interaction site for protein phosphatase 2A (PP2A) that induces dephosphorylation of AXIN (30). Thus, AXIN is the core protein of the destruction complex that mediates the whole assembly of the destruction complex. Although AXIN can hold all proteins, the interaction between APC and β-catenin is required for active complex formation (31). GSK3β phosphorylates both AXIN (32, 33) and APC, which further increases its β-catenin binding affinity (34). CK1α binds to the first ARM domain of β-catenin (35) and mediates the first regulatory phosphorylation at Ser45 (36); this process requires AXIN-CK1α complex formation (29). Additionally, α-catenin must be dissociated from β-catenin to provide CK1 access. This dissociation is achieved by Tyr142 phosphorylation, which is mediated by tyrosine kinases FEline Sarcoma (FES)-related (FER) and FYN (35, 37). FYN is a member of SRC family of protein tyrosine kinases (SFKs). CK1α-induced Ser45 phosphorylation creates a priming site for GSK3β, which is necessary and sufficient for GSK3β-mediated phosphorylation at Thr41, Ser37, and Ser33 (29, 36).

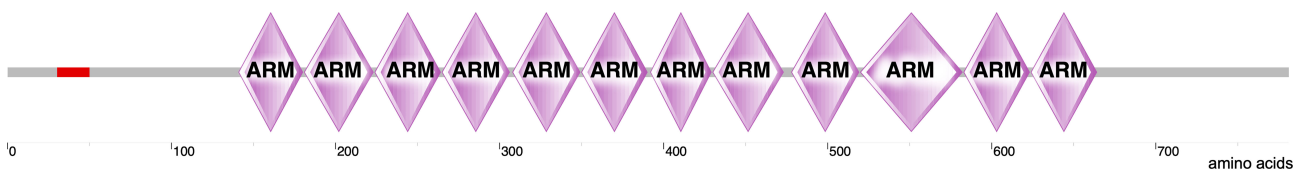

FIGURE 1 | Structure of β-catenin. The structure of β-catenin was generated by SMART (http://smart.embl-heidelberg.de/smart/show_motifs.pl?ID=P35222) and modified using Canvas X draw. It includes an N-terminal domain where several regulatory phosphorylation sites are located (red). This domain follows twelve ARM domains and a long C-terminal domain.

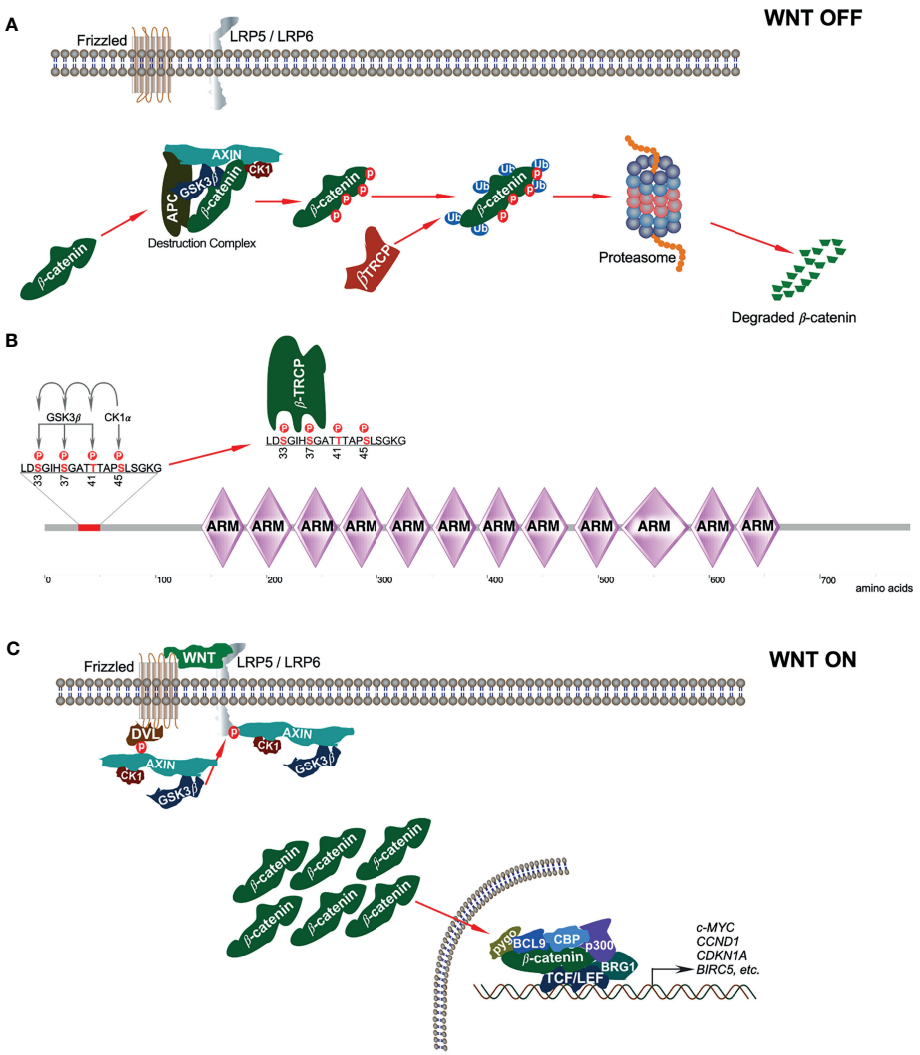

FIGURE 2 | Canonical WNT signaling. **(A)** In absence of canonical WNT ligands, β-catenin is associated with the destruction complex. This interaction leads to phosphorylation-dependent ubiquitination of β-catenin and thereby its degradation in the proteasome. **(B)** In the destruction complex, CK1α phosphorylates β-catenin on Ser45 residue that initiates sequential phosphorylation of Thr41, Ser37, and Ser33 phosphorylation by GSK3β. Ser33 and Ser37 phosphorylation sites facilitate β-TRCP interaction with β-catenin. **(C)** In the presence of classical WNT ligands, a destruction complex cannot be formed and thus, β-catenin is stabilized from degradation.

Ser33 and Ser37 in β-catenin create docking sites for the E3 ubiquitin ligase, β-transducing repeat-containing protein (β-TRCP) (**Figure 2B**) that ubiquitinates β-catenin and targets it for proteasomal degradation after forming a complex with Skp1 and Cullin (24, 38). Mutation of Ser37 thus results in stabilization of β-catenin (39).

The destruction complex is ultimately responsible for the phosphorylation of β-catenin, thereby priming it for ubiquitin-mediated proteasomal degradation (31). However, when canonical WNT ligands bind to their respective Fz receptor and LRP5/6 co-receptors, the result is the activation of the canonical WNT signaling pathway (40). Due to this, the phosphoprotein dishevelled (DVL, DVL1/2/3, segment polarity protein) is activated and recruited to the plasma membrane where it interacts with the cytoplasmic domain of Fz (41). DVL then recruits the destruction complex to the plasma membrane, thereby promoting interaction between LRP5/6 and AXIN (42, 43). GSK3β and CDK14 facilitate LRP5/6 phosphorylation that further enables AXIN-CK1-GSK3β complex recruitment (9). Recruitment of this complex to WNT receptors disrupts it and thereby inhibits CK1-GSK3β-mediated β-catenin phosphorylation, resulting in the stabilization and accumulation of β-catenin in the cytoplasm (**Figure 2C**).

Inhibition of CK1, WNT signaling activation, and DVL overexpression suppresses Ser45 phosphorylation (29). Moreover, GSK3β can be inactivated through Ser9 phosphorylation by AKT. These events result in the stabilization and accumulation of β-catenin in the cytoplasm

(44). β-catenin activity in the canonical WNT pathway can also be regulated in a GSK3β and β-TrCP-independent manner.

It was observed in Drosophila that upon canonical WNT signaling, Arrow (LRP5/6) recruits AXIN to the membrane, which leads to degradation of AXIN. Thus, the scaffolding member of the destruction complex, AXIN, is no longer present to form the destruction complex (45). A more recent study demonstrated that an E3 ubiquitin ligase, tripartite motif-containing protein 11 (TRIM11), serves as an oncogene in lymphomas by promoting cell proliferation through activation of the β-catenin signaling. This regulation is brought about by TRIM11-mediated ubiquitination and degradation of AXIN1, part of the destruction complex of β-catenin (46). Thus, inactivation or degradation of any of the components forming the β-catenin destruction complex results in the stabilization and accumulation of β-catenin in the cytoplasm.

Stabilized β-catenin then translocates to the nucleus, where it interacts with different transcription factors, notably T-cell factor (TCF), and lymphoid enhancing factor (LEF). The repressor of the TCF/LEF complex, Groucho, is displaced upon this interaction, whose function is to compact chromatin (44). Thereafter, transcriptional co-activators and histone modifiers are recruited, which is sometimes referred to as WNT enhanceosome. These include the cyclic adenosine monophosphate response element (CREB)-binding protein (CBP), its closely related homolog p300, B-cell lymphoma 9 (BCL9), pygopus, and ATP-dependent helicase Brahma-related gene 1 (BRG1, also known as SMARCA4) (44, 47). Chromatin is remodeled by the WNT enhanceosome and results in the transcription of WNT/β-catenin target genes that are involved in cell survival and growth such as *c-MYC*, *CCND1*, *CDKN1A*, and *BIRC5* (40). *C-MYC* is a proto-oncogene that further activates cyclin D1 and also inhibits the tumor suppressors p21 and p27, thereby leading to uncontrolled cell proliferation (48, 49).

MUTATIONS OF COMPONENTS INVOLVED IN THE CANONICAL WNT/β-CATENIN PATHWAY

After having understood the regulation of β-catenin in the canonical WNT pathway, we now know that mutations in any of the components of this pathway can lead to its deregulation, which can contribute to a variety of diseases. Herein, we will focus on such mutations contributing to cancer. APC plays an important role in β-catenin degradation, and mutation in APC impairs destruction complex formation. Over 70% of colorectal adenocarcinoma patients carry mutations in the APC gene (**Figure 3A**) that lead to the stabilization of β-catenin. APC has long been known to be an important initiator gene for the majority of colorectal cancers. However, a recent study suggests that colorectal cancer tumors with a single APC mutation can have a survival benefit, whereas tumors lacking any APC mutations convey a worse prognosis (50). Other cancers display a lower number of APC mutations, whereas endometrial carcinoma, esophagogastric adenocarcinoma, and melanoma exhibit over 10% APC mutations. An aberrant APC promoter mutation is found in early endometrial carcinoma, which decreases with cancer progression (51), suggesting that loss of APC function is an early event in endometrial carcinoma. β-catenin mutations in N-terminal serine/threonine residues or adjacent residues that interrupt CK1- and GSK3β-induced regulatory serine/threonine phosphorylations have been found in several cancers (**Figure 3B**). In endometrial carcinoma, 20-40% of patients carry mutations in β-catenin (52). It is also frequently mutated in hepatocellular carcinoma (15-33%) (53).

However, β-catenin is not mutated in pediatric T-ALL, and even if it is found to be mutated in any T-ALL cell line or patient sample, this holds no clinical significance (54). The most common activating missense mutation found in the endometroid carcinoma subtype of epithelial ovarian cancer (EOC) is in the β-catenin gene, *CTNNB1*, accounting for 54% of cases (55). This mutation occurred within the amino-terminal domain of β-catenin (55), which is positively correlated with its nuclear localization and expression of the β-catenin target genes. GSK3β phosphorylates the amino-terminal domain of β-catenin, leading to its degradation. Thus, mutations within this domain help β-catenin in evading degradation instead of accumulating in the nucleus (56). Moreover, loss-of-function mutations in genes encoding several components of the destruction complex, such as AXIN, APC, and GSK3β, were also reported in EOC, although not frequently (57). Thus, β-catenin target genes, such as *cMyc*, *CCND1*, and *VEGF*, were constitutively activated due to the disrupted WNT pathways contributed by the various mutations in its different components, which aided in cancer progression (58).

NON-CANONICAL WNT SIGNALING PATHWAY

Non-canonical WNT ligands such as WNT4, WNT5A, WNT5B, WNT7A, WNT7B, and WNT11 bind to Frizzled receptors (Fzd2, Fzd3, Fzd4, Fzd5, and Fzd6), and ROR1/ROR2 (receptor tyrosine kinase-like orphan receptor) or RYK acts as co-receptors to initiate non-canonical signaling (**Figure 4**). This pathway has always been defined as the one where β-catenin does not accumulate in the nucleus (59). It generally governs intercalation, cellular movement, and directed migration culminating in convergence and extension along the anterior/posterior axis of the organism (60, 61). Based on the phenotypic response, non-canonical signaling can be classified into two branches: WNT/PCP (Planar Cell Polarity) and the WNT-cGMP (cyclic guanosine monophosphate)/Ca^{2+} pathways (61, 62).

The first branch of the non-canonical pathway – PCP signaling occurs through WNT-Fz receptor interaction without the involvement of LRP5/6 co-receptors. This results in activation of the DVL protein, which in turn activates a small GTPase such as RAC (63). Activated RAC further stimulates JNK activation (64). DVL also forms a complex with DSH

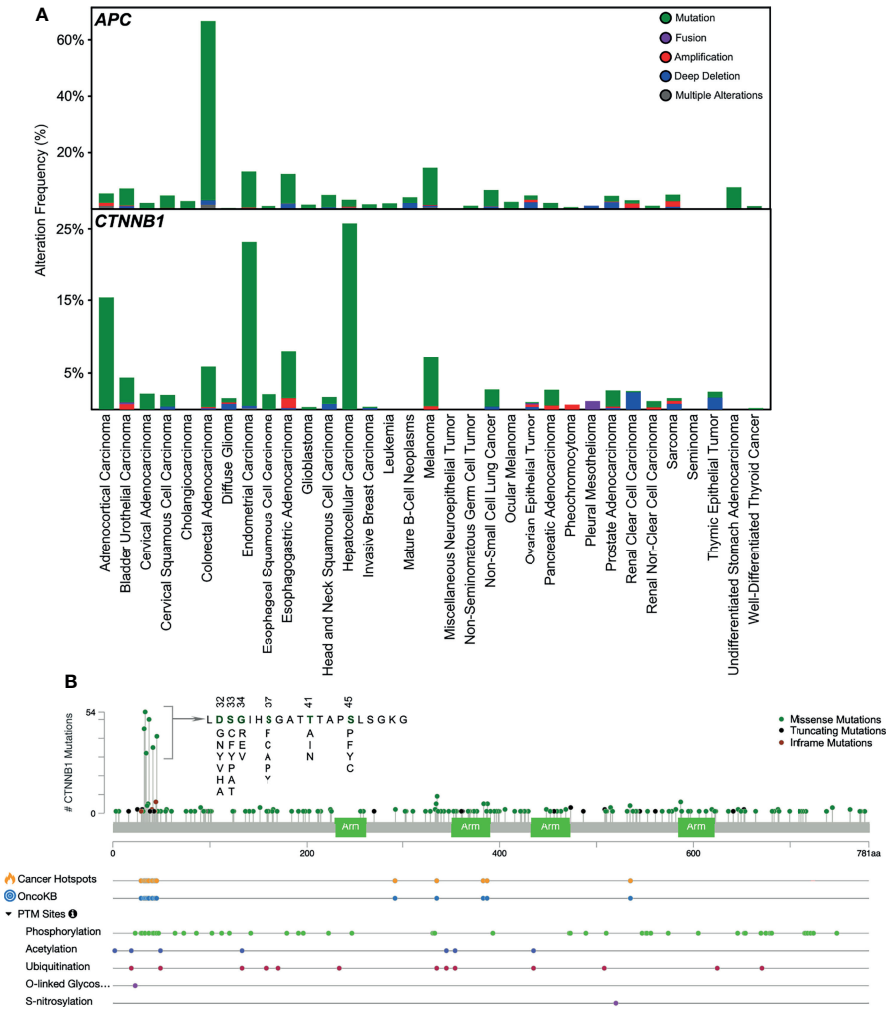

FIGURE 3 | Mutations in APC and β-catenin. **(A)** Mutations in *APC* and *CTNNB1* (β-catenin) in different cancers have been collected from cbioportal. **(B)** Mutation frequency in *CTNNB1* gene and other post-translational modifications collected from cbioportal. TCGA PanCancer Atlas Studies (http://www.cbioportal.org/study/summary?id=5c8a7d55e4b046111fee2296) was used.

associated activator of morphogenesis 1 (DAAM1), which results in the activation of other GTPases: RHO and, subsequently, Rho-associated kinase (ROCK) and myosin (63). The actin remodeling process associated with cell polarization and motility is controlled by signals emanating from both RAC and RHO activation (64). Non-canonical WNT ligands such as WNT5A also interact with ROR family orphan receptor tyrosine kinases such as ROR2 to activate JNK, RHOA, etc. This has been shown to antagonize the canonical WNT signaling pathway by inhibiting the transcriptional activation potential of the β-catenin/TCF complex, thus reducing the expression of *Cyclin D1* (65, 66).

The second branch of the non-canonical pathway – WNT/Ca^{2+} signaling is characterized by WNT-Fz-induced phospholipase C (PLC) activation that increases cytoplasmic Ca^{2+} levels. Several Ca^{2+}-responsive enzymes such as protein kinase C (PKC), calcineurin, and calcium/calmodulin-dependent protein kinase II (CaMKII) are activated upon sensing the intracellular Ca^{2+} flux (67). CaMKII further activates the transcription factors nuclear factor of activated T cells (NFAT), TGF-β activated kinase (TAK1), and Nemo-like kinase (NLK), all of which result in decrease in the levels of intracellular cGMP, which antagonizes the canonical WNT signaling (68, 69). Moreover, TAK1 activates NLK, which in turn phosphorylates TCF. This prevents the β-catenin-TCF complex from binding DNA, thereby inhibiting gene transcription (70). The WNT/Ca^{2+} signaling regulates various developmental processes such as cytoskeletal rearrangements, cellular adhesion, dorsoventral patterning, and tissue separation in embryos (71).

The non-canonical WNT signaling pathway also has the potential to inhibit canonical WNT signaling by promoting the proteasomal degradation of β-catenin through an alternative E3 ubiquitin ligase complex containing APC, Ebi, and Siah1 or Siah2 (72, 73). This does not involve GSK3β or β-TrCP and

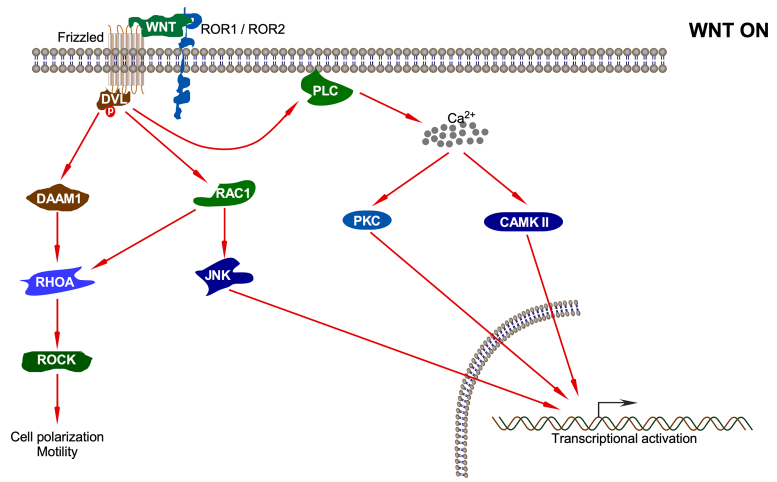

FIGURE 4 | Non-canonical WNT pathway. Upon interaction of the non-canonical WNT ligand with Fz and ROR1/ROR2, several pathways including DAAM1-RHOA-ROCK, RAC1-JNK, PKC, and CAMKII pathways are activated which results in different cellular processes and transcriptional activation of different sets of genes.

neither requires activation of CaMKII or NFAT (74). Thus, the antagonism of canonical WNT signaling by non-canonical WNTs involves multiple mechanisms that may or may not involve calcium (71).

COACTIVATORS REGULATING THE OUTPUT OF THE WNT SIGNALING PATHWAYS

The canonical WNT signaling pathway is dependent on β-catenin, whereas the non-canonical WNT signaling pathway is independent of β-catenin (75). Once in the nucleus, β-catenin interacts with members of the TCF/LEF family of transcription factors. β-catenin can also interact with a variety of other transcription factors like FOXO, HIF1, Sox family members, nuclear receptors, etc. Thus, nuclear β-catenin can perform divergent functions, which adds complexity to the interpretation of canonical WNT signaling (76). Transcriptional coactivators like cAMP response element-binding protein (CREB)-binding protein (CBP) or its closely related homolog, p300, are key regulators of RNA polymerase II-mediated transcription (77). β-catenin can recruit either CBP or p300 along with other components of the basal transcriptional machinery to generate a transcriptionally active complex, which leads to the expression of a variety of downstream target genes (78). Differential utilization of these coactivators by β-catenin can lead to different cellular outputs (75). Canonical WNT signaling pathway mediated by WNT3A stabilizes β-catenin and leads to its association with the coactivator CBP for transcribing genes related to self-renewal, potency, and proliferation (77). However, the non-canonical WNT signaling pathway mediated by WNT5A induces the activation of various kinases such as PKC, CaMKII, SIK, AMPK, and MAPK (5, 8, 79). PKC further phosphorylates Ser89 of p300, which increases its affinity for β-catenin (77). The association of coactivator p300 with β-catenin drives the gene expression program from a proliferative state to a differentiative state; that also governs planar cell polarity, convergent extension, and cytoskeletal reorganization (80). Thus, coordinated integration between both canonical and non-canonical WNT signaling pathways is extremely crucial for regulating cell proliferation with differentiation and adhesion (75). Canonical and non-canonical WNT signaling pathways are, hence, highly dynamic, coupled, and not mutually exclusive with cross-talk occurring between them, which is dependent on the type of cell, tissue, and specific stage of development (77).

KINASES REGULATING THE ACTIVITY OF β-CATENIN

Alternative signal transduction pathways from various growth factor receptors and ion channels can activate a myriad of kinases, which also have the potential to phosphorylate either CBP or p300, thereby controlling differential utilization of coactivators by β-catenin. Moreover, these kinases can phosphorylate β-catenin directly (77), thereby playing key roles in regulating the localization, expression, and function of β-catenin (81). We will be discussing some of those kinases in the following sections.

Cell Cycle-Associated Kinases

Aurora kinase A (AURKA) is required for centrosome function and spindle assembly during mitosis that, once activated, phosphorylates Polo-like kinase 1 (PLK1) at Thr210 in presence of the co-factor Bora (82–85). PLK1 is the master regulator of the cell cycle, playing an important role in M-phase progression (86). PLK1 in turn phosphorylates several substrates, FOXM1 being one of them. FOXM1 then transcribes

target genes involved in cell cycle progression, cell proliferation, genomic stability, chemoresistance, and DNA damage repair (87–89). All components of the AURKA-PLK1-FOXM1 axis appear to be hyperactivated due to multiple events associated with a BCR-ABL fusion protein that promotes resistance to tyrosine kinase inhibitors in chronic myeloid leukemia (CML) (90–94). The AURKA-PLK1-FOXM1 axis interacts with β-catenin, which supports the resistance of BCR-ABL+ leukemic stem cells to tyrosine kinase inhibitors (86, 95–97). PLK1 physically interacts with β-catenin and phosphorylates it on Ser718 in the M phase of the cell cycle, indicating an important M-phase specific function of β-catenin such as the regulation of centrosomes (86). Deregulated PLK1 expression has been reported in many cancers, which in turn could alter β-catenin regulation in the M phase, thus leading to abnormal cell cycle control and chromosome instability (79, 86, 98). Moreover, PLK1 regulates the activity of another cell cycle regulatory kinase, NIMA-related protein kinase 2 (Nek2). Nek2 phosphorylates Thr41, Ser37, and Ser33 at the N-terminus of β-catenin along with some five additional sites; these are the amino acid residues phosphorylated by GSK3β as well. This inhibits the interaction of β-catenin with β-TRCP, thereby stabilizing it. Nek2 regulates centrosome disjunction/splitting; thus, β-catenin stabilized by Nek2 accumulates at centrosomes in mitosis, regulating the centrosome cycle (81). AURKA sequesters AXIN from the destruction complex, while FOXM1 associates with β-catenin, thereby enabling its nuclear import and recruitment to the TCF/LEF transcription complex to support leukemic cell proliferation and survival (99). So, all 3 components of the AURKA-PLK1-FOXM1 axis regulate β-catenin transcriptional activity. Inhibition of these components ultimately results in the dephosphorylation of FOXM1, causing the release of β-catenin from its binding, which leads to its cytoplasmic relocation and degradation. The proliferation and survival of BCR-ABL+ cells are thus blocked by the inhibition of the β-catenin-mediated transcriptional activity (100).

Protein Kinase C (PKC)

Once activated, β-catenin is translocated to the nucleus. Its stability is regulated by the E3 ubiquitin ligase tripartite motif-containing protein 33 (TRIM33), which is independent of GSK3β and β-TRCP (101). However, this regulation is dependent on the PKC family member PKCδ, which is activated upon prolonged WNT stimulation. PKCδ phosphorylates β-catenin at Ser715, thereby facilitating its interaction with TRIM33. β-catenin is then targeted for degradation, shutting off the WNT pathway. Apart from inhibiting the canonical WNT pathway mediated by WNT3a, TRIM33 can inhibit EGF-induced β-catenin transactivation (101). TRIM33 is thus known to act as a tumor suppressor in various cancers including clear cell renal cell carcinoma (102), chronic myelomonocytic leukemia (103), hepatocellular carcinoma (104), and pancreatic cancer (105). In fact, PKC is a family of 10 protein serine/threonine kinases that are encoded by 9 genes (106–109). PKC family members are divided into three subfamilies: classical (PKCα, PKCβ1, PKCβ2, and PKCγ), novel (PKCδ, PKCε, PKCη, and PKCθ) and atypical (PKCζ and PKCι) (108, 109). Classical and novel PKC isoforms display dependency on second messengers for activation. For example, classical PKC isoforms are diacylglycerol (DAG) and Ca^{2+}-responsive while novel PKC isoforms are dependent on DAG. While several PKC family members have been implicated in tumorigenesis, PKCδ acts as a tumor suppressor, as its main function is to induce apoptosis, apart from regulating β-catenin degradation (101, 108–114). Another PKC family member that serves as a tumor suppressor in intestinal cancer is the atypical PKCζ that induces Ser45 phosphorylation of β-catenin, which is independent of CK1α and is thus important for GSK3β-mediated phosphorylation (115). The classical PKC isoform PKCα induces phosphorylation of β-catenin at N-terminal serine residues, which in turn results in enhanced proteasomal degradation of β-catenin and a reduction of transcriptional regulations (116). Furthermore, PKCα phosphorylates ROR1 (RORα) at Ser35, which can eventually limit the transcriptional regulation of β-catenin (117). Collectively, these studies suggest that several PKC isoforms play important roles in the regulation of WNT/β-catenin signaling.

Protein Kinase A (PKA)

The cyclic AMP (cAMP)-dependent protein kinase, protein kinase A (PKA), has diverse cellular functions including cell proliferation, differentiation, cell cycle regulation, and apoptosis. The cAMP/PKA pathway plays a highly complex and cell-specific role in regulating cell growth, as it stimulates growth for some cell types while inhibiting others (118, 119). PKA can even have contrasting effects of promoting or inhibiting cell proliferation in the same cell type, such as the vascular smooth muscle cells, depending on the agonist that stimulates its activity (120, 121). The presenilin1 complex in Alzheimer's disease contains presenilin1, GSK3β, the catalytic subunit of PKA and β-catenin. PKA induces Ser45 phosphorylation on β-catenin, thereby enhancing GSK3β-dependent phosphorylation of β-catenin and its subsequent proteasomal degradation, which is independent of the WNT-controlled AXIN complex (122). However, in contrast, activation of PKA has also been shown to increase β-catenin accumulation in both the cytosol and nucleus of HEK293 cells after stimulation with prostaglandin E2 (PGE2) (123). PKA phosphorylates β-catenin on Ser552 and Ser675 that stabilize β-catenin by inhibiting its ubiquitination without affecting the formation of the destruction complex and GSK3β-dependent phosphorylation (123–125). PKA-induced phosphorylation of β-catenin at Ser675 promotes TCF/LEF transactivation and binding to its transcriptional coactivator CREB-binding protein (CBP) (124). Thus, the phosphorylation of β-catenin by PKA at different serine residues determines the outcome of β-catenin regulation.

Receptor Tyrosine Kinases (RTKs)

Receptor tyrosine kinase (RTK) consists of a family of around 60 mammalian protein tyrosine kinases (106, 107). The RTK epidermal growth factor receptor (EGFR) activates AKT that directly phosphorylates β-catenin on Ser552, which increases the cytosolic and nuclear β-catenin levels and transcriptional regulation, thereby promoting tumor cell invasion (126).

Furthermore, the proliferation of PTEN-deficient intestinal stem cells that initiate intestinal polyposis is driven by AKT activation where AKT phosphorylates β-catenin on Ser552 (127). Ultraviolet (UV) irradiation activates EGFR in keratinocytes, resulting in the phosphorylation of β-catenin at Tyr654, which is responsible for its dissociation from the E-cadherin/β-catenin/α-catenin complex (128). Furthermore, UV-induced EGFR activation allows for the nuclear translocation of β-catenin and transcriptional activation through interaction with TCF4 (128). Fibroblast growth factor-2 (FGF-2) activates MAP kinase signaling in osteoblasts, which in turn phosphorylates β-catenin. The phosphorylation is mediated by MEKK2 (MAP3K2) at Ser675 that stabilizes β-catenin and increases its activity by recruiting the deubiquitinase USP15 (129). In colorectal cancer, a loss-of-function mutation in APC is very common, stabilizing β-catenin due to the lack of destruction complex. However, 60% of colorectal cancer patients carry mutations in KRAS and BRAF genes that result in uncontrolled MAPK signaling. Oncogenic activation of KRAS/BRAF/MEK signaling increases the transcriptional activities of β-catenin/TCF4 and c-MYC promoter and increases the mRNA levels of c-Myc, AXIN2, and Lef1 (130). Another MAPK, p38γ, phosphorylates β-catenin at Ser605 (131). FGFR2, FGFR3, EGFR, and TRKA increase the cytosolic β-catenin concentration by dissociating β-catenin from cadherin complex through direct phosphorylation at Tyr142 (132). The RTK MET interacts with β-catenin in hepatocytes, colon cancer, and breast cancer cell lines; this association occurs at the region of cell-cell contact (133, 134). The association is constitutive but can be abrogated by hepatocyte growth factor (HGF) stimulation. HGF induces tyrosine phosphorylation of β-catenin at Tyr654 and Tyr670, resulting in its dissociation from MET (135). Hepatocyte growth factor-like protein (HGFL) induced RON activation, which resulted in tyrosine phosphorylation of β-catenin at Tyr654 and Tyr670, inducing its nuclear accumulation and transcriptional activation in breast cancer (136). Type-1 insulin-like growth factor (IGF-1) causes the nuclear translocation of β-catenin in the context of IGF-1R signaling, which leads to the activation of β-catenin target genes such as *c-MYC* and *cyclin* (137–141). This is brought about by the direct binding of sequences between amino acid residues 695 and 781 in the C-terminus of β-catenin to sequences located between amino acid residue 600 and the C-terminus of insulin receptor substrate-1 (IRS-1), in both the nucleus and the cytoplasm (142). The PTB domain of IRS-1 then translocates the β-catenin-IRS-1 complex to the nucleus (143). β-catenin binding to IRS-1 with its C-terminus may thus prevent phosphorylation at its N-terminus by GSK3β, which primes β-catenin for ubiquitination and degradation (8, 144). So, IRS-1, a docking protein for both IGF-1 and insulin receptors, can regulate the subcellular localization and activity of β-catenin in cells that are responsive to the mitogenic action of IGF-1 (142, 145).

Janus Kinase 3 (JAK3)

Adherens junctions are multiprotein complexes in cell-cell junctions that connect neighboring cells to maintain the epithelial tissue structure (146). β-catenin is an adherens junctions-associated protein that links the cytoplasmic domain of cadherins to the α-catenin-associated actin cytoskeleton and has been implicated in adherens junctions remodeling (16). Janus kinase 3 (JAK3) is a non-receptor tyrosine kinase that transmits intracellular signals through interactions with the γ chain of several cytokine receptors upon stimulation with cytokines (147). It associates with β-catenin in adherens junctions and phosphorylates Tyr30, Tyr64, and Tyr86 (148). However, JAK3-mediated phosphorylation is required prior to the Tyr654 phosphorylation of β-catenin. Phosphorylation on those sites by JAK3 suppressed EGF-induced epithelial-mesenchymal transition (EMT) and, rather, induced epithelial barrier functions by adherens junctions localization of phosphorylated β-catenin *via* its association with α-catenin. Moreover, a reverse effect was seen with increased EMT and compromised epithelial barrier functions upon the loss of JAK3-mediated β-catenin phosphorylation, which even abrogated the localization of β-catenin in the adherens junctions (148).

p21-Activated Kinase (PAK)

p21-activated kinase (PAK) is a family of six protein serine/threonine kinases that acts mainly as the effector proteins for the Rho GTPases CDC42 and RAC (149). PAK-family proteins regulate various cellular processes including cell proliferation and cell survival, cell motility, cytoskeletal reorganization, oncogenic transformation, and gene transcription (149, 150). JNK2 and PAK1 both are the downstream effectors of RAC1. More advanced colon cancer samples often contained K-Ras mutation, which elevated two signaling branches: K-Ras/RAC1/JNK2 cascade and K-Ras/RAC1/PAK1 cascade (151–154). Thus, JNK2-mediated phosphorylation of β-catenin at Ser191 and Ser605 increased, which led to its nuclear translocation (151, 152). Additionally, RAC1 induces β-catenin Ser191 and Ser605 phosphorylation, which is mediated by JNK2; phosphorylation on those sites is required for the nuclear localization of β-catenin (151, 155). Apart from RAC1, the EGF and IGF signaling pathways may induce PAK1 expression (156–158). Another kinase, PAK4, shuttles between the nucleus and cytoplasm and interacts with β-catenin in both cellular compartments (159). It was observed that both PAK1 and PAK4 mediated phosphorylation of β-catenin on Ser675 stabilizes it by inhibiting its degradation and thus promotes TCF/LEF transcriptional activity (159, 160). Therefore, one downstream effector of RAC1 mediates the nuclear translocation of β-catenin, while the other downstream effector promotes its transcriptional activity.

Tyrosine Kinases

Several tyrosine phosphorylation sites have been identified on β-catenin and have been shown to play important roles. In the presence of a disrupted cellular contact and active TGF-β1, E-cadherin and the epithelial integrin α3β1 associate with TGF-β1 receptors, where Tyr654 in β-catenin gets phosphorylated by the epithelial integrin in primary alveolar epithelial cells (AECs) and the phosphorylated β-catenin forms a complex with phospho-

SMAD2, resulting in EMT initiation in idiopathic pulmonary fibrosis (IPF) (161, 162). This epithelial integrin-mediated cross-talk between WNT and TGF-β1 signaling pathways, which is required for pulmonary fibrogenesis and EMT, is done with the help of TGF-β1mediated activation of SRC family kinases (163). In a hypoxic condition, reactive oxygen species (ROS) activates SRC that phosphorylates β-catenin on Tyr654. This tyrosine-phosphorylated β-catenin gets complexed with SRC and HIF1α in primary human lung adenocarcinomas and lung tumor cell lines to promote the transcriptional activity of HIF1α and hypoxia-induced EMT (164). Another substrate identified for SRC in β-catenin is Tyr86 (165). An SFK FYN induces tyrosine phosphorylation of β-catenin at Tyr142 and disrupts its association with α-catenin (37). Other tyrosine kinases such as FER, FES, and c-MET also participate in the phosphorylation of Tyr142 (37). This disrupts the binding of α-catenin to β-catenin and, instead, favors the binding of β-catenin to the nuclear transporter B-cell lymphoma 9 (Bcl9), which acts as a co-activator in WNT signaling (166). Protein tyrosine kinase (PTK6) is a distant SRC family member. It is regulated by C-terminal tyrosine phosphorylation, which is similar to SRC but lacks an N-terminal myristoylation site and, therefore, cannot localize to the membrane-like other SRCs. PTK6 interacts with both the cytoplasmic and nuclear β-catenin and directly phosphorylates β-catenin at several tyrosine residues including Tyr64, Tyr142, Tyr331, and Tyr333 (167). In the nucleus, PTK6 inhibits β-catenin function, which was shown to be independent of tyrosine phosphorylation, suggesting a possible kinase-independent role of PTK6 in the transcriptional regulation of β-catenin function (167).

BCR-ABL Fusion Protein

The BCR-ABL fusion protein, which is frequently found in chronic myeloid leukemia (CML), physically interacts with β-catenin and phosphorylates it at Tyr86 and Tyr654 (168). Phosphorylation of these tyrosine sites by BCR-ABL prevents the association of β-catenin with AXIN/GSK3β complex; thereby, serine/threonine phosphorylation is prevented. This subsequently increases the cytosolic and nuclear accumulation of β-catenin that is required for self-renewal of BCR-ABL-positive CML cells (169). This process can be reversed by tyrosine phosphatase SHP1, where SHP1-mediated dephosphorylation of Tyr86 and Tyr654 restores GSK3β-dependent serine/threonine phosphorylation and, thereby, β-catenin degradation (170). In another mechanism, BCR-ABL tyrosine kinase controls β-catenin mediated transcriptional activity indirectly, without physical interaction. Chibby1 (CBY1) is a small protein that represses β-catenin transcriptional activation; it interacts with the C-terminal activation domain of β-catenin that hinders its binding with the TCF/LEF transcription factors (171). The scaffolding protein 14-3-3 drives the nuclear export of CBY1 and β-catenin by forming a stable tripartite complex with them (172, 173). However, BCR-ABL fusion protein downregulates CBY1 at the transcriptional level by promoter hypermethylation and at the post-transcriptional level by directing CBY1 toward proteasome-dependent degradation through SUMOylation (171–173). This retains β-catenin in the nucleus and sustains its activation, which is required for the proliferation of CML cells (174).

Casein Kinase 2 (CK2)

Casein kinase 2 (CK2) is ubiquitously expressed in the nucleus and cytoplasm of eukaryotic cells (175). CK2 phosphorylates many transcription factors, tumor suppressors, and proto-oncoproteins involved in cancer, thereby regulating a multitude of cellular processes. One such important function is the regulation of protein stability, thus contributing to cell proliferation and transformation (176). It also plays an important role in embryonic development. CK2 phosphorylates β-catenin at Thr393, which leads to its stabilization and increases its contributions in transcriptional regulations (176). This is probably mediated by decreased affinity to AXIN in the destruction complex (177). Another study identified Ser29, Thr102, and Thr112 in β-catenin as CK2 phosphorylation sites that were required for interaction with α-catenin. CK2 phosphorylation of these residues was also important for degradation of β-catenin, as pre-phosphorylation of β-catenin by CK2 stabilizes its binding to components of the destruction complex, AXIN, and GSK3β, further enhancing the activity of GSK3β. Thus, the cytoplasmic turnover of β-catenin is controlled by the combined action of CK2 and GSK3β (178). Therefore, CK2 appears to have dual roles in β-catenin regulation: one for canonical WNT signaling and the other for cell adhesion (166).

Protein Kinase D1 (PKD1)

Protein kinase D1 (PKD1) lies downstream of the signaling pathways initiated by diacylglycerol and PKC. Diacylglycerol dictates the intracellular localization of PKD1, while PKC activates it by phosphorylation (179). PKD1 served as a tumor suppressor in advanced prostate cancer, where its expression was downregulated; later, it was found that it interacted with E-cadherin (180, 181). PKD1 interacts with β-catenin and phosphorylates it on Thr112 and Thr120 that inhibit the nuclear localization of β-catenin, thereby decreasing its transcriptional activity. This was probably because these threonine phosphorylations on β-catenin increased its interaction with α-catenin and E-cadherin, thereby linking the cytoskeleton. This suggests that Thr120 phosphorylation is critical for cell-cell adhesion (182, 183). However, it has been suggested that PKD1 expression is transcriptionally repressed by β-catenin, indicating the involvement of a negative auto-regulatory loop (184).

In summary, β-catenin activity is tightly controlled by a series of tyrosine and serine/threonine kinases (summarized in **Table 1**). Phosphorylation on a specific β-catenin residue or several residues can affect its stability, localization, and interaction with other partners (**Figure 5**). For example, phosphorylation by tyrosine or serine/threonine kinases in the N-terminal region (except for Tyr86 and Ser191) tags β-catenin for degradation or inhibits its nuclear translocation. On the other hand, phosphorylation of the C-terminal region increases the stability of β-catenin as well as its nuclear translocation (except

TABLE 1 | Kinases regulating β-catenin activity.

Sites	Kinases	Function	Reference
S29, T102	CK2	Degradation, interaction with α-catenin.	(176, 178)
Y30	JAK3	Interaction with α-catenin.	(148)
S33, S37, T41	GSK3β, NEK2	Degradation, contributes to mitosis.	(24, 36, 38, 81)
S45	CK1α, PKA, PKCζ	Degradation, regulation of phosphorylation.	(36, 115, 122, 123)
Y64	JAK3, PTK6	Inhibits function in the nucleus, interaction with α-catenin.	(148, 167)
Y86	BCR-ABL, JAK3, SRC	Increases the cytosolic and nuclear accumulation, interaction with α-catenin.	(148, 165, 168, 169)
T112	CK2, PKD1	Degradation, interaction with α-catenin, inhibits the nuclear localization.	(178, 182)
T120	PKD1	Interaction with α-catenin, inhibits the nuclear localization	(182, 183)
Y142	PTK6, FYN, FER, FGFR2, FGFR3, EGFR, TRKA	Inhibits function in the nucleus, dissociation from adherence junctions, cytoplasmic accumulation.	(25, 35, 37, 132, 167)
S191	JNK2	Nuclear translocation.	(151, 152)
Y331, Y333	PTK6	Inhibits function in nucleus.	(167)
T393	CK2	Stabilization, enhances contributions in transcriptional regulations	(176)
S552	PKA, AKT	Inhibits ubiquitination, stabilization, transcriptional regulation, and promoting tumor cell invasion.	(124, 126, 127)
S605	JNK2, p38γ	Nuclear translocation.	(131, 151, 152)
Y654	MET, EGFR, SRC, BCR-ABL	Dissociation from the E-cadherin/β-catenin/α-catenin complex, nuclear translocation.	(128, 135, 164, 168, 169)
Y670	MET	Nuclear translocation.	(135)
S675	PAK1, PAK4, MEKK2, PKA	Stabilization, inhibits ubiquitination, contributes to TCF/LEF transactivation.	(123, 124, 129, 159, 160)
S715	PKCδ	Facilitate interaction with TRIM33 and degradation.	(101)
S718	PLK1	Regulation of centrosomes in M phase	(86)

for Ser718). Nevertheless, different regions of β-catenin display affinity to different regulatory proteins probably due to phosphorylation modifications (8). Since a deregulated β-catenin function can contribute to malignancy, kinases involved in the regulation of β-catenin stability, localization, and function can be attractive targets for therapeutic implications. Pharmacological inhibitors against BCR-ABL, EGFR, and MET have been developed for several cancers (185–187) and probably can be repurposed to regulate β-catenin activity. However, inhibition of kinases that promote β-catenin degradation or inhibits its function can result in transcriptional activation of WNT/β-catenin target genes.

CONCLUSION

Like other cellular signaling events, WNT/β-catenin signaling is tightly controlled by protein phosphorylation and dephosphorylation. For example, in classical WNT/β-catenin signaling, the formation and activity of the destruction complex are phosphorylation-dependent, which further regulates the stability of β-catenin in a phosphorylation-dependent manner (8). Nevertheless, as discussed above, several kinases are involved in the regulation of this evolutionarily conserved pathway modulating cellular adhesion, polarity, motility, migration, proliferation, and differentiation (188–190).

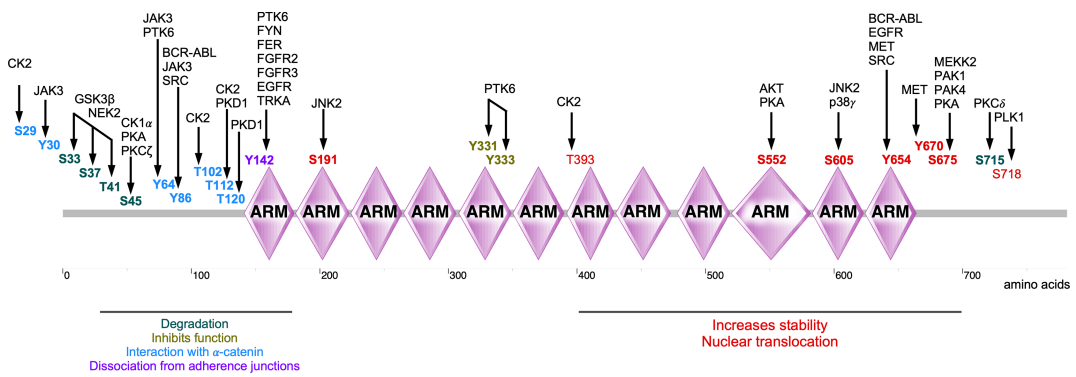

FIGURE 5 | Phosphorylations sites of β-catenin. Several kinases are involved in the phosphorylation of β-catenin, thereby regulating its stability, localization, and activity of β-catenin.

Much is already known about WNT/β-catenin signaling and the roles of its components in various cancers. However, there are still several possible missing links that need to be studied in the regulation of WNT/β-catenin. For instance, aurora family kinases seem to be involved in the stabilization of β-catenin (191). However, the exact mechanism of how β-catenin stabilization is mediated by aurora family kinases remains to be determined. Although WNT/β-catenin signaling is highly simplified in the figures depicted in this review, the interaction between various signaling proteins as described above makes it highly complicated. Both the canonical and non-canonical pathways involving β-catenin intersect at many levels, which adds several layers of complexity. Thus, attempts should be made to precisely define and dissect these pathways, so that they can be better targeted as therapies in the future.

AUTHOR CONTRIBUTIONS

KS and JK outlined the content, reviewed the literature, and wrote the manuscript. All authors contributed to the article and approved the submitted version.

FUNDING

This research was supported by the Kungliga Fysiografiska Sällskapet i Lund (KS), the Crafoord Foundation (JK), Magnus Bergvalls Stiftelse (JK), the Swedish Cancer Society (JK), and the Swedish Childhood Cancer Foundation (JK).

REFERENCES

1. Perugorria MJ, Olaizola P, Labiano I, Esparza-Baquer A, Marzioni M, Marin JJG, et al. Wnt-Beta-Catenin Signalling in Liver Development, Health and Disease. *Nat Rev Gastroenterol Hepatol* (2019) 16(2):121–36. doi: 10.1038/s41575-018-0075-9
2. Parsons MJ, Tammela T, Dow LE. WNT as a Driver and Dependency in Cancer. *Cancer Discov* (2021) 11(10):2413–29. doi: 10.1158/2159-8290.CD-21-0190
3. Kleeman SO, Leedham SJ. Not All Wnt Activation Is Equal: Ligand-Dependent Versus Ligand-Independent Wnt Activation in Colorectal Cancer. *Cancers (Basel)* (2020) 12(11):3355. doi: 10.3390/cancers12113355
4. Vallee A, Lecarpentier Y, Vallee JN. The Key Role of the WNT/beta-Catenin Pathway in Metabolic Reprogramming in Cancers Under Normoxic Conditions. *Cancers (Basel)* (2021) 13(21):5557. doi: 10.3390/cancers13215557
5. Bell IJ, Horn MS, Van Raay TJ. Bridging the Gap Between Non-Canonical and Canonical Wnt Signaling Through Vangl2. *Semin Cell Dev Biol* (2021). doi: 10.1016/j.semcdb.2021.10.004
6. Lojk J, Marc J. Roles of Non-Canonical Wnt Signalling Pathways in Bone Biology. *Int J Mol Sci* (2021) 22(19):10840. doi: 10.3390/ijms221910840
7. Trejo-Solis C, Escamilla-Ramirez A, Jimenez-Farfan D, Castillo-Rodriguez RA, Flores-Najera A, Cruz-Salgado A. Crosstalk of the Wnt/beta-Catenin Signaling Pathway in the Induction of Apoptosis on Cancer Cells. *Pharmaceuticals (Basel)* (2021) 14(9):871. doi: 10.3390/ph14090871
8. Yu F, Yu C, Li F, Zuo Y, Wang Y, Yao L, et al. Wnt/beta-Catenin Signaling in Cancers and Targeted Therapies. *Signal Transduct Target Ther* (2021) 6(1):307. doi: 10.1038/s41392-021-00701-5
9. Nusse R, Clevers H. Wnt/beta-Catenin Signaling, Disease, and Emerging Therapeutic Modalities. *Cell* (2017) 169(6):985–99. doi: 10.1016/j.cell.2017.05.016
10. Hiremath IS, Goel A, Warrier S, Kumar AP, Sethi G, Garg M. The Multidimensional Role of the Wnt/beta-Catenin Signaling Pathway in Human Malignancies. *J Cell Physiol* (2021) 273:199–238. doi: 10.1002/jcp.30561
11. Taank Y, Agnihotri N. Understanding the Regulation of Beta-Catenin Expression and Activity in Colorectal Cancer Carcinogenesis: Beyond Destruction Complex. *Clin Transl Oncol* (2021) 23(12):2448–59. doi: 10.1007/s12094-021-02686-7
12. Mege RM, Ishiyama N. Integration of Cadherin Adhesion and Cytoskeleton at Adherens Junctions. *Cold Spring Harb Perspect Biol* (2017) 9(5):a028738. doi: 10.1101/cshperspect.a028738
13. Menck K, Heinrichs S, Baden C, Bleckmann A. The WNT/ROR Pathway in Cancer: From Signaling to Therapeutic Intervention. *Cells* (2021) 10(1):142. doi: 10.3390/cells10010142
14. Söderholm S, Cantù C. The WNT/beta-Catenin Dependent Transcription: A Tissue-Specific Business. *WIREs Mech Dis* (2021) 13(3):e1511. doi: 10.1002/wsbm.1511
15. Zhao B, Xue B. Self-Regulation of Functional Pathways by Motifs Inside the Disordered Tails of Beta-Catenin. *BMC Genomics* (2016) 179Suppl 5):484. doi: 10.1186/s12864-016-2825-9
16. Xing Y, Takemaru K, Liu J, Berndt JD, Zheng JJ, Moon RT, et al. Crystal Structure of a Full-Length Beta-Catenin. *Structure* (2008) 16(3):478–87. doi: 10.1016/j.str.2007.12.021
17. Valenta T, Hausmann G, Basler K. The Many Faces and Functions of Beta-Catenin. *EMBO J* (2012) 31(12):2714–36. doi: 10.1038/emboj.2012.150
18. Kumar R, Bashyam MD. Multiple Oncogenic Roles of Nuclear Beta-Catenin. *J Biosci* (2017) 42(4):695–707. doi: 10.1007/s12038-017-9710-9
19. Masuda T, Ishitani T. Context-Dependent Regulation of the Beta-Catenin Transcriptional Complex Supports Diverse Functions of Wnt/beta-Catenin Signaling. *J Biochem* (2017) 161(1):9–17. doi: 10.1093/jb/mvw072
20. Shapiro L, Weis WI. Structure and Biochemistry of Cadherins and Catenins. *Cold Spring Harb Perspect Biol* (2009) 1(3):a003053. doi: 10.1101/cshperspect.a003053
21. Yu W, Yang L, Li T, Zhang Y. Cadherin Signaling in Cancer: Its Functions and Role as a Therapeutic Target. *Front Oncol* (2019) 9:989. doi: 10.3389/fonc.2019.00989
22. Wang B, Li X, Liu L, Wang M. Beta-Catenin: Oncogenic Role and Therapeutic Target in Cervical Cancer. *Biol Res* (2020) 53(1):33. doi: 10.1186/s40659-020-00301-7
23. Vergara D, Stanca E, Guerra F, Priore P, Gaballo A, Franck J, et al. Beta-Catenin Knockdown Affects Mitochondrial Biogenesis and Lipid Metabolism in Breast Cancer Cells. *Front Physiol* (2017) 8:544. doi: 10.3389/fphys.2017.00544
24. Tominaga J, Fukunaga Y, Abelardo E, Nagafuchi A. Defining the Function of Beta-Catenin Tyrosine Phosphorylation in Cadherin-Mediated Cell-Cell Adhesion. *Genes Cells* (2008) 13(1):67–77. doi: 10.1111/j.1365-2443.2007.01149.x
25. Brembeck FH, Rosario M, Birchmeier W. Balancing Cell Adhesion and Wnt Signaling, the Key Role of Beta-Catenin. *Curr Opin Genet Dev* (2006) 16(1):51–9. doi: 10.1016/j.gde.2005.12.007
26. Spink KE, Polakis P, Weis WI. Structural Basis of the Axin-Adenomatous Polyposis Coli Interaction. *EMBO J* (2000) 19(10):2270–9. doi: 10.1093/emboj/19.10.2270
27. Yamamoto H, Kishida S, Kishida M, Ikeda S, Takada S, Kikuchi A. Phosphorylation of Axin, a Wnt Signal Negative Regulator, by Glycogen Synthase Kinase-3beta Regulates Its Stability. *J Biol Chem* (1999) 274(16):10681–4. doi: 10.1074/jbc.274.16.10681
28. Xing Y, Clements WK, Kimelman D, Xu W. Crystal Structure of a Beta-Catenin/Axin Complex Suggests a Mechanism for the Beta-Catenin Destruction Complex. *Genes Dev* (2003) 17(22):2753–64. doi: 10.1101/gad.1142603
29. Amit S, Hatzubai A, Birman Y, Andersen JS, Ben-Shushan E, Mann M, et al. Axin-Mediated CKI Phosphorylation of Beta-Catenin at Ser 45: A Molecular Switch for the Wnt Pathway. *Genes Dev* (2002) 16(9):1066–76. doi: 10.1101/gad.230302

30. Strovel ET, Wu D, Sussman DJ. Protein Phosphatase 2Calpha Dephosphorylates Axin and Activates LEF-1-Dependent Transcription. *J Biol Chem* (2000) 275(4):2399–403. doi: 10.1074/jbc.275.4.2399
31. Stamos JL, Weis WI. The Beta-Catenin Destruction Complex. *Cold Spring Harb Perspect Biol* (2013) 5(1):a007898. doi: 10.1101/cshperspect.a007898
32. Jho E, Lomvardas S. Costantini F. A GSK3beta Phosphorylation Site in Axin Modulates Interaction With Beta-Catenin and Tcf-Mediated Gene Expression. *Biochem Biophys Res Commun* (1999) 266(1):28–35. doi: 10.1006/bbrc.1999.1760
33. Kim SE, Huang H, Zhao M, Zhang X, Zhang A, Semonov MV, et al. Wnt Stabilization of Beta-Catenin Reveals Principles for Morphogen Receptor-Scaffold Assemblies. *Science* (2013) 340(6134):867–70. doi: 10.1126/science.1232389
34. Ha NC, Tonozuka T, Stamos JL, Choi HJ, Weis WI. Mechanism of Phosphorylation-Dependent Binding of APC to Beta-Catenin and Its Role in Beta-Catenin Degradation. *Mol Cell* (2004) 15(4):511–21. doi: 10.1016/j.molcel.2004.08.010
35. Bustos VH, Ferrarese A, Venerando A, Marin O, Allende JE, Pinna LA. The First Armadillo Repeat Is Involved in the Recognition and Regulation of Beta-Catenin Phosphorylation by Protein Kinase CK1. *Proc Natl Acad Sci USA* (2006) 103(52):19725–30. doi: 10.1073/pnas.0609424104
36. Liu C, Li Y, Semenov M, Han C, Baeg GH, Tan Y, et al. Control of Beta-Catenin Phosphorylation/Degradation by a Dual-Kinase Mechanism. *Cell* (2002) 108(6):837–47. doi: 10.1016/s0092-8674(02)00685-2
37. Piedra J, Miravet S, Castano J, Palmer HG, Heisterkamp N, Garcia de Herreros A, et al. P120 Catenin-Associated Fer and Fyn Tyrosine Kinases Regulate Beta-Catenin Tyr-142 Phosphorylation and Beta-Catenin-Alpha-Catenin Interaction. *Mol Cell Biol* (2003) 23(7):2287–97. doi: 10.1128/mcb.23.7.2287-2297.2003
38. Wu G, Xu G, Schulman BA, Jeffrey PD, Harper JW, Pavletich NP. Structure of a Beta-TrCP1-Skp1-Beta-Catenin Complex: Destruction Motif Binding and Lysine Specificity of the SCF(beta-TrCP1) Ubiquitin Ligase. *Mol Cell* (2003) 11(6):1445–56. doi: 10.1016/s1097-2765(03)00234-x
39. Orford K, Crockett C, Jensen JP, Weissman AM, Byers SW. Serine Phosphorylation-Regulated Ubiquitination and Degradation of Beta-Catenin. *J Biol Chem* (1997) 272(40):24735–8. doi: 10.1074/jbc.272.40.24735
40. Niehrs C. The Complex World of WNT Receptor Signalling. *Nat Rev Mol Cell Biol* (2012) 13(12):767–79. doi: 10.1038/nrm3470
41. Tauriello DV, Jordens I, Kirchner K, Slootstra JW, Kruitwagen T, Bouwman BA, et al. Wnt/beta-Catenin Signaling Requires Interaction of the Dishevelled DEP Domain and C Terminus With a Discontinuous Motif in Frizzled. *Proc Natl Acad Sci USA* (2012) 109(14):E812–20. doi: 10.1073/pnas.1114802109
42. Anastas JN, Moon RT. WNT Signalling Pathways as Therapeutic Targets in Cancer. *Nat Rev Cancer* (2013) 13(1):11–26. doi: 10.1038/nrc3419
43. Bienz M. Signalosome Assembly by Domains Undergoing Dynamic Head-to-Tail Polymerization. *Trends Biochem Sci* (2014) 39(10):487–95. doi: 10.1016/j.tibs.2014.08.006
44. Fiedler M, Graeb M, Mieszczanek J, Rutherford TJ, Johnson CM, Bienz M. An Ancient Pygo-Dependent Wnt Enhanceosome Integrated by Chip/LDB-SSDP. *Elife* (2015) 4:e09073. doi: 10.7554/eLife.09073
45. Tolwinski NS, Wehrli M, Rives A, Erdeniz N, DiNardo S, Wieschaus E. Wg/Wnt Signal Can Be Transmitted Through Arrow/LRP5,6 and Axin Independently of Zw3/Gsk3beta Activity. *Dev Cell* (2003) 4(3):407–18. doi: 10.1016/s1534-5807(03)00063-7
46. Hou Y, Ding M, Wang C, Yang X, Ye T, Yu H. TRIM11 Promotes Lymphomas by Activating the Beta-Catenin Signaling and Axin1 Ubiquitination Degradation. *Exp Cell Res* (2020) 387(2):111750. doi: 10.1016/j.yexcr.2019.111750
47. Takemaru KI, Moon RT. The Transcriptional Coactivator CBP Interacts With Beta-Catenin to Activate Gene Expression. *J Cell Biol* (2000) 149(2):249–54. doi: 10.1083/jcb.149.2.249
48. Shtutman M, Zhurinsky J, Simcha I, Albanese C, D'Amico M, Pestell R, et al. The Cyclin D1 Gene Is a Target of the Beta-Catenin/LEF-1 Pathway. *Proc Natl Acad Sci USA* (1999) 96(10):5522–7. doi: 10.1073/pnas.96.10.5522
49. He TC, Sparks AB, Rago C, Hermeking H, Zawel L, da Costa LT, et al. Identification of C-MYC as a Target of the APC Pathway. *Science* (1998) 281(5382):1509–12. doi: 10.1126/science.281.5382.1509
50. Schell MJ, Yang M, Teer JK, Lo FY, Madan A, Coppola D, et al. A Multigene Mutation Classification of 468 Colorectal Cancers Reveals a Prognostic Role for APC. *Nat Commun* (2016) 7:11743. doi: 10.1038/ncomms11743
51. Ignatov A, Bischoff J, Ignatov T, Schwarzenau C, Krebs T, Kuester D, et al. APC Promoter Hypermethylation Is an Early Event in Endometrial Tumorigenesis. *Cancer Sci* (2010) 101(2):321–7. doi: 10.1111/j.1349-7006.2009.01397.x
52. Banno K, Yanokura M, Iida M, Masuda K, Aoki D. Carcinogenic Mechanisms of Endometrial Cancer: Involvement of Genetics and Epigenetics. *J Obstet Gynaecol Res* (2014) 40(8):1957–67. doi: 10.1111/jog.12442
53. de La Coste A, Romagnolo B, Billuart P, Renard CA, Buendia MA, Soubrane O, et al. Somatic Mutations of the Beta-Catenin Gene are Frequent in Mouse and Human Hepatocellular Carcinomas. *Proc Natl Acad Sci USA* (1998) 95(15):8847–51. doi: 10.1073/pnas.95.15.8847
54. Bigas A, Guillen Y, Schoch L, Arambilet D. Revisiting Beta-Catenin Signaling in T-Cell Development and T-Cell Acute Lymphoblastic Leukemia. *Bioessays* (2020) 42(2):e1900099. doi: 10.1002/bies.201900099
55. Wu R, Zhai Y, Fearon ER, Cho KR. Diverse Mechanisms of Beta-Catenin Deregulation in Ovarian Endometrioid Adenocarcinomas. *Cancer Res* (2001) 61(22):8247–55.
56. Gamallo C, Palacios J, Moreno G, Calvo de Mora J, Suarez A, Armas A. Beta-Catenin Expression Pattern in Stage I and II Ovarian Carcinomas : Relationship With Beta-Catenin Gene Mutations, Clinicopathological Features, and Clinical Outcome. *Am J Pathol* (1999) 155(2):527–36. doi: 10.1016/s0002-9440(10)65148-6
57. Nguyen VHL, Hough R, Bernaudo S, Peng C. Wnt/beta-Catenin Signalling in Ovarian Cancer: Insights Into Its Hyperactivation and Function in Tumorigenesis. *J Ovarian Res* (2019) 12(1):122. doi: 10.1186/s13048-019-0596-z
58. Hanahan D, Weinberg RA. Hallmarks of Cancer: The Next Generation. *Cell* (2011) 144(5):646–74. doi: 10.1016/j.cell.2011.02.013
59. Veeman MT, Axelrod JD, Moon RT. A Second Canon. Functions and Mechanisms of Beta-Catenin-Independent Wnt Signaling. *Dev Cell* (2003) 5(3):367–77. doi: 10.1016/s1534-5807(03)00266-1
60. Keller R. Shaping the Vertebrate Body Plan by Polarized Embryonic Cell Movements. *Science* (2002) 298(5600):1950–4. doi: 10.1126/science.1079478
61. Mlodzik M. Planar Cell Polarization: Do the Same Mechanisms Regulate Drosophila Tissue Polarity and Vertebrate Gastrulation? *Trends Genet* (2002) 18(11):564–71. doi: 10.1016/s0168-9525(02)02770-1
62. Xiao Q, Chen Z, Jin X, Mao R, Chen Z. The Many Postures of Noncanonical Wnt Signaling in Development and Diseases. *BioMed Pharmacother* (2017) 93:359–69. doi: 10.1016/j.biopha.2017.06.061
63. Marlow F, Topczewski J, Sepich D, Solnica-Krezel L. Zebrafish Rho Kinase 2 Acts Downstream of Wnt11 to Mediate Cell Polarity and Effective Convergence and Extension Movements. *Curr Biol* (2002) 12(11):876–84. doi: 10.1016/s0960-9822(02)00864-3
64. Habas R, Dawid IB, He X. Coactivation of Rac and Rho by Wnt/Frizzled Signaling Is Required for Vertebrate Gastrulation. *Genes Dev* (2003) 17(2):295–309. doi: 10.1101/gad.1022203
65. Yan L, Du Q, Yao J, Liu R. ROR2 Inhibits the Proliferation of Gastric Carcinoma Cells *via* Activation of Non-Canonical Wnt Signaling. *Exp Ther Med* (2016) 12(6):4128–34. doi: 10.3892/etm.2016.3883
66. Yuan Y, Niu CC, Deng G, Li ZQ, Pan J, Zhao C, et al. The Wnt5a/Ror2 Noncanonical Signaling Pathway Inhibits Canonical Wnt Signaling in K562 Cells. *Int J Mol Med* (2011) 27(1):63–9. doi: 10.3892/ijmm.2010.560
67. De A. Wnt/Ca2+ Signaling Pathway: A Brief Overview. *Acta Biochim Biophys Sin (Shanghai)* (2011) 43(10):745–56. doi: 10.1093/abbs/gmr079
68. Saneyoshi T, Kume S, Amasaki Y, Mikoshiba K. The Wnt/calcium Pathway Activates NF-AT and Promotes Ventral Cell Fate in Xenopus Embryos. *Nature* (2002) 417(6886):295–9. doi: 10.1038/417295a
69. Wang HY, Malbon CC. Wnt Signaling, Ca2+, and Cyclic GMP: Visualizing Frizzled Functions. *Science* (2003) 300(5625):1529–30. doi: 10.1126/science.1085259
70. Ishitani T, Ninomiya-Tsuji J, Nagai S, Nishita M, Meneghini M, Barker N, et al. The TAK1-NLK-MAPK-Related Pathway Antagonizes Signalling

Between Beta-Catenin and Transcription Factor TCF. *Nature* (1999) 399 (6738):798–802. doi: 10.1038/21674
71. Kohn AD, Moon RT. Wnt and Calcium Signaling: Beta-Catenin-Independent Pathways. *Cell Calcium* (2005) 38(3-4):439–46. doi: 10.1016/j.ceca.2005.06.022
72. Liu J, Stevens J, Rote CA, Yost HJ, Hu Y, Neufeld KL, et al. Siah-1 Mediates a Novel Beta-Catenin Degradation Pathway Linking P53 to the Adenomatous Polyposis Coli Protein. *Mol Cell* (2001) 7(5):927–36. doi: 10.1016/s1097-2765(01)00241-6
73. Matsuzawa SI, Reed JC. Siah-1, SIP, and Ebi Collaborate in a Novel Pathway for Beta-Catenin Degradation Linked to P53 Responses. *Mol Cell* (2001) 7 (5):915–26. doi: 10.1016/s1097-2765(01)00242-8
74. Topol L, Jiang X, Choi H, Garrett-Beal L, Carolan PJ, Yang Y. Wnt-5a Inhibits the Canonical Wnt Pathway by Promoting GSK-3-Independent Beta-Catenin Degradation. *J Cell Biol* (2003) 162(5):899–908. doi: 10.1083/jcb.200303158
75. Lai KKY, Nguyen C, Lee KS, Lee A, Lin DP, Teo JL, et al. Convergence of Canonical and Non-Canonical Wnt Signal: Differential Kat3 Coactivator Usage. *Curr Mol Pharmacol* (2019) 12(3):167–83. doi: 10.2174/1874467212666190304121131
76. Le NH, Franken P, Fodde R. Tumour-Stroma Interactions in Colorectal Cancer: Converging on Beta-Catenin Activation and Cancer Stemness. *Br J Cancer* (2008) 98(12):1886–93. doi: 10.1038/sj.bjc.6604401
77. Teo JL, Kahn M. The Wnt Signaling Pathway in Cellular Proliferation and Differentiation: A Tale of Two Coactivators. *Adv Drug Delivery Rev* (2010) 62(12):1149–55. doi: 10.1016/j.addr.2010.09.012
78. Moon RT. Wnt/beta-Catenin Pathway. *Sci STKE* (2005) 2005(271):cm1. doi: 10.1126/stke.2712005cm1
79. Park JE, Hymel D, Burke TR Jr, Lee KS. Current Progress and Future Perspectives in the Development of Anti-Polo-Like Kinase 1 Therapeutic Agents. *F1000Res* (2017) 6:1024. doi: 10.12688/f1000research.11398.1
80. Rieger ME, Zhou B, Solomon N, Sunohara M, Li C, Nguyen C, et al. P300/Beta-Catenin Interactions Regulate Adult Progenitor Cell Differentiation Downstream of WNT5a/Protein Kinase C (PKC). *J Biol Chem* (2016) 291 (12):6569–82. doi: 10.1074/jbc.M115.706416
81. Mbom BC, Siemers KA, Ostrowski MA, Nelson WJ, Barth AI. Nek2 Phosphorylates and Stabilizes Beta-Catenin at Mitotic Centrosomes Downstream of Plk1. *Mol Biol Cell* (2014) 25(7):977–91. doi: 10.1091/mbc.E13-06-0349
82. Van Horn RD, Chu S, Fan L, Yin T, Du J, Beckmann R, et al. Cdk1 Activity Is Required for Mitotic Activation of Aurora A During G2/M Transition of Human Cells. *J Biol Chem* (2010) 285(28):21849–57. doi: 10.1074/jbc.M110.141010
83. Lindon C, Grant R, Min M. Ubiquitin-Mediated Degradation of Aurora Kinases. *Front Oncol* (2015) 5:307. doi: 10.3389/fonc.2015.00307
84. Cyphers S, Ruff EF, Behr JM, Chodera JD, Levinson NM. A Water-Mediated Allosteric Network Governs Activation of Aurora Kinase a. *Nat Chem Biol* (2017) 13(4):402–8. doi: 10.1038/nchembio.2296
85. Macurek L, Lindqvist A, Lim D, Lampson MA, Klompmaker R, Freire R, et al. Polo-Like Kinase-1 Is Activated by Aurora A to Promote Checkpoint Recovery. *Nature* (2008) 455(7209):119–23. doi: 10.1038/nature07185
86. Arai T, Haze K, Iimura-Morita Y, Machida T, Iida M, Tanaka K, et al. Identification of Beta-Catenin as a Novel Substrate of Polo-Like Kinase 1. *Cell Cycle* (2008) 7(22):3556–63. doi: 10.4161/cc.7.22.7072
87. Wierstra I. The Transcription Factor FOXM1 (Forkhead Box M1): Proliferation-Specific Expression, Transcription Factor Function, Target Genes, Mouse Models, and Normal Biological Roles. *Adv Cancer Res* (2013) 118:97–398. doi: 10.1016/B978-0-12-407173-5.00004-2
88. Asteriti IA, De Mattia F, Guarguaglini G. Cross-Talk Between AURKA and Plk1 in Mitotic Entry and Spindle Assembly. *Front Oncol* (2015) 5:283. doi: 10.3389/fonc.2015.00283
89. Fu Z, Malureanu L, Huang J, Wang W, Li H, van Deursen JM, et al. Plk1-Dependent Phosphorylation of FoxM1 Regulates a Transcriptional Programme Required for Mitotic Progression. *Nat Cell Biol* (2008) 10 (9):1076–82. doi: 10.1038/ncb1767
90. Seke Etet PF, Vecchio L, Nwabo Kamdje AH. Signaling Pathways in Chronic Myeloid Leukemia and Leukemic Stem Cell Maintenance: Key Role of Stromal Microenvironment. *Cell Signal* (2012) 24(9):1883–8. doi: 10.1016/j.cellsig.2012.05.015
91. Yang J, Ikezoe T, Nishioka C, Udaka K, Yokoyama A. Bcr-Abl Activates AURKA and AURKB in Chronic Myeloid Leukemia Cells *via* AKT Signaling. *Int J Cancer* (2014) 134(5):1183–94. doi: 10.1002/ijc.28434
92. Zhang J, Yuan C, Wu J, Elsayed Z, Fu Z. Polo-Like Kinase 1-Mediated Phosphorylation of Forkhead Box Protein M1b Antagonizes Its SUMOylation and Facilitates its Mitotic Function. *J Biol Chem* (2015) 290 (6):3708–19. doi: 10.1074/jbc.M114.634386
93. Marumoto T, Zhang D, Saya H. Aurora-A - A Guardian of Poles. *Nat Rev Cancer* (2005) 5(1):42–50. doi: 10.1038/nrc1526
94. Benada J, Burdova K, Lidak T, von Morgen P, Macurek L. Polo-Like Kinase 1 Inhibits DNA Damage Response During Mitosis. *Cell Cycle* (2015) 14 (2):219–31. doi: 10.4161/15384101.2014.977067
95. Zhao C, Blum J, Chen A, Kwon HY, Jung SH, Cook JM, et al. Loss of Beta-Catenin Impairs the Renewal of Normal and CML Stem Cells *In Vivo*. *Cancer Cell* (2007) 12(6):528–41. doi: 10.1016/j.ccr.2007.11.003
96. Zhang N, Wei P, Gong A, Chiu WT, Lee HT, Colman H, et al. FoxM1 Promotes Beta-Catenin Nuclear Localization and Controls Wnt Target-Gene Expression and Glioma Tumorigenesis. *Cancer Cell* (2011) 20(4):427–42. doi: 10.1016/j.ccr.2011.08.016
97. Xia Z, Wei P, Zhang H, Ding Z, Yang L, Huang Z, et al. AURKA Governs Self-Renewal Capacity in Glioma-Initiating Cells *via* Stabilization/Activation of Beta-Catenin/Wnt Signaling. *Mol Cancer Res* (2013) 11(9):1101–11. doi: 10.1158/1541-7786.MCR-13-0044
98. Iliaki S, Beyaert R, Afonina IS. Polo-Like Kinase 1 (PLK1) Signaling in Cancer and Beyond. *Biochem Pharmacol* (2021) 193:114747. doi: 10.1016/j.bcp.2021.114747
99. Joshi K, Banasavadi-Siddegowda Y, Mo X, Kim SH, Mao P, Kig C, et al. MELK-Dependent FOXM1 Phosphorylation Is Essential for Proliferation of Glioma Stem Cells. *Stem Cells* (2013) 31(6):1051–63. doi: 10.1002/stem.1358
100. Mancini M, De Santis S, Monaldi C, Bavaro L, Martelli M, Castagnetti F, et al. Hyper-Activation of Aurora Kinase a-Polo-Like Kinase 1-FOXM1 Axis Promotes Chronic Myeloid Leukemia Resistance to Tyrosine Kinase Inhibitors. *J Exp Clin Cancer Res* (2019) 38(1):216. doi: 10.1186/s13046-019-1197-9
101. Xue J, Chen Y, Wu Y, Wang Z, Zhou A, Zhang S, et al. Tumour Suppressor TRIM33 Targets Nuclear Beta-Catenin Degradation. *Nat Commun* (2015) 6:6156. doi: 10.1038/ncomms7156
102. Xu Y, Wu G, Zhang J, Li J, Ruan N, Zhang J, et al. TRIM33 Overexpression Inhibits the Progression of Clear Cell Renal Cell Carcinoma *In Vivo* and *In Vitro*. *BioMed Res Int* (2020) 2020:8409239. doi: 10.1155/2020/8409239
103. Aucagne R, Droin N, Paggetti J, Lagrange B, Largeot A, Hammann A, et al. Transcription Intermediary Factor 1gamma Is a Tumor Suppressor in Mouse and Human Chronic Myelomonocytic Leukemia. *J Clin Invest* (2011) 121 (6):2361–70. doi: 10.1172/JCI45213
104. Herquel B, Ouararhni K, Khetchoumian K, Ignat M, Teletin M, Mark M, et al. Transcription Cofactors TRIM24, TRIM28, and TRIM33 Associate to Form Regulatory Complexes That Suppress Murine Hepatocellular Carcinoma. *Proc Natl Acad Sci USA* (2011) 108(20):8212–7. doi: 10.1073/pnas.1101544108
105. Vincent DF, Yan KP, Treilleux I, Gay F, Arfi V, Kaniewski B, et al. Inactivation of TIF1gamma Cooperates With Kras to Induce Cystic Tumors of the Pancreas. *PloS Genet* (2009) 5(7):e1000575. doi: 10.1371/journal.pgen.1000575
106. Kazi JU, Kabir NN, Soh JW. Bioinformatic Prediction and Analysis of Eukaryotic Protein Kinases in the Rat Genome. *Gene* (2008) 410(1):147–53. doi: 10.1016/j.gene.2007.12.003
107. Kabir NN, Kazi JU. Comparative Analysis of Human and Bovine Protein Kinases Reveals Unique Relationship and Functional Diversity. *Genet Mol Biol* (2011) 34(4):587–91. doi: 10.1590/S1415-47572011005000035
108. Kazi JU. The Mechanism of Protein Kinase C Regulation. *Front Biol* (2011) 6 (4):328–36. doi: 10.1007/s11515-011-1070-5
109. Kazi JU, Kabir NN, Rönnstrand L. Protein Kinase C (PKC) as a Drug Target in Chronic Lymphocytic Leukemia. *Med Oncol* (2013) 30(4):757. doi: 10.1007/s12032-013-0757-7
110. Isakov N. Protein Kinase C (PKC) Isoforms in Cancer, Tumor Promotion and Tumor Suppression. *Semin Cancer Biol* (2018) 48:36–52. doi: 10.1016/j.semcancer.2017.04.012

111. Newton AC. Protein Kinase C as a Tumor Suppressor. *Semin Cancer Biol* (2018) 48:18–26. doi: 10.1016/j.semcancer.2017.04.017
112. Perletti GP, Marras E, Concari P, Piccinini F, Tashjian AH Jr. PKCdelta Acts as a Growth and Tumor Suppressor in Rat Colonic Epithelial Cells. *Oncogene* (1999) 18(5):1251–6. doi: 10.1038/sj.onc.1202408
113. Kazi JU, Soh JW. Isoform-Specific Translocation of PKC Isoforms in NIH3T3 Cells by TPA. *Biochem Biophys Res Commun* (2007) 364(2):231–7. doi: 10.1016/j.bbrc.2007.09.123
114. Kabir NN, Rönnstrand L, Kazi JU. Protein Kinase C Expression Is Deregulated in Chronic Lymphocytic Leukemia. *Leuk Lymphoma* (2013) 54(10):2288–90. doi: 10.3109/10428194.2013.769220
115. Llado V, Nakanishi Y, Duran A, Reina-Campos M, Shelton PM, Linares JF, et al. Repression of Intestinal Stem Cell Function and Tumorigenesis Through Direct Phosphorylation of Beta-Catenin and Yap by PKCzeta. *Cell Rep* (2015) 10(5):740–54. doi: 10.1016/j.celrep.2015.01.007
116. Gwak J, Cho M, Gong SJ, Won J, Kim DE, Kim EY, et al. Protein-Kinase-C-Mediated Beta-Catenin Phosphorylation Negatively Regulates the Wnt/beta-Catenin Pathway. *J Cell Sci* (2006) 119(Pt 22):4702–9. doi: 10.1242/jcs.03256
117. Lee JM, Kim IS, Kim H, Lee JS, Kim K, Yim HY, et al. RORalpha Attenuates Wnt/beta-Catenin Signaling by PKCalpha-Dependent Phosphorylation in Colon Cancer. *Mol Cell* (2010) 37(2):183–95. doi: 10.1016/j.molcel.2009.12.022
118. Stork PJ, Schmitt JM. Crosstalk Between cAMP and MAP Kinase Signaling in the Regulation of Cell Proliferation. *Trends Cell Biol* (2002) 12(6):258–66. doi: 10.1016/s0962-8924(02)02294-8
119. Cao W, Li J, Hao Q, Vadgama JV, Wu Y. AMP-Activated Protein Kinase: A Potential Therapeutic Target for Triple-Negative Breast Cancer. *Breast Cancer Res* (2019) 21(1):29. doi: 10.1186/s13058-019-1107-2
120. Hogarth DK, Sandbo N, Taurin S, Kolenko V, Miano JM, Dulin NO. Dual Role of PKA in Phenotypic Modulation of Vascular Smooth Muscle Cells by Extracellular ATP. *Am J Physiol Cell Physiol* (2004) 287(2):C449–56. doi: 10.1152/ajpcell.00547.2003
121. Marino A, Hausenloy DJ, Andreadou I, Horman S, Bertrand L, Beauloye C. AMP-Activated Protein Kinase: A Remarkable Contributor to Preserve a Healthy Heart Against ROS Injury. *Free Radic Biol Med* (2021) 166:238–54. doi: 10.1016/j.freeradbiomed.2021.02.047
122. Kang DE, Soriano S, Xia X, Eberhart CG, De Strooper B, Zheng H, et al. Presenilin Couples the Paired Phosphorylation of Beta-Catenin Independent of Axin: Implications for Beta-Catenin Activation in Tumorigenesis. *Cell* (2002) 110(6):751–62. doi: 10.1016/s0092-8674(02)00970-4
123. Hino S, Tanji C, Nakayama KI, Kikuchi A. Phosphorylation of Beta-Catenin by Cyclic AMP-Dependent Protein Kinase Stabilizes Beta-Catenin Through Inhibition of Its Ubiquitination. *Mol Cell Biol* (2005) 25(20):9063–72. doi: 10.1128/MCB.25.20.9063-9072.2005
124. Taurin S, Sandbo N, Qin Y, Browning D, Dulin NO. Phosphorylation of Beta-Catenin by Cyclic AMP-Dependent Protein Kinase. *J Biol Chem* (2006) 281(15):9971–6. doi: 10.1074/jbc.M508778200
125. Li CC, Le K, Kato J, Moss J, Vaughan M. Enhancement of Beta-Catenin Activity by BIG1 Plus BIG2 *via* Arf Activation and cAMP Signals. *Proc Natl Acad Sci USA* (2016) 113(21):5946–51. doi: 10.1073/pnas.1601918113
126. Fang D, Hawke D, Zheng Y, Xia Y, Meisenhelder J, Nika H, et al. Phosphorylation of Beta-Catenin by AKT Promotes Beta-Catenin Transcriptional Activity. *J Biol Chem* (2007) 282(15):11221–9. doi: 10.1074/jbc.M611871200
127. He XC, Yin T, Grindley JC, Tian Q, Sato T, Tao WA, et al. PTEN-Deficient Intestinal Stem Cells Initiate Intestinal Polyposis. *Nat Genet* (2007) 39(2):189–98. doi: 10.1038/ng1928
128. Jean C, Blanc A, Prade-Houdellier N, Ysebaert L, Hernandez-Pigeon H, Al Saati T, et al. Epidermal Growth Factor Receptor/Beta-Catenin/T-Cell Factor 4/Matrix Metalloproteinase 1: A New Pathway for Regulating Keratinocyte Invasiveness After UVA Irradiation. *Cancer Res* (2009) 69(8):3291–9. doi: 10.1158/0008-5472.CAN-08-1909
129. Greenblatt MB, Shin DY, Oh H, Lee KY, Zhai B, Gygi SP, et al. MEKK2 Mediates an Alternative Beta-Catenin Pathway That Promotes Bone Formation. *Proc Natl Acad Sci USA* (2016) 113(9):E1226–35. doi: 10.1073/pnas.1600813113
130. Lemieux E, Cagnol S, Beaudry K, Carrier J, Rivard N. Oncogenic KRAS Signalling Promotes the Wnt/beta-Catenin Pathway Through LRP6 in Colorectal Cancer. *Oncogene* (2015) 34(38):4914–27. doi: 10.1038/onc.2014.416
131. Yin N, Qi X, Tsai S, Lu Y, Basir Z, Oshima K, et al. P38gamma MAPK is Required for Inflammation-Associated Colon Tumorigenesis. *Oncogene* (2016) 35(8):1039–48. doi: 10.1038/onc.2015.158
132. Krejci P, Aklian A, Kaucka M, Sevcikova E, Prochazkova J, Masek JK, et al. Receptor Tyrosine Kinases Activate Canonical WNT/beta-Catenin Signaling *via* MAP Kinase/LRP6 Pathway and Direct Beta-Catenin Phosphorylation. *PloS One* (2012) 7(4):e35826. doi: 10.1371/journal.pone.0035826
133. Hiscox S, Jiang WG. Association of the HGF/SF Receptor, C-Met, With the Cell-Surface Adhesion Molecule, E-Cadherin, and Catenins in Human Tumor Cells. *Biochem Biophys Res Commun* (1999) 261(2):406–11. doi: 10.1006/bbrc.1999.1002
134. Monga SP, Mars WM, Pediaditakis P, Bell A, Mule K, Bowen WC, et al. Hepatocyte Growth Factor Induces Wnt-Independent Nuclear Translocation of Beta-Catenin After Met-Beta-Catenin Dissociation in Hepatocytes. *Cancer Res* (2002) 62(7):2064–71.
135. Zeng G, Apte U, Micsenyi A, Bell A, Monga SP. Tyrosine Residues 654 and 670 in Beta-Catenin Are Crucial in Regulation of Met-Beta-Catenin Interactions. *Exp Cell Res* (2006) 312(18):3620–30. doi: 10.1016/j.yexcr.2006.08.003
136. Wagh PK, Gray JK, Zinser GM, Vasiliauskas J, James L, Monga SP, et al. Beta-Catenin Is Required for Ron Receptor-Induced Mammary Tumorigenesis. *Oncogene* (2011) 30(34):3694–704. doi: 10.1038/onc.2011.86
137. Guo Q, Kim A, Li B, Ransick A, Bugacov H, Chen X, et al. A Beta-Catenin-Driven Switch in TCF/LEF Transcription Factor Binding to DNA Target Sites Promotes Commitment of Mammalian Nephron Progenitor Cells. *Elife* (2021) 10:e64444. doi: 10.7554/eLife.64444
138. Morali OG, Delmas V, Moore R, Jeanney C, Thiery JP, Larue L. IGF-II Induces Rapid Beta-Catenin Relocation to the Nucleus During Epithelium to Mesenchyme Transition. *Oncogene* (2001) 20(36):4942–50. doi: 10.1038/sj.onc.1204660
139. Playford MP, Bicknell D, Bodmer WF, Macaulay VM. Insulin-Like Growth Factor 1 Regulates the Location, Stability, and Transcriptional Activity of Beta-Catenin. *Proc Natl Acad Sci USA* (2000) 97(22):12103–8. doi: 10.1073/pnas.210394297
140. Satyamoorthy K, Li G, Vaidya B, Patel D, Herlyn M. Insulin-Like Growth Factor-1 Induces Survival and Growth of Biologically Early Melanoma Cells Through Both the Mitogen-Activated Protein Kinase and Beta-Catenin Pathways. *Cancer Res* (2001) 61(19):7318–24.
141. Reiss K, Valentinis B, Tu X, Xu SQ, Baserga R. Molecular Markers of IGF-I-Mediated Mitogenesis. *Exp Cell Res* (1998) 242(1):361–72. doi: 10.1006/excr.1998.4113
142. Chen J, Wu A, Sun H, Drakas R, Garofalo C, Cascio S, et al. Functional Significance of Type 1 Insulin-Like Growth Factor-Mediated Nuclear Translocation of the Insulin Receptor Substrate-1 and Beta-Catenin. *J Biol Chem* (2005) 280(33):29912–20. doi: 10.1074/jbc.M504516200
143. Prisco M, Santini F, Baffa R, Liu M, Drakas R, Wu A, et al. Nuclear Translocation of Insulin Receptor Substrate-1 by the Simian Virus 40 T Antigen and the Activated Type 1 Insulin-Like Growth Factor Receptor. *J Biol Chem* (2002) 277(35):32078–85. doi: 10.1074/jbc.M204658200
144. Gao ZH, Seeling JM, Hill V, Yochum A, Virshup DM. Casein Kinase I Phosphorylates and Destabilizes the Beta-Catenin Degradation Complex. *Proc Natl Acad Sci USA* (2002) 99(3):1182–7. doi: 10.1073/pnas.032468199
145. Gorgisen G, Gulacar IM, Ozes ON. The Role of Insulin Receptor Substrate (IRS) Proteins in Oncogenic Transformation. *Cell Mol Biol (Noisy-le-grand)* (2017) 63(1):1–5. doi: 10.14715/cmb/2017.63.1.1
146. Campbell HK, Maiers JL, DeMali KA. Interplay Between Tight Junctions & Adherens Junctions. *Exp Cell Res* (2017) 358(1):39–44. doi: 10.1016/j.yexcr.2017.03.061
147. Senkevitch E, Durum S. The Promise of Janus Kinase Inhibitors in the Treatment of Hematological Malignancies. *Cytokine* (2017) 98:33–41. doi: 10.1016/j.cyto.2016.10.012
148. Mishra J, Das JK, Kumar N. Janus Kinase 3 Regulates Adherens Junctions and Epithelial Mesenchymal Transition Through Beta-Catenin. *J Biol Chem* (2017) 292(40):16406–19. doi: 10.1074/jbc.M117.811802
149. Rane CK, Minden A. P21 Activated Kinase Signaling in Cancer. *Semin Cancer Biol* (2019) 54:40–9. doi: 10.1016/j.semcancer.2018.01.006

150. Wang K, Baldwin GS, Nikfarjam M, He H. P21-Activated Kinase Signalling in Pancreatic Cancer: New Insights Into Tumour Biology and Immune Modulation. *World J Gastroenterol* (2018) 24(33):3709–23. doi: 10.3748/wjg.v24.i33.3709
151. Wu X, Tu X, Joeng KS, Hilton MJ, Williams DA, Long F. Rac1 Activation Controls Nuclear Localization of Beta-Catenin During Canonical Wnt Signaling. *Cell* (2008) 133(2):340–53. doi: 10.1016/j.cell.2008.01.052
152. Phelps RA, Chidester S, Dehghanizadeh S, Phelps J, Sandoval IT, Rai K, et al. A Two-Step Model for Colon Adenoma Initiation and Progression Caused by APC Loss. *Cell* (2009) 137(4):623–34. doi: 10.1016/j.cell.2009.02.037
153. Yao D, Li C, Rajoka MSR, He Z, Huang J, Wang J, et al. P21-Activated Kinase 1: Emerging Biological Functions and Potential Therapeutic Targets in Cancer. *Theranostics* (2020) 10(21):9741–66. doi: 10.7150/thno.46913
154. Nheu T, He H, Hirokawa Y, Walker F, Wood J, Maruta H. PAK Is Essential for RAS-Induced Upregulation of Cyclin D1 During the G1 to S Transition. *Cell Cycle* (2004) 3(1):71–4. doi: 10.4161/cc.3.1.593
155. Al Thawadi H, Abu-Kaoud N, Al Farsi H, Hoarau-Vechot J, Rafii S, Rafii A, et al. VE-Cadherin Cleavage by Ovarian Cancer Microparticles Induces Beta-Catenin Phosphorylation in Endothelial Cells. *Oncotarget* (2016) 7(5):5289–305. doi: 10.18632/oncotarget.6677
156. Sun J, Khalid S, Rozakis-Adcock M, Fantus IG. Jin T. P-21-Activated Protein Kinase-1 Functions as a Linker Between Insulin and Wnt Signaling Pathways in the Intestine. *Oncogene* (2009) 28(35):3132–44. doi: 10.1038/onc.2009.167
157. Fu H, Zhang W, Yuan Q, Niu M, Zhou F, Qiu Q, et al. PAK1 Promotes the Proliferation and Inhibits Apoptosis of Human Spermatogonial Stem Cells *via* PDK1/KDR/ZNF367 and ERK1/2 and AKT Pathways. *Mol Ther Nucleic Acids* (2018) 12:769–86. doi: 10.1016/j.omtn.2018.06.006
158. Barbe C, Loumaye A, Lause P, Ritvos O, Thissen JP. P21-Activated Kinase 1 Is Permissive for the Skeletal Muscle Hypertrophy Induced by Myostatin Inhibition. *Front Physiol* (2021) 12:677746. doi: 10.3389/fphys.2021.677746
159. Li Y, Shao Y, Tong Y, Shen T, Zhang J, Li Y, et al. Nucleo-Cytoplasmic Shuttling of PAK4 Modulates Beta-Catenin Intracellular Translocation and Signaling. *Biochim Biophys Acta* (2012) 1823(2):465–75. doi: 10.1016/j.bbamcr.2011.11.013
160. Zhu G, Wang Y, Huang B, Liang J, Ding Y, Xu A, et al. A Rac1/PAK1 Cascade Controls Beta-Catenin Activation in Colon Cancer Cells. *Oncogene* (2012) 31(8):1001–12. doi: 10.1038/onc.2011.294
161. Kim KK, Wei Y, Szekeres C, Kugler MC, Wolters PJ, Hill ML, et al. Epithelial Cell Alpha3beta1 Integrin Links Beta-Catenin and Smad Signaling to Promote Myofibroblast Formation and Pulmonary Fibrosis. *J Clin Invest* (2009) 119(1):213–24. doi: 10.1172/JCI36940
162. Xu L, Cui WH, Zhou WC, Li DL, Li LC, Zhao P, et al. Activation of Wnt/beta-Catenin Signalling Is Required for TGF-Beta/Smad2/3 Signalling During Myofibroblast Proliferation. *J Cell Mol Med* (2017) 21(8):1545–54. doi: 10.1111/jcmm.13085
163. Ulsamer A, Wei Y, Kim KK, Tan K, Wheeler S, Xi Y, et al. Axin Pathway Activity Regulates *In Vivo* Py654-Beta-Catenin Accumulation and Pulmonary Fibrosis. *J Biol Chem* (2012) 287(7):5164–72. doi: 10.1074/jbc.M111.322123
164. Xi Y, Wei Y, Sennino B, Ulsamer A, Kwan I, Brumwell AN, et al. Identification of Py654-Beta-Catenin as a Critical Co-Factor in Hypoxia-Inducible Factor-1alpha Signaling and Tumor Responses to Hypoxia. *Oncogene* (2013) 32(42):5048–57. doi: 10.1038/onc.2012.530
165. Roura S, Miravet S, Piedra J, Garcia de Herreros A, Dunach M. Regulation of E-Cadherin/Catenin Association by Tyrosine Phosphorylation. *J Biol Chem* (1999) 274(51):36734–40. doi: 10.1074/jbc.274.51.36734
166. Daugherty RL, Gottardi CJ. Phospho-Regulation of Beta-Catenin Adhesion and Signaling Functions. *Physiol (Bethesda)* (2007) 22:303–9. doi: 10.1152/physiol.00020.2007
167. Palka-Hamblin HL, Gierut JJ, Bie W, Brauer PM, Zheng Y, Asara JM, et al. Identification of Beta-Catenin as a Target of the Intracellular Tyrosine Kinase PTK6. *J Cell Sci* (2010) 123(Pt 2):236–45. doi: 10.1242/jcs.053264
168. Coluccia AM, Vacca A, Dunach M, Mologni L, Redaelli S, Bustos VH, et al. Bcr-Abl Stabilizes Beta-Catenin in Chronic Myeloid Leukemia Through Its Tyrosine Phosphorylation. *EMBO J* (2007) 26(5):1456–66. doi: 10.1038/sj.emboj.7601485
169. Jamieson CH, Ailles LE, Dylla SJ, Muijtjens M, Jones C, Zehnder JL, et al. Granulocyte-Macrophage Progenitors as Candidate Leukemic Stem Cells in Blast-Crisis CML. *N Engl J Med* (2004) 351(7):657–67. doi: 10.1056/NEJMoa040258
170. Simoneau M, Coulombe G, Vandal G, Vezina A, Rivard N. SHP-1 Inhibits Beta-Catenin Function by Inducing Its Degradation and Interfering With Its Association With TATA-Binding Protein. *Cell Signal* (2011) 23(1):269–79. doi: 10.1016/j.cellsig.2010.09.011
171. Takemaru K, Yamaguchi S, Lee YS, Zhang Y, Carthew RW, Moon RT. Chibby, a Nuclear Beta-Catenin-Associated Antagonist of the Wnt/Wingless Pathway. *Nature* (2003) 422(6934):905–9. doi: 10.1038/nature01570
172. Li FQ, Mofunanya A, Harris K, Takemaru K. Chibby Cooperates With 14-3-3 to Regulate Beta-Catenin Subcellular Distribution and Signaling Activity. *J Cell Biol* (2008) 181(7):1141–54. doi: 10.1083/jcb.200709091
173. Takemaru K, Fischer V, Li FQ. Fine-Tuning of Nuclear-Catenin by Chibby and 14-3-3. *Cell Cycle* (2009) 8(2):210–3. doi: 10.4161/cc.8.2.7394
174. Mancini M, Soverini S, Gugliotta G, Santucci MA, Rosti G, Cavo M, et al. Chibby 1: A New Component of Beta-Catenin-Signaling in Chronic Myeloid Leukemia. *Oncotarget* (2017) 8(50):88244–50. doi: 10.18632/oncotarget.21166
175. Borgo C, D'Amore C, Sarno S, Salvi M, Ruzzene M. Protein Kinase CK2: A Potential Therapeutic Target for Diverse Human Diseases. *Signal Transduct Target Ther* (2021) 6(1):183. doi: 10.1038/s41392-021-00567-7
176. Song DH, Dominguez I, Mizuno J, Kaut M, Mohr SC, Seldin DC. CK2 Phosphorylation of the Armadillo Repeat Region of Beta-Catenin Potentiates Wnt Signaling. *J Biol Chem* (2003) 278(26):24018–25. doi: 10.1074/jbc.M212260200
177. Wu H, Symes K, Seldin DC, Dominguez I. Threonine 393 of Beta-Catenin Regulates Interaction With Axin. *J Cell Biochem* (2009) 108(1):52–63. doi: 10.1002/jcb.22260
178. Bek S, Kemler R. Protein Kinase CKII Regulates the Interaction of Beta-Catenin With Alpha-Catenin and Its Protein Stability. *J Cell Sci* (2002) 115 (Pt 24):4743–53. doi: 10.1242/jcs.00154
179. Youssef I, Ricort JM. Deciphering the Role of Protein Kinase D1 (PKD1) in Cellular Proliferation. *Mol Cancer Res* (2019) 17(10):1961–74. doi: 10.1158/1541-7786.MCR-19-0125
180. Jaggi M, Rao PS, Smith DJ, Wheelock MJ, Johnson KR, Hemstreet GP, et al. E-Cadherin Phosphorylation by Protein Kinase D1/protein Kinase C {mu} Is Associated With Altered Cellular Aggregation and Motility in Prostate Cancer. *Cancer Res* (2005) 65(2):483–92. doi: 10.1158/0008-5472.483.65.2
181. Syed V, Mak P, Du C, Balaji KC. Beta-Catenin Mediates Alteration in Cell Proliferation, Motility and Invasion of Prostate Cancer Cells by Differential Expression of E-Cadherin and Protein Kinase D1. *J Cell Biochem* (2008) 104 (1):82–95. doi: 10.1002/jcb.21603
182. Du C, Jaggi M, Zhang C, Balaji KC. Protein Kinase D1-Mediated Phosphorylation and Subcellular Localization of Beta-Catenin. *Cancer Res* (2009) 69(3):1117–24. doi: 10.1158/0008-5472.CAN-07-6270
183. Aberle H, Schwartz H, Hoschuetzky H, Kemler R. Single Amino Acid Substitutions in Proteins of the Armadillo Gene Family Abolish Their Binding to Alpha-Catenin. *J Biol Chem* (1996) 271(3):1520–6. doi: 10.1074/jbc.271.3.1520
184. Nickkholgh B, Sittadjody S, Rothberg MB, Fang X, Li K, Chou JW, et al. Beta-Catenin Represses Protein Kinase D1 Gene Expression by Non-Canonical Pathway Through MYC/MAX Transcription Complex in Prostate Cancer. *Oncotarget* (2017) 8(45):78811–24. doi: 10.18632/oncotarget.20229
185. Rossari F, Minutolo F, Orciuolo E. Past, Present, and Future of Bcr-Abl Inhibitors: From Chemical Development to Clinical Efficacy. *J Hematol Oncol* (2018) 11(1):84. doi: 10.1186/s13045-018-0624-2
186. Du X, Yang B, An Q, Assaraf YG, Cao X, Xia J. Acquired Resistance to Third-Generation EGFR-TKIs and Emerging Next-Generation EGFR Inhibitors. *Innovation (N Y)* (2021) 2(2):100103. doi: 10.1016/j.xinn.2021.100103
187. Wang Q, Yang S, Wang K, Sun SY. MET Inhibitors for Targeted Therapy of EGFR TKI-Resistant Lung Cancer. *J Hematol Oncol* (2019) 12(1):63. doi: 10.1186/s13045-019-0759-9
188. Hong Y. aPKC: The Kinase That Phosphorylates Cell Polarity. *F1000Res* (2018) 7:903. doi: 10.12688/f1000research.14427.1

189. Jones MC, Zha J, Humphries MJ. Connections Between the Cell Cycle, Cell Adhesion and the Cytoskeleton. *Philos Trans R Soc Lond B Biol Sci* (2019) 374(1779):20180227. doi: 10.1098/rstb.2018.0227
190. Chen Y, Chen Z, Tang Y, Xiao Q. The Involvement of Noncanonical Wnt Signaling in Cancers. *BioMed Pharmacother* (2021) 133:110946. doi: 10.1016/j.biopha.2020.110946
191. Shah K, Ahmed M, Kazi JU. The Aurora Kinase/Beta-Catenin Axis Contributes to Dexamethasone Resistance in Leukemia. *NPJ Precis Oncol* (2021) 5(1):13. doi: 10.1038/s41698-021-00148-5

Conflict of Interest: The authors declare that the research was conducted in the absence of any commercial or financial relationships that could be construed as a potential conflict of interest.

frontiers | Frontiers in Oncology

TYPE Original Research
PUBLISHED 25 July 2022
DOI 10.3389/fonc.2022.911316

OPEN ACCESS

EDITED BY
Simone Patergnani,
University of Ferrara, Italy

REVIEWED BY
Esmaa Bouhamida,
University of Ferrara, Italy
Yilin Yu,
Fujian Medical University, China

*CORRESPONDENCE
Wei Liu
liuweixy3@csu.edu.cn

SPECIALTY SECTION
This article was submitted to Molecular and Cellular Oncology, a section of the journal Frontiers in Oncology

RECEIVED 02 April 2022
ACCEPTED 28 June 2022
PUBLISHED 25 July 2022

CITATION
Wang J, Yang Q, Tang M and Liu W (2022) Validation and analysis of expression, prognosis and immune infiltration of WNT gene family in non-small cell lung cancer. *Front. Oncol.* 12:911316. doi: 10.3389/fonc.2022.911316

Validation and analysis of expression, prognosis and immune infiltration of WNT gene family in non-small cell lung cancer

Jianglin Wang[1], Qingping Yang[2], Mengjie Tang[3] and Wei Liu[1]*

[1]Department of Pharmacy, The Third Xiangya Hospital, Central South University, Changsha, China, [2]Department of Pharmacy, Zunyi Medical University, Zunyi, China, [3]Department of Pathology, Hunan Cancer Hospital, The Affiliated Cancer Hospital of Xiangya School of Medicine, Central South University, Changsha, China

Early diagnosis and prognosis prediction of non-small cell lung cancer (NSCLC) have been challenging. Signaling cascades involving the Wingless-type (WNT) gene family play important biological roles and show prognostic value in various cancers, including NSCLC. On this basis, this study aimed to investigate the significance of WNTs in the prognosis and tumor immunity in NSCLC by comprehensive analysis. Expression and methylation levels of WNTs were obtained from the ONCOMINE, TIMER, and UALCAN. The dataset obtained from The Cancer Genome Atlas (TCGA) was utilized for prognostic analysis. cBioPortal was used to perform genetic alterations and correlation analysis of WNTs. R software was employed for functional enrichment and pathway analysis, partial statistics, and graph drawing. TRRUST was used to find key transcription factors. GEPIA was utilized for the analysis of expression, pathological staging, etc. Correlative analysis of immune infiltrates from TIMER. TISIDB was used for further immune infiltration validation analysis. Compared with that of normal tissues, WNT2/2B/3A/4/7A/9A/9B/11 expressions decreased, while WNT3/5B/6/7B/8B/10A/10B/16 expressions increased in lung adenocarcinoma (LUAD); WNT2/3A/7A/11 expressions were lessened, while WNT2B/3/5A/5B/6/7B/10A/10B/16 expressions were enhanced in squamous cell lung cancer (LUSC). Survival analysis revealed that highly expressed WNT2B and lowly expressed WNT7A predicted better prognostic outcomes in LUAD and LUSC. In the study of immune infiltration levels, WNT2, WNT9B, and WNT10A were positively correlated with six immune cells in LUAD; WNT1, WNT2, and WNT9B were positively correlated with six immune cells in LUSC, while WNT7B was negatively correlated. Our study indicated that WNT2B and WNT7A might have prognostic value in LUAD, and both of them might be important prognostic factors in LUSC and correlated to immune cell infiltration in LUAD and LUSC to a certain extent. Considering the prognostic value of WNT2B and WNT7A in NSCLC, we validated their mRNA and protein

expression levels in NSCLC by performing qRT-PCR, western blot, and immunohistochemical staining on NSCLC pathological tissues and cell lines. This study may provide some direction for the subsequent exploration of the prognostic value of the WNTs and their role as biomarkers in NSCLC.

KEYWORDS

NSCLC, LUAD, LUSC, WNT gene family, prognosis, immune infiltration

Introduction

Lung cancer has a high incidence rate, accounting for 11.4% of cases and 18% of cancer mortality worldwide. By 2020, it has been the second most common cancer and the leading cause of death worldwide. There was little progress in its early screening and survival (1, 2). Non-small cell lung cancer (NSCLC) is the most common histological subtype in lung cancer patients, about 85% of these patients. It can be mainly divided into lung adenocarcinoma (LUAD), squamous cell lung cancer (LUSC), and large cell lung carcinoma, of which LUAD and LUSC are the most common (3, 4). For NSCLC therapeutic targets, molecular therapy, immune checkpoint inhibition, and lung cancer vaccination have made many advances (5–7). Nonetheless, lung cancer still has a 5-year survival rate lower than all other cancer types (8).

The Wingless-type (WNT) protein family consists of many cysteine-rich secreted glycoproteins, with a molecular weight of about 40 kDa, and 19 WNT genes have been identified in the human genome (9). WNT binds to members of the Frizzled (Fzd) receptor family on the cell surface to activate downstream effectors inside the cell, activating signal transduction cascades through three different pathways in the organism, i.e., the canonical WNT pathway, the non-canonical WNT/planar cell polarity (PCP) pathway, and the non-canonical WNT/calcium pathway (10). At the cellular level, WNT proteins participate in the regulation of cell proliferation, cell morphology, cell motility, and cell fate, playing an extensive role in organism development; moreover, dysregulation of WNT signaling also works during tumor formation (11, 12). WNT signaling serves as a molecular rheostat in organisms and participates in multiple physiological processes, including embryonic development, lineage commitment, adult stem cell homeostasis, and tissue regeneration (12). The transmission of WNT signaling and the generation and secretion of WNT ligands involve specialized and complex mechanisms (11–13). Conduction of WNT signaling has been demonstrated in many types of cancer (12), including but not limited to colorectal cancer (14), liver cancer (15), prostate cancer (16), skin cancer (17), melanoma (18) and lung cancer (12, 13). The WNT pathway plays an important biological role and represents prognostic value in NSCLC, and β-catenin produced by downstream activation of WNT ligands is indispensable in NSCLC development (12, 13, 19). Activation by WNT ligands in the canonical WNT pathway increases the concentrations of β-catenin in the cytoplasm, which binds to transcription factors of the T-cell factor (TCF)/Lymphoid enhancer-binding factor (LEF) family in the nucleus so as to drive transcription of WNT/β-catenin target genes. Some genomic data also suggest that an important component in lung cancer development is intrinsic WNT signaling within cancer cells (12). However, comprehensive studies on the expression and prognosis of the WNT family in NSCLC or its subtypes are lacking.

Our study used a publicly available tumor database to perform bioinformatics analysis of WNT gene family expression, prognosis, and immune infiltration in LUAD and LUSC so as to find reliable biomarkers and detailed prognosis of the WNT family in NSCLC.

Materials and methods

ONCOMINE database

ONCOMINE (https://www.ONCOMINE.org) is an online microarray database that allows differential expression analysis in many types of cancer (20). In this study, we compared the mRNA transcript expression differences of WNT genes by using Student's t-test in this database, and the cut-off values of *p* value and fold-change were as follows: *p* value of 1E-4, fold-change of 2, gene rank of 10%.

Tumor immune estimation resource (TIMER)

TIMER (https://cistrome.shinyapps.io/timer/) is an online tool that can systematically assess the infiltration level of immune cells in different cancer types and their clinical impact (21). In the "DiffExp" module, the expression level

distribution of WNTs was displayed using boxplots, and the statistical significance of differential expression was assessed using the Wilcoxon test. Scatter plots representing the correlation of infiltration levels between WNT genes and the six immune cells were obtained by the "Gene" module. Then, by using the "Survival" module, the clinical correlation between WNTs and tumor immunity was explored by Cox regression analysis, including risk ratio and statistical significance. The level of tumor invasion between WNTs and tumors with different somatic copy number alterations was compared using the Wilcoxon rank-sum test in the "SCNA" module defined by GISTIC2.0. The heatmap of the correlation between WNTs and immune scores was created using the R software v4.0.3 package pheatmap (v1.0.12). The lollipop chart using the R software v4.0.3 package GSVA (v1.34.0) built-in algorithm ssGSEA to verify the relationship between WNTs expression and immune cells. The dataset used contained mRNA sequence data from 516 lung adenocarcinomas and 501 squamous cell lung cancers from TCGA tumors.

UALCAN database

UALCAN (http://ualcan.path.uab.edu) is a comprehensive network resource that is taken from publicly available cancer genomics data (TCGA, MET500, and CPTAC) (22). In this study, the mRNA transcript expression and methylation data of WNT gene family were obtained by using the expression analysis module and methylation level module of UALCAN.

Gene expression profiling interactive analysis (GEPIA)

GEPIA (http://gepia.cancer-pku.cn) is a web-based data mining platform with large RNA sequencing data from TCGA and GTEx (23). "Pathological Stage Plot" in the "ExpressionDIY" function is used for the correlation study of the pathological stage of WNTs in NSCLC patients. "Multiple Gene Comparison" module was used to obtain WNTs relative expression data, and matrix plots were created by the R v4.0.3 software package ggplot2 (v.3.3.5). Gene expression correlation analysis was performed in the "Correlation" module.

Prognostic analysis

From the TCGA dataset (https://portal.gdc.com), to obtain raw counts and corresponding clinical information of RNA sequencing data of NSCLC tumors. For Kaplan-Meier (KM) curves, p values and hazard ratios (HR) with 95% confidence intervals (CI) were derived by log-rank test and univariate Cox proportional hazards regression, $p < 0.05$ was considered statistically significant. The above analysis method was created by the R software v4.0.3 package ggplot2 (v.3.3.5). The survival analysis results were verified by the Kaplan-Meier plotter (https://kmplot.com/) (24), the microarray database included caBIG, GEO, and TCGA. We obtained KM survival plots with hazard ratios and log-rank p values by univariate Cox regression analysis. For prognostic models of prognosis-related genes and clinical factors, univariate and multivariate Cox proportional hazards analyses were first performed, with risk scores including age, gender, pTNM stage of the tumor, and expression levels of prognosis-related genes. Based on the univariate and multivariate Cox regression analysis results, variables with significant differences in prognosis were extracted to construct a nomogram and predict the 1-year, 3-year, and 5-year survival rates of NSCLC patients. The above analysis was created using the R software v4.0.3 packages forestplot (v2.0.0) and rms (v6.2-0).

cBioPortal database

The portal (https://www.cbioportal.org/) simplifies molecular profiling data from cancer tissues and cell lines into easily understood genetic, epigenetic, gene expression and proteomics events. It contains large cancer genomics datasets and has functions such as visualization, download and analysis (25). Based on the TCGA database, we analyzed 586 lung adenocarcinoma samples (TCGA, Firehose Legacy) and 511 squamous cell lung cancer samples (TCGA, Firehose Legacy) obtained from cBioPortal. mRNA expression z-scores (RNA Seq V2 RSEM) enter a z-score threshold ± 2.0, and protein expression z-scores (RPPA) enter a z-score threshold ± 2.0. Pearson's correlation coefficient and p value were obtained by the "Co-expression" module, and the correlation heatmap between genes was constructed using the R software v4.0.3 package pheatmap (v1.0.12).

Gene ontology (GO) and Kyoto encyclopedia of genes and genomes (KEGG) analysis

GO enrichment analysis examined the function of the WNT gene family from three levels: Biology Process, Molecular Function, and Cellular Component. KEGG is then used for pathway analysis. Histogram is implemented by R software v4.0.3 package clusterprofiler (v3.18.1) (26), the threshold is set as follows: p value cut-off of 0.05, q value cut-off of 0.05, minGSSize = 5, maxGSSize = 5000, The p value correction method uses Benjamini-Hochberg (BH). Protein-protein interaction (PPI) networks were constructed by STRING and Cytoscape. STRING database (https://string-db.org/) is designed to collect, score, and integrate all publicly available sources of

protein-protein interaction information, supplemented by computational predictions (27). We constructed a protein interaction network of WNTs by the "Multipleproteins" function in STRING and performed GO and KEGG analyses.

TRRUST

TRRUST (https://www.grnpedia.org/trrust/) is a TF-target interaction database based on text mining, including 8444 regulatory interactions of 800 transcription factors (TFs) in humans (28). A list of genes is entered on this website to query key TFs.

TISIDB

TISIDB (http://cis.hku.hk/TISIDB/index.php) is a web portal containing multiple heterogeneous data on tumor and immune system interactions (29). We used TISIDB to reveal the relations between the abundance of tumor-infiltrating lymphocytes (TILs) and the expression of WNTs.

Lung tissue samples

During January and March 2022, we collected 20 pairs of NSCLC tissues and adjacent normal tissues from the Third Xiangya Hospital of Central South University. These tissues were used to detect the expression levels of WNTs mRNA by quantitative real-time PCR (qRT-PCR). The Ethics Committee of the Third Xiangya Hospital of Central South University has approved the study. The approval number is I-22054.

Cell culture

Human normal lung epithelial cell line (BEAS-2B), LUAD cell line (PC9) and LUSC cell line (NCI-H520) were obtained from American Type Culture Collection (ATCC) (Manassas, VA, USA). All cell lines were cultured in DMEM (Gibco, Carlsbad, CA) supplemented with 10% FBS (Gibco) and 1% pen/strep (Gibco) at 5% CO_2 and 37°C.

Quantitative real-time PCR (qRT-PCR)

According to the manufacturer's instructions, total RNA was isolated from tissues or cells using Trizol reagent (TaKaRa, Japan). One microgram of RNA was reverse transcribed into cDNA using the Revert Aid First Strand cDNA Synthesis Kit (Thermo, USA). Quantitative RT-PCR was then performed with Pro Taq HS Premix Probe qPCR Kit (Accurate, Hunan, China). The amplification program consisted of one cycle of predenaturation at 95°C for 5 min, 37 cycles of denaturation at 95°C for 30 s, annealing at 61°C for 30 s, and extension at 72°C for 10 min. The GAPDH gene was used as an endogenous control gene for normalizing the expression of target genes. Each sample was analyzed in triplicate. Primer sequences are shown in **Supplementary Table S1**.

Western blot

RIPA lysis buffer (Thermo Fisher Scientific, USA) containing protease and phosphatase inhibitors was used to lyse tissues. Protein lysates were separated by SDS-PAGE gels (Thermo Fisher Scientific, USA), blotted onto PVDF membrane (Roche, Switzerland) for analysis and incubated at 4°C overnight with the following primary antibodies: anti-WNT2B antibody (1:1000 dilution; Bioss, China), anti-WNT7A antibody (1:1000 dilution; Bioss, China), and anti-GAPDH antibody (1:2000 dilution; Cell Signaling Technology, USA). The results of the western blot analyses were performed with Image J software.

Immunohistochemical staining

Immunohistochemistry was performed in 20 NSCLC tissues and adjacent normal tissues. Paraffin-embedded sections were stained to determine the expression level of proteins. Sections were incubated overnight at 4°C with anti-WNT2B antibody (1:100 dilution; Bioss, China), or anti-WNT7A antibody (1:100 dilution; Bioss, China). After washing with phosphate-buffered saline (PBS), the slides were incubated with a goat anti-rabbit IgG secondary antibody conjugated to fluorescein isothiocyanate (ZSDB-BIO, China) for 30 mins. They were washed with PBS and then incubated with an antifade reagent (Invitrogen, USA). Finally, staining was observed using an Olympus CX41 fluorescence microscope (Olympus, Japan). The results of the analyses were performed with Image J software.

Results

mRNA transcription and methylation levels of the WNT gene family in LUAD and LUSC

Members of the WNT gene family and their respective specific chromosomal regions are presented in **Table 1**. We first examined the mRNA transcription of 19 WNT genes in lung cancer by the ONCOMINE database, as can be seen from **Figure 1A**. The detailed expression results in lung cancer are shown in **Table 2**, in which the expression levels of WNT2/2B/3A/7A/11 in lung cancer were significantly lower than those in

TABLE 1 WNT gene family members and chromosome location.

HGNC ID (gene)	Approved symbol	Approved name	Previous symbols	Aliases	Chromosome
HGNC:12774	WNT1	WNT family member 1	INT1		12q13.12
HGNC:12780	WNT2	WNT family member 2	INT1L1	IRP	7q31.2
HGNC:12781	WNT2B	WNT family member 2B	WNT13	XWNT2	1p13.2
HGNC:12782	WNT3	WNT family member 3	INT4	MGC131950,MGC138321,MGC138323	17q21.31-q21.32
HGNC:15983	WNT3A	WNT family member 3A			1q42.13
HGNC:12783	WNT4	WNT family member 4		WNT-4	1p36.12
HGNC:12784	WNT5A	WNT family member 5A		hWNT5A	3p14.3
HGNC:16265	WNT5B	WNT family member 5B			12p13.33
HGNC:12785	WNT6	WNT family member 6			2q35
HGNC:12786	WNT7A	WNT family member 7A		WNT-7A	3p25.1
HGNC:12787	WNT7B	WNT family member 7B			22q13.31
HGNC:12788	WNT8A	WNT family member 8A		WNT8D	5q31.2
HGNC:12789	WNT8B	WNT family member 8B			10q24.31
HGNC:12778	WNT9A	WNT family member 9A	WNT14		1q42.13
HGNC:12779	WNT9B	WNT family member 9B	WNT15	WNT14B	17q21.32
HGNC:13829	WNT10A	WNT family member 10A			2q35
HGNC:12775	WNT10B	WNT family member 10B		WNT-12,SHFM6	12q13.12
HGNC:12776	WNT11	WNT family member 11			11q13.5
HGNC:16267	WNT16	WNT family member 16			7q31.31

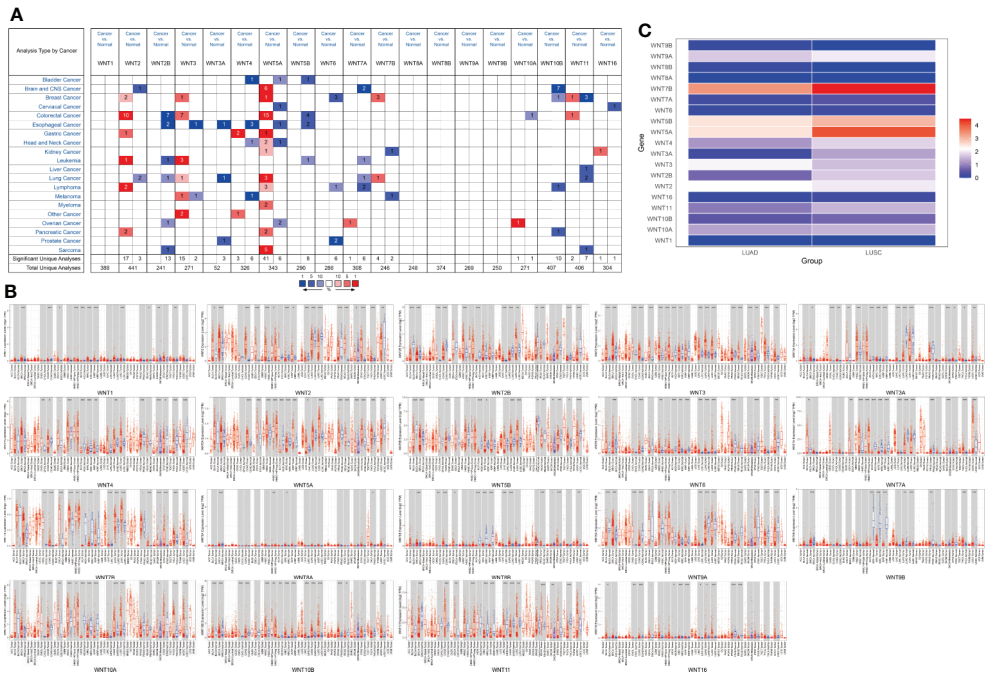

FIGURE 1
The mRNA transcription levels of the WNT gene family in LUAD and LUSC. **(A)** The mRNA transcription levels of WNT gene family in lung cancer (ONCOMINE). Red for overexpression, blue for downregulated expression. **(B)** Differential expression of WNT gene family in different tumor tissues and normal tissues (TIMER). Statistical significance of differential expression was assessed using the Wilcoxon test (*p* value significant codes: 0 ≤ *** < 0.001 ≤ ** < 0.01 ≤ * < 0.05 ≤. < 0.1). **(C)** The expression matrix plots for WNT gene family in LUAD and LUSC. Indicates the relative expression level among WNT genes.

TABLE 2 The significant changes of WNTs mRNA expression in transcription level between different types of Lung cancer.

Gene	Types of lung cancer *vs.* normal	Fold change	*p* value	t-Test	References
WNT2	Lung Adenocarcinoma *vs.* Normal	-2.089	3.63E-5	-4.473	Su Lung Statistics (30)
	Large Cell Lung Carcinoma *vs.* Normal	-3.134	1.53E-8	-8.323	Hou Lung Statistics (31)
WNT2B	Lung Adenocarcinoma *vs.* Normal	-2.063	1.77E-9	-8.935	Okayama Lung Statistics (32)
WNT3	Lung Adenocarcinoma *vs.* Normal	2.581	5.94E-10	9.100	Okayama Lung Statistics (32)
WNT3A	Lung Adenocarcinoma *vs.* Normal	-3.974	4.29E-30	-17.652	Selamat Lung Statistics (33)
WNT5A	Squamous Cell Lung Carcinoma *vs.* Normal	14.130	2.16E-7	6.311	Bhattacharjee Lung Statistics (34)
	Squamous Cell Lung Carcinoma *vs.* Normal	3.729	4.20E-6	6.292	Garber Lung Statistics (35)
	Squamous Cell Lung Carcinoma *vs.* Normal	3.897	4.95E-12	9.815	Hou Lung Statistics (31)
WNT7A	Small Cell Lung Carcinoma *vs.* Normal	-4.772	6.12E-5	-4.754	Bhattacharjee Lung Statistics (34)
WNT7B	Lung Adenocarcinoma *vs.* Normal	3.579	4.25E-14	10.960	Okayama Lung Statistics (32)
WNT11	Lung Adenocarcinoma *vs.* Normal	-2.512	4.12E-5	-4.540	Bhattacharjee Lung Statistics (34)
	Lung Adenocarcinoma *vs.* Normal	-3.138	1.31E-9	-7.752	Okayama Lung Statistics (32)

normal tissues, while those of WNT3/5A/7B expressions were significantly higher, with altered expression levels of WNT5A and WNT7A in LUSC and the others are in LUAD.

Additionally, we used TIMER to assess differences in expression levels of the WNT gene family in various cancers and normal tissues. As shown in **Figure 1B**, in LUAD, WNT3/5B/6/7B/8B/10A/10B/16 expressions significantly increased, WNT2/2B/3A/4/7A/9A/9B/11 expressions significantly decreased, and the results of WNT1 and WNT5A presented no statistical significance. In LUSC, the expressions of WNT2B/3/5A/5B/6/7B/10A/10B/16 were significantly promoted, while the expressions of WNT1/2/3A/7A/9A/9B/11 were significantly inhibited; the results of WNT4 and WNT8B were not statistically significant in LUSC, and WNT8A expression showed no statistical significance in LUAD and LUSC. **Figure 1C** showed the relative expression levels of WNT genes in LUAD and LUSC. Among the 19 WNT genes, WNT7B presented the highest relative expression level in LUAD, while the relative expression level of WNT5A/5B/7B was higher in LUSC than in LUAD, consistent with the above expression results.

Moreover, UALCAN was used to explore the expression differences of the WNT gene family in normal tissues and in LUAD and LUSC, with the results shown in **Figure 2A**. In LUAD, the expression of WNT2/2B/3A/4/7A/9A/9B/11 was lower than that in normal tissues, while the expressions of WNT1/3/5B/6/7B/8B/10A/10B/16 were higher than that in normal tissues, presenting statistical significance; WNT5A and WNT8A results were not statistically significant; WNT2/3A/7A/11 were less expressed in LUSC than in normal tissues, while WNT2B/3/4/5A/5B/6/7B/8B/10A/10B/16 showed the opposite circumstance with statistical significance; WNT1/8A/9A/9B expressions were not statistically significant in LUSC. In summary, according to the comparison between databases, LUAD represented lessened WNT2/2B/3A/4/7A/9A/9B/11 expressions and enhanced WNT3/5B/6/7B/8B/10A/10B/16 expressions compared with normal tissues; in contrast, LUSC presented prohibited WNT2/3A/7A/11 expressions and promoted WNT2B/3/5A/5B/6/7B/10A/10B/16 expressions.

In addition, UALCAN was employed to explore the methylation levels of WNTs in LUAD and LUSC, with the results depicted in **Figure 2B**. In both LUAD and LUSC, the methylation levels of WNT1/2/2B/3/3A/6/7A/9B/10A/10B/16 were significantly improved, while those of WNT8B and WNT11 were significantly diminished. For WNT8A and WNT9A, their methylation levels were significantly boosted in LUAD but declined in LUSC. The methylation level of WNT5B significantly dropped in LUSC but not in LUAD, and that of WNT7B significantly went up in LUSC but not in LUAD.

Prognostic value of WNTs in patients with LUAD and LUSC

This section first analyzed the correlation between the WNT gene and different pathological stages of LUAD and LUSC. As shown in **Figure 3A**, WNT2, WNT2B, and WNT11 were significantly correlated with pathological stages of LUAD patients, while WNTs presented no statistical significance in the correlation with LUSC (**Figure 3B**), indicating that the mRNA expression of WNT2, WNT2B, and WNT11 was significantly correlated with individual cancer stages of LUAD patients.

Next, data were extracted from The Cancer Genome Atlas (TCGA) dataset (https://portal.gdc.com). Raw counts and corresponding clinical information of RNA sequencing data were obtained from 516 LUAD patients and 501 LUSC patients for survival analysis. The clinical information of corresponding

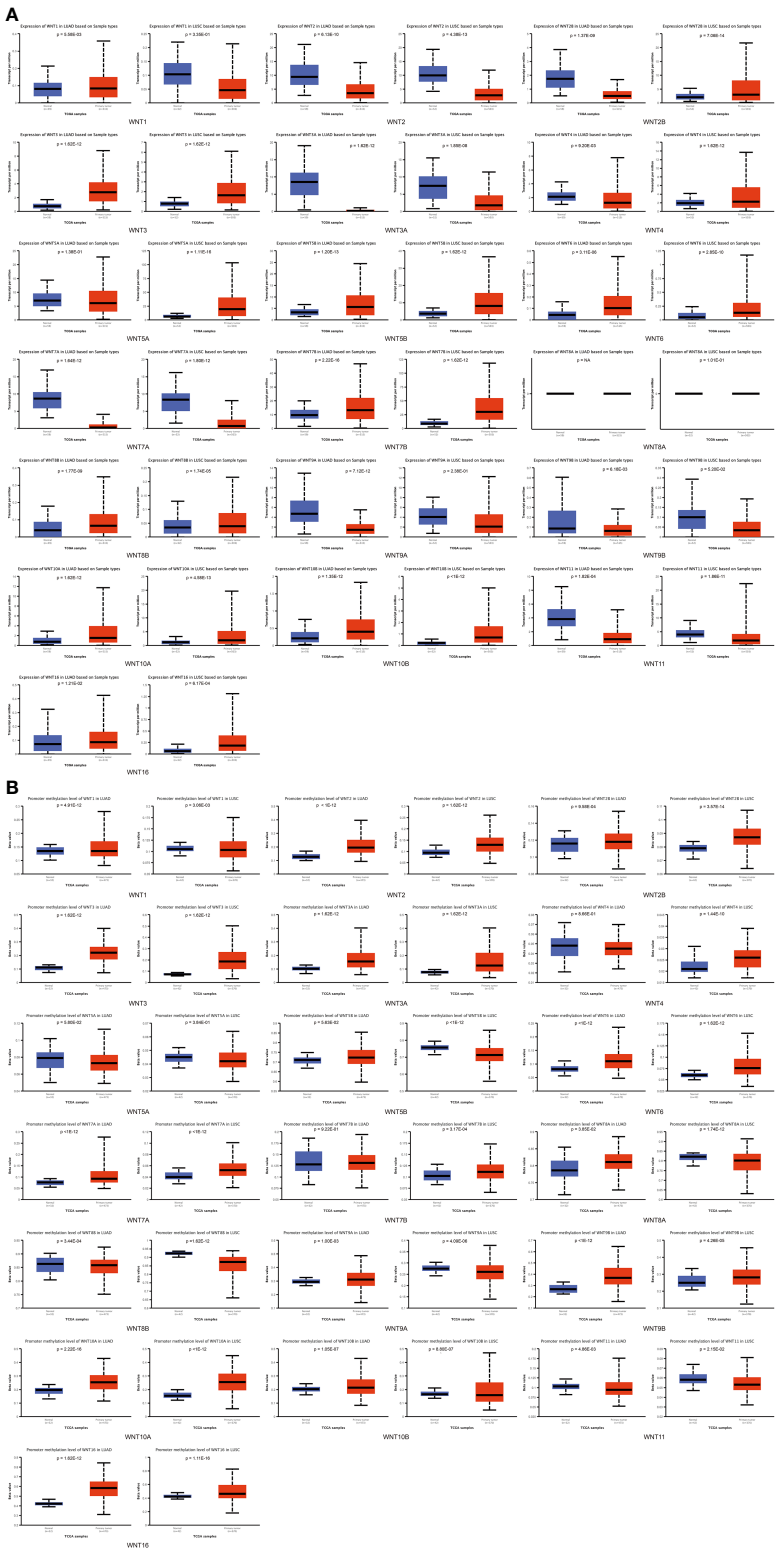

FIGURE 2
Compared with normal tissues, the WNT gene family's mRNA expression and methylation levels in LUAD and LUSC (UALCAN). **(A)** The mRNA transcription levels of the WNT gene family in LUAD and LUSC. **(B)** The methylation level of the WNT gene family in LUAD and LUSC. $p < 0.05$ was considered statistically significant.

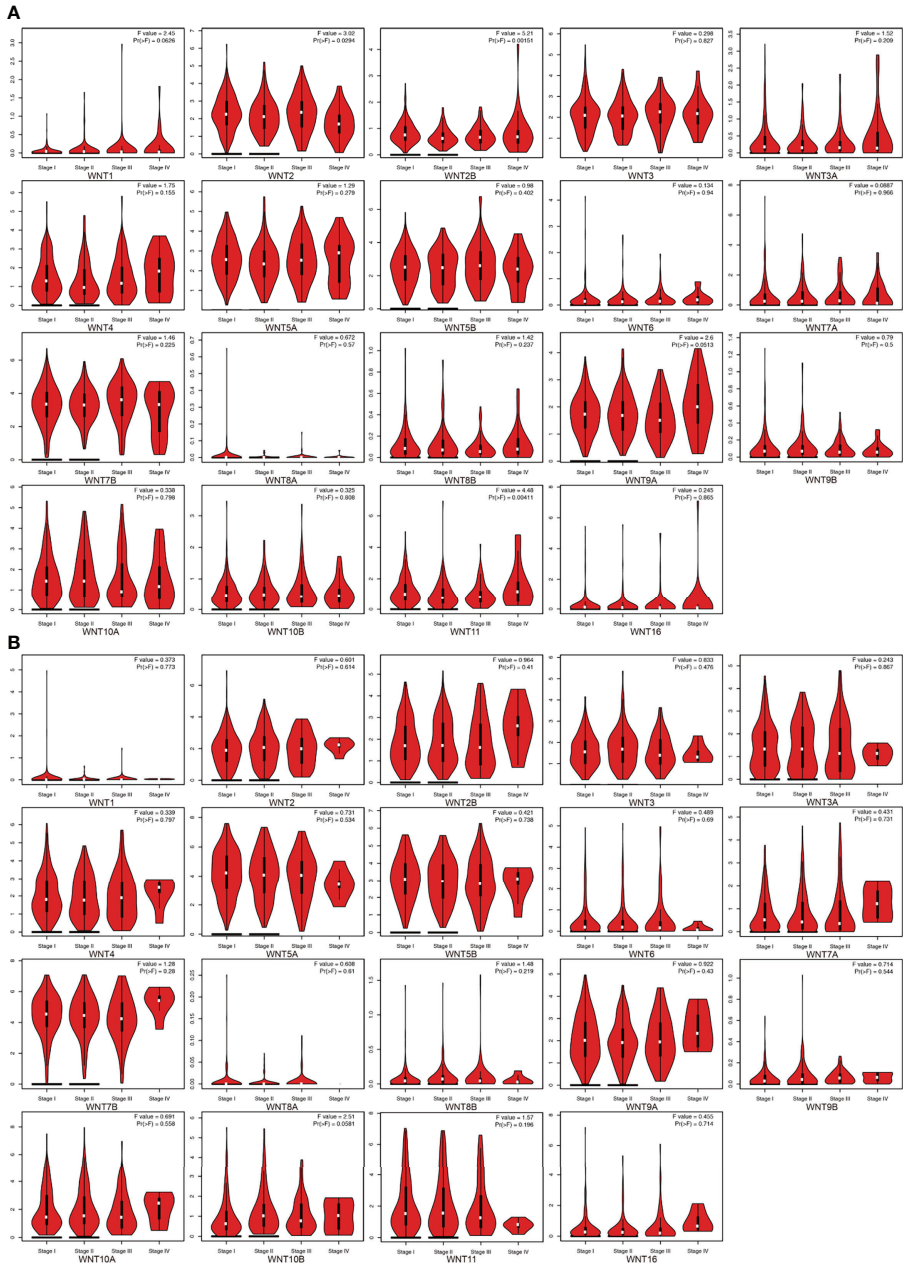

FIGURE 3
The mRNA expression of WNT gene family in different pathological stages of LUAD and LUSC (GEPIA). **(A)** Correlation between WNT gene family and pathological stage in patients with LUAD. **(B)** Correlation between WNT gene family and pathological stage in patients with LUSC.

patients is shown in Supplementary Table S2. Figures 4A, B showed the overall survival (OS) curves in LUAD and LUSC. In LUAD patients, higher WNT2B expression and lower WNT7A expression were associated with a better prognosis. Similarly, higher expression of WNT2B and WNT8B and lower expression of WNT7A predicted better prognostic outcomes in LUSC patients. In addition, WNT8A expression was zero in more than half of the samples of LUAD and LUSC, which was thus not presented in this section. Then, the survival outcomes of WNTs in NSCLC were validated by the Kaplan-Meier plotter (Supplementary Figure 1), and higher WNT2B expression and lower WNT7A expression were associated with better prognostic outcomes in LUAD and LUSC, compatible with our results in TCGA. However, the results

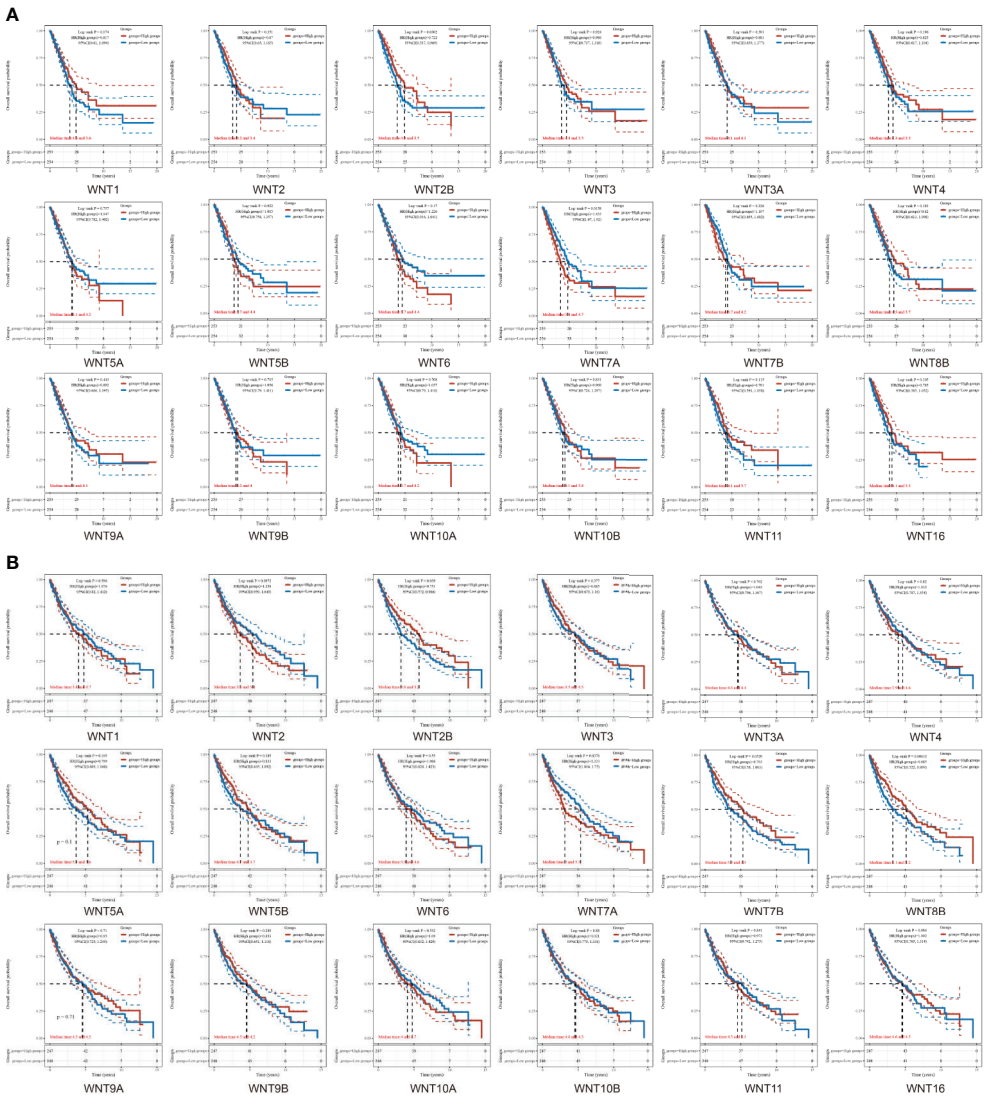

FIGURE 4
The overall survival (OS) curves of WNTs in LUAD and LUSC. **(A)** Kaplan-Meier survival analysis of WNTs in LUAD. **(B)** Kaplan-Meier survival analysis of WNTs in LUSC.

of WNT8B in LUSC were not significant, and thus WNT2B and WNT7A in LUAD and LUSC were selected for further analysis.

For the prognosis-related genes obtained from the survival analysis, a prognostic model was constructed (Figures 5A-H) to explore their clinical impact on the disease process of patients. For the univariate (Figure 5A) and multivariate (Figure 5B) analysis of LUAD, WNT7A and pTNM stage were significantly different variables; in contrast, WNT7A was not statistically significant for the prediction of the LUAD process (Figure 5C). The univariate (Figure 5E) and multivariate (Figure 5F) analyses of LUSC indicated that WNT7A, WNT2B, and pTNM stage were significantly different variables. Figure 5G illustrated that WNT7A and WNT2B were statistically significant in predicting the LUSC process. Taken together, our results showed that WNT2B and WNT7A might have prognostic value in LUAD, and both of them might be independent prognostic factors for LUSC patients.

Genetic alterations and association analysis of the WNT gene family in LUAD and LUSC patients

Through the cBioPortal online tool, we obtained the LUAD (TCGA, Firehose Legacy, http://gdac.broadinstitute.org/runs/

10.3389/fonc.2022.911316

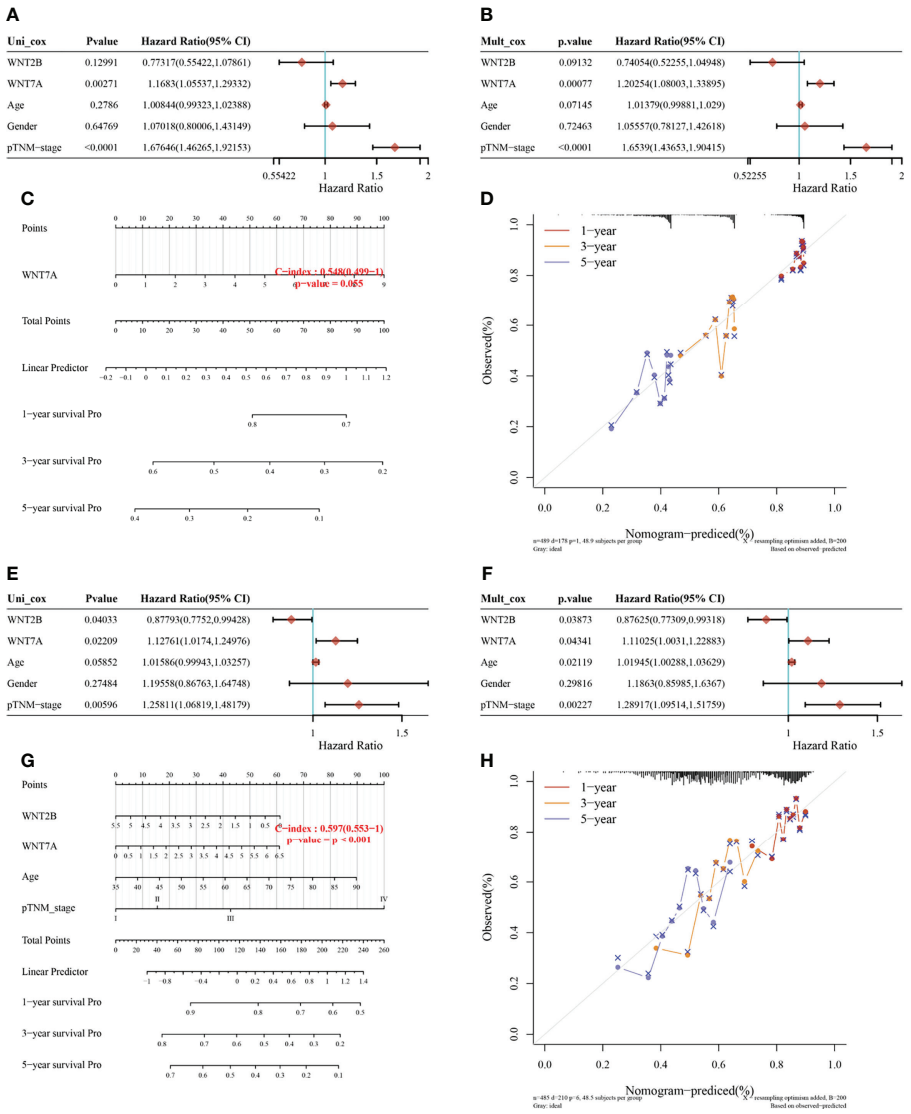

FIGURE 5
Univariate and multivariate Cox regression analysis of WNT gene expression and clinical characteristics and the nomogram predicting 1-y, 3-y, and 5-y survival in patients with LUAD and LUSC. **(A, B, E, F)** Hazard ratio and *p* value of constituents involved in univariate and multivariate Cox regression in LUAD **(A, B)** and LUSC **(E, F)**. **(C, G)** Nomogram to predict the 1-y, 3-y and 5-y overall survival of LUAD **(C)** and LUSC **(G)** patients. **(D, H)** Calibration curve for the overall survival nomogram model in the discovery group. The dashed diagonal line represents the ideal nomogram, and the red, orange and blue represent the 1-y, 3-y and 5-y observed nomograms. **(D)** for LUAD. **(H)** for LUSC.

stddata__2016_01_28/data/LUAD/20160128/) and the LUSC (TCGA, Firehose Legacy, http://gdac.broadinstitute.org/runs/stddata__2016_01_28/data/LUSC/20160128/) datasets from TCGA to analyze the genetic alterations and associations of WNT genes in NSCLC patients. As shown in **Figures 6A, B**, the WNT gene family represented different degrees of mutations in LUAD and LUSC. The mutation rate of WNT9A was the highest (11%) in LUAD (**Figure 6A**), while that of WNT5B was the highest (10%) in LUSC (**Figure 6B**). mRNA High and mRNA Low were the most common genetic changes in LUAD and LUSC.

In addition, Pearson's correlation coefficients of relevant genes were obtained by the analysis of mRNA expression (RNA Seq V2 RSEM) samples (**Figures 6C, D**) and visualized by R software. A moderate correlation was observed between WNT1 and WNT10B (*p* value = 2.07e-40) in LUAD (**Figure 6C**), as well as between WNT4 and WNT10A (*p* value = 8.53e-25), WNT5A and WNT11 (*p* value = 5.96e-

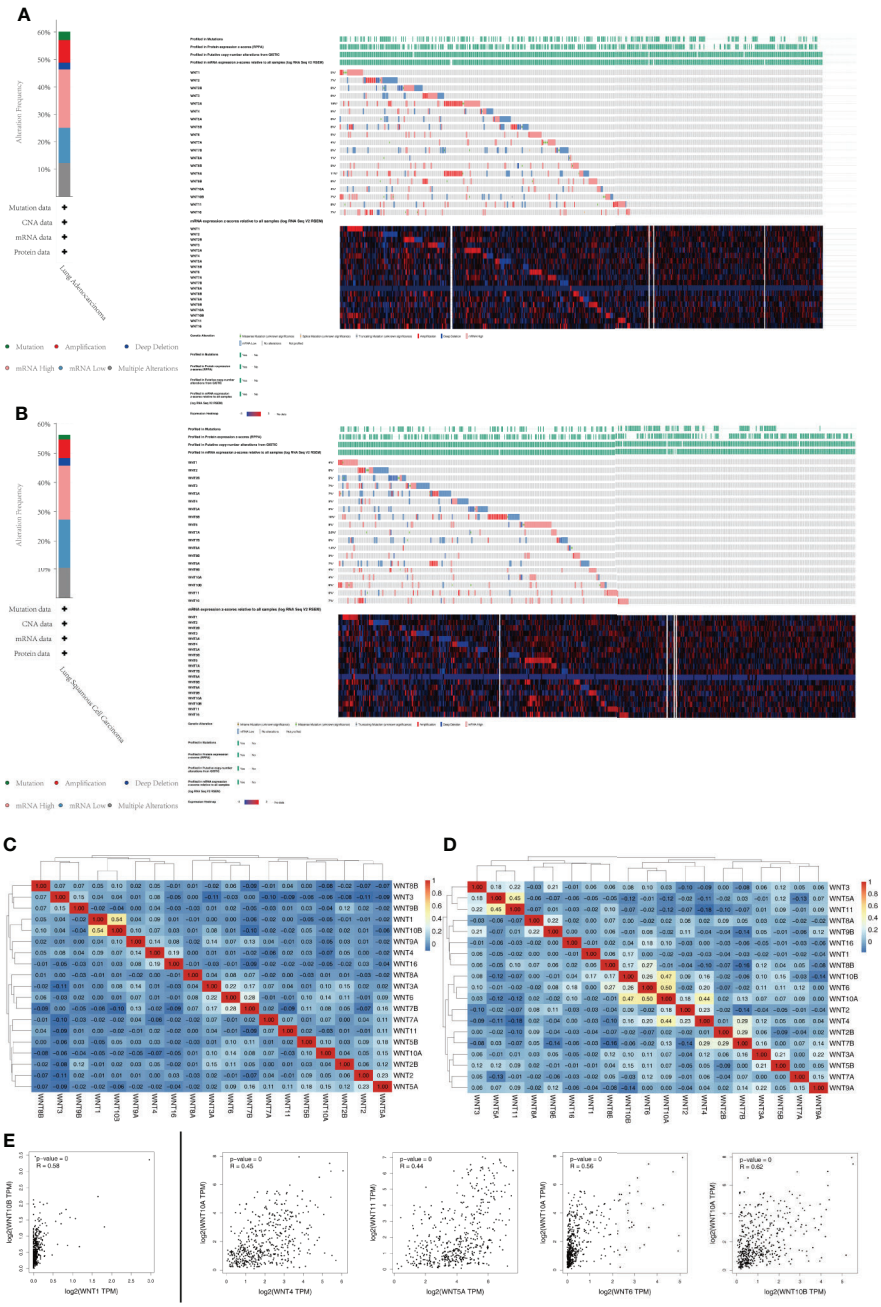

FIGURE 6
Genetic alterations and association analysis of the WNT gene family in NSCLC patients. **(A)** Genetic alterations of the WNT Gene Family in LUAD (cBioPortal). **(B)** Genetic alterations of the WNT Gene Family in LUSC (cBioPortal). **(C, D)** Correlation analysis heatmap between different WNT genes in LUAD **(C)** and LUSC **(D)**. **(E)** Correlation analysis between different WNT genes (GEPIA).

26), WNT6 and WNT10A (p value = 1.99e-32), and WNT10A and WNT10B (p value = 3.81e-29) in LUSC (Figure 6D). A total of 19 members of the WNT gene family were analyzed by the Correlation Analysis module of GEPIA, and similar correlation expression results were obtained, as shown in Figure 6E. In LUAD, WNT1 was moderately correlated with WNT10B (R = 0.58, p value = 0). However, In LUSC, moderate correlation was observed between WNT4 and WNT10A (R = 0.45, p value = 0), WNT5A and WNT11 (R = 0.44, p value = 0), and WNT6 and WNT10A (R = 0.56, p value = 0); moreover, a strong correlation

was observed between WNT10A and WNT10B (R = 0.62, p value = 0).

Functional enrichment and pathway analysis of the WNT gene family

To further predict the functional role of the WNT gene family, we performed GO enrichment and KEGG pathway analysis of WNT gene family members with differential expression. Figure 7A showed that, in Biological Process, WNT genes were mainly enriched in canonical WNT signaling pathway, cellular response to retinoic acid, pattern specification process, regulation of animal organ morphogenesis, regionalization, immune system development, developmental induction, cell fate commitment, positive regulation of myeloid leukocyte cytokine production involved in immune response, etc. In the part of Molecular Function (Figure 7B), WNTs were mainly enriched in signaling receptor binding, molecular function regulator, receptor regulator activity, receptor ligand activity, G protein-coupled receptor binding, Fzd binding, protein domain specific binding, cytokine activity, regulatory region nucleic acid binding, co-receptor binding, etc. Additionally, WNT genes in Cellular Component (Figure 7C) were mainly enriched in extracellular region, Golgi apparatus part, vesicle membrane, cytoplasmic vesicle membrane, endoplasmic reticulum lumen, endocytic vesicle, endocytic vesicle membrane, Golgi lumen, collagen-containing extracellular matrix, WNT signalosome, etc. Subsequently, KEGG pathway enrichment analysis (Figure 7D) identified that WNT genes were mainly enriched in Signaling pathways regulating pluripotency of stem cells, mTOR signaling pathway, Hippo signaling pathway, WNT signaling pathway, Basal cell carcinoma, Breast cancer, Gastric cancer, Cushing syndrome, Hepatocellular carcinoma, melanogenesis, etc.

The PPI network analysis graph was constructed by STRING (Figure 7E) and Cytoscape (Figure 7F). STRING contained 19 nodes and 171 edges, PPI enrichment p value < 1.0e-16. As can be seen in Figure 7F, members of the WNT gene family had a close relationship with the Fzd receptor family, lipoprotein receptor-related protein (LRP) family, secreted Fzd-related proteins (SFRPs), and WNT inhibitory protein (WIF) family. Taken together, the functional enrichment and pathway analysis results for WNTs were as we know. The biological functions of

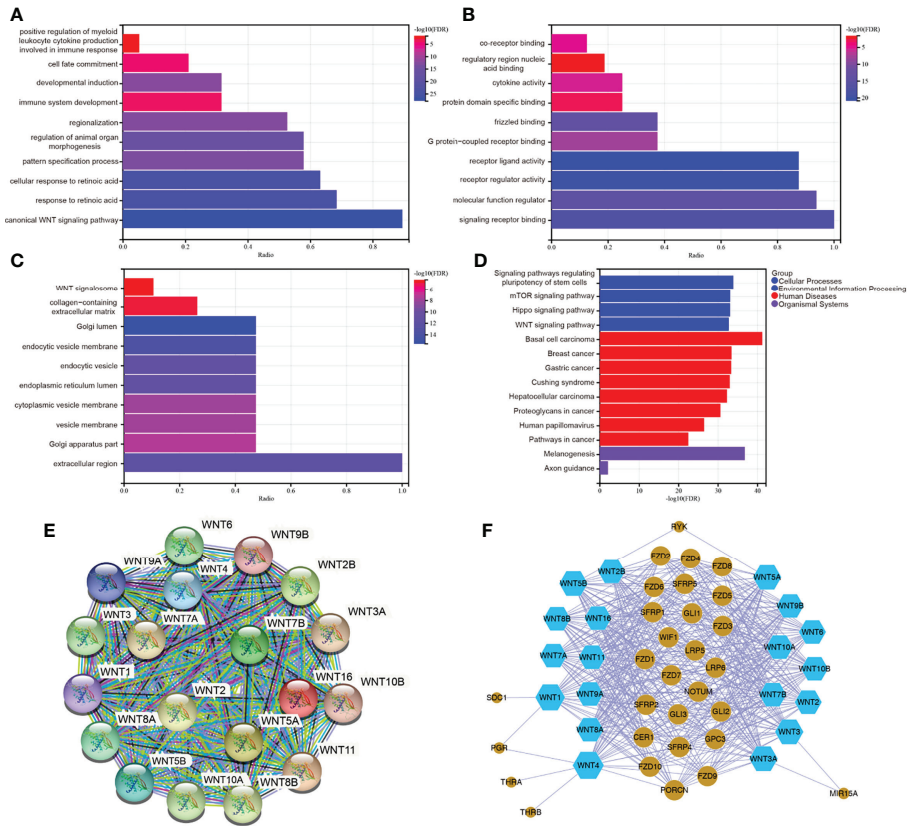

FIGURE 7
(A–D) GO and KEGG enrichment analysis of WNT gene family. **(E, F)** Protein-protein interaction network of WNT gene family. **(E)** for STRING. **(F)** for Cytoscape.

the WNT gene family were mainly related to the canonical and non-canonical WNT signaling pathways, G-protein-coupled receptor binding, immune system development, and partial regulation of immune response.

Transcription factor analysis of the WNT gene family in LUAD and LUSC patients

Compared with that of normal tissues, the transcriptional expression of WNTs was significantly altered in both LUAD and LUSC patients. Since transcription factors were involved in the human transcription initiation, we used the TRRUST database to explore the key transcription factors of WNT genes in humans. Among 19 WNT genes, WNT2, WNT2B, WNT3, WNT3A, WNT4, WNT5A, WNT7B, and WNT11 were included in the TRRUST database. We found that PITX2 was a key transcription factor associated with WNT gene regulation (**Table 3**).

Analysis of WNT gene family immune infiltration in LUAD and LUSC

Through the TIMER database, we explored the correlation between the WNT gene and immune cell infiltration (**Figure 8**). In LUAD, WNT2, WNT9B, and WNT10A represented a significantly positive correlation with six immune cells, including B cell, CD4+ T cell, CD8+ T cell, dendritic cell, macrophage, and neutrophil; WNT3 and WNT8B were positively correlated with tumor purity, while WNT1/2/2B/6/7A/7B/9A/9B/10A/10B/16 were negatively correlated with tumor purity. In LUSC, WNT1, WNT2, WNT7B, and WNT9B were significantly correlated with six immune cells, among which WNT1, WNT2, and WNT9B were positively correlated, and WNT7B was negatively correlated. However, the effect of WNTs on tumor purity in LUSC was slightly poorer than that in LUAD, and WNT3/5A/8B/11 were positively correlated with tumor purity, while WNT1/2/4/6/7A/98/10A were negatively correlated with tumor purity. For WNT2B and WNT7A, which might have prognostic value in LUAD and LUSC, as can be seen, in LUAD, WNT2B was positively correlated with all immune infiltration cells except CD8+ T cell; WNT7A was positively correlated with CD4+ T cell, macrophage, neutrophil and dendritic cell. In LUSC, WNT2B was negatively correlated with CD8+ T cell, neutrophil and dendritic cell; WNT7A was significantly correlated with B cell, CD4+ T cell and macrophage, among which CD4+ T cell and macrophage were positively correlated, and B cell was negatively correlated. Subsequently, we validated the association of WNT2B and WNT7A with immune cell infiltration by the TISIDB database. **Figures 9A, C** represented the relationship between WNT2B and WNT7A and tumor-infiltrating lymphocytes (TILs) in different cancer types. **Figure 9B** showed that, in LUAD and LUSC, except for CD4+ T cell and neutrophil, the correlation between WNT2B and other TILs infiltration levels was the same as the results obtained in TIMER. Similarly, **Figure 9D** represented that except for CD4+ T cell and B cell, the correlation between WNT7A and other TILs infiltration levels was the same as the results obtained in TIMER. Additionally, based on the dataset containing mRNA sequence data from TCGA, we constructed a heatmap of the correlation between WNTs and immune scores (**Supplementary Figure 2**), as well as a lollipop chart (**Supplementary Figure 3**) implemented by the ssGSEA algorithm to show the correlation between WNT2B and WNT7A and the level of immune cell infiltration, and these results are generally compatible with ours. Next, using a Cox proportional hazards model in TIMER, we explored the clinical relevance of WNTs with LUAD and LUSC tumor immunity, with the results shown in **Tables 4** and **5**. As can be seen, B cell ($p < 0.001$), WNT2B ($p < 0.05$), WNT3A ($p < 0.05$), WNT6 ($p < 0.05$) and WNT7A ($p < 0.05$) were significantly associated with clinical outcomes in LUAD (**Table 4**) but not in LUSC (**Table 5**).

Moreover, for the 19 genes of WNTs, we compared the tumor infiltration level with different degrees of somatic copy number alterations (SCNA) in LUAD and LUSC patients, with the results illustrated in **Figure 10**. We found that all significant copy number change types appeared in arm-level deletion, arm-level gain, deep deletion, and high amplification. In LUAD, WNT7B and WNT8A were significantly correlated with deep deletion and arm-level deletion of six immune cells, respectively, and WNT3A and WNT9A were significantly correlated with high amplification of six immune cells. In LUSC, WNT4, WNT5A, WNT7A, and WNT8B were significantly correlated with arm-level deletion of six immune cells; WNT3 and WNT9B were significantly correlated with the arm-level gain of six immune cells; WNT7B was significantly correlated with high amplification of six immune cells. For WNT2B and WNT7A, WNT2B is significantly correlated with arm-level deletion of CD8+ T Cell, CD4+ T cell, macrophage, neutrophil and dendritic cell in LUAD; in LUSC, WNT2B showed a significant correlation with CNA levels in all immune cells except for CD8+ T cells. Similarly, WNT7A showed a

TABLE 3 The key regulated factor of WNT genes in human.

Key TF	Description	List of overlapped genes	*p* value	Q value
PITX2	paired-like homeodomain 2	WNT2, WNT5A (36)	5.25E-05	5.25E-05

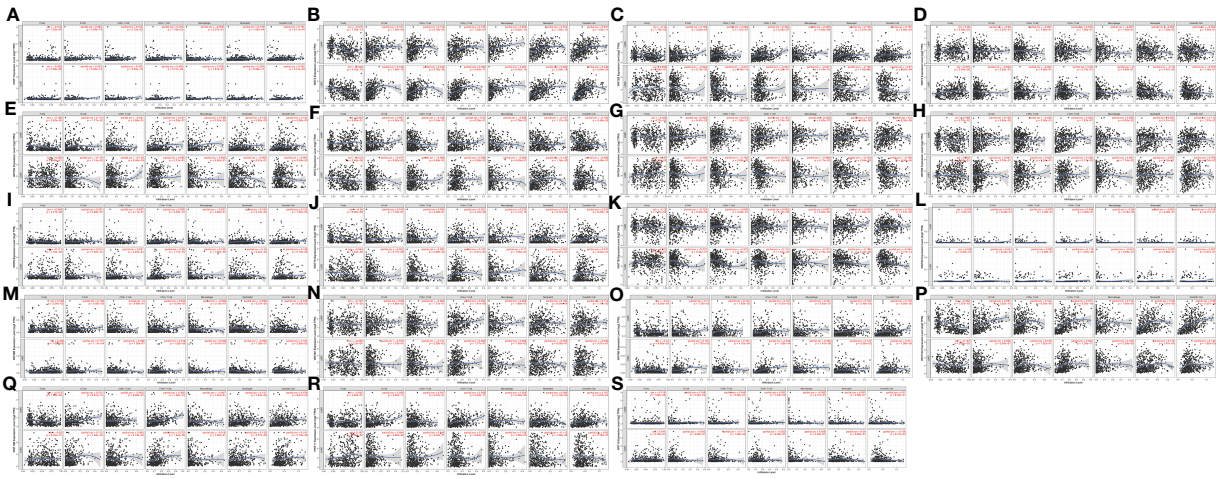

FIGURE 8
Correlation of WNT genes with immune cell infiltration in LUAD and LUSC (TIMER). **(A)** WNT1. **(B)** WNT2. **(C)** WNT2B. **(D)** WNT3. **(E)** WNT3A. **(F)** WNT4. **(G)** WNT5A. **(H)** WNT5B. **(I)** WNT6. **(J)** WNT7A. **(K)** WNT7B. **(L)** WNT8A. **(M)** WNT8B. **(N)** WNT9A. **(O)** WNT9B. **(P)** WNT10A. **(Q)** WNT10B. **(R)** WNT11. **(S)** WNT16.

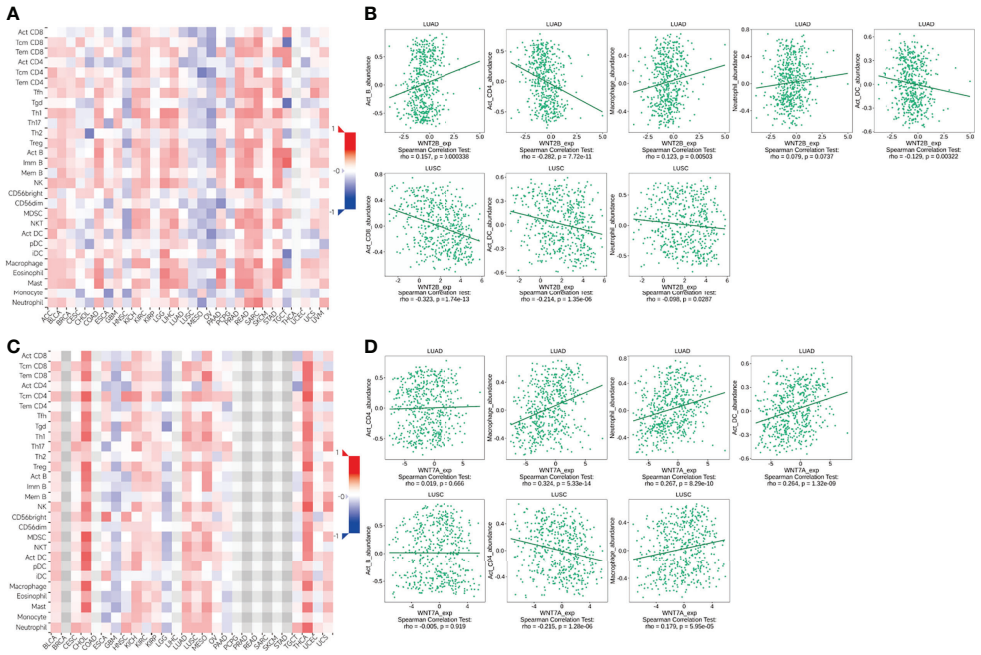

FIGURE 9
The association of WNT2B and WNT7A with immune cell infiltration (TISIDB). **(A, C)** The landscape of relationship between WNT2B **(A)** and WNT7A **(C)** expression and TILs in different types of cancer (red is positive correlated and blue is negative correlated). **(B)** Relationship between WNT2B and immune infiltration levels of B cell, CD4+ T cell, macrophage, neutrophil, dendritic cell in LUAD, and CD8+ T cell, neutrophil, dendritic cell in LUSC. **(D)** Relationship between WNT7A and immune infiltration levels of CD4+ T cells, macrophage, neutrophil, dendritic cell in LUAD, and B cell, CD4+ T cell, macrophage in LUSC.

TABLE 4 The Cox proportional hazard model of WNT genes with tumor-infiltrating immune cells in LUAD patients.

	Coef	HR	95%CI_l	95%CI_u	*p* value	Sig
B_cell	-5.084	0.006	0.000	0.099	<0.001	***
CD8_Tcell	0.564	1.758	0.297	10.414	0.534	
CD4_Tcell	2.396	10.976	0.599	201.099	0.106	
Macrophage	-0.007	0.993	0.066	15.018	0.996	
Neutrophil	-1.150	0.317	0.006	16.594	0.569	
Dendritic	-0.420	0.657	0.158	2.731	0.563	
WNT1	0.470	1.600	0.903	2.837	0.108	
WNT2	0.119	1.127	0.940	1.351	0.197	
WNT2B	-0.529	0.589	0.355	0.978	0.041	*
WNT3	-0.080	0.923	0.740	1.151	0.477	
WNT3A	-0.389	0.678	0.483	0.950	0.024	*
WNT4	-0.031	0.970	0.831	1.131	0.694	
WNT5A	-0.050	0.951	0.802	1.129	0.568	
WNT5B	-0.021	0.979	0.851	1.127	0.771	
WNT6	0.441	1.555	1.033	2.342	0.035	*
WNT7A	0.133	1.142	1.002	1.301	0.047	*
WNT7B	0.097	1.102	0.953	1.274	0.192	
WNT8A	-11.301	0.000	0.000	48.751	0.145	
WNT8B	-0.561	0.570	1.442	0.236		
WNT9A	0.060	1.062	0.847	1.332	0.601	
WNT9B	-0.251	0.778	0.252	2.407	0.663	
WNT10A	0.038	1.038	0.890	1.212	0.633	
WNT10B	0.140	1.150	0.762	1.735	0.506	
WNT11	0.030	1.030	0.859	1.236	0.749	
WNT16	-0.126	0.882	0.679	1.146	0.347	

p value significant codes: 0 ≤ *** < 0.001 ≤ ** < 0.01 ≤ * < 0.05 ≤. < 0.1.

significant correlation with CNA levels of all immune cells in LUAD except for CD8+ T Cell; and WNT7A showed a significant correlation with CNA levels of all immune cells in LUSC.

Validation of the mRNA and protein expression levels of WNT2B and WNT7A in LUAD and LUSC

To validate the mRNA expression levels of WNT2B and WNT7A in adjacent normal tissues, LUAD tissues, and LUSC tissues, qRT-PCR was performed (**Figure 11**). The results indicated that the expressions of WNT2B and WNT7A were downregulated in tissue samples from 10 LUAD cases. Moreover, WNT2B expression was upregulated, while WNT7A expression was downregulated in tissue samples from 10 LUSC cases (**Figure 11A**). In addition, compared with normal lung epithelial cell line (BEAS-2B), WNT2B and WNT7A were significantly underexpressed in the LUAD cell line (PC9), WNT2B was significantly highly expressed in the LUSC cell line (NCI-H520), and WNT7A was significantly underexpressed in LUSC cell line (NCI-H520) (**Figure 11B**). These results were consistent with the results of bioinformatics analysis. Next, the protein expression levels of WNT2B and WNT7A were validated by western blot (**Figures 11C–F**) and immunohistochemical staining (**Figures 11G–J**), which were consistent with the mRNA expression levels.

Discussion

At the beginning of this study, we obtain the complete mRNA expression of WNT in LUAD and LUSC through three databases. In LUAD patients, WNT2/2B/3A/4/7A/9A/9B/11 expressions decrease, and WNT3/5B/6/7B/8B/10A/10B/16 expressions increase. In contrast, in LUSC patients, WNT2/3A/7A/11 expressions are decreased, and WNT2B/3/5A/5B/6/7B/10A/10B/16 expressions are increased. As in our findings, WNT2 is overexpressed in NSCLC (37). A higher expression of WNT2 was associated with a worse survival prognosis in some studies (38). In addition, anti-WNT2 antibodies could induce specific apoptosis in NSCLC by inhibiting WNT signaling (37), making anti-WNT2 monoclonal antibodies one of the strategies

TABLE 5 The Cox proportional hazard model of WNT genes with tumor-infiltrating immune cells in LUSC patients.

	Coef	HR	95%CI_l	95%CI_u	*p* value	Sig
B_cell	1.297	3.657	0.305	43.804	0.306	
CD8_Tcell	-1.087	0.337	0.055	2.086	0.242	
CD4_Tcell	0.575	1.777	0.124	25.500	0.672	
Macrophage	0.321	1.378	0.120	15.796	0.796	
Neutrophil	1.162	3.196	0.117	87.541	0.492	
Dendritic	0.244	1.277	0.304	5.360	0.739	
WNT1	0.336	1.399	0.956	2.047	0.084	.
WNT2	-0.003	0.997	0.851	1.166	0.966	
WNT2B	-0.130	0.878	0.764	1.010	0.068	.
WNT3	0.057	1.059	0.848	1.323	0.614	
WNT3A	0.012	1.012	0.877	1.168	0.871	
WNT4	-0.073	0.930	0.800	1.081	0.344	
WNT5A	0.009	1.009	0.896	1.136	0.878	
WNT5B	-0.103	0.902	0.801	1.016	0.088	.
WNT6	-0.049	0.952	0.776	1.169	0.639	
WNT7A	0.103	1.108	0.977	1.257	0.111	
WNT7B	-0.029	0.971	0.842	1.119	0.685	
WNT8A	3.795	44.478	0.026	76678.348	0.318	
WNT8B	-0.229	0.796	0.309	2.051	0.636	
WNT9A	0.022	1.022	0.879	1.189	0.772	
WNT9B	-1.721	0.179	0.032	0.997	0.050	.
WNT10A	0.092	1.096	0.969	1.240	0.146	
WNT10B	-0.015	0.985	0.834	1.163	0.855	
WNT11	0.018	1.018	0.920	1.127	0.728	
WNT16	0.010	1.010	0.848	1.202	0.913	

p value significant codes: 0 ≤ *** < 0.001 ≤ ** < 0.01 ≤ * < 0.05 ≤. < 0.1.

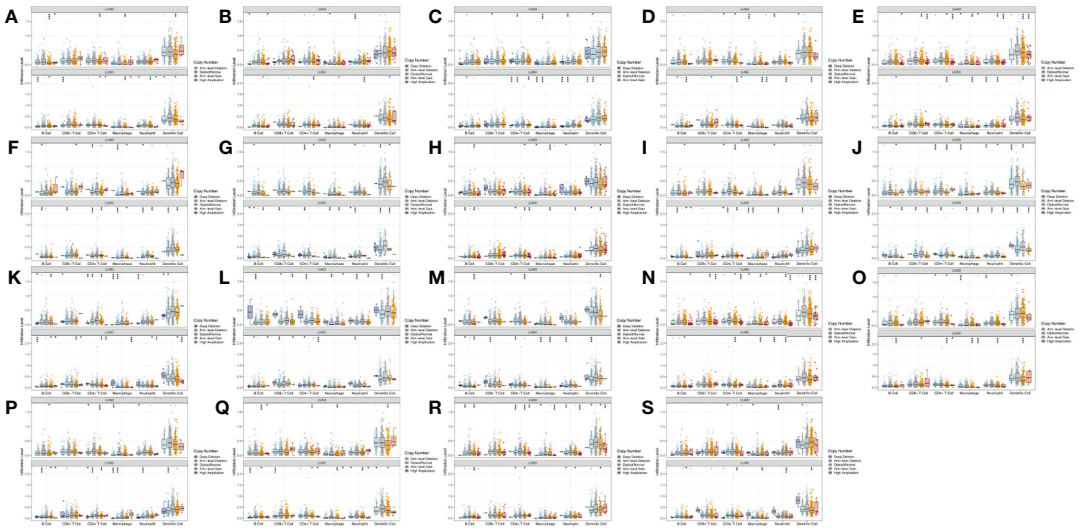

FIGURE 10
Comparison of tumor infiltration levels among tumors with different SCNA for WNTs in LUAD and LUSC samples (*p* value significant codes: 0 ≤ *** < 0.001 ≤ ** < 0.01 ≤ * < 0.05 ≤. < 0.1). **(A)** WNT1. **(B)** WNT2. **(C)** WNT2B. **(D)** WNT3. **(E)** WNT3A. **(F)** WNT4. **(G)** WNT5A. **(H)** WNT5B. **(I)** WNT6. **(J)** WNT7A. **(K)** WNT7B. **(L)** WNT8A. **(M)** WNT8B. **(N)** WNT9A. **(O)** WNT9B. **(P)** WNT10A. **(Q)** WNT10B. **(R)** WNT11. **(S)** WNT16.

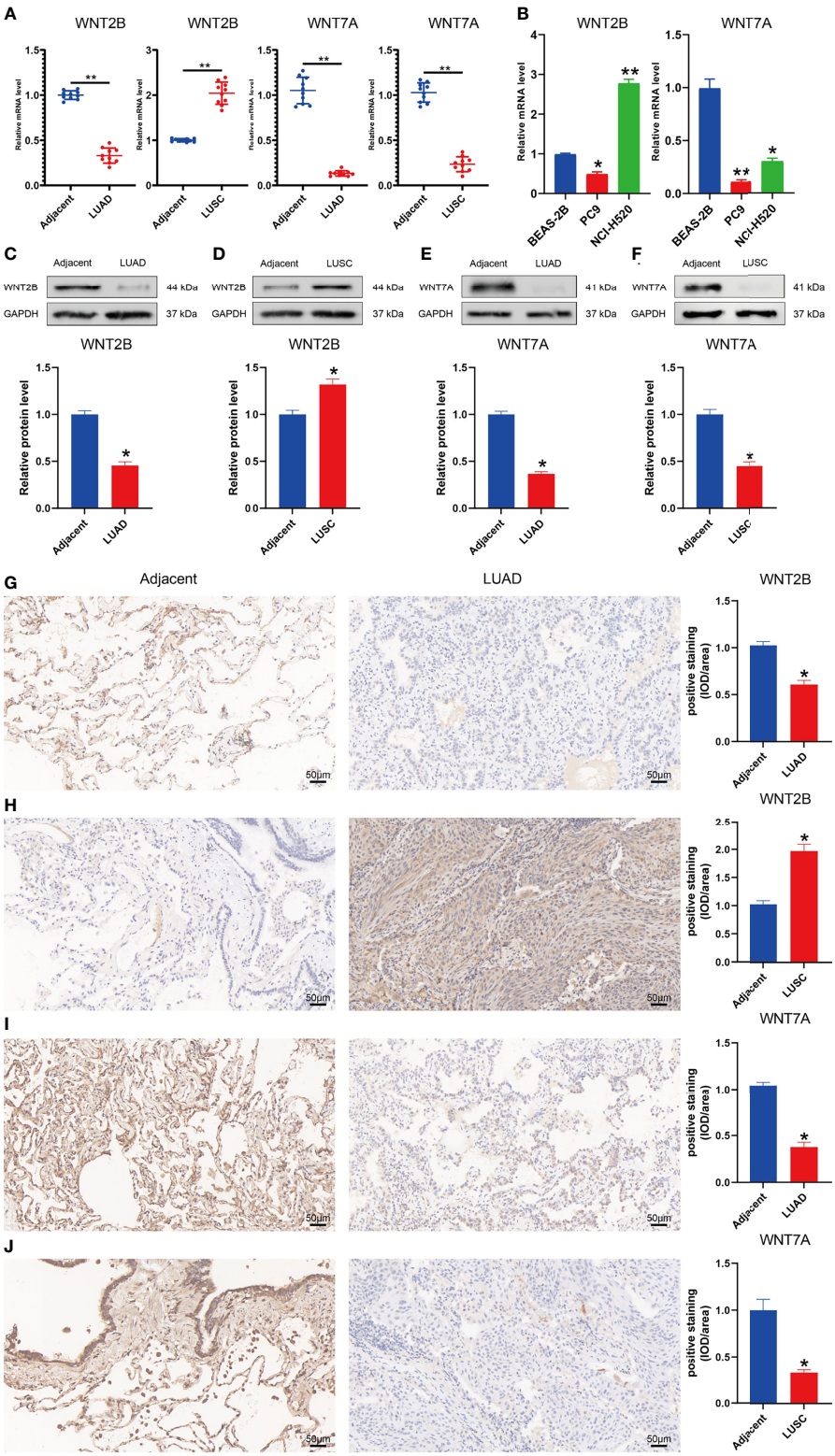

FIGURE 11
Validation of mRNA and protein expression levels of WNT2B and WNT7A in NSCLC. **(A)** Comparison of mRNA expression levels of WNTs in 20 paired NSCLC tissues and adjacent normal tissue samples by qRT-PCR. **(B)** Comparison of mRNA expression levels of WNTs in LUAD cell line (PC9) and LUSC cell line (NCI-H520) with human normal lung epithelial cell line (BEAS-2B). **(C–F)** The western blot analyses. **(G–J)** The immunohistochemical staining in 20 NSCLC tissues and adjacent normal tissues.

for treating lung cancer. Robert A Winn et al. carried out cell experiments and found that the mRNA expression level of WNT7A was significantly reduced in NSCLC cells and primary tumors (39), consistent with our down-regulation found.

In addition, according to the methylation analysis of the UALCAN database, in LUAD, the methylation levels of WNT1/2/2B/3/3A/6/7A/8A/9A/9B/10A/10B/16 are significantly enhanced, while those of WNT8B and WNT11 are significantly reduced; in LUSC, the methylation levels of WNT1/2/2B/3/3A/4/6/7A/7B/9B/10A/10B/16 are significantly promoted, while those of WNT5B/8A/8B/9A/11 are significantly inhibited. Methylation of WNTs has been demonstrated to show a partial correlation with tumor development (40). Tae-Hyung Kim et al. investigated a correlation between WNT7A promoter methylation and loss of E-cadherin expression by detecting WNT7A promoter methylation in NSCLC patients (40). E-cadherin loss was closely related to the poor prognosis and survival of many cancers (41), suggesting that promoter methylation-induced WNT7A loss might be an important prognostic factor in NSCLC. The 3p25 is the chromosome location of the WNT7A (**Table 1**). Cytogenetic analysis reveals that 3p25 is a common genetic deletion site in lung cancer, and similar regions also include 3p21.3 and 3p14-cen (42). The elevated methylation levels of WNT7A may be associated with its loss of expression (43).

In the next prognostic value and survival analysis, we first explore the WNT expression at different pathological stages of LUAD and LUSC patients. With the LUAD development, the WNT2 expression decreases as a whole, reaching the lowest level when the tumor progresses to stage IV; the expression of WNT2B presents no obvious change but tends to decrease with the disease progression, of which a few patients show a sudden rise in the expression in stage IV; WNT11 showed an increase in the expression with the tumor development. The results indicate that WNT2/2B/11 may be able to predict the tumor progression of LUAD patients. Next, we obtain the prognostic outcomes shown by the WNT gene with different degrees of expression in NSCLC patients by KM survival curves, and the survival results are also validated by another open database. In our study, highly expressed WNT2B and lowly expressed WNT7A predict better prognosis in LUAD and LUSC patients. After regression analysis and screening, the prediction results of WNT7A during the LUAD are not significant enough, according to the significant differential results obtained by univariate and multivariate Cox analyses of RNA-seq data from LUAD samples in TCGA. Despite this, we believe that WNT2B and WNT7A may act the important prognostic values in LUAD and LUSC, based on the significant differences shown in KM curves. The nomogram provides some guidance for WNT7A and WNT2B in predicting disease progression and survival in LUSC patients clinically.

WNT7A bound to Fzd9 and promoted epithelial differentiation of NSCLC cells by activating the cJun N-terminal kinases (JNKs) pathway (44). Moreover, the low expression of WNT7A in NSCLC might play a role in lung cancer progression through its effect on E-cadherin transcription (45). WNT7A could also induce hypertrophy of muscle fibers by driving activation of the AKT/mTOR signaling pathway (46). In addition, WNT7A acted as an upstream signaling molecule of the WNT canonical pathway (47). Its overexpression could transcriptionally activate WNT target genes through the WNT/β-catenin signaling pathway, thus leading to cancer development, or it could bind to some WNT receptors to promote the malignant phenotype of cancer (48), partially corroborating our findings. Some studies have suggested that the up-regulated expression of WNT2B promoted the malignant behavior of NSCLC (49, 50). After methodological comparison, we believe that the reason for the difference in the above results with our study may be relevant to the different cell types of NSCLC. That is, the previous studies focus on all NSCLC patients; in contrast, in this study, the prognostic analysis for WNT2B is based on the clinical samples of LUAD and LUSC patients. In addition, in our results, the transcriptional expression of WNT2B is divergent in LUAD and LUSC patients, implying the different roles of WNT2B in tumor progression in LUAD and LUSC. More research is required to explore the lung cancer field where WNT2B is located, which may be a breakthrough point in subsequent studies. WNT8B is one of the typical WNT ligands, transcriptionally regulated by zinc finger transcription factor 191 (ZNF 191) and playing an important role in hepatocellular carcinoma (HCC) proliferation through the canonical WNT pathway (serving as a new prognostic marker for HCC) (51). Few related studies were found on WNT8B in lung cancer, which may provide some directions for future research. It is worth mentioning that in the existing studies, WNT7A and WNT2B played different roles in the prognosis of different cancer types, which may be attributed to their various mechanisms of action in diverse cancer cell lines and the activated signaling pathways. More critically, our study is the first to use clinical samples to link the WNT expression with different cell types in LUAD and LUSC, providing more insights and evidence for the subsequent research of the WNT gene family in the prognosis of LUAD and LUSC patients. We look forward to more subsequent extensive studies of WNTs in different cell types of NSCLC.

Immediately afterward, we explore the WNT gene mutation in LUAD and LUSC by cBioPortal. All WNT genes are detected to show different degrees of mutation, of which mRNA High and mRNA Low are the most common genetic changes in LUAD and LUSC. The mutations presented by WNTs showed significant phenotypes in mice, *Caenorhabditis elegans*, and *Drosophila* (10). Heparin-sulfated forms of proteoglycans (HSPG) were involved in the WNT transport and played a role in stabilizing WNT proteins or assisting their transmission between cells. In *Drosophila*, loss of

HSPG or mutations in genes encoding enzymes that modify them could lead to the generation of phenotypes similar to wingless mutants (9). Since it is associated with the biological role of stem cells (9), WNT pathway mutations are very common in cancer, especially in tissues relying on WNT for self-repair (11). However, mutations in WNT pathway components frequently appeared in colorectal cancer (19, 52). Although some studies have shown that mutations in β-catenin and its pathway components caused downstream activation of WNT signaling in LUAD (53), this mutation was still rare in lung cancer (13, 54). Analysis of RNA-seq and miRNA-seq data from several NSCLC patients suggested that alterations in WNT9A might impact cancer progression by affecting the interference between lncRNAs, miRNAs, and mRNAs (55). WNT5B signaled through the non-canonical WNT signaling pathway, which was usually used as an antagonist of the canonical WNT signaling pathway and played a role in the proliferation, differentiation, and migration of cells (56). Pairwise WNT genes presenting tight links in correlation analysis might play a synergistic or similar role in cancer progression. And both WNT5A and WNT11 act through the non-canonical WNT/calcium signaling pathway. It was found that when the mRNA of WNT5A or WNT11 was injected into one-cell zebrafish embryos, both of the mRNA of WNT5A or WNT11 could double the frequency of calcium transients in the enveloping layer of the blastodisc (57). Similar to WNT11 (58, 59), WNT5A has also been shown to help to inhibit cell migration and invasiveness in cancer cell lines (60).

According to the functional enrichment and pathway analysis results, we can see that WNT genes are highly enriched in WNT signaling pathways, immune system development and Fzd receptor/G protein-coupled receptor binding, etc. These functions are highly correlated with the action mode of the WNT gene family in the body. For example, overexpression of WNT4, WNT5A, and WNT11 has been found to play a role in early embryo development through the non-canonical WNT signaling pathway (57, 61). As an important regulator of cell growth and differentiation, WNT5A has also been demonstrated to participate in the tumor growth inhibition through the non-canonical WNT/calcium signaling pathway (62). WNT11 acted as a non-canonical WNT pathway ligand and similarly activated the WNT/calcium signaling pathway (63). WNT signaling might also serve as an essential regulator of stem cell proliferation or self-renewal selection in the body. For example, WNT3A promoted the self-renewal of hematopoietic stem cells *in vitro* (9). It turned out that there was overexpression of some WNT pathway components and active WNT signaling in most NSCLC (13). Mark Shapiro et al. performed immunoblot analysis on tumor and normal lung tissues from several patients with stage I NSCLC after resection, confirming that activation of the WNT pathway was significantly associated with high tumor recurrence rates (64).

It is well-known that transcription factors play an important role in the transcription process in humans. Therefore, we query key WNT-associated transcription factors in humans. Paired-like homeodomain transcription factor 2 (PITX2) is one of the bicoid/paired-like homeobox gene family, which is located at position 4q25 of the chromosome and is a transcription factor involved in the anterior structure development (65). PITX2 could promote cancer progression by activating the WNT gene and regulating the WNT/β-catenin pathway (36). In addition, PITX2 was also found to be a target gene of LEF1 (66). During WNT/β-catenin pathway regulation, PITX2 could activate specific growth regulatory genes, such as cyclin D1, cyclin D2 and c-Myc Kioussi (67). Jing Luo et al. investigated the involvement of PITX2 in the WNT/β-catenin pathway in LUAD, showing that PITX2 was a potential up-regulated oncogene in LUAD, and PITX2 was overexpressed in LUAD and relevant to poor prognosis. They also found that PITX2 could activate the WNT/β-catenin pathway by enhancing WNT3A transcription, thereby exerting an oncogenic effect (68).

After this, we explore the association between the WNT gene family and six immune cells, including B cell, CD4+ T Cell, CD8+ T Cell, dendritic cell, macrophage, and neutrophil. The prognosis-related genes WNT2B and WNT7A are significantly correlated with immune cell infiltration and the infiltration level of different SCNAs in both LUAD and LUSC. WNT signaling has been demonstrated to regulate immune cell function, significantly inhibit the maturation and differentiation of T cells and dendritic cells (69), and alter the differentiation of CD4+ cells and CD8+ effector T cells (70, 71). WNT signaling plays an important role in the tumor immune microenvironment, and WNT signaling can promote naive T cell maturation and control the proliferation and survival of progenitor B-cells and B-1 cells (72, 73). Moreover, WNT signaling can also increase the level of β-catenin in malignant cells, which leads to the subsistence of Regulatory T cells (Tregs), differentiation of CD4 + T cells into Th17 subtypes and secretion of IL10 and IL12 in dendritic cells (74). In addition, the canonical WNT signaling pathway was identified as one of the important immune evasion-related oncogenic pathway signals (75). Therefore, relevant WNT signaling pathways have been increasingly recognized as a potential target for cancer therapy. NFAT is a transcription factor regulated by the calcium/calmodulin-dependent protein phosphatase calcineurin and a downstream factor of WNT5A, localizing in the cytoplasm of resting T cells (76, 77). NFAT could enhance the expression of IL-2, an important mediator of graft-versus-host disease, under the stimulation of T cells, while cyclosporine A (CsA) acted as an immunosuppressive agent by reducing the nuclear accumulation of NFAT and then IL-2 expression (78). However, in the presence of CsA, T cell treatment with WNT5A resulted in nuclear accumulation of NFAT, enabling WNT5A to lead to CsA resistance through the WNT/heterotrimeric GTP-binding protein pathway (57). Through the B cell proliferation in WNT5A-deficient mice, WNT5A was found to inhibit B cell proliferation through WNT/calcium to act as a tumor suppressor (62). Immune escape has been a key in cancer research in recent decades, and the advent of treatments such as molecular therapy and immune checkpoint inhibition for cancer has also shed light on the conquest of lung cancer (5–7). Overall, based on the

results in TIMER and TISIDB, our results suggest that there may be a degree of correlation between WNT2B and WNT7A and the level of immune cell infiltration. Based on limitations such as study objectives and experimental samples, etc, we did not conduct further experiments to verify the relationship between WNTs and immune cells, therefore, this field still needs to be explored through a large number of experiments. Furthermore, because of new drug resistance mechanisms, gene polymorphisms, and other reasons, many studies are still expected to support the research and treatment methods in this field.

Finally, we validate the mRNA and protein expression levels of WNT2B and WNT7A in NSCLC by qRT-PCR, western blot, and immunohistochemical staining, obtaining consistent experimental results with our analysis, further increasing the credibility and accuracy of our conclusions.

In summary, our study provides some insights into the WNT gene family in NSCLC patients about differential expression profile, potential prognostic value, immune infiltration level, etc. Nevertheless, this study still has some limitations. First, we did not perform the gene knockdown or overexpression of WNT2B and WNT7A to investigate the effects of WNT2B and WNT7A on prognostically relevant functions such as proliferation and migration of NSCLC, which will be the research focus of our team in the next phase. Second, based on existing studies, the role of some WNT genes in cancer conduction is not exhaustive, and the detailed mechanism of these genes still needs numerous subsequent studies. Our research is expected to provide further exploration direction and reference significance for subsequent research in this field.

Conclusion

This paper, for the first time, explored the comprehensive situation of the WNT gene family in LUAD and LUSC by bioinformatics methods and the differences of the WNT gene family in LUAD and LUSC fields. According to the survival analysis results, WNT2B and WNT7A might have prognostic value in LUAD, and both of them might be important prognostic factors for LUSC patients. In addition, WNT2B and WNT7A might show some correlation with immune cell infiltration of LUAD and LUSC, but their specific prognosis and immune infiltration-related mechanisms need further experimental validation. This study may provide some direction for the subsequent exploration of the biomarker or prognostic value of the WNT gene family in NSCLC.

Data availability statement

The original contributions presented in the study are included in the article/**Supplementary Material**. Further inquiries can be directed to the corresponding author.

Ethics statement

The studies involving human participants were reviewed and approved by the ethics committee of the Third Xiangya Hospital of Central South University. Written informed consent for participation was not required for this study in accordance with the national legislation and the institutional requirements.

Author contributions

WL and MT designed the study. JW and QY prepared the manuscript. All authors contributed to the article and approved the submitted version.

Funding

This study was supported by the Hunan Province Natural Science Foundation (No. 2021JJ40939, No. 2022JJ40253), the Scientific research project of Hunan Health Commission (No. 202203014949, No. 202102041763, No. 20200985), the Changsha Municipal Natural Science Foundation (No. kq2014267), and the Hunan Cancer Hospital Climb Plan (No. 2020QH001).

Conflict of interest

The authors declare that the research was conducted in the absence of any commercial or financial relationships that could be construed as a potential conflict of interest.

Publisher's note

Supplementary material

The Supplementary Material for this article can be found online at: https://www.frontiersin.org/articles/10.3389/fonc.2022.911316/full#supplementary-material

References

1. Ferlay J, Ervik M, Lam F, Colombet M, Mery L, Piñeros M, et al. Global Cancer Observatory: Cancer Today. Lyon, France: International Agency for Research on Cancer. Available from: https://gco.iarc.fr/today.

2. Schwartz AG, Cote ML. Epidemiology of lung cancer. *Adv Exp Med Biol* (2016) 893:21–41. doi: 10.1007/978-3-319-24223-1_2

3. Molina JR, Yang P, Cassivi SD, Schild SE, Adjei AA. Non-small cell lung cancer: Epidemiology, risk factors, treatment, and survivorship. *Mayo Clin Proc* (2008) 83(5):584–94. doi: 10.4065/83.5.584

4. Travis WD, Brambilla E, Noguchi M, Nicholson AG, Geisinger K, Yatabe Y, et al. Diagnosis of lung cancer in small biopsies and cytology: Implications of the 2011 international association for the study of lung Cancer/American thoracic Society/European respiratory society classification. *Arch Pathol Lab Med* (2013) 137(5):668–84. doi: 10.5858/arpa.2012-0263-RA

5. Sankar K, Gadgeel SM, Qin A. Molecular therapeutic targets in non-small cell lung cancer. *Expert Rev Anticancer Ther* (2020) 20(8):647–61. doi: 10.1080/14737140.2020.1787156

6. Rafei H, El-Bahesh E, Finianos A, Nassereddine S, Tabbara I. Immune-based therapies for non-small cell lung cancer. *Anticancer Res* (2017) 37(2):377–87. doi: 10.21873/anticanres.11330

7. Steendam CM, Dammeijer F, Aerts J, Cornelissen R. Immunotherapeutic strategies in non-small-cell lung cancer: The present and the future. *Immunotherapy* (2017) 9(6):507–20. doi: 10.2217/imt-2016-0151

8. Bade BC, Dela Cruz CS. Lung cancer 2020: Epidemiology, etiology, and prevention. *Clinics Chest Med* (2020) 41(1):1–24. doi: 10.1016/j.ccm.2019.10.001

9. Logan CY, Nusse R. The wnt signaling pathway in development and disease. *Annu Rev Cell Dev Biol* (2004) 20:781–810. doi: 10.1146/annurev.cellbio.20.010403.113126

10. Cadigan KM, Nusse R. Wnt signaling: A common theme in animal development. *Genes Dev* (1997) 11(24):3286–305. doi: 10.1101/gad.11.24.3286

11. Clevers H, Nusse R. Wnt/B-catenin signaling and disease. *Cell* (2012) 149(6):1192–205. doi: 10.1016/j.cell.2012.05.012

12. Parsons MJ, Tammela T, Dow LE. Wnt as a Driver and Dependency in Cancer. *Cancer discovery* (2021) 11(10):2413-29. doi 10.1158/2159-8290.Cd-21-0190

13. Stewart DJ. Wnt signaling pathway in non-small cell lung cancer. *J Natl Cancer Inst* (2014) 106(1):djt356. doi: 10.1093/jnci/djt356

14. Cheng X, Xu X, Chen D, Zhao F, Wang W. Therapeutic potential of targeting the Wnt/B-catenin signaling pathway in colorectal cancer. *Biomed Pharmacother* (2019) 110:473–81. doi: 10.1016/j.biopha.2018.11.082

15. He S, Tang S. Wnt/B-catenin signaling in the development of liver cancers. *Biomed Pharmacother* (2020) 132:110851. doi: 10.1016/j.biopha.2020.110851

16. Gounari F, Signoretti S, Bronson R, Klein L, Sellers WR, Kum J, et al. Stabilization of beta-catenin induces lesions reminiscent of prostatic intraepithelial neoplasia, but terminal squamous transdifferentiation of other secretory epithelia. *Oncogene* (2002) 21(26):4099–107. doi: 10.1038/sj.onc.1205562

17. Tan SH, Barker N. Wnt signaling in adult epithelial stem cells and cancer. *Prog Mol Biol Trans Sci* (2018) 153:21–79. doi: 10.1016/bs.pmbts.2017.11.017

18. Gajos-Michniewicz A, Czyz M. Wnt Signaling in Melanoma. *Int J Mol Scie* (2020) 21(14):4852. doi 10.3390/ijms21144852

19. Mazieres J, He B, You L, Xu Z, Jablons DM. Wnt signaling in lung cancer. *Cancer Lett* (2005) 222(1):1–10. doi: 10.1016/j.canlet.2004.08.040

20. Rhodes DR, Yu J, Shanker K, Deshpande N, Varambally R, Ghosh D, et al. Oncomine: A cancer microarray database and integrated data-mining platform. *Neoplasia* (2004) 6(1):1–6. doi: 10.1016/s1476-5586(04)80047-2

21. Li T, Fan J, Wang B, Traugh N, Chen Q, Liu JS, et al. Timer: A web server for comprehensive analysis of tumor-infiltrating immune cells. *Cancer Res* (2017) 77(21):e108–e10. doi: 10.1158/0008-5472.Can-17-0307

22. Chandrashekar DS, Bashel B, Balasubramanya SAH, Creighton CJ, Ponce-Rodriguez I, Chakravarthi BVSK, et al. Ualcan: A portal for facilitating tumor subgroup gene expression and survival analyses. *Neoplasia* (2017) 19(8):649–58. doi: 10.1016/j.neo.2017.05.002

23. Tang Z, Li C, Kang B, Gao G, Li C, Zhang Z. Gepia: A web server for cancer and normal gene expression profiling and interactive analyses. *Nucleic Acids Res* (2017) 45(W1):W98–W102. doi: 10.1093/nar/gkx247

24. Győrffy B, Surowiak P, Budczies J, Lánczky A. Online survival analysis software to assess the prognostic value of biomarkers using transcriptomic data in non-small-cell lung cancer. *PloS One* (2013) 8(12):e82241. doi: 10.1371/journal.pone.0082241

25. Gao J, Aksoy BA, Dogrusoz U, Dresdner G, Gross B, Sumer SO, et al. Integrative analysis of complex cancer genomics and clinical profiles using the cbioportal. *Sci Signal* (2013) 6(269):pl1–pl. doi: 10.1126/scisignal.2004088

26. Yu G, Wang LG, Han Y, He QY. Clusterprofiler: An r package for comparing biological themes among gene clusters. *Omics* (2012) 16(5):284–7. doi: 10.1089/omi.2011.0118

27. Szklarczyk D, Gable AL, Lyon D, Junge A, Wyder S, Huerta-Cepas J, et al. String V11: Protein-protein association networks with increased coverage, supporting functional discovery in genome-wide experimental datasets. *Nucleic Acids Res* (2019) 47(D1):D607–d13. doi: 10.1093/nar/gky1131

28. Han H, Cho JW, Lee S, Yun A, Kim H, Bae D, et al. Trrust V2: An expanded reference database of human and mouse transcriptional regulatory interactions. *Nucleic Acids Res* (2018) 46(D1):D380–d6. doi: 10.1093/nar/gkx1013

29. Ru B, Wong CN, Tong Y, Zhong JY, Zhong SSW, Wu WC, et al. Tisidb: An integrated repository portal for tumor-immune system interactions. *Bioinformatics (Oxford England)* (2019) 35(20):4200–2. doi: 10.1093/bioinformatics/btz210

30. Su LJ, Chang CW, Wu YC, Chen KC, Lin CJ, Liang SC, et al. Selection of Ddx5 as a novel internal control for q-Rt-Pcr from microarray data using a block bootstrap re-sampling scheme. *BMC Genomics* (2007) 8:140. doi: 10.1186/1471-2164-8-140

31. Hou J, Aerts J, den Hamer B, van Ijcken W, den Bakker M, Riegman P, et al. Gene expression-based classification of non-small cell lung carcinomas and survival prediction. *PLoS One* (2010) 5(4):e10312. doi: 10.1371/journal.pone.0010312

32. Okayama H, Kohno T, Ishii Y, Shimada Y, Shiraishi K, Iwakawa R, et al. Identification of genes upregulated in alk-positive and Egfr/Kras/Alk-negative lung adenocarcinomas. *Cancer Res* (2012) 72(1):100–11. doi: 10.1158/0008-5472.Can-11-1403

33. Selamat SA, Chung BS, Girard L, Zhang W, Zhang Y, Campan M, et al. Genome-scale analysis of DNA methylation in lung adenocarcinoma and integration with mrna expression. *Genome Res* (2012) 22(7):1197–211. doi: 10.1101/gr.132662.111

34. Bhattacharjee A, Richards WG, Staunton J, Li C, Monti S, Vasa P, et al. Classification of human lung carcinomas by mrna expression profiling reveals distinct adenocarcinoma subclasses. *Proc Natl Acad Sci U S A* (2001) 98(24):13790–5. doi: 10.1073/pnas.191502998

35. Garber ME, Troyanskaya OG, Schluens K, Petersen S, Thaesler Z, Pacyna-Gengelbach M, et al. Diversity of gene expression in adenocarcinoma of the lung. *Proc Natl Acad Sci U S A* (2001) 98(24):13784–9. doi: 10.1073/pnas.241500798

36. Basu M, Roy SS. Wnt/B-catenin pathway is regulated by Pitx2 homeodomain protein and thus contributes to the proliferation of human ovarian adenocarcinoma cell, skov-3. *J Biol Chem* (2013) 288(6):4355–67. doi: 10.1074/jbc.M112.409102

37. You L, He B, Xu Z, Uematsu K, Mazieres J, Mikami I, et al. Inhibition of wnt-2-mediated signaling induces programmed cell death in non-small-cell lung cancer cells. *Oncogene* (2004) 23(36):6170–4. doi: 10.1038/sj.onc.1207844

38. Huang C, Ma R, Xu Y, Li N, Li Z, Yue J, et al. Wnt2 promotes non-small cell lung cancer progression by activating Wnt/B-catenin pathway. *Am J Cancer Res* (2015) 5(3):1032–46.

39. Winn RA, Marek L, Han SY, Rodriguez K, Rodriguez N, Hammond M, et al. Restoration of wnt-7a expression reverses non-small cell lung cancer cellular transformation through frizzled-9-Mediated growth inhibition and promotion of cell differentiation. *J Biol Chem* (2005) 280(20):19625–34. doi: 10.1074/jbc.M409392200

40. Yang YL, Chen MW, Xian L. Prognostic and clinicopathological significance of downregulated e-cadherin expression in patients with non-small cell lung cancer (Nsclc): A meta-analysis. *PLoS One* (2014) 9(6):e99763. doi: 10.1371/journal.pone.0099763

41. Wong SHM, Fang CM, Chuah LH, Leong CO, Ngai SC. E-cadherin: Its dysregulation in carcinogenesis and clinical implications. *Crit Rev Oncol Hematol* (2018) 121:11–22. doi: 10.1016/j.critrevonc.2017.11.010

42. Hibi K, Takahashi T, Yamakawa K, Ueda R, Sekido Y, Ariyoshi Y, et al. Three distinct regions involved in 3p deletion in human lung cancer. *Oncogene* (1992) 7(3):445–9.

43. Tennis MA, Vanscoyk MM, Wilson LA, Kelley N, Winn RA. Methylation of Wnt7a is modulated by Dnmt1 and cigarette smoke condensate in non-small cell lung cancer. *PLoS One* (2012) 7(3):e32921. doi: 10.1371/journal.pone.0032921

44. Heasley LE, Winn RA. Analysis of Wnt7a-stimulated jnk activity and cjun phosphorylation in non-small cell lung cancer cells. *Methods Mol Biol (Clifton NJ)* (2008) 468:187–96. doi: 10.1007/978-1-59745-249-6_14

45. Ohira T, Gemmill RM, Ferguson K, Kusy S, Roche J, Brambilla E, et al. Wnt7a induces e-cadherin in lung cancer cells. *Proc Natl Acad Sci U S A* (2003) 100 (18):10429–34. doi: 10.1073/pnas.1734137100

46. Schmidt M, Poser C, von Maltzahn J. Wnt7a counteracts cancer cachexia. *Mol Ther Oncolytics* (2020) 16:134–46. doi: 10.1016/j.omto.2019.12.011

47. Liu Y, Meng F, Xu Y, Yang S, Xiao M, Chen X, et al. Overexpression of Wnt7a is associated with tumor progression and unfavorable prognosis in endometrial cancer. *Int J Gynecol Cancer* (2013) 23(2):304–11. doi: 10.1097/IGC.0b013e31827c7708

48. Kirikoshi H, Katoh M. Expression of Wnt7a in Human Normal Tissues and Cancer, and Regulation of Wnt7a and Wnt7b in Human Cancer. *Int J Oncol* (2002) 21(4):895-900. doi 10.3892/ijo.21.4.895

49. Wang B, Sun L, Li J, Jiang R. Mir-577 suppresses cell proliferation and epithelial-mesenchymal transition by regulating the Wnt2b mediated Wnt/B-catenin pathway in non-small cell lung cancer. *Mol Med Rep* (2018) 18(3):2753–61. doi: 10.3892/mmr.2018.9279

50. Wu Y, Cheng K, Liang W, Wang X. Lncrna Rpph1 promotes non-small cell lung cancer progression through the mir-326/Wnt2b axis. *Oncol Lett* (2020) 20 (4):105. doi: 10.3892/ol.2020.11966

51. Liu Y, Wu D, Cheng H, Chen L, Zhang W, Zou L, et al. Wnt8b, transcriptionally regulated by Znf191, promotes cell proliferation of hepatocellular carcinoma *Via* wnt signaling. *Cancer Sci* (2021) 112(2):629–40. doi: 10.1111/cas.14738

52. Suzuki H, Watkins DN, Jair KW, Schuebel KE, Markowitz SD, Chen WD, et al. Epigenetic inactivation of sfrp genes allows constitutive wnt signaling in colorectal cancer. *Nat Genet* (2004) 36(4):417–22. doi: 10.1038/ng1330

53. Juan J, Muraguchi T, Iezza G, Sears RC, McMahon M. Diminished wnt -> B-catenin -> c-myc signaling is a barrier for malignant progression of Brafv600e-induced lung tumors. *Genes Dev* (2014) 28(6):561–75. doi: 10.1101/gad.233627.113

54. Ueda M, Gemmill RM, West J, Winn R, Sugita M, Tanaka N, et al. Mutations of the beta- and gamma-catenin genes are uncommon in human lung, breast, kidney, cervical and ovarian carcinomas. *Br J Cancer* (2001) 85 (1):64–8. doi: 10.1054/bjoc.2001.1863

55. Zheng C, Li X, Qian B, Feng N, Gao S, Zhao Y, et al. The lncrna myocardial infarction associated transcript-centric competing endogenous rna network in non-small-cell lung cancer. *Cancer Manag Res* (2018) 10:1155–62. doi: 10.2147/cmar.S163395

56. Suthon S, Perkins RS, Bryja V, Miranda-Carboni GA, Krum SA. Wnt5b in physiology and disease. *Front Cell Dev Biol* (2021) 9:667581. doi: 10.3389/fcell.2021.667581

57. Kohn AD, Moon RT. Wnt and calcium signaling: Beta-Catenin-Independent pathways. *Cell Calcium* (2005) 38(3-4):439–46. doi: 10.1016/j.ceca.2005.06.022

58. Ouko L, Ziegler TR, Gu LH, Eisenberg LM, Yang VW. Wnt11 signaling promotes proliferation, transformation, and migration of Iec6 intestinal epithelial cells. *J Biol Chem* (2004) 279(25):26707–15. doi: 10.1074/jbc.M402877200

59. Toyama T, Lee HC, Koga H, Wands JR, Kim M. Noncanonical Wnt11 inhibits hepatocellular carcinoma cell proliferation and migration. *Mol Cancer Res* (2010) 8(2):254–65. doi: 10.1158/1541-7786.Mcr-09-0238

60. Syed Khaja AS, Helczynski L, Edsjö A, Ehrnström R, Lindgren A, Ulmert D, et al. Elevated level of Wnt5a protein in localized prostate cancer tissue is associated with better outcome. *PloS One* (2011) 6(10):e26539. doi: 10.1371/journal.pone.0026539

61. Du SJ, Purcell SM, Christian JL, McGrew LL, Moon RT. Identification of distinct classes and functional domains of wnts through expression of wild-type and chimeric proteins in xenopus embryos. *Mol Cell Biol* (1995) 15(5):2625–34. doi: 10.1128/mcb.15.5.2625

62. Liang H, Chen Q, Coles AH, Anderson SJ, Pihan G, Bradley A, et al. Wnt5a inhibits b cell proliferation and functions as a tumor suppressor in hematopoietic tissue. *Cancer Cell* (2003) 4(5):349–60. doi: 10.1016/s1535-6108(03)00268-x

63. Veeman MT, Axelrod JD, Moon RT. A second canon. functions and mechanisms of beta-Catenin-Independent wnt signaling. *Dev Cell* (2003) 5 (3):367–77. doi: 10.1016/s1534-5807(03)00266-1

64. Shapiro M, Akiri G, Chin C, Wisnivesky JP, Beasley MB, Weiser TS, et al. Wnt pathway activation predicts increased risk of tumor recurrence in patients with stage I nonsmall cell lung cancer. *Ann Surg* (2013) 257(3):548–54. doi: 10.1097/SLA.0b013e31826d81fd

65. Logan M, Pagán-Westphal SM, Smith DM, Paganessi L, Tabin CJ. The transcription factor Pitx2 mediates situs-specific morphogenesis in response to left-right asymmetric signals. *Cell* (1998) 94(3):307–17. doi: 10.1016/s0092-8674(00)81474-9

66. Kioussi C, Briata P, Baek SH, Rose DW, Hamblet NS, Herman T, et al. Identification of a Wnt/Dvl/Beta-catenin –> Pitx2 pathway mediating cell-Type-Specific proliferation during development. *Cell* (2002) 111(5):673–85. doi: 10.1016/s0092-8674(02)01084-x

67. Briata P, Ilengo C, Corte G, Moroni C, Rosenfeld MG, Chen CY, et al. The Wnt/Beta-Catenin–>Pitx2 pathway controls the turnover of Pitx2 and other unstable mrnas. *Mol Cell* (2003) 12(5):1201–11. doi: 10.1016/s1097-2765(03)00407-6

68. Luo J, Yao Y, Ji S, Sun Q, Xu Y, Liu K, et al. Pitx2 enhances progression of lung adenocarcinoma by transcriptionally regulating Wnt3a and activating Wnt/B-catenin signaling pathway. *Cancer Cell Int* (2019) 19:96. doi: 10.1186/s12935-019-0800-7

69. Staal FJ, Luis TC, Tiemessen MM. Wnt signalling in the immune system: Wnt is spreading its wings. *Nat Rev Immunol* (2008) 8(8):581–93. doi: 10.1038/nri2360

70. Hong Y, Manoharan I, Suryawanshi A, Majumdar T, Angus-Hill ML, Koni PA, et al. B-catenin promotes regulatory T-cell responses in tumors by inducing vitamin a metabolism in dendritic cells. *Cancer Res* (2015) 75(4):656–65. doi: 10.1158/0008-5472.Can-14-2377

71. Fu C, Liang X, Cui W, Ober-Blöbaum JL, Vazzana J, Shrikant PA, et al. B-catenin in dendritic cells exerts opposite functions in cross-priming and maintenance of Cd8+ T cells through regulation of il-10. *Proc Natl Acad Sci U S A* (2015) 112(9):2823–8. doi: 10.1073/pnas.1414167112

72. Rothenberg EV, Moore JE, Yui MA. Launching the T-Cell-Lineage developmental programme. *Nat Rev Immunol* (2008) 8(1):9–21. doi: 10.1038/nri2232

73. Osugui L, de Roo JJ, de Oliveira VC, Sodré ACP, Staal FJT, Popi AF. B-1 cells and b-1 cell precursors prompt different responses to wnt signaling. *PLoS One* (2018) 13(6):e0199332. doi: 10.1371/journal.pone.0199332

74. Patel S, Alam A, Pant R, Chattopadhyay S. Wnt signaling and its significance within the tumor microenvironment: Novel therapeutic insights. *Front Immunol* (2019) 10:2872. doi: 10.3389/fimmu.2019.02872

75. Pai SG, Carneiro BA, Mota JM, Costa R, Leite CA, Barroso-Sousa R, et al. Wnt/Beta-catenin pathway: Modulating anticancer immune response. *J Hematol Oncol* (2017) 10(1):101. doi: 10.1186/s13045-017-0471-6

76. Rao A, Luo C, Hogan PG. Transcription factors of the nfat family: Regulation and function. *Annu Rev Immunol* (1997) 15:707–47. doi: 10.1146/annurev.immunol.15.1.707

77. Saneyoshi T, Kume S, Amasaki Y, Mikoshiba K. The Wnt/Calcium pathway activates nf-at and promotes ventral cell fate in xenopus embryos. *Nature* (2002) 417(6886):295–9. doi: 10.1038/417295a

78. Shaw KT, Ho AM, Raghavan A, Kim J, Jain J, Park J, et al. Immunosuppressive drugs prevent a rapid dephosphorylation of transcription factor Nfat1 in stimulated immune cells. *Proc Natl Acad Sci U S A* (1995) 92 (24):11205–9. doi: 10.1073/pnas.92.24.11205

frontiers | Frontiers in Oncology

ORIGINAL RESEARCH
published: 28 July 2022
doi: 10.3389/fonc.2022.854702

A-Kinase Interacting Protein 1 Knockdown Restores Chemosensitivity *via* Inactivating PI3K/AKT and β-Catenin Pathways in Anaplastic Thyroid Carcinoma

Haiyan Zheng[†], *Qingyuan Lin*[†] *and Yamin Rao*[*]

Department of Pathology, Ninth People's Hospital, Shanghai Jiao Tong University School of Medicine, Shanghai, China

OPEN ACCESS

Edited by:
Gary Piazza,
Auburn University, United States

Reviewed by:
Rozita Bagheri-Yarmand,
University of Texas MD Anderson Cancer Center, United States
Adam Keeton,
Auburn University Harrison School of Pharmacy, United States

***Correspondence:**
Yamin Rao
raoyaya2006@126.com

[†]*These authors have contributed equally to this work*

Specialty section:
This article was submitted to Molecular and Cellular Oncology, a section of the journal Frontiers in Oncology

Received: *14 January 2022*
Accepted: *19 April 2022*
Published: *28 July 2022*

Citation:
Zheng H, Lin Q and Rao Y (2022) A-Kinase Interacting Protein 1 Knockdown Restores Chemosensitivity via Inactivating PI3K/AKT and β-Catenin Pathways in Anaplastic Thyroid Carcinoma. Front. Oncol. 12:854702. doi: 10.3389/fonc.2022.854702

Background: A-kinase interacting protein 1 (AKIP1) promotes tumor progression and chemoresistance in several malignancies; meanwhile, it is related to higher tumor size and recurrence risk of papillary thyroid carcinoma, while the role of AKIP1 in anaplastic thyroid carcinoma (ATC) is unclear. The aim of this study is to explore the effect of AKIP1 knockdown on cell malignant behaviors and doxorubicin resistance in ATC.

Methods: AKIP1 knockdown was conducted in ATC cell lines (8505C and CAL-62 cells) by siRNA; then, cell viability, apoptosis, invasion, PI3K/AKT and β-catenin pathways, and doxorubicin sensitivity were detected. Subsequently, doxorubicin-resistant 8505C cells (8505C/Dox) were established. Additionally, AKIP1 was modified in 8505C and 8505C/Dox cells that underwent doxorubicin treatment by siRNA or overexpression plasmid, followed by cellular function and pathway detection.

Results: AKIP1 was elevated in FRO, 8505C, CAL-62, and KHM-5M cells compared to control cells (all $p < 0.05$). Subsequently, AKIP1 knockdown elevated apoptosis, inhibited viability and invasion, and inactivated PI3K/AKT and β-catenin pathways in 8505C and CAL-62 cells (all $p < 0.05$). AKIP1 knockdown decreased relative cell viability in doxorubicin-treated 8505C and CAL-62 cells; then, AKIP1 was elevated in 8505C/Dox cells compared to 8505C cells (all $p < 0.05$). Furthermore, AKIP1 knockdown restored doxorubicin sensitivity (reflected by decreased cell viability and invasion, and increased apoptosis), but inactivated PI3K/AKT and β-catenin pathways in doxorubicin-treated 8505C/Dox cells. However, AKIP1 overexpression presented an opposite effect on these functions and pathways in doxorubicin-treated 8505C cells.

Conclusion: AKIP1 knockdown decreases cell survival and invasion while promoting sensitivity to doxorubicin *via* inactivating PI3K/AKT and β-catenin pathways in ATC.

Keywords: AKIP1, anaplastic thyroid carcinoma, doxorubicin sensitivity, cell malignant behaviors, PI3K/AKT and β-catenin pathways

INTRODUCTION

Anaplastic thyroid carcinoma (ATC), a rare but the most malignant type of thyroid carcinomas, is characterized by poor differentiation, a highly aggressive nature, and quick metastasis (1–4). Currently, treatments of ATC typically consist of surgery, chemotherapy, radiotherapy, molecular targeted therapy, etc. (1, 5, 6). However, these comprehensive treatments of ATC still fail to demonstrate an obvious survival benefit for ATC patients due to its intrinsic characteristics; thus, ATC is viewed as a devastating disease with a high mortality rate (5). Hence, exploring the potential molecular mechanism and possible target to improve treatment of ATC is crucial and urgent.

A-kinase interacting protein 1 (AKIP1), originally named breast cancer-associated protein 3, facilitates the nuclear translocation of catalytic subunit of protein kinase A (7, 8). Recently, it has been reported that AKIP1 is viewed as a tumor promoter (7–11). For instance, it is proposed that AKIP1 induces the nuclear factor kappa-B (NF-κB)-dependent chemokines to promote angiogenesis and tumor growth in cervical cancer (8). Moreover, AKIP1 elevates vascular endothelial growth factor-C (VEGF-C) to accelerate angiogenesis and lymphangiogenesis in human esophageal squamous cell carcinoma (9). Another interesting study discloses that AKIP1 activates Zinc Finger E-Box Binding Homeobox 1 (ZEB1) to facilitate tumor metastasis in non-small cell lung cancer (10). In addition, AKIP1 is also considered as a regulator of treatment resistance in malignancies (11, 12). For example, AKIP1 upregulates C-X-C motif chemokine ligand (CXCL)1 and CXCL8 to decrease chemoradiation sensitivity in glioblastoma (12). Additionally, AKIP1 interacts with Tap73 to modulate the radiotherapy sensitivity of cervical cancer cells (11). Importantly, recent research has presented that AKIP1 is correlated with advanced tumor features and higher recurrence risk in papillary thyroid carcinoma (13). According to the above-mentioned information, we deduce that AKIP1 may play an important role in tumor progression and treatment resistance in ATC, while related data are scarce.

In the current study, AKIP1 modification was conducted in ATC cell lines, followed by detection of cellular functions, chemotherapy resistance, and downstream pathways, aiming to explore the potential of AKIP1 as a treatment target for ATC. The current study discovered that AKIP1 knockdown inhibited cell viability and invasion but promoted cell apoptosis, as well as restored doxorubicin sensitivity *via* inactivating PI3K/AKT and β-catenin pathways in ATC, indicating that targeting AKIP1 might provide a new treatment choice for ATC.

METHODS

Cell Lines

Human normal thyroid cell line (Nthy-ori 3-1) was purchased from the European Collection of Authenticated Cell Cultures (ECACC). Human ATC cell lines, including FRO, 8505C, C643, CAL-62, and KHM-5M, were purchased from the National Collection of Authenticated Cell Cultures (Shanghai, China). Cells were maintained in DMEM (Lonza, Swiss) (8505C and CAL-62) or RPMI-1640 medium (Lonza, Swiss) (Nthy-ori 3-1, FRO, C643, and KHM-5M) containing 10% fetal bovine serum (FBS) (Sigma, USA) and 1% penicillin/streptomycin (Beyotime, China) at 37°C in an incubator with 5% CO_2. The doxorubicin-resistant 8505C cells (8505C/Dox) were established from the parental 8505C cells by exposing cells to gradually increasing concentrations of doxorubicin (Sigma, USA) from 0.1 μM to 10 μM over 8 months (14). 8505C/Dox cells were cultured in culture medium containing 2 μM doxorubicin to maintain drug resistance phenotype.

Cell Transfection

The AKIP1 siRNA (si-AKIP1) and negative control (si-NC) were commercially designed and synthesized by Shanghai GenePharma Co., Ltd. (Shanghai, China). The AKIP1 overexpression plasmids (pcDNA-AKIP1) and negative control (pcDNA-NC) were obtained from Guangzhou Ribobio Co., Ltd. (Guangzhou, China). ATC cells were cultured and transfected with 50 nM siRNA (si-AKIP1 or si-NC) or 0.8 μg of plasmids (pcDNA-AKIP1 or pcDNA-NC) with Lipofectamine® 3000 (Invitrogen, USA) for 6 h. The AKIP1 siRNA sequence was as follows: sense, 5' GTGGGCTCAAATGACTTAATT 3'; antisense, 5' TTAAGTCATTTGAGCCCACTT 3'. The non-transfected cells served as normal controls.

Drug Sensitivity Assay

The 8505C cells were incubated with 0, 0.2, 0.4, 0.8, 1.6, 3.2, and 6.4 μM doxorubicin; CAL-62 cells were incubated with 0, 0.02, 0.04, 0.08, 0.16, 0.32, and 0.64 μM doxorubicin; and 8505C/Dox cells were incubated with 0, 2, 4, 8, 16, 32, and 64 μM doxorubicin (15, 16). After 48 h of treatment, CCK-8 assay was performed by the methods mentioned in the *Cell Viability Assay* subsection and half maximal inhibitory concentration (IC_{50}) was calculated using the sigmoidal dose–response function of the GraphPad Prism software (Version 7.0) (17).

Doxorubicin Treatment

To assess whether AKIP1 participated in the drug resistance of ATC cells, the 8505C cells were transfected with pcDNA-AKIP1 and cultured with 1.6 μM doxorubicin (selected by IC_{50}); meanwhile, 8505C/Dox cells were transfected with si-AKIP1 and cultured with 16 μM doxorubicin. Briefly, 8505C cells were divided into five groups, including the Normal group (non-treated), the pcDNA-NC group (transfected with NC plasmids), the pcDNA-AKIP1 group (transfected with AKIP1 overexpression plasmids), the pcDNA-NC and Dox group (transfected with NC plasmids and treated with 1.6 μM doxorubicin), and the pcDNA-AKIP1 and Dox group (transfected with AKIP1 overexpression plasmids and treated with 1.6 μM doxorubicin). Analogously, 8505C/Dox cells were divided into five groups, including the Normal group (non-treated), the si-NC group (transfected with NC siRNA), the si-AKIP1 group (transfected with AKIP1 siRNA), the si-NC and Dox group (transfected with NC siRNA and treated with 16 μM doxorubicin), and the si-AKIP1 and Dox group (transfected with

AKIP1 siRNA and treated with 16 μM doxorubicin). After 48 h of treatment, further assays were carried out.

Reverse Transcription Quantitative Polymerase Chain Reaction for AKIP1 Expression

In brief, total RNA from ATC cells was extracted *via* Beyozol (Beyotime, China). Reverse transcription of RNA was completed by the GeneAce Reverse Transcriptase Kit (Nippon, Japan). The PCR program was implemented using the SYBR® Premix DimmerEraser™ kit (Takara, Japan). The thermal cycle of qPCR was as follows: 1 cycle, 95°C for 30 s; 40 cycles, 95°C for 5 s and 61°C for 30 s. The AKIP1 mRNA expression was evaluated based on the $2^{-\Delta\Delta Ct}$ method with GAPDH as an endogenous control. The primer sequences were listed as follows (5'→3'): AKIP1 forward, CATGGACAACTGTTTGG CGG, AKIP1 reverse: TAGAGCCAGCCTTGCTGAAC; GAPDH forward, GAGTCCACTGGCGTCTTCAC, GAPDH reverse, ATCTTGAGGCTGTTGTCATACTTCT.

Western Blotting

Western blotting assays of ATC cells were implemented at 48 h after treatment. First of all, ATC cells were lysed by RIPA comprising 1 mM PMSF (Selleck, USA) and the concentration of total proteins was quantified using the bicinchoninic acid kit (Beyotime, China). Secondly, 40 μg of proteins was separated by SDS-PAGE and transferred onto a nitrocellulose membrane (Pall, USA). Then, membranes were blocked using 5% nonfat milk (Beyotime, China), hatched with primary antibodies overnight at 4°C, and subsequently incubated with secondary antibody (1:10,000) (Affinity, China) for 1 h at 37°C. Finally, blots were detected *via* ECL-PLUS kit (Beyotime, China) and analyzed using ImageJ software (version 1.8.0, NIH). The primary antibodies used in this study were bought from Abcam (Cambridge, USA) and listed as follows: anti-AKIP1 (1:500, ab135996), anti-p-PI3K (1:1,000, ab182651), anti-PI3K (1:1,500, ab86714), anti-p-AKT^{Ser473} (1:1,000, ab81283), anti-AKT (1:1,500, ab8805), anti-β-catenin (1:1,000, ab68813), anti-GAPDH (1:5,000, ab181602), and anti-Histone H3 (1:5,000, ab1791).

Cell Viability Assay

Cell viability was evaluated by the Cell Counting Kit-8 (CCK-8) (Sigma, USA) assay. In brief, ATC cells were plated in 96-well plates (2×10^3 cells/well) and cultured for 48 h and 72 h. Then, 10 μl of CCK-8 reagent was added and further cultured for another 2 h at 37°C. Finally, the optical density (OD) values at 450 nm were assessed with a microplate reader (Molecular Devices, USA).

Cell Apoptosis Assay

Cell apoptosis rate was detected using the TUNEL apoptosis kit (Sangon, China). Briefly, at 48 h and 72 h after treatment, ATC cells (1×10^4 cells/well) were fixed with 4% paraformaldehyde (Sangon, China) and permeabilized with 0.1% Triton X-100 (Sangon, China). Then, cells were incubated with TUNEL reagent for 20 min and DAPI solution (Sigma, USA) for 10 min at room temperature (RT), successively. The apoptotic cells were viewed and imaged with a microscope (Olympus, Japan).

Cell Invasion Assay

At 48 h after treatment, the invasion ability of ATC cells was assessed by the transwell assay. In brief, cells were adjusted to 5×10^4 cells/well with serum-free medium and plated into the upper chamber of Matrigel-coated transwell chamber plates (Life, USA). The lower chambers were covered with 600 μl of DMEM containing 10% FBS. At 24 h after culture, the invasive cells were counted under a microscope after being stained with crystal violet (Beyotime, China) for 10 min at RT (16, 18).

Statistical Analysis

The experiment was performed in triplicate. One-way ANOVA with Tukey's or Dunnett's post-hoc test and Student's *t*-test were used for comparisons. All statistical analyses were calculated by GraphPad Prism. $p < 0.05$ was considered to be statistically significant.

RESULTS

AKIP1 Expression

No difference was found in AKIP1 between Nthy-ori3-1 cells and C643 cells ($p > 0.05$), while AKIP1 was increased in FRO, 8505C, CAL-62, and KHM-5M cells compared to Nthy-ori 3-1 cells (all $p < 0.05$); since AKIP1 was dramatically elevated in 8505C and CAL-62 cells, these two cell lines were selected for further experiments (**Figures 1A–C**). Moreover, 8505C and CAL-62 cells were transfected with AKIP1 siRNA or NC siRNA; data showed that AKIP1 was decreased in 8505C and CAL-62 cells transfected with AKIP1 siRNA compared to those transfected with NC siRNA, suggesting successful transfection (**Figures 1D–H**).

AKIP1 Knockdown Decreased Cell Survival and Invasion in ATC Cell Lines

In order to explore the regulation of AKIP1 on cellular functions, cell viability, apoptosis, and invasion assays were conducted. The data showed that AKIP1 knockdown elevated apoptosis but declined cell viability and invasive cell count in both 8505C and CAL-62 cells at 48 h after transfection (all $p < 0.05$); moreover, the rates of inhibition of survival of 8505C and CAL-62 cells transfected with si-AKIP1 were 37.14% and 25.82%, respectively, at 48 h after transfection; meanwhile, the apoptosis rate of normal 8505C cells, and 8505C cells transfected with si-NC and si-AKIP1 was 5.52%, 5.54%, and 14.93%, respectively; moreover, the apoptosis rate of normal CAL-62 cells, and CAL-62 cells transfected with si-NC and si-AKIP1 was 4.92%, 5.26%, and 12.52%, respectively (**Figures 2A–H**). Furthermore, cell viability and apoptosis presented similar trends at 72 h after AKIP1 knockdown (**Supplementary Figures 1A–E**).

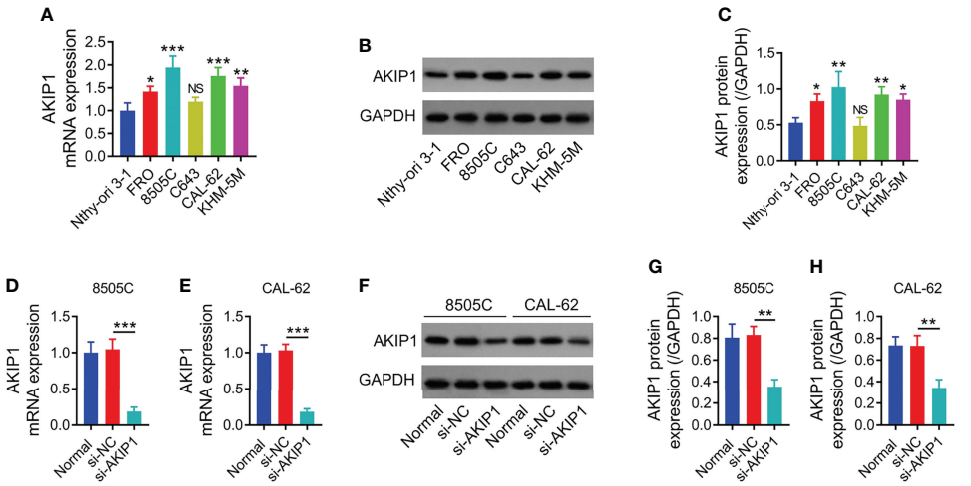

FIGURE 1 | Detection of AKIP1 expression. Comparison of AKIP1 mRNA expression between human normal thyroid cell line and ATC cell lines **(A)**; example image of AKIP1 protein in human normal thyroid cell line and ATC cell lines through Western blot **(B)**; comparison of AKIP1 protein expression between human normal thyroid cell line and ATC cell lines **(C)**; comparison of AKIP1 mRNA expression among groups in 8505C cells **(D)** and CAL-62 cells **(E)** after transfection; detection of AKIP1 protein expression by Western blot in 8505C cells and CAL-62 cells after transfection **(F)**; comparison of AKIP1 protein expression among groups in 8505C cells **(G)** and CAL-62 cells **(H)** after transfection by one-way ANOVA followed by Dunnett's post-hoc test. ATC, anaplastic thyroid carcinoma; AKIP1, A-kinase interacting protein 1; NS, not significant; $^{*}p < 0.05$; $^{**}p < 0.01$; $^{***}p < 0.001$.

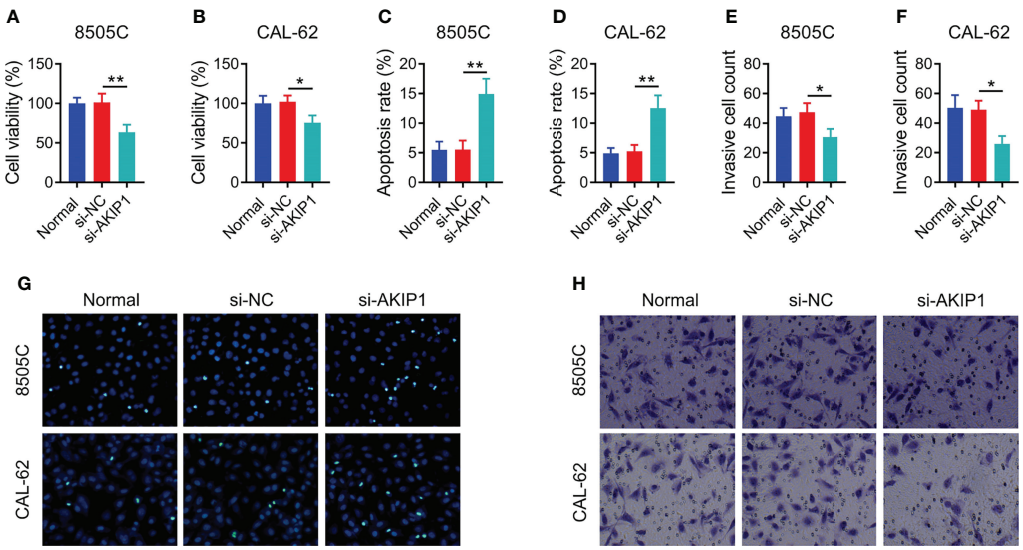

FIGURE 2 | Cellular functions in ATC cell lines at 48 h after siRNA transfection. Comparison of relative cell viability among groups in 8505C cells **(A)** and CAL-62 cells **(B)** after transfection; comparison of apoptosis among groups in 8505C cells **(C)** and CAL-62 cells **(D)** after transfection; comparison of invasive cell count among groups in 8505C cells **(E)** and CAL-62 cells **(F)** after transfection by one-way ANOVA followed by Dunnett's post-hoc test; example image of cell apoptosis through TUNEL Apoptosis Assay Kit **(G)** and example image of cell invasion through transwell assay **(H)** in 8505C cells and CAL-62 cells after transfection. ATC, anaplastic thyroid carcinoma; siRNA, small interfering RNA; AKIP1, A-kinase interacting protein 1; $^{*}p < 0.05$; $^{**}p < 0.01$.

AKIP1 Knockdown Suppressed PI3K/AKT and β-Catenin Pathways in ATC Cell Lines

Previous studies have presented that AKIP1 modulates PI3K/AKT and β-catenin pathways to regulate tumor progression (12, 19, 20); thus, the effect of AKIP1 knockdown on these pathways in ATC cell lines was explored by Western blot, which revealed that AKIP1 knockdown inhibited the phosphorylation of PI3K and AKT in 8505C and CAL-62 cells (both $p < 0.05$); meanwhile, AKIP1 knockdown inhibited expression of β-catenin in CAL-62 cells ($p < 0.05$) but not in 8505C cells ($p > 0.05$) (**Figures 3A–C**). Furthermore, AKIP1 knockdown inhibited the nuclear

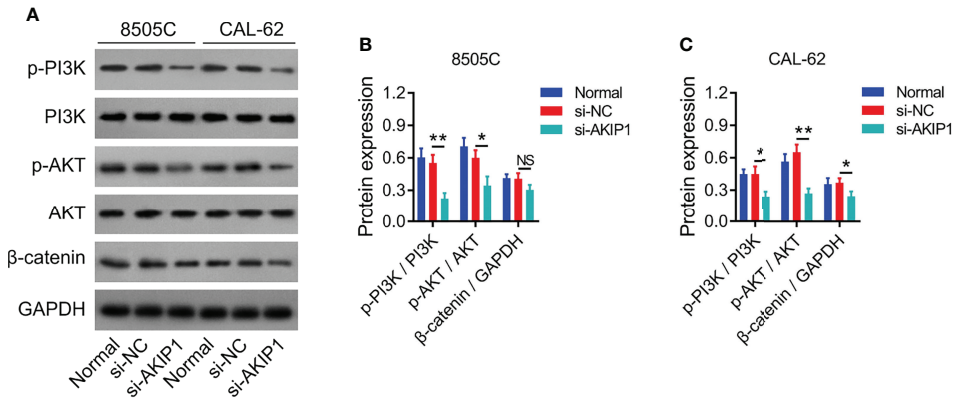

FIGURE 3 | PI3K/AKT and β-catenin pathways in ATC cell lines after siRNA transfection. Detection of p-PI3K, PI3K, p-AKT, AKT, and β-catenin protein expressions by Western blot in 8505C cells and CAL-62 cells after transfection **(A)**; comparison of p-PI3K/PI3K, p-AKT/AKT, and β-catenin expressions among groups in 8505C cells **(B)** and CAL-62 cells **(C)** after transfection by one-way ANOVA followed by Dunnett's post-hoc test. ATC, anaplastic thyroid carcinoma; siRNA, small interfering RNA; AKIP1, A-kinase interacting protein 1; NS, not significant; PI3K, phosphatidylinositol-3-kinase; AKT, protein kinase B; GAPDH, glyceraldehyde-3-phosphate dehydrogenase; *$p < 0.05$; **$p < 0.01$.

translocation of β-catenin in 8505C and CAL-62 cells (both $p < 0.01$) (**Supplementary Figures 2A–C**).

AKIP1 Was Elevated in 8505C/Dox Cells

Relative cell viability was declined along with the increasing concentration of doxorubicin in 8505C and CAL-62 cells; meanwhile, the IC_{50} concentration of doxorubicin was identified as 1.77 μM in 8505C cells and 0.16 μM in CAL-62 cells (**Figures 4A, B**). Furthermore, 1.6 μM doxorubicin was used to treat 8505C cells and 0.16 μM doxorubicin was used to treat CAL-62 cells after transfection; data showed that AKIP1 knockdown decreased relative cell viability in 8505C cells and CAL-62 cells under doxorubicin treatment (both $p < 0.05$) (**Figures 4C, D**). In addition, AKIP1 knockdown declined relative cell viability in 0.8 μM, 1.6 μM, and 3.2 μM doxorubicin-treated 8505C cells; meanwhile, AKIP1 knockdown decreased relative cell viability in 0.04 μM, 0.08 μM, 0.16 μM, and 0.32 μM doxorubicin-treated CAL-62 cells (all $p < 0.05$) (**Supplementary Figures 3A, B**). To explore whether AKIP1 participated in drug resistance of ATC, 8505C/Dox cells with an IC_{50} concentration of 18.2 μM were established (**Figure 4E**). Furthermore, AKIP1 was elevated in 8505C/Dox cells compared to 8505C cells (both $p < 0.05$) (**Figures 4F–H**).

AKIP1 Knockdown Enhanced Doxorubicin Sensitivity, and Inactivated PI3K/AKT and β-Catenin Pathways in 8505C/Dox Cells

To further explore the effect of AKIP1 on drug resistance in ATC cell lines, 8505C cells were transfected with AKIP1 or NC overexpression plasmids; meanwhile, 8505C/Dox cells were transfected with AKIP1 siRNA or NC siRNA; data showed that AKIP1 was elevated in 8505C cells transfected with the AKIP1 overexpression plasmid compared to those transfected with the NC overexpression plasmid (both $p < 0.001$), while AKIP1 was declined in 8505C/Dox cells transfected with AKIP1 siRNA compared to NC siRNA (both $p < 0.01$) (**Figures 5A–E**). Moreover, AKIP1 overexpression elevated relative cell viability in 0.8 μM, 1.6 μM, 3.2 μM, and 6.4 μM doxorubicin-treated 8505C cells; moreover, AKIP1 knockdown decreased relative cell viability in 8 μM, 16 μM, 32 μM, and 64 μM doxorubicin-treated 8505C/Dox cells, as well as promoted the doxorubicin sensitivity in 8505C/Dox cells (IC_{50} in normal cells: 18.50 μm, IC_{50} in siRNA-AKIP1 cells: 10.05 μm) (**Figures 5F, G**).

To further verify the effect of AKIP1 on drug resistance in ATC cell lines, 8505C cells after transfection were treated by 1.6 μM doxorubicin and 8505C/Dox cells after transfection were treated by 16 μM doxorubicin. Data presented that AKIP1 overexpression elevated relative cell viability and invasive cell count, but decreased apoptosis rate in doxorubicin-treated 8505C cells (all $p < 0.05$); furthermore, AKIP1 knockdown decreased relative cell viability and invasive cell count, but elevated apoptosis rate in doxorubicin-treated 8505C/Dox cells (all $p < 0.05$) (**Figures 6A–J**). Moreover, AKIP1 overexpression increased p-AKT and β-catenin in doxorubicin-treated 8505C cells, while AKIP1 knockdown decreased p-PI3K, p-AKT, and β-catenin in doxorubicin-treated 8505C/Dox cells (all $p < 0.05$) (**Figures 7A–D**). In addition, AKIP1 overexpression increased the nuclear translocation of β-catenin in doxorubicin-treated 8505C cells, while AKIP1 knockdown declined the nuclear translocation of β-catenin in doxorubicin-treated 8505C/Dox cells (both $p < 0.05$) (**Supplementary Figures 4A–C**).

DISCUSSION

ATC accounts for only 2% of all thyroid carcinomas; although it is rare, ATC is viewed as one of the invariably lethal diseases worldwide (1–3). Until now, the prognosis of ATC is relatively poor due to the characteristics of ATC, such as aggressive nature and metastasis at an early stage (4–6). Moreover, partly because

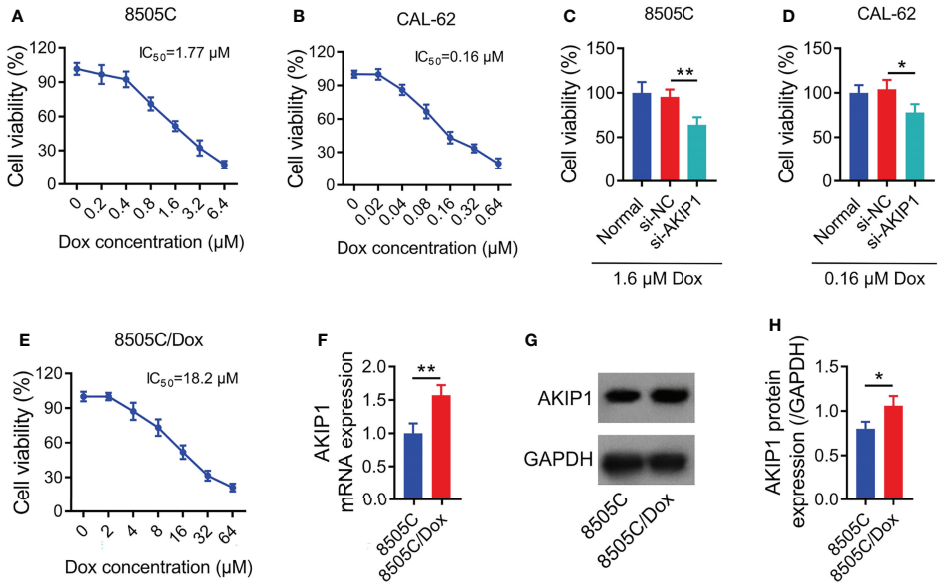

FIGURE 4 | AKIP1 involved in doxorubicin sensitivity in ATC cell lines. Relative cell viability of 8505C cells **(A)** and CAL-62 cells **(B)** under different concentrations of doxorubicin treatment without siRNA transfection; comparison of relative cell viability between groups in 8505C cells after siRNA transfection under 1.6 μM doxorubicin treatment **(C)** and CAL-62 cells after siRNA transfection under 0.16 μM doxorubicin treatment **(D)**; relative cell viability under different concentrations of doxorubicin treatment in 8505C/Dox cells without siRNA transfection **(E)**; comparison of AKIP1 mRNA expression between 8505C cells and 8505C/Dox cells without siRNA transfection or doxorubicin treatment **(F)**; detection of AKIP1 protein expression by Western blot in 8505C cells and 8505C/Dox cells without siRNA transfection or doxorubicin treatment **(G)**; comparison of AKIP1 protein expression between 8505C cells and 8505C/Dox cells without siRNA transfection or doxorubicin treatment **(H)** by one-way ANOVA followed by Dunnett's post-hoc test and Student's *t*-test. ATC, anaplastic thyroid carcinoma; AKIP1, A-kinase interacting protein 1; Dox, doxorubicin; IC_{50}, half maximal inhibitory concentration; $^{*}p < 0.05$; $^{**}p < 0.01$.

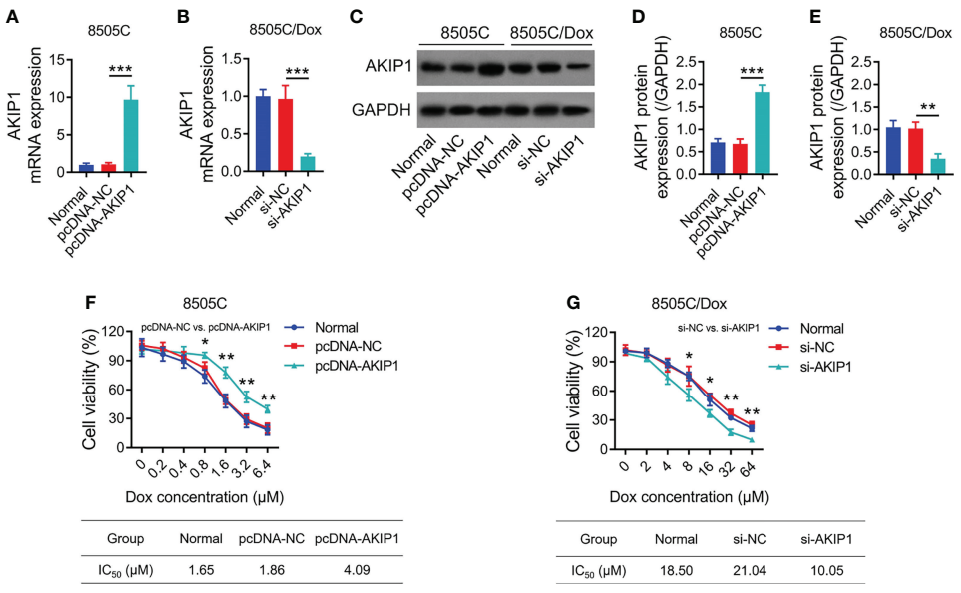

Group	Normal	pcDNA-NC	pcDNA-AKIP1
IC_{50} (μM)	1.65	1.86	4.09

Group	Normal	si-NC	si-AKIP1
IC_{50} (μM)	18.50	21.04	10.05

FIGURE 5 | AKIP1 modification regulated ATC cell viability under different concentrations of doxorubicin. Comparison of AKIP1 mRNA expression among groups in 8505C cells **(A)** and 8505C/Dox **(B)** after AKIP1 modification; detection of AKIP1 protein expression by Western blot in 8505C cells and 8505C/Dox after AKIP1 modification **(C)**; comparison of AKIP1 protein expression among groups in 8505C cells **(D)** and 8505C/Dox **(E)** after AKIP1 modification; comparison of relative cell viability among groups in 8505C cells after AKIP1 modification under 0–6.4 μM doxorubicin treatment **(F)** and 8505C/Dox after AKIP1 modification under 0–64 μM doxorubicin treatment **(G)** by one-way ANOVA followed by Dunnett's post-hoc test. ATC, anaplastic thyroid carcinoma; AKIP1, A-kinase interacting protein 1; Dox, doxorubicin; IC_{50}, half maximal inhibitory concentration; siRNA, small interfering RNA; NC, negative control $^{*}p < 0.05$; $^{**}p < 0.01$; $^{***}p < 0.001$.

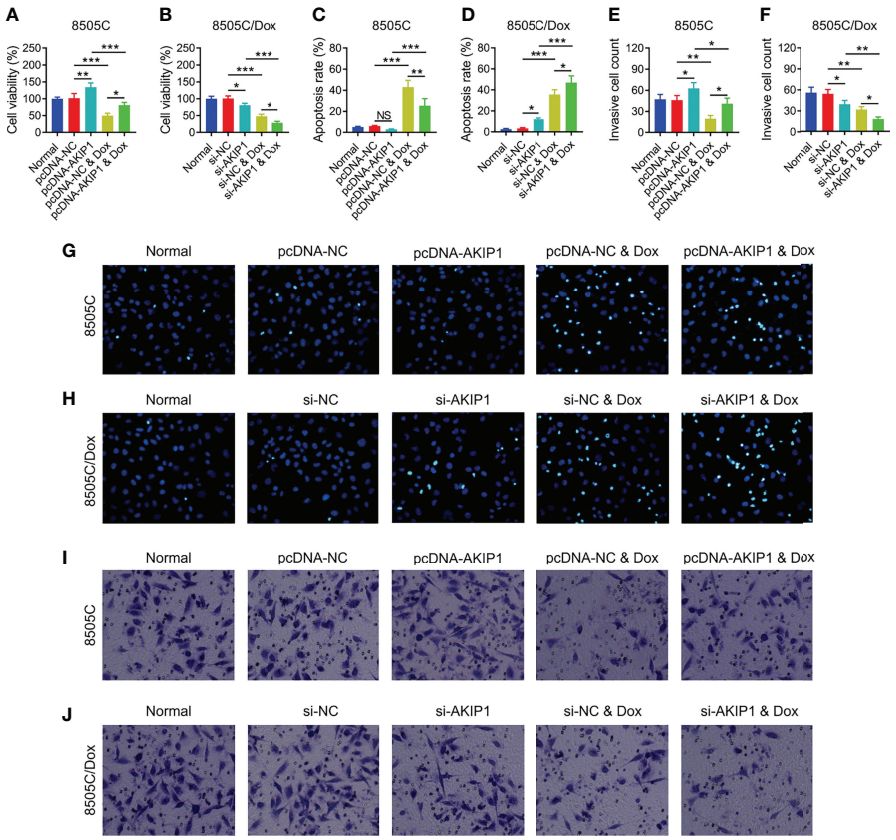

FIGURE 6 | ATC cellular functions after AKIP1 modification and doxorubicin treatment. Comparison of relative cell viability among groups in 8505C cells **(A)** and 8505C/Dox cells **(B)** after AKIP1 modification and doxorubicin treatment; comparison of apoptosis rate among groups in 8505C cells **(C)** and 8505C/Dox cells **(D)** after AKIP1 modification and doxorubicin treatment; comparison of invasive cell count among groups in 8505C cells **(E)** and 8505C/Dox cells **(F)** after AKIP1 modification and doxorubicin treatment by one-way ANOVA followed by Tukey's post-hoc test; example image of cell apoptosis through TUNEL Apoptosis Assay Kit in 8505C cells **(G)** and 8505C/Dox cells **(H)** after AKIP1 modification and doxorubicin treatment; example image of cell invasion through transwell assay in 8505C cells **(I)** and 8505C/Dox cells **(J)** after AKIP1 modification and doxorubicin treatment. ATC, anaplastic thyroid carcinoma; AKIP1, A-kinase interacting protein 1; Dox, doxorubicin; NC, negative control; siRNA, small interfering RNA; TUNEL, terminal deoxynucleotidyl transferase-mediated dUTP-biotin nick end labeling; NS, not significant; $^{*}p < 0.05$; $^{**}p < 0.01$; $^{***}p < 0.001$.

ATC lacks thyroid-like phenotype and function, the treatment option of ATC is very limited; meanwhile, ATC usually presents an unfavorable response rate to chemotherapy and other available therapies (21). Given that ATC is a worldwide threat and extremely hard to manage, exploring the potential target to improve treatment is crucial. In the current study, we explored the interaction of AKIP1 with chemosensitivity and pathways in ATC. Interestingly, we discovered that AKIP1 knockdown could inhibit ATC cell survival and invasion while enhancing doxorubicin sensitivity *via* inhibiting PI3K/AKT and β-catenin pathways.

Over the past decades, AKIP1 has drawn a lot of attention in oncology research, due to its important biological role in multiple malignancies (8, 19, 22, 23). For instance, AKIP1 promotes breast cancer cell motility *via* suppressing Akt/glycogen synthase kinase3β/Snail pathways (22); moreover, AKIP1 elevates hepatocellular carcinoma (HCC) metastasis through Wnt/β-catenin/cyclic AMP response element-binding protein pathways (19); furthermore, AKIP1 facilitates gastric cancer metastasis and cell growth and through activating epithelial–mesenchymal transition (23); additionally, AKIP1 accelerates glioblastoma viability, mobility, and chemoradiation resistance *via* the NF-κB pathway (12); meanwhile, AKIP1 is also considered as a molecular determinant of protein kinase in the NF-κB pathway (24); furthermore, AKIP1 is able to bind the p65 subunit of NF-κB and modulate its transcriptional activity (25). Thus, combined with previous studies, we hypothesize that AKIP1 also takes part in the pathophysiology of ATC, while the information about this issue is scarce. In the current study, we disclosed that AKIP1 was elevated in ATC cell lines compared to the human normal thyroid cell line; meanwhile, we also found that AKIP1 knockdown elevated apoptosis but inhibited relative cell viability and cell invasion in ATC cell lines, which was consistent with the results of previous research about other malignancies (8, 19, 22, 23). The possible explanations might be that (1) AKIP1 knockdown could inhibit ATC cell survival and invasion through several approaches (such as inactivating slug-induced epithelial–mesenchymal transition and

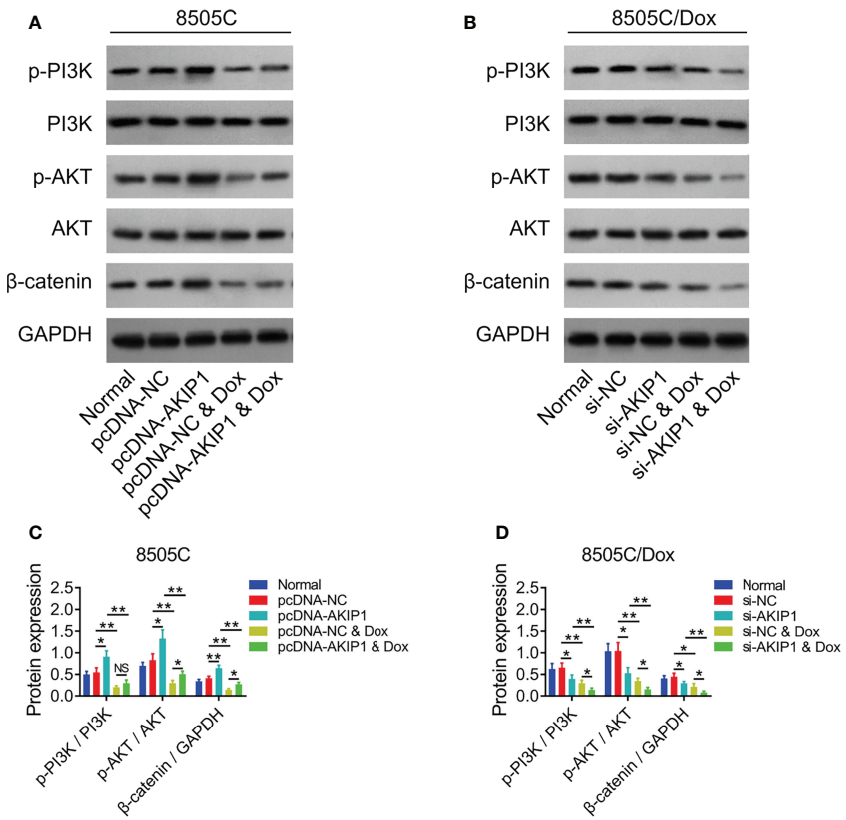

FIGURE 7 | PI3K/AKT and β-catenin pathways after AKIP1 modification and doxorubicin treatment in ATC cell lines. Detection of p-PI3K, PI3K, p-AKT, AKT, and β-catenin protein expressions by Western blot in 8505C cells **(A)** and 8505C/Dox cells **(B)** after AKIP1 modification and doxorubicin treatment; comparison of p-PI3K/PI3K, p-AKT/AKT, and β-catenin expressions among groups in 8505C cells **(C)** and 8505C/Dox cells **(D)** after AKIP1 modification and doxorubicin treatment by one-way ANOVA followed by Tukey's post-hoc test. ATC, anaplastic thyroid carcinoma; AKIP1, A-kinase interacting protein 1; Dox, doxorubicin; NS, not significant; NC, negative control; siRNA, small interfering RNA; PI3K, phosphatidylinositol-3-kinase; AKT, protein kinase B; GAPDH, glyceraldehyde-3-phosphate dehydrogenase; *, $p < 0.05$; **, $p < 0.01$.

downregulating CXC-chemokines) (8, 23) and (2) AKIP1 knockdown might decrease ATC cell survival and invasion through modulating PI3K/AKT and β-catenin pathways (results of our subsequent research).

The PI3K/AKT pathway is viewed as a vital modulator among numerous cancers, such as breast cancer and lung adenocarcinoma (26–30). Importantly, a variety of previous studies suggest that the PI3K/AKT pathway also plays an important role in tumor progression and drug resistance in ATC (31–33). For instance, inhibition of the PI3K/AKT pathway suppresses ATC aggressiveness, such as decreasing cell invasion and survival (31–34); meanwhile, inactivating the PI3K/AKT pathway elevates chemosensitivity in ATC (35). In addition, β-catenin dysregulation is usually found in different malignancies, including ATC (32, 36, 37). For instance, β-catenin inactivation declined cell survival and invasiveness in ATC (31, 36, 38); moreover, β-catenin inactivation is able to elevate iodine uptake in ATC (36). In addition, AKIP1 is reported to regulate PI3K/AKT and β-catenin pathways in several malignancies (12, 19, 20). Inspired by previous data, in the current study, we explored the interaction of AKIP1 with PI3K/AKT and β-catenin pathways in ATC, and data showed that AKIP1 knockdown inactivated PI3K/AKT and β-catenin pathways in ATC cell lines.

It is a big challenge for chemoresistance to elevate outcome among ATC patients, which is regulated by several pathways, including PI3K/AKT and β-catenin pathways (6, 21, 26, 36). Moreover, AKIP1 is proposed to modulate chemoresistance in several cancers (11, 12). Thus, we hypothesized that AKIP1 could regulate chemosensitivity through PI3K/AKT and β-catenin pathways in ATC. In the current research, we chose doxorubicin in the chemosensitivity assay, because doxorubicin is the main cornerstone recommended by the National Comprehensive Cancer Network guideline for the treatment of ATC (39, 40). Surprisingly, we discovered that AKIP1 knockdown elevated apoptosis rate, decreased relative cell viability and invasive cell count, and inactivated PI3K/AKT and β-catenin pathways in chemo-resistant ATC cells under doxorubicin treatment, indicating that AKIP1 knockdown restored doxorubicin sensitivity *via* inhibiting PI3K/AKT and β-catenin pathways in ATC. The possible reasons might be that (1) AKIP1 knockdown could decrease excretion of C-X-C motif

chemokine ligand families, which consequently elevated chemosensitivity (19, 20, 31) and (2) AKIP1 knockdown could inactivate PI3K/AKT and β-catenin pathways to decline stemness, which indirectly elevated chemosensitivity (41–43).

To be conclusive, AKIP1 knockdown decreases cell survival and invasion, while restoring doxorubicin sensitivity through inactivating PI3K/AKT and β-catenin pathways in ATC, indicating that AKIP1 may be a potential target to improve the treatment of ATC.

DATA AVAILABILITY STATEMENT

The datasets presented in this study can be found in online repositories. The names of the repository/repositories and accession number(s) can be found in the article/ **Supplementary Material**.

AUTHOR CONTRIBUTIONS

HZ and QL designed the research study. HZ, QL, and YR performed the research. YR provided help and advice on administration. HZ and QL analyzed the data. HZ, QL, and YR wrote the manuscript. All authors contributed to editorial changes in the manuscript. All authors read and approved the final manuscript.

FUNDING

This work was supported by the Project of Biobank (No.YBKB201911) from Shanghai Ninth People's Hospital, Shanghai Jiao Tong University School of Medicine and the Cross Disciplinary Research Projects of Ninth People's Hospital, Shanghai Jiao Tong University School of Medicine (JYJC202106).

SUPPLEMENTARY MATERIAL

The Supplementary Material for this article can be found online at: https://www.frontiersin.org/articles/10.3389/fonc.2022.854702/full#supplementary-material

REFERENCES

1. Yang J, Barletta JA. Anaplastic Thyroid Carcinoma. *Semin Diagn Pathol* (2020) 37(5):248–56. doi: 10.1053/j.semdp.2020.06.005
2. Lim AM, Solomon BJ. Immunotherapy for Anaplastic Thyroid Carcinoma. *J Clin Oncol* (2020) 38(23):2603–4. doi: 10.1200/JCO.20.01437
3. Molinaro E, Romei C, Biagini A, Sabini E, Agate L, Mazzeo S, et al. Anaplastic Thyroid Carcinoma: From Clinicopathology to Genetics and Advanced Therapies. *Nat Rev Endocrinol* (2017) 13(11):644–60. doi: 10.1038/nrendo.2017.76
4. Saini S, Tulla K, Maker AV, Burman KD, Prabhakar BS. Therapeutic Advances in Anaplastic Thyroid Cancer: A Current Perspective. *Mol Cancer* (2018) 17(1):154. doi: 10.1186/s12943-018-0903-0
5. Rao SN, Zafereo M, Dadu R, Busaidy NL, Hess K, Cote GJ, et al. Patterns of Treatment Failure in Anaplastic Thyroid Carcinoma. *Thyroid* (2017) 27(5):672–81. doi: 10.1089/thy.2016.0395
6. Perrier ND, Brierley JD, Tuttle RM. Differentiated and Anaplastic Thyroid Carcinoma: Major Changes in the American Joint Committee on Cancer Eighth Edition Cancer Staging Manual. *CA Cancer J Clin* (2018) 68(1):55–63. doi: 10.3322/caac.21439
7. Keprova A, Korinkova L, Krizova I, Hadravova R, Kaufman F, Pichova I, et al. Various AKIP1 Expression Levels Affect its Subcellular Localization But Have No Effect on NF-kappaB Activation. *Physiol Res* (2019) 68(3):431–43. doi: 10.33549/physiolres.933961
8. Zhang W, Wu Q, Wang C, Yang L, Liu P, Ma C. AKIP1 Promotes Angiogenesis and Tumor Growth by Upregulating CXC-Chemokines in Cervical Cancer Cells. *Mol Cell Biochem* (2018) 448(1-2):311–20. doi: 10.1007/s11010-018-3335-7
9. Lin C, Song L, Liu A, Gong H, Lin X, Wu J, et al. Overexpression of AKIP1 Promotes Angiogenesis and Lymphangiogenesis in Human Esophageal Squamous Cell Carcinoma. *Oncogene* (2015) 34(3):384–93. doi: 10.1038/onc.2013.559
10. Guo X, Zhao L, Cheng D, Mu Q, Kuang H, Feng K. AKIP1 Promoted Epithelial-Mesenchymal Transition of non-Small-Cell Lung Cancer *via* Transactivating ZEB1. *Am J Cancer Res* (2017) 7(11):2234–44.
11. Leung TH, Ngan HY. Interaction of TAp73 and Breast Cancer-Associated Gene 3 Enhances the Sensitivity of Cervical Cancer Cells in Response to Irradiation-Induced Apoptosis. *Cancer Res* (2010) 70(16):6486–96. doi: 10.1158/0008-5472.CAN-10-0688
12. Han D, Zhang N, Zhao S, Liu H, Wang X, Yang M, et al. AKIP1 Promotes Glioblastoma Viability, Mobility and Chemoradiation Resistance *via* Regulating CXCL1 and CXCL8 Mediated NF-kappaB and AKT Pathways. *Am J Cancer Res* (2021) 11(4):1185–205.
13. Zhang L, Tao H, Ke K, Ma C. A-Kinase Interacting Protein 1 as a Potential Biomarker of Advanced Tumor Features and Increased Recurrence Risk in Papillary Thyroid Carcinoma Patients. *J Clin Lab Anal* (2020) 34(10):e23452. doi: 10.1002/jcla.23452
14. Liang Y, Song X, Li Y, Su P, Han D, Ma T, et al. Circkdm4c Suppresses Tumor Progression and Attenuates Doxorubicin Resistance by Regulating miR-548p/PBLD Axis in Breast Cancer. *Oncogene* (2019) 38(42):6850–66. doi: 10.1038/s41388-019-0926-z
15. Garg M, Kanojia D, Mayakonda A, Ganesan TS, Sadhanandhan B, Suresh S, et al. Selinexor (KPT-330) has Antitumor Activity Against Anaplastic Thyroid Carcinoma *In Vitro* and *In Vivo* and Enhances Sensitivity to Doxorubicin. *Sci Rep* (2017) 7(1):9749. doi: 10.1038/s41598-017-10325-x
16. Lin B, Lu B, Hsieh IY, Liang Z, Sun Z, Yi Y, et al. Synergy of GSK-J4 With Doxorubicin in KRAS-Mutant Anaplastic Thyroid Cancer. *Front Pharmacol* (2020) 11:632. doi: 10.3389/fphar.2020.00632
17. Tian S, Lou L, Tian M, Lu G, Tian J, Chen X. MAPK4 Deletion Enhances Radiation Effects and Triggers Synergistic Lethality With Simultaneous PARP1 Inhibition in Cervical Cancer. *J Exp Clin Cancer Res* (2020) 39(1):143. doi: 10.1186/s13046-020-01644-5
18. Li R, Wan T, Qu J, Yu Y, Zheng R. Long non-Coding RNA DLEUI Promotes Papillary Thyroid Carcinoma Progression by Sponging miR-421 and Increasing ROCK1 Expression. *Aging (Albany NY)* (2020) 12(20):20127–38. doi: 10.18632/aging.103642
19. Cui Y, Wu X, Lin C, Zhang X, Ye L, Ren L, et al. AKIP1 Promotes Early Recurrence of Hepatocellular Carcinoma Through Activating the Wnt/beta-Catenin/CBP Signaling Pathway. *Oncogene* (2019) 38(27):5516–29. doi: 10.1038/s41388-019-0807-5
20. Zhang X, Liu S, Zhu Y. A-Kinase-Interacting Protein 1 Promotes EMT and Metastasis *via* PI3K/Akt/IKKbeta Pathway in Cervical Cancer. *Cell Biochem Funct* (2020) 38(6):782–91. doi: 10.1002/cbf.3547

21. Amaral M, Afonso RA, Gaspar MM, Reis CP. Anaplastic Thyroid Cancer: How Far can We Go? *EXCLI J* (2020) 19:800–12. doi: 10.17179/excli2020-1302
22. Mo D, Li X, Li C, Liang J, Zeng T, Su N, et al. Overexpression of AKIP1 Predicts Poor Prognosis of Patients With Breast Carcinoma and Promotes Cancer Metastasis Through Akt/GSK-3beta/Snail Pathway. *Am J Transl Res* (2016) 8(11):4951–9.
23. Chen D, Cao G, Liu Q. A-Kinase-Interacting Protein 1 Facilitates Growth and Metastasis of Gastric Cancer Cells *via* Slug-Induced Epithelial-Mesenchymal Transition. *J Cell Mol Med* (2019) 23(6):4434–42. doi: 10.1111/jcmm.14339
24. Gao N, Hibi Y, Cueno M, Asamitsu K, Okamoto T. A-Kinase-Interacting Protein 1 (AKIP1) Acts as a Molecular Determinant of PKA in NF-kappaB Signaling. *J Biol Chem* (2010) 285(36):28097–104. doi: 10.1074/jbc.M110.116566
25. King CC, Sastri M, Chang P, Pennypacker J, Taylor SS. The Rate of NF-kappaB Nuclear Translocation is Regulated by PKA and A Kinase Interacting Protein 1. *PLoS One* (2011) 6(4):e18713. doi: 10.1371/journal.pone.0018713
26. Milosevic Z, Pesic M, Stankovic T, Dinic J, Milovanovic Z, Stojsic J, et al. Targeting RAS-MAPK-ERK and PI3K-AKT-mTOR Signal Transduction Pathways to Chemosensitize Anaplastic Thyroid Carcinoma. *Transl Res* (2014) 164(5):411–23. doi: 10.1016/j.trsl.2014.06.005
27. Yang J, Nie J, Ma X, Wei Y, Peng Y, Wei X. Targeting PI3K in Cancer: Mechanisms and Advances in Clinical Trials. *Mol Cancer* (2019) 18(1):26. doi: 10.1186/s12943-019-0954-x
28. Aoki M, Fujishita T. Oncogenic Roles of the PI3K/AKT/mTOR Axis. *Curr Top Microbiol Immunol* (2017) 407:153–89. doi: 10.1007/82_2017_6
29. Yan W, Ma X, Zhao X, Zhang S. Baicalein Induces Apoptosis and Autophagy of Breast Cancer Cells *via* Inhibiting PI3K/AKT Pathway *In Vivo* and Vitro. *Drug Des Devel Ther* (2018) 12:3961–72. doi: 10.2147/DDDT.S181939
30. Yu M, Qi B, Xiaoxiang W, Xu J, Liu X. Baicalein Increases Cisplatin Sensitivity of A549 Lung Adenocarcinoma Cells *via* PI3K/Akt/NF-kappaB Pathway. *BioMed Pharmacother* (2017) 90:677–85. doi: 10.1016/j.biopha.2017.04.001
31. Kim SH, Kang JG, Kim CS, Ihm SH, Choi MG, Yoo HJ, et al. 17-Allylamino-17-Demethoxygeldanamycin and Herbimycin A Induce Cell Death by Modulating Beta-Catenin and PI3K/AKT Signaling in FRO Anaplastic Thyroid Carcinoma Cells. *Anticancer Res* (2015) 35(10):5453–60.
32. Kim SH, Kang JG, Kim CS, Ihm SH, Choi MG, Yoo HJ, et al. CCAAT/Enhancer-Binding Protein-Homologous Protein Sensitizes to SU5416 by Modulating P21 and PI3K/Akt Signal Pathway in FRO Anaplastic Thyroid Carcinoma Cells. *Horm Metab Res* (2013) 45(1):9–14. doi: 10.1055/s-0032-1323680
33. Xing M. Genetic Alterations in the Phosphatidylinositol-3 Kinase/Akt Pathway in Thyroid Cancer. *Thyroid* (2010) 20(7):697–706. doi: 10.1089/thy.2010.1646
34. Nozhat Z, Mohammadi-Yeganeh S, Azizi F, Zarkesh M, Hedayati M. Effects of Metformin on the PI3K/AKT/FOXO1 Pathway in Anaplastic Thyroid Cancer Cell Lines. *Daru* (2018) 26(2):93–103. doi: 10.1007/s40199-018-0208-2
35. Francipane MG, Eterno V, Spina V, Bini M, Scerrino G, Buscemi G, et al. Suppressor of Cytokine Signaling 3 Sensitizes Anaplastic Thyroid Cancer to Standard Chemotherapy. *Cancer Res* (2009) 69(15):6141–8. doi: 10.1158/0008-5472.CAN-09-0994
36. Lan L, Basourakos S, Cui D, Zuo X, Deng W, Huo L, et al. ATRA Increases Iodine Uptake and Inhibits the Proliferation and Invasiveness of Human Anaplastic Thyroid Carcinoma SW1736 Cells: Involvement of Beta-Catenin Phosphorylation Inhibition. *Oncol Lett* (2017) 14(6):7733–8. doi: 10.3892/ol.2017.7225
37. Valenta T, Hausmann G, Basler K. The Many Faces and Functions of Beta-Catenin. *EMBO J* (2012) 31(12):2714–36. doi: 10.1038/emboj.2012.150
38. Sastre-Perona A, Santisteban P. Wnt-Independent Role of Beta-Catenin in Thyroid Cell Proliferation and Differentiation. *Mol Endocrinol* (2014) 28 (5):681–95. doi: 10.1210/me.2013-1377
39. Smallridge RC, Ain KB, Asa SL, Bible KC, Brierley JD, Burman KD, et al. American Thyroid Association Guidelines for Management of Patients With Anaplastic Thyroid Cancer. *Thyroid* (2012) 22(11):1104–39. doi: 10.1089/thy.2012.0302
40. Haddad RI, Lydiatt WM, Ball DW, Busaidy NL, Byrd D, Callender G, et al. Anaplastic Thyroid Carcinoma, Version 2.2015. *J Natl Compr Canc Netw* (2015) 13(9):1140–50. doi: 10.6004/jnccn.2015.0139
41. Madsen RR. PI3K in Stemness Regulation: From Development to Cancer. *Biochem Soc Trans* (2020) 48(1):301–15. doi: 10.1042/BST20190778
42. Basu S, Cheriyamundath S, Ben-Ze'ev A. Cell-Cell Adhesion: Linking Wnt/beta-Catenin Signaling With Partial EMT and Stemness Traits in Tumorigenesis. *F1000Res* (2018) 7:F1000 Faculty Rev-1488. doi: 10.12688/f1000research.15782.1
43. Prasad S, Ramachandran S, Gupta N, Kaushik I, Srivastava SK. Cancer Cells Stemness: A Doorstep to Targeted Therapy. *Biochim Biophys Acta Mol Basis Dis* (2020) 1866(4):165424. doi: 10.1016/j.bbadis.2019.02.019

Conflict of Interest: The authors declare that the research was conducted in the absence of any commercial or financial relationships that could be construed as a potential conflict of interest.

Advantages of publishing in Frontiers

OPEN ACCESS
Articles are free to read for greatest visibility and readership

FAST PUBLICATION
Around 90 days from submission to decision

HIGH QUALITY PEER-REVIEW
Rigorous, collaborative, and constructive peer-review

TRANSPARENT PEER-REVIEW
Editors and reviewers acknowledged by name on published articles

Frontiers
Avenue du Tribunal-Fédéral 34
1005 Lausanne | Switzerland

Visit us: www.frontiersin.org
Contact us: frontiersin.org/about/contact

REPRODUCIBILITY OF RESEARCH
Support open data and methods to enhance research reproducibility

DIGITAL PUBLISHING
Articles designed for optimal readership across devices

FOLLOW US
@frontiersin

IMPACT METRICS
Advanced article metrics track visibility across digital media

EXTENSIVE PROMOTION
Marketing and promotion of impactful research

LOOP RESEARCH NETWORK
Our network increases your article's readership